Detrital Zircon Studies in Silurian Basins of Southern New Brunswick

by

Robert John Dokken

A thesis submitted in partial fulfillment of the requirements for the degree of

Master of Science

Department of Earth and Atmospheric Sciences

University of Alberta

Abstract

The Appalachian orogen in eastern Canada resulted from the Paleozoic convergence of the continents Laurentia and Gondwana during the closure of the intervening Iapetus Ocean. In New Brunswick, the Fredericton Trough and Mascarene Basin were filled in the Silurian within the peri-Gondwanan domain of Ganderia during associated convergence and ocean closure. Detrital zircon geochronological studies demonstrate that the northern formations of the Fredericton Trough were juxtaposed with Laurentia in the early Silurian; however, southern portions of the trough were still separated from Laurentia at this time, indicating the persistence of the Iapetus Ocean. These southern formations record the arrival of Laurentian detritus by the mid-Wenlock, indicating that components of Ganderia were juxtaposed with Laurentia by this time, coinciding with ocean closure. The location of the terminal Iapetan suture, marking the closure of the last portion of Iapetus Ocean, is approximated by the Fredericton Fault, which bisects the trough. Analogous studies in the Mascarene back-arc basin, to the south of the Fredericton Trough, show that it was separated from Laurentia until at least the late Llandovery, and may suggest juxtaposition with a composite Laurentia by 423 ± 1 Ma. These combined results suggest a scenario where Ganderian terranes were successively accreted to Laurentia in the Silurian, as recorded by the progressively increasing extent of Laurentian detritus in juxtaposed terranes.

Acknowledgments

Firstly, I would like to gratefully acknowledge the mentorship of Dr. John Waldron, whose experience and insight has been invaluable over a number of years. Numerous faculty and staff at the University of Alberta have been a great assistance to this project; to name a few, Andy DuFrane greatly assisted with analysis and data reduction, and Nathan Gerein and Richard Stern facilitated sample imaging. Many others from the Department of Earth and Atmospheric Sciences have been helpful and willing to share their knowledge, whether in courses, presentations, or discussion. Les Fyffe, Adrian Park, and Susan Johnson aided in field work and sample collection by identifying fossil localities, providing field maps, assisting with field work in-person, and otherwise sharing their knowledge of New Brunswick geology. Correspondence with Allan Ludman has provided helpful insights into related geological puzzles in Maine. Cees van Staal has provided encouragement and constructive feedback. Funding was provided through a Natural Sciences and Engineering Research Council of Canada Discovery Grant to Dr. John Waldron. Lastly, I would like to thank my family and friends for their continued support.

Contents

List of figures

Chapter 1: Introduction

1. Overview of Appalachian geology

1.1 Description and background to study of the orogen

The Paleozoic Appalachian orogen in eastern Canada is a belt of deformed rock, up to 600 km wide at its broadest point, extending through Newfoundland, the Maritime provinces, and a portion of southern Quebec. The orogen is bounded to the west by rocks of the Canadian Shield, and to the east by the Atlantic Continental Shelf (Williams, 1995). It continues southward through the United States, and is correlated northwards with the Caledonides in eastern Greenland and Europe (Figure 1.1).

The Appalachian region has been very well-studied and thoroughly mapped over centuries of work. For much of the century previous to the advent of plate tectonic theory, the Appalachians were the type example of geosynclinal theory (Dana, 1873; Hall, 1883), a mountain belt formed from subsidence, compression, and uplift. Subsequent study saw the development and application of plate tectonic theory, some of which was pioneered in the Appalachians (Wilson, 1966; Dewey, 1969; Bird and Dewey, 1970), leading to the current framework of the orogen as the end result of a cycle of subduction, ocean closing, terrane accretion, and continental collision (Williams, 1995).

The Appalachian orogen has traditionally been divided into several regions of similar lithology, stratigraphy, fossil biota, and structural characteristics (Williams, 1979): these are the Humber, Dunnage, Gander, Avalon, and Meguma Zones. The Humber Zone “miogeocline” (Kay, 1951) is interpreted as the Paleozoic passive margin of Laurentia, or ancient North America. The remaining successively outboard zones are regarded as suspect terranes (Williams and Hatcher, 1982, 1983), accreted to the margin of Laurentia during the Paleozoic closure of an ancient seaway, the Iapetus Ocean (Harland and Gayer, 1972). More recent subdivision (Hibbard and

Figure 1.1: Map of the Appalachian-Caledonide orogen.

Pangean (pre-Mesozoic) reconstruction after Waldron and others (2014b) and references therein. Lithotectonic divisions after van Staal and others (1998) and Hibbard and others (2006, 2007).

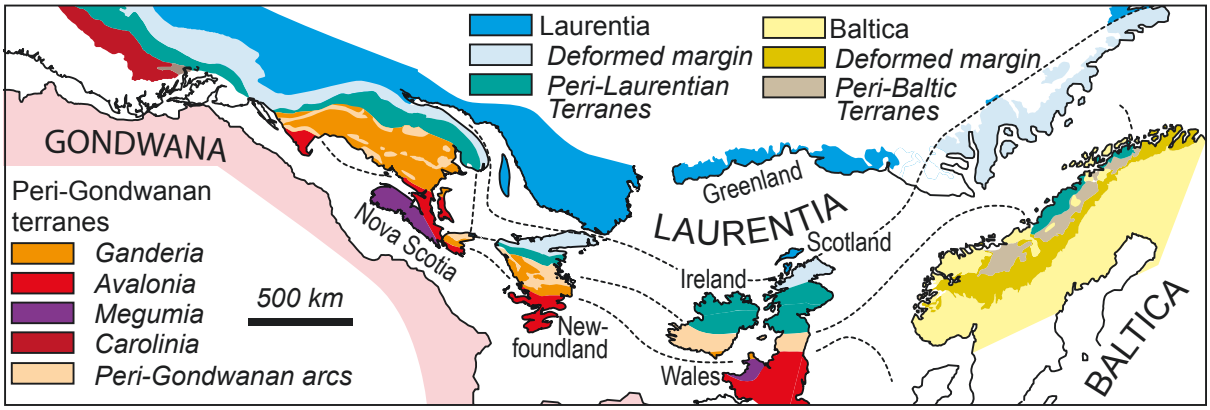

others, 2006, 2007) has attempted to clearly designate lithotectonic zones as those of Laurentian affinity, peri-Laurentian (separated at some point from the continent), or peri-Gondwanan. Gondwana was an assembling supercontinent in the Paleozoic, opposite Laurentia across the Iapetus Ocean. A number of peri-Gondwanan microcontinental domains, including Ganderia and Avalonia, rifted from Gondwana in the early Paleozoic and were assimilated into the Appalachian orogen.

1.2 Tectonic history and development of the Appalachian orogen

Research in recent decades has attempted to synthesize knowledge of Appalachian geology and produce a cohesive model of the tectonic setting and formation of the orogen (e.g. Williams, 1979; van Staal and others, 1998; Hibbard and others 2006, 2007; van Staal and others, 2009).

Laurentia was an independent continent in the late Neoproterozoic (Li and others, 2008), one fragment resulting from the protracted breakup of the Proterozoic supercontinent Rodinia. The Iapetus Ocean developed to south of Laurentia from about 570 – 550 Ma (Williams and Hiscott, 1987), resulting in a Laurentian passive margin by the early Cambrian (Cawood and others, 2001). This ocean separated Laurentia from Gondwana, an assembling supercontinent which included Amazonia and West Africa. Appalachian orogenesis resulted from the convergence of Laurentia with Gondwana, as the Iapetus Ocean closed, and material (microcontinental, oceanic, arc) within the ocean was successively accreted to the Laurentian margin.

Accretion at the Laurentian margin began taking place in the late Cambrian to Late Ordovician, notably including the collision of the peri-Laurentian Notre Dame arc in the Early Ordovician (van Staal and others, 2009). This deformation has been identified as Taconic orogenesis, which terminated with the Late Ordovician accretion of the Popelogan arc terrane, rifted from the margin of Ganderia, to the active Laurentian margin. This event was the first contact of peri-Gondwanan material with Laurentia, and also coincided with the closure, according to van Staal and others (1998), of the “main tract” of the Iapetus Ocean, leaving only a remnant behind. This

remnant was the 600-800 km wide Tetagouche-Exploits backarc basin (van Staal and others, 2012), which had opened between Ganderia and the rifted Popelogan arc.

The deformation which closely followed is interpreted (ex. van Staal and others, 2009) to have resulted from the accretion of Ganderia to Laurentia in the Silurian, which involved the subduction and closure of the Tetagouche-Exploits seaway (and microcontinental material within it), in what is referred to as Salinic orogenesis. This may have marked the closure of the last remnant of the Iapetus Ocean (Reusch and van Staal, 2012).

Deformation in the late Silurian to Early Devonian is interpreted (ex. van Staal and others, 2009) to result from the convergence and accretion at Ganderia's opposite (southern) margin of Avalonia, another arc terrane rifted from the margin of Gondwana. This is referred to as the Acadian orogeny (van Staal and others, 2009). Accretion is interpreted to have taken place following the stepping back of a northwest-dipping subduction zone behind previously accreted material, continuing the progressive growth of a composite Laurentia.

Lastly, further deformation took place in the Middle Devonian to Early Carboniferous, interpreted to result from the accretion of the Meguma terrane (or Megumia: Waldron and others, 2011; Figure 1.1) to the Laurentian margin (now represented by accreted peri-Gondwanan terranes) in Neo-Acadian orogenesis (van Staal and others, 2009). This heralded the assembly of Laurentia, Gondwana, and other continental domains into the supercontinent of Pangaea by the end of the Paleozoic; the Appalachian orogen was effectively one of the seams of this assembly.

1.3 Appalachian-Caledonide connections

The Caledonides feature similar rocks and terranes (Bluck and others, 1992) to the Appalachian orogen, and ongoing research has attempted to correlate sutures and terranes, and compare tectonic histories. There are, however, notable differences between the orogens (van Staal and others, 1998; McKerrow and others, 2000; Waldron and others, 2014a).

The Caledonide orogen includes deformed rocks in the British Isles, Scandinavia, and Eastern Greenland, attributed to the Paleozoic closure of the Iapetus Ocean, and involving the continents of Laurentia, Baltica, and microcontinental domains of peri-Gondwana (McKerrow and others, 2000). Ordovician (Grampian) deformation in the British Isles probably resulted from arc-continent collision (Dewey and Mange, 1999; Soper and others, 1999), and is considered equivalent to the Taconic orogeny in the Canadian Appalachians (van Staal and others, 1998; McKerrow and others, 2000). In the Silurian, the closure of the Iapetus Ocean resulted in collision of Ganderia with Laurentia by about 430 Ma along the Solway Line (Waldron and others, 2014a). This is in contrast to the Early (Macdonald and others, 2014) and Late Ordovician (van Staal and others, 2009) arrival of Ganderian fragments in the New England and Newfoundland Appalachians, respectively. Later Devonian (Acadian) deformation following Iapetan closure may have been related to the convergence of Avalonia, or other convergence across the Rheic Ocean (Woodcock and Soper, 2006) which divided Gondwana from separated peri-Gondwanan material (van Staal and others, 2012).

1.4 Purpose of study

Constraints on the timing of closure of the Iapetus Ocean are complicated by diachronous or isolated orogenic events within the Appalachian-Caledonide orogen. While previous interpretation (e.g. van Staal and others, 1998) suggests that the main tract of the Iapetus Ocean closed with the accretion of the first piece of Ganderia with Laurentia, at least a portion of Iapetus persisted in the form of the Tetagouche-Exploits seaway, or Sea of Exploits (Waldron and others, 2014a, 2014b), which evolved from its origin as a back-arc basin into a seaway of significant width (van Staal and others, 2012), and the closure of which resulted in the accretion of many other peri-Gondwanan fragments (van Staal and others, 2008). As a result Silurian Salinic orogenesis involves many possible sutures, and the accretion of the final mass of Ganderia, coinciding with the closure of the Tetagouche-Exploits seaway and the terminal Iapetan suture.

This thesis presents new detrital zircon data from two Silurian basins in the Appalachians of southern New Brunswick. Previous work has demonstrated that Laurentian detritus, marked by distinctive zircon age distributions, is found pervasively and abundantly in accreted terranes (e.g. Cawood and Nemchin, 2001; Moecher and Samson, 2006; Pollock and others, 2007; Waldron and others, 2012; Macdonald and others, 2014; Waldron and others, 2014a). Peri-Gondwanan terranes that have not been accreted preserve a contrasting detrital zircon signature, typically including abundant Neoproterozoic zircon and lacking the diagnostic detritus shed from the Laurentian margin. Analyzing detrital zircon signatures from basin sediments deposited upon suspect terranes can then be used to determine when peri-Gondwanan material, or Ganderia in particular, was accreted to Laurentia.

The Silurian Fredericton Trough, trending northeast-southwest in southern New Brunswick, is filled by turbidites interpreted to have been deposited along the margins of the Tetagouche-Exploits seaway: to the north, along the margin of composite Laurentia, and to the south along the margin of the final piece of Ganderia. It is ideally located to provide constraints on the timing and location of the terminal Iapetan suture. The Silurian volcanic-sedimentary Mascarene Basin sits upon Ganderian terranes to the south of the Fredericton Trough, further outboard with respect to Laurentia, and can likewise be studied for evidence of Laurentian detritus to indicate the timing of accretion.

2. Overview of methods

2.1 Introduction to U-Pb geochronology

Uranium-lead (U-Pb) geochronology produces age data by measuring the ratios between the parent and daughter isotopes of two distinct decay chains from uranium to a stable isotope of lead: $^{238}U \rightarrow {}^{206}Pb$, and $^{235}U \rightarrow {}^{207}Pb$. A third decay chain, from thorium to lead, is sometimes also measured: $^{232}Th \rightarrow {}^{208}Pb$. These cycles account for three of the four stable isotopes of lead; the fourth, ^{204}Pb, is not radiogenic.

A singular advantage to the U-Th-Pb system is the wide range of half-lives and decay constants of each decay series. ^{238}U-^{206}Pb has a half-life of approximately 4.47 Ga, ^{235}U-^{207}Pb of 0.704 Ga, and ^{232}Th-^{208}Pb of 14.01 Ga. Measuring more than one of these parent-daughter ratios allows each to cross-check the other for the internal consistency of the U-Pb (or U-Th-Pb) system as a whole.

A disadvantage of the U-Pb system in its simplest form is the relative mobility of uranium and lead – it is not necessarily a closed system – leading to difficulties in dating rocks which have undergone low-grade metamorphism or even superficial weathering (Dickin, 2008). However, by employing each of the two U-Pb decay schemes together, even disturbed rocks can yield valuable and accurate age data. This is particularly true of U-Pb zircon dating. Zircon is a ubiquitous and robust mineral that incorporates uranium at the time of crystallization, but little initial lead; combined with the helpful redundancy of U-Pb analysis, reliable age data can be obtained in a diverse assortment of rocks, some of which may otherwise be difficult to analyze.

2.2 Method overview

Modern analytical methods can accommodate either individually selected zircons and other mineral grains, or thin section and grain mounts via in situ techniques. Three commonly used methods are thermal ionization mass spectrometry (variants include isotope dilution and/or chemical abrasion, ID-TIMS or CA-TIMS), laser ablation inductively coupled mass spectrometry (LA-ICPMS), and secondary ion mass spectrometry (SIMS). Backscattered electron imaging (BSE) or cathodoluminescence imaging (CL) is often performed before analysis of selected zircons, epoxy mounts, or thin sections, to identify internal structures which may affect the analysis, such as oscillatory zoning, inherited cores, inclusions, overgrowths, metamict textures, and alteration.

TIMS has been used for several decades, and has long been the mainstay of U-Pb analysis (Schoene, 2014). It involves purifying U and Pb by column chemistry, and then depositing a

sample onto a metal filament, which is heated to ionize the sample, and analyzed by the mass spectrometer. This method is used to analyze carefully selected single grains. It is the most precise technique, but also the slowest and most costly for the typically large number of analyses involved in detrital samples.

LA-ICPMS is a technique widely used to accommodate in situ analysis of epoxy grain mounts and thin sections, and has the additional advantage of being able to analyze many distinct grains in a short period of time, at relatively little cost, and with reasonable precision and accuracy for most geologic problems. It is a relatively recent technique that began to be applied to U-Pb geochronology in the 1990s (Dickin, 2005; Schoene, 2014), and has since been widely adopted. Laser ablation apparatus may be combined with different types of mass spectrometers, such as multi-collector or quadrupole instruments (LA-MC-ICPMS or LA-Q-ICPMS). It is often the preferred method for detrital zircon studies due to its efficiency in analyzing a large number of grains.

SIMS was developed in the 1970s (Dickin, 2005; Schoene, 2014), and soon applied effectively to analyzing one or many zircons with complex histories. An advantage of the technique is its ability to sputter small spot sizes with much shallower pit depths than in laser ablation, making it the ideal technique in terms of in situ spatial resolution, and the least destructive of standard methods. However, it is more expensive and time-consuming than LA-ICPMS.

2.3 Detrital zircon geochronology

Detrital zircon geochronology is a subfield which studies sedimentary rocks specifically, where a given sample may have zircons of many different ages representing various sources.

One useful application of this method is the study of provenance, or determining the sources or source regions of a given rock unit. When many zircons from a single sedimentary rock are analyzed they can form a fingerprint-like spectrum of ages, and these spectra can be used to

distinguish between rocks of substantially different source regions.

A consideration of these studies is the number of grains required for a statistically sound analysis while balancing the cost and time invested. The number of zircons required is dependent on the number of discrete populations in a sample, and the desired confidence level that a fraction is not missed (Vermeesch, 2004). Typical reported figures range from dozens to hundreds of analyses, and techniques are increasingly being developed to efficiently accommodate large numbers of grains.

One problem which must constantly be addressed by researchers employing this method is the depositional environment of the rocks chosen for study. For example, extant fluvial systems draining known source terranes have been shown to underrepresent or not record the ages of those terranes (Eriksson and others, 2003). The ideal system is one in which detritus can be widely and consistently distributed, such as in a foreland basin or continental margin.

2.4 Data representation and statistical analyses

Accurately representing detrital zircon data presents several unique challenges. The goal is to present the typically large quantities of data in an easily visualized plot, which accurately represents the general trend of the age spectra for the entire sample while also allowing an outside reader to discern information about measurements from individual grains. Analyses should be easily comparable between different researchers, with relative consistency between different data sets and authors. In other words the same data should appear the same, regardless of who has plotted it, so as to encourage more objective interpretations.

Probability density plots (PDPs; Figure 1.2) have been widely used to this end, having been greatly facilitated by the availability and ease of software such as Isoplot (Ludwig, 2012). In these plots, each individual analysis is represented as a normal distribution, with a mean corresponding to the age and standard deviation to the analytical error. The final probability

Figure 1.2: Detrital zircon probability density plots.

Individual analyses are shown as normal distributions (red), with their age and analytical error corresponding to the mean and standard deviation of each curve. The resulting probability density curve is shown at a different scale (blue).

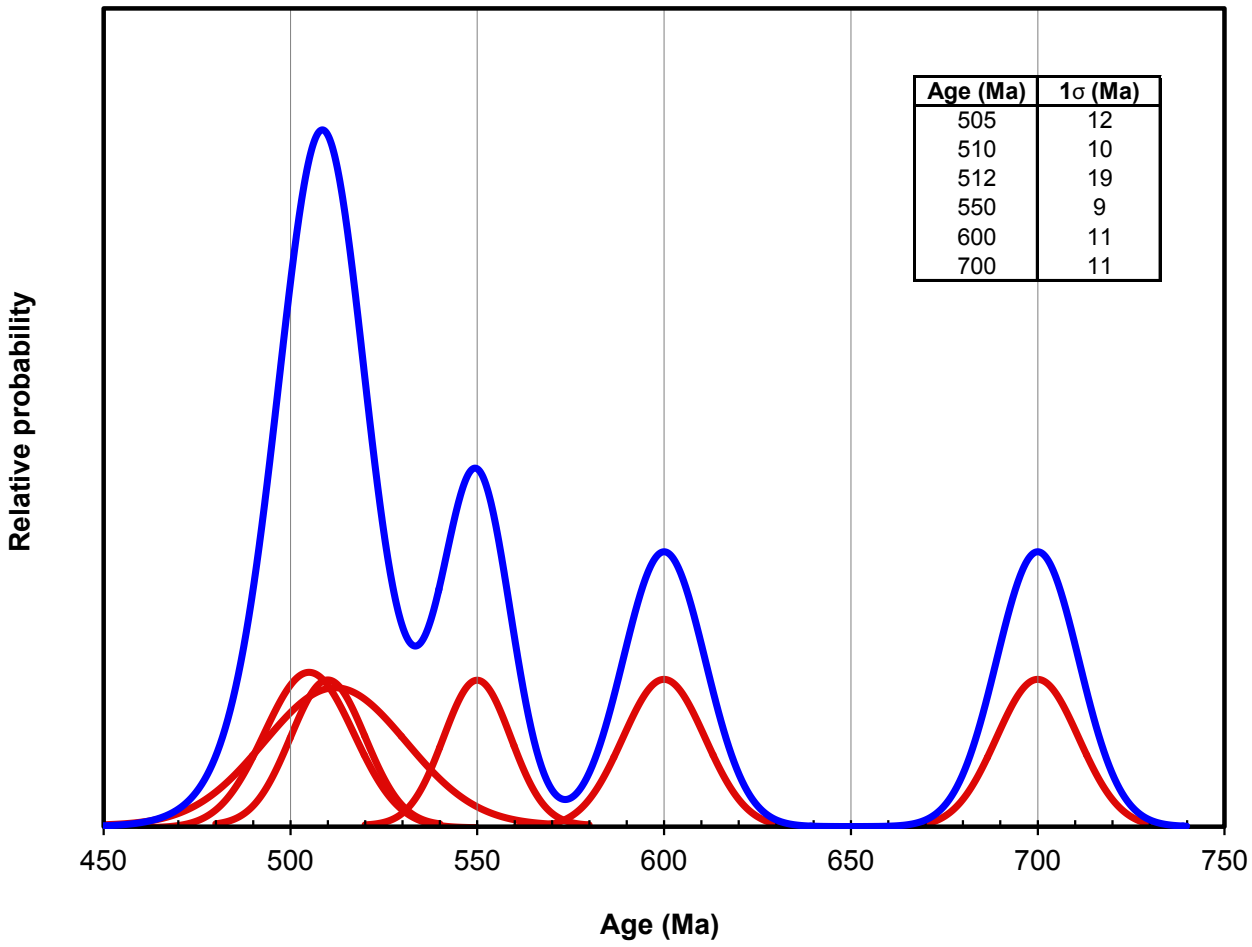

density function is effectively the sum of each of these individual curves. In the theoretical analysis of an infinite number of grains all possible zircon ages must fall within the curve, the integral of which is 1.0 (Guynn and Gehrels, 2010). The vertical scale on these plots is relative and arbitrary; a large number of zircon analyses at a certain age will result in a higher peak than a population of only a few grains. Similarly, broader peaks are less precise than sharp, narrow peaks. These plots are reproducible with relative consistency between different researchers, and they present age data in an easily comprehendible format. However, they may lack a sound statistical basis (Vermeesch, 2012), leading many researchers to seek other means for presenting their data. Additionally, these plots do not inherently indicate how many analyses form a given peak. This makes it difficult to distinguish between a robust data set of many analyses, or a sparse data set of only a few grains. Even within the plot itself, peak heights cannot be directly compared in a way that indicates the number of analyses in each.

Standard histograms are often shown in addition to (or in place of) PDPs, and avoid their statistical problems, in addition to incorporating information on how many grains of a given age group were analyzed. These plots consist of bins (including all analyses of a given age range along the horizontal axis) whose height along the vertical axis corresponds to the number of analyses falling within that range. However, these graphs have parameters which, depending on the researcher's preference, can significantly affect the representation of the data. Bin width, for example, may undersmooth or oversmooth a data set. If individual age measurements typically include an error of 10 Ma, then bins of 1 Ma imply more detail than can be justified; alternately, bins of 100 Ma may lose meaningful data. Comparing these two plots (Figure 1.3) demonstrates inconsistencies in their visual representation, complicating the comparison of different data sets, from different authors. Additionally, the start location of bins (Figure 1.3) can also significantly change the appearance of a data set. For example, a significant population of zircons from a single source may be split into multiple bins, appearing inconsistent with what may be suggested from a single, more prominent bin. These difficulties mean that visual comparisons of different data sets may be unreliable on their own.

Figure 1.3: Detrital zircon histograms.

Comparison of bin start and width affecting representation of the same sample (Burtts Corner Fm., n=113, see Chapter 2). Probability density curves in red, histogram bins in blue.

A: Bin start 0, width 100. B: Bin start 50, width 100. C: Bin start 0, width 50. D: Bin start 0, width 25 (note the different vertical scale).

Note the shifted bins of B relative to A, changes in relative bin heights (e.g. 700 Ma), and gaps where there were none previously. In C, note the different bin heights at ca. 1000 Ma and 450 Ma, where they were nearly equal in A and B. The bin width in D approximates the mean 2σ analytical uncertainty of the analyses, and closely follows the shape of the probability density curve.

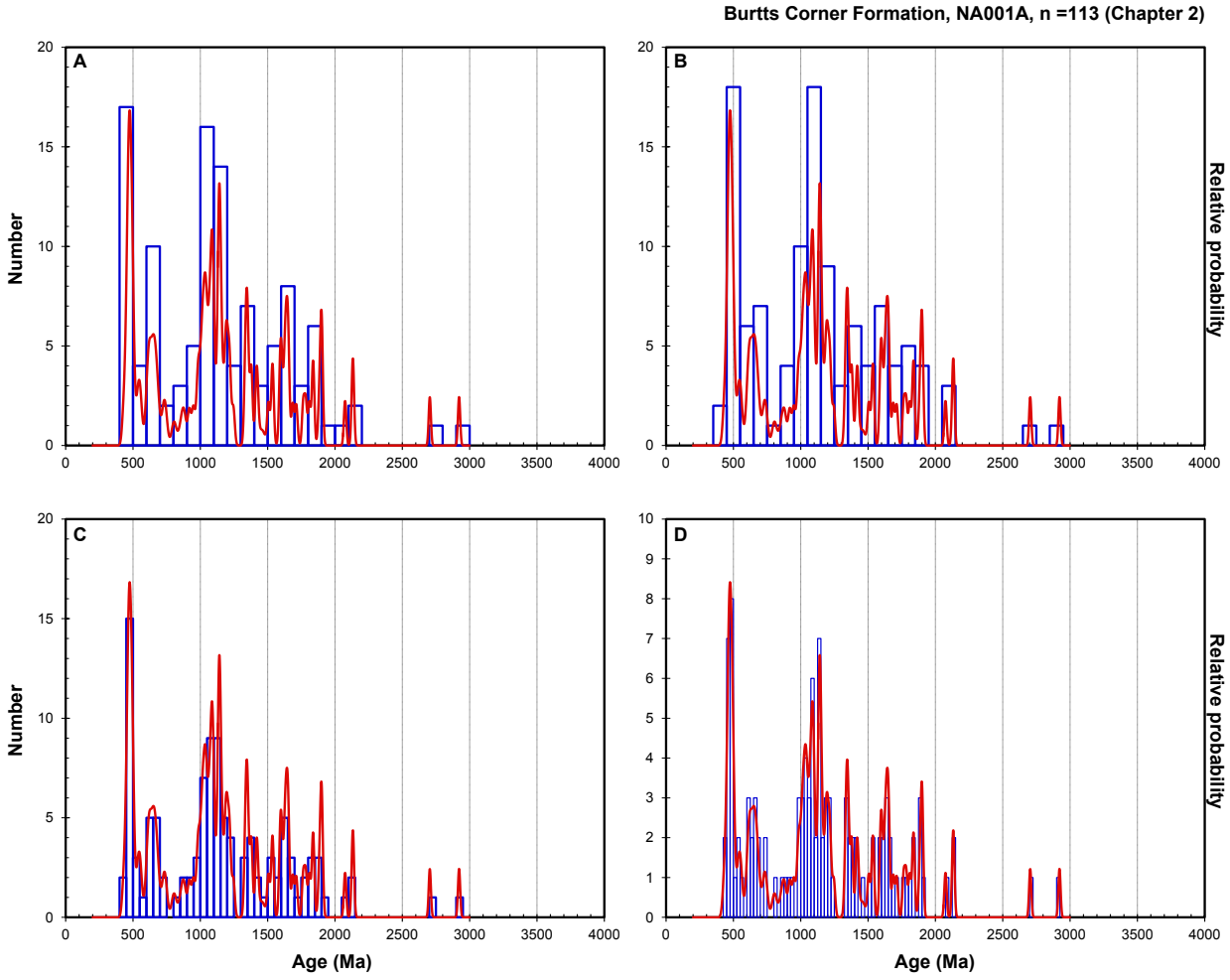

Cumulative density plots (CDPs; Figure 1.4) are perhaps a less intuitive way to visualize data, but enable a data set to be reproduced consistently, while avoiding some of the statistical pitfalls of PDPs and the potential inconsistencies of histograms. Age is plotted on the x-axis, and cumulative probability on the y-axis: thus a sample with a large proportion of grains at 500 Ma will produce a steep line at this point; a sample with few or no zircons from 500 Ma to 1000 Ma will yield a shallow or horizontal line in this range. Although these plots do show the proportion (or probability) of a given age population in the sample, they still do not typically show the number of grains in as precise a manner as histograms. The basic cumulative density plot is represented as a step function (Figure 1.4), with vertical lines where an age is reported, and horizontal lines where there are no analyses of that age range. With detrital zircon data, analytical uncertainty is typically incorporated in a manner analogous to PDPs, by summing individual normal distributions with a mean equal to the age, and standard deviation equal to the analytical error. This has the effect of rounding the corners and sloping the lines of the step function (Figure 1.4).

Kernel density plots (KDPs; Figure 1.5) are another option in visualizing detrital zircon age data, superficially similar to PDPs, but with a sound statistical basis underlying their construction (Vermeesch, 2012). However, they have a tendency to oversmooth datasets and risk obscuring real information from the measured ages (Gehrels, 2013). This can be addressed by arbitrating the "bandwidth" associated with the plot (Figure 1.5); the result may be very similar to standard PDPs. These plots may not be as easily reproducible as PDPs, since the bandwidth and other parameters may be determined differently by various researchers, but they are otherwise an excellent method to visually represent age distributions.

Kolmogorov-Smirnov (K-S; Figure 1.6) tests are a statistical method which allow one to objectively compare detrital zircon samples; more specifically, a two-sample test can test the null hypothesis that two data sets are the same, or taken from the same population (Gehrels and others, 2006; Guynn and Gehrels, 2010). The test functions by measuring the maximum

Figure 1.4: Detrital zircon cumulative density plots.

Plotting the same data as Figure 1.2. In purple, data are plotted as a step function (not accounting for analytical error). In blue, the data are plotted to account for uncertainty by summing up normal distributions, as in PDPs.

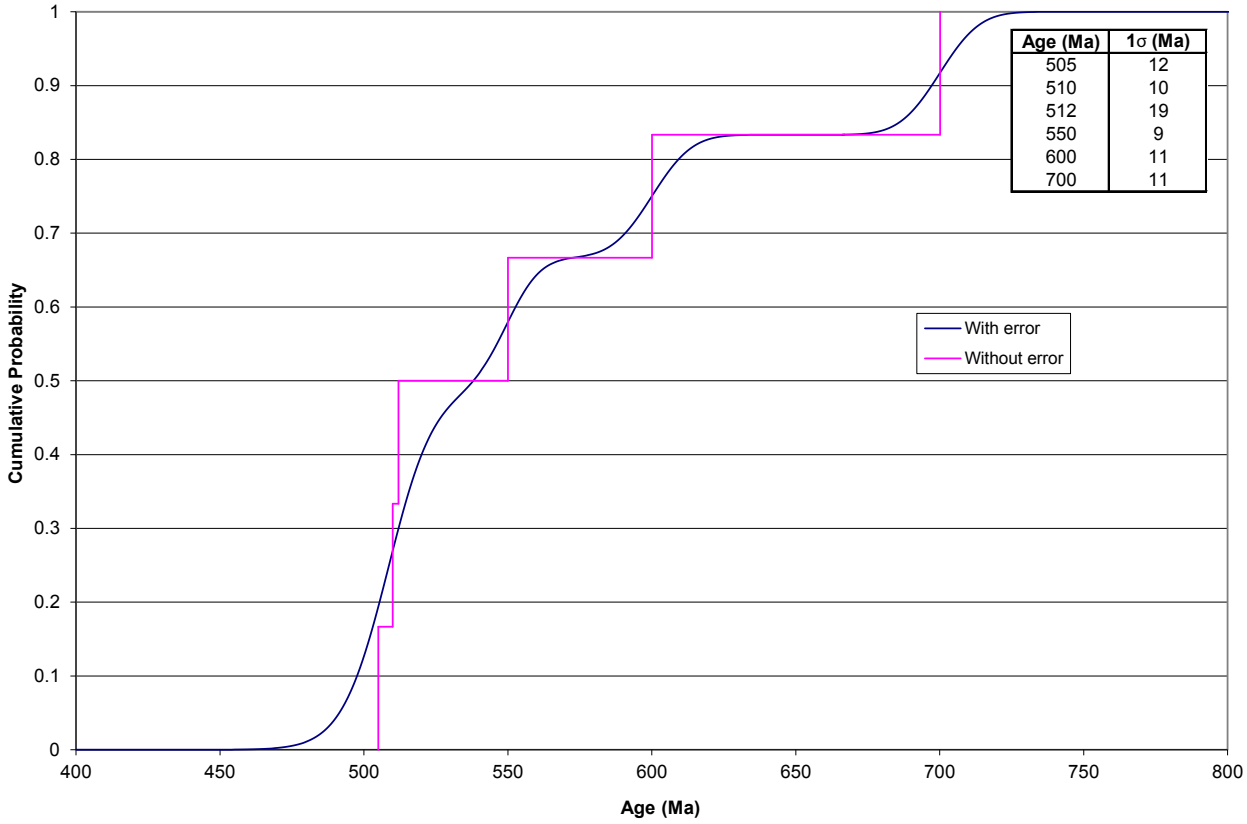

Figure 1.5: Detrital zircon kernel density plots.

Kernel density plots shown in blue, probability density plots in red, for the Burtts Corner Formation (Chapter 2).

A: Bandwidth of 12.2 Ma (mean of the analytical errors, 1σ). B: Adaptive kernel density (Vermeesch, 2012) with starting bandwidth of 12.2 Ma. C: Bandwidth of 24.4 Ma (mean of 2σ). D. Adaptive kernel density with starting bandwidth of 24.4 Ma.

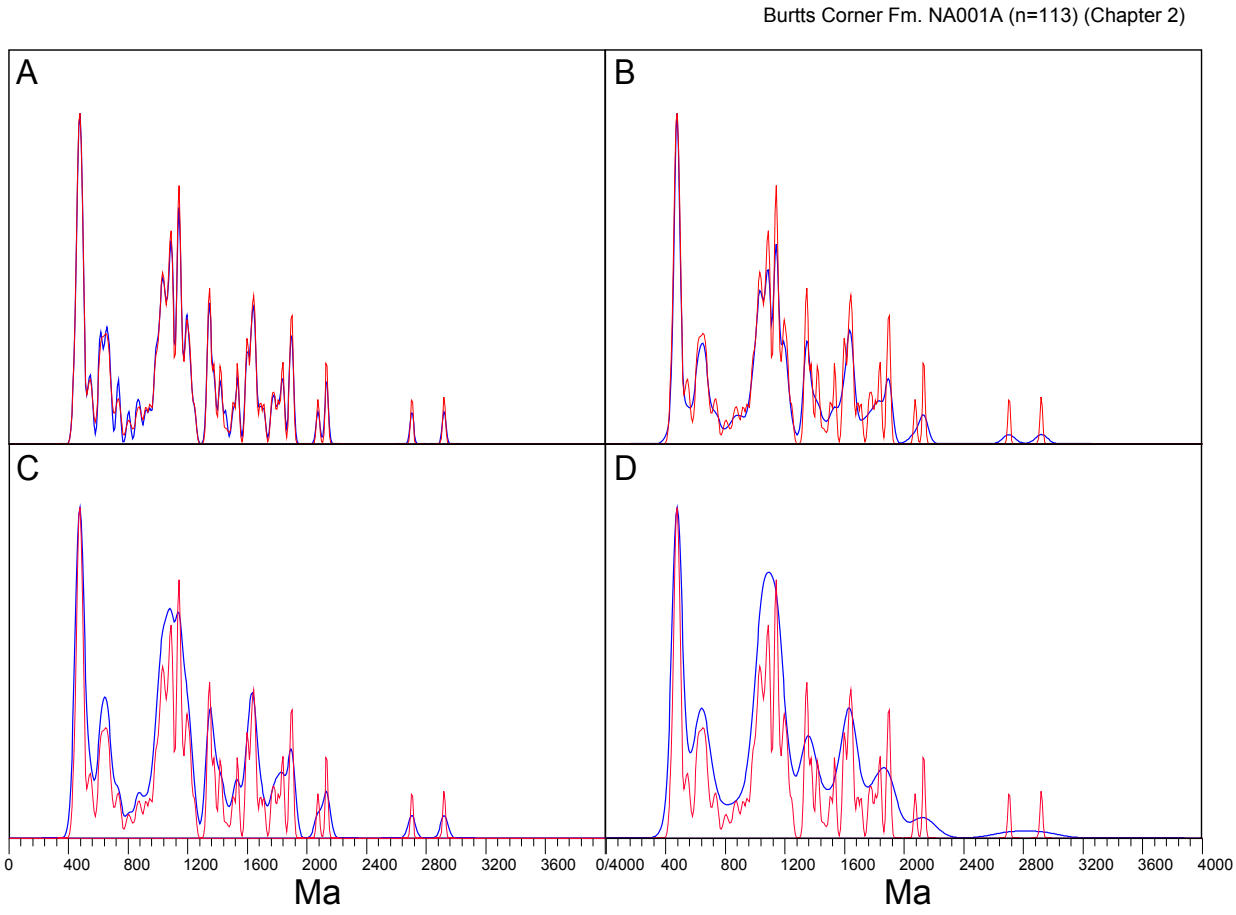

difference between two cumulative density curves. If this value D is greater than a critical value (dependent on the number of analyses), then the null hypothesis is rejected, and the two samples were probably not drawn from the same parent population. The significance of measured D values is expressed as P, or the probability that observed D values are a result of random sampling error. High P-values mean than two samples are probably not from different populations; low P-values indicate that they are probably from different populations. The value of P is also correlated to confidence level; so at a 95% level of confidence, the null hypothesis is rejected for P values of less than 0.05 (the compared samples probably did not come from the same population).

Concordia plots are also useful in studying detrital zircon distributions. The standard concordia diagram (Wetherill, 1956; Appendix A; Appendix B) plots $^{206}Pb/^{238}U$ on the y-axis, and $^{207}Pb/^{235}U$ on the x-axis; the concordia curve is drawn where these ratios correspond to the same age. These plots are not typically used for comparing provenance between different detrital zircon samples, but they are valuable tools in studying the causes of discordance within a sample, and can be used to calculate discordia lines, and help estimate the crystallization age of discordant zircon. A common alternative to the Wetherill diagram is the Tera-Wasserburg concordia (Tera and Wasserburg, 1972a, 1972b), plotting $^{207}Pb/^{206}Pb$ on the y-axis and $^{238}U/^{206}Pb$ on the x-axis. These diagrams are often preferred when dealing with young analyses, as they can show those discordia lines more clearly (Dickin, 2005).

Lastly, weighted means are frequently used within a sample to estimate the age of discrete populations (Schoene, 2014). For example, the youngest grains in a detrital sample may be averaged in this way to suggest the maximum depositional age. These figures are typically accompanied by measures of goodness of fit, such as the MSWD (mean square of weighted deviates, York, 1969). An MSWD > 1 indicates that the means are overscattered, compared to what would be expected given the assigned analytical uncertainties. An MSWD < 1 shows the scatter is less than what would be expected with the analytical uncertainties, and assigned errors

Figure 1.6: Detrital zircon Kolmogorov-Smirnov (K-S) tests.

A: Schematic graph showing the maximum difference (D-value) between two cumulative density functions.

B: Tables of P-values and D-values resulting from K-S analysis between four samples. Yellow cells in the first table highlight those tests which do not reject the null hypothesis at 95% confidence (P>0.05); they are probably not from different populations. Note that the test without error in the CDF is more stringent; red cells highlight comparisons that reject the null hypothesis here, but do not in the K-S test using error.

A

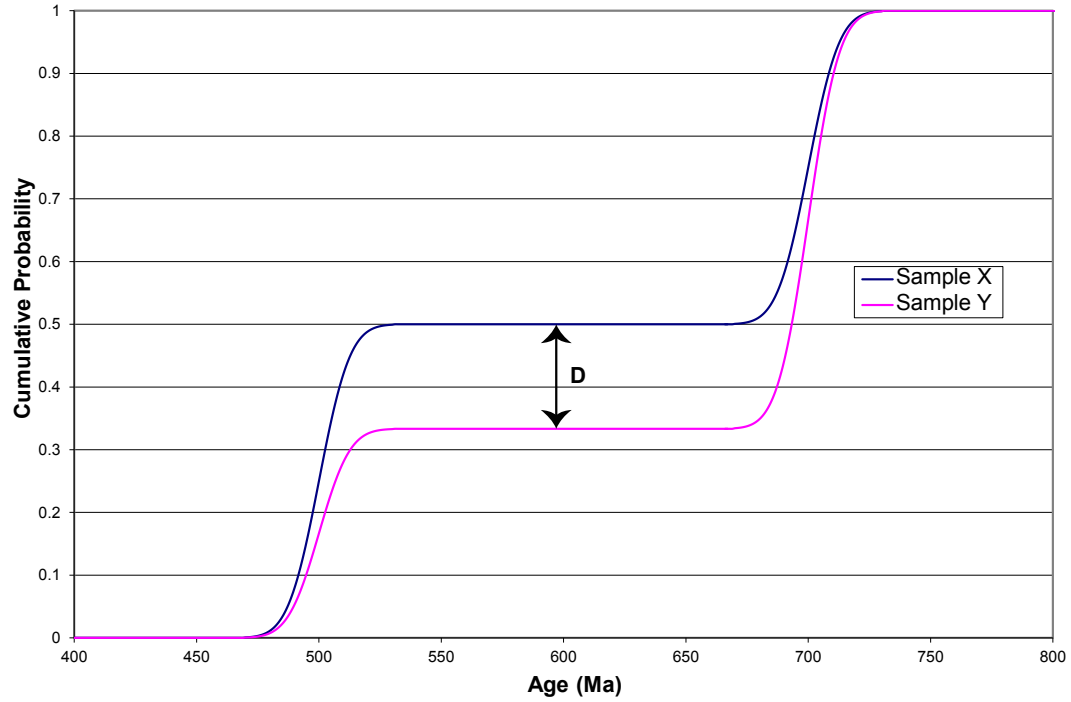

B

K-S P-values using error in the CDF

	Sample 1	Sample 2	Sample 3	Sample 4
Sample 1		**0.333**	**0.059**	0.000
Sample 2	**0.333**		**0.910**	0.000
Sample 3	**0.059**	**0.910**		0.000
Sample 4	0.000	0.000	0.000	

D-values using error in the CDF

	Sample 1	Sample 2	Sample 3	Sample 4
Sample 1		0.180	0.199	0.683
Sample 2	0.180		0.109	0.833
Sample 3	0.199	0.109		0.822
Sample 4	0.683	0.833	0.822	

K-S P-values for no error

	Sample 1	Sample 2	Sample 3	Sample 4
Sample 1		0.264	**0.043**	0.000
Sample 2	0.264		0.692	0.000
Sample 3	**0.043**	0.692		0.000
Sample 4	0.000	0.000	0.000	

D-values for no error

	Sample 1	Sample 2	Sample 3	Sample 4
Sample 1		0.191	0.208	0.694
Sample 2	0.191		0.138	0.833
Sample 3	0.208	0.138		0.822
Sample 4	0.694	0.833	0.822	

are over-estimated.

3. Organization

This thesis is presented in paper format, organized in a manner intended for future publication. Chapter 2 presents the results of our detrital zircon study in the Fredericton Trough, a version of which is being prepared for publication under the authorship Dokken, R.J., Waldron, J.W.F. and DuFrane, S.A., who provided information on the operating conditions of the instrumentation used for analyses. Chapter 3 presents our work from the Mascarene Basin, and will be prepared for publication under the same authorship. Chapter 4 summarizes our conclusions and suggests avenues for further research.

4. References

Bird, J.M., and Dewey, J.F., 1970, Lithosphere plate-continental margin tectonics and the evolution of the Appalachian orogen: Geological Society of America Bulletin, v. 81, n. 4, p. 1031-1059.

Bluck, B.J., Gibbons, W., and Ingham, J.K., 1992, Terranes, *in* Cope, J.C.W., Ingham, J.K. and Rawson, P.F., editors, Atlas of palaeogeography and lithofacies: United Kingdom, Geological Society of London, Memoirs, v. 13, p. 1-4.

Cawood, P.A., and Nemchin, A.A., 2001, Paleogeographic development of the East Laurentian margin: constraints from U-Pb dating of detrital zircons in the Newfoundland Appalachians: Geological Society of America Bulletin, v. 113, n. 9, p. 1234-1246.

Cawood, P.A., McCausland, P.J.A., and Dunning, G.R., 2001, Opening Iapetus: constraints from the Laurentian margin in Newfoundland: Geological Society of America Bulletin, v. 113, n. 4, p. 443-453.

Dana, J.D., 1873, On some results of the earth's contraction from cooling including a discussion

of the origin of mountains and the nature of the earth's interior: American Journal of Science, v. 5, n. 30, p. 423-443.

Dewey, J.F., 1969, Evolution of the Appalachian/Caledonian orogen: Nature, v. 222, n. 5189, p. 124-129.

Dewey, J.F., and Mange, M., 1999, Petrography of Ordovician and Silurian sediments in the western Irish Caledonides; tracers of a short-lived Ordovician continent-arc collision orogeny and the evolution of the Laurentian Appalachian-Caledonian margin: Geological Society of London, Special Publications, v. 164, p. 55-107.

Dickin, A.P., 2005, Radiogenic isotope geology: United Kingdom, Cambridge University Press, 492 p.

Eriksson, K., Campbell, I., Palin, J., and Allen, C., 2003, Predominance of Grenvillian magmatism recorded in detrital zircons from modern Appalachian rivers: The Journal of Geology, v. 111, n. 6, p. 707-717.

Gehrels, G., 2013, U-Pb geochronology and Hf isotope geochemistry applied to detrital minerals: Geological Society of America, Annual Meeting, Short Course 521, 216 p.

Gehrels, G., Valencia, V., and Pullen, A., 2006, Detrital zircon geochronology by laser-ablation multicollector ICPMS at the Arizona Laserchron Center, *in* Olszewski, T.D., editor, Geochronology: Emerging Opportunities: Paleontological Society Papers, v. 12, p. 67-76.

Guynn, J., and Gehrels, G., 2010, Comparison of detrital zircon age distributions using the K-S test: University of Arizona, Department of Geosciences, 16 p.

Hall, J., 1883, Contributions to the geological history of the American continent: American Association for the Advancement of Science, Proceedings, p. 29-69.

Harland, W.B., and Gayer, R.A., 1972, The Arctic Caledonides and earlier Oceans: Geological

Magazine, v. 109, n. 4, p. 289-314.

Hibbard, J.P., van Staal, C.R., Rankin, D.W., and Williams, H., 2006, Lithotectonic map of the Appalachian Orogen, Canada-United States of America: Geological Survey of Canada, Map 2096A, scale 1:1,500,000.

Hibbard, J.P., van Staal, C.R., and Rankin, D.W., 2007, A comparative analysis of pre-Silurian crustal building blocks of the northern and the southern Appalachian Orogen: American Journal of Science, v. 307, n. 1, p. 23-45.

Kay, M., 1951, North American geosynclines: Geological Society of America, Memoirs, v. 48, p. 1-132.

Li, Z.X., Bogdanova, S.V., Collins, A.S., Davidson, A., De Waele, B., Ernst, R.E., Fitzsimons, I.C.W., Fuck, R.A., Gladkochub, D.P., Jacobs, J., Karlstrom, K.E., Lu, S., Natapov, L.M., Pease, V., Pisarevsky, S.A., Thrane, K., and Vernikovsky, V., 2008, Assembly, configuration, and breakup history of Rodinia: a synthesis, *in* Bogdanova, S.V., Li, Z.X., Moores, E.M. and Pisaresvky, S.A., editors, Testing the Rodinia hypothesis: records in its building blocks: Precambrian Research, v. 160, n. 1-2, p. 179-210.

Ludwig, K.R., 2012, User's manual for Isoplot 3.75: Berkeley Geochronology Center Special Publication, 5, 75 p.

Macdonald, F.A., Ryan-Davis, J., Coish, R.A., Crowley, J.L., and Karabinos, P., 2014, A newly identified Gondwanan terrane in the northern Appalachian mountains: implications for the Taconic orogeny and closure of the Iapetus Ocean: Geology, v. 42, n. 6, p. 539-542.

McKerrow, W.S., Mac Niocaill, C., and Dewey, J.F., 2000, The Caledonian Orogeny redefined: Journal of the Geological Society of London, v. 157, n. 6, p. 1149-1154.

Moecher, D.P., and Samson, S.D., 2006, Differential zircon fertility of source terranes and natural bias in the detrital zircon record: Implications for sedimentary provenance analysis:

Earth and Planetary Science Letters, v. 247, n. 3–4, p. 252-266.

Pollock, J.C., Wilton, D.H.C., van Staal, C.R., and Morrissey, K.D., 2007, U-Pb detrital zircon geochronological constraints on the Early Silurian collision of Ganderia and Laurentia along the Dog Bay Line: the terminal Iapetan suture in the Newfoundland Appalachians: American Journal of Science, v. 307, n. 2, p. 399-433.

Reusch, D.N., and van Staal, C.R., 2012, The Dog Bay-Liberty Line and its significance for Silurian tectonics of the Northern Appalachian Orogen: Canadian Journal of Earth Sciences, v. 49, n. 1, p. 239-258.

Schoene, B., 2014, U–Th–Pb Geochronology, *in* Holland, H.D. and Turekian, K.K., editors, Treatise on Geochemistry (Second Edition): Oxford, Elsevier, p. 341-378.

Soper, N.J., Ryan, P.D., and Dewey, J.F., 1999, Age of the Grampian Orogeny in Scotland and Ireland: Journal of the Geological Society of London, v. 156, n. 6, p. 1231-1236.

Tera, F., and Wasserburg, G.J., 1972a, U-Th-Pb systematics in lunar highland samples from the Luna 20 and Apollo 16 missions: Earth and Planetary Science Letters, v. 17, n. 1, p. 36-51.

Tera, F., and Wasserburg, G.J., 1972b, U-Th-Pb systematics in three Apollo 14 basalts and the problem of initial Pb in lunar rocks: Earth and Planetary Science Letters, v. 14, n. 3, p. 281-304.

van Staal, C.R., Dewey, J.F., Mac Niocaill, C., and McKerrow, W.S., 1998, The Cambrian-Silurian tectonic evolution of the Northern Appalachians and British Caledonides: history of a complex, west and southwest Pacific-type segment of Iapetus, *in* Blundell, D.J. and Scott, A.C., editors, Lyell: the Past is the Key to the Present: Geological Society of London, Special Publications, v. 143, p. 199-242.

van Staal, C.R., Currie, K.L., Rowbotham, G., Rogers, N., and Goodfellow, W., 2008, Pressure-temperature paths and exhumation of Late Ordovician-Early Silurian blueschists and

associated metamorphic nappes of the Salinic Brunswick subduction complex, Northern Appalachians: Geological Society of America Bulletin, v. 120, n. 11-12, p. 1455-1477.

van Staal, C.R., Whalen, J.B., Valverde-Vaquero, P., Zagorevski, A., and Rogers, N., 2009, Pre-Carboniferous, episodic accretion-related, orogenesis along the Laurentian margin of the Northern Appalachians, *in* Murphy, J.B., Keppie, J.D. and Hynes, A.J., editors, Ancient orogens and modern analogues: Geological Society of London, Special Publications, v. 327, p. 271-316.

van Staal, C.R., Barr, S.M., and Murphy, J.B., 2012, Provenance and tectonic evolution of Ganderia: constraints on the evolution of the Iapetus and Rheic Oceans: Geology, v. 40, n. 11, p. 987-990.

Vermeesch, P., 2004, How many grains are needed for a provenance study?: Earth and Planetary Science Letters, v. 224, n. 3-4, p. 441-451.

Vermeesch, P., 2012, On the visualisation of detrital age distributions: Chemical Geology, v. 312-313, p. 190-194.

Waldron, J.W.F., Schofield, D.I., White, C.E., and Barr, S.M., 2011, Cambrian successions of the Meguma Terrane, Nova Scotia, and Harlech Dome, north Wales: dispersed fragments of a peri-Gondwanan basin?: Journal of the Geological Society of London, v. 168, n. 1, p. 83-98.

Waldron, J.W.F., McNicoll, V.J., and van Staal, C.R., 2012, Laurentia-derived detritus in the Badger Group of central Newfoundland: deposition during closing of the Iapetus Ocean: Canadian Journal of Earth Sciences, v. 49, n. 1, p. 207-221.

Waldron, J.W.F., Schofield, D.I., Dufrane, S.A., Floyd, J.D., Crowley, Q.G., Simonetti, A., Dokken, R.J., and Pothier, H.D., 2014a, Ganderia–Laurentia collision in the Caledonides of Great Britain and Ireland: Journal of the Geological Society of London, v. 171, n. 4, p. 555-569.

Waldron, J.W.F., Schofield, D.I., Murphy, J.B., and Thomas, C.W., 2014b, How was the Iapetus Ocean infected with subduction?: Geology, v. 42, n. 12, p. 1095-1098.

Wetherill, G.W., 1956, Discordant uranium-lead ages: Transaction of the American Geophysical Union, v. 37, p. 320-326.

Williams, H., 1979, Appalachian Orogen in Canada: Canadian Journal of Earth Sciences, v. 16, n. 3, p. 792-807.

Williams, H., 1995, Introduction, *in* Geology of the Appalachian-Caledonian Orogen in Canada and Greenland: Geological Survey of Canada, Geology of Canada, v. 6, p. 3-19.

Williams, H., and Hatcher, R.D., Jr., 1982, Suspect terranes and accretionary history of the Appalachian Orogen: Geology, v. 10, n. 10, p. 530-536.

Williams, H., and Hatcher, R.D., Jr., 1983, Appalachian suspect terranes, *in* Hatcher, R.D., Jr., Williams, H. and Zietz, I., editors, Contributions to the tectonics and geophysics of mountain chains: Geological Society of America, Memoirs, v. 158, p. 33-53.

Williams, H., and Hiscott, R.N., 1987, Definition of the Iapetus rift-drift transition in western Newfoundland: Geology, v. 15, n. 11, p. 1044-1047.

Wilson, J.T., 1966, Did the Atlantic close and then re-open?: Nature, v. 211, n. 5050, p. 676-681.

Woodcock, N.H., and Soper, N.J., 2006, The Acadian Orogeny: the Mid-Devonian phase of deformation that formed slate belts in England and Wales, *in* Brenchley, P.J. and Rawson, P.F., editors, The geology of England and Wales: p. 131-146.

York, D., 1969, Least squares fitting of a straight line with correlated errors: Earth and Planetary Science Letters, v. 5, n. 5, p. 320-324.

Chapter 2: Detrital zircon geochronology of the Fredericton Trough: Constraints on the Silurian closure of remnant Iapetus Ocean

The Fredericton Trough in the Appalachians of southwestern New Brunswick is filled by the Silurian Kingsclear Group, consisting mainly of turbidites, deposited during convergence of Laurentia with components of the peri-Gondwanan domain Ganderia. Its tectonic setting has been interpreted as a successor basin, trench, foredeep or foreland basin. We present new detrital zircon U-Pb data from four formations of the Kingsclear Group, collected north and south of the Fredericton Fault, which bisects the trough. South of the Fredericton Fault, detrital zircon ages from an early Silurian (Llandovery) unit show a late Neoproterozoic peak, typical of peri-Gondwanan provenance. Detrital zircons from a younger Silurian unit (Wenlock - Ludlow, intruded by the Pocomoonshine pluton, 422.7 ± 3 Ma) display a distinctive asymmetric peak at ~1.0 Ga with a tail of older Proterozoic zircons, suggesting Laurentian provenance. North of the Fredericton Fault, a Llandovery sample also shows a signature consistent with Laurentian sources. In a mid-Silurian (Wenlock) unit zircon peaks indicate mixed Laurentian and peri-Gondwanan sources, consistent with exhumation of the Miramichi terrane to the north. The absence of Laurentian material in Llandovery strata south of the fault, contrasted with a strong Laurentian signature in rocks to the north, suggests that a remnant of the Iapetus Ocean, in which turbidites of the Kingsclear Group were deposited, persisted until at least the mid-Silurian. The timing of its closure is constrained by the arrival of Laurentian detritus south of the Fredericton Fault before 422.7 ± 3 Ma, and probably by the mid-Wenlock.

1. Introduction

The Appalachians of eastern Canada record a complex history of orogenesis, resulting from the convergence of Gondwanan elements with Laurentia during the closure of the Iapetus

Ocean. Previous work has divided the orogen into distinct lithotectonic domains based on their Laurentian or Gondwanan origin (Figure 2.1; Williams, 1979; Hibbard and others, 2006; Hibbard and others, 2007). Ganderia (van Staal and others, 1998; Hibbard and others, 2006, 2007; Pollock and others, 2012) is a peri-Gondwanan microcontinental domain underlying much of New Brunswick, which probably rifted from the margin of Amazonia (van Staal and others, 1996, 1998) in the mid-Cambrian (van Staal and others, 2012), and underwent a complex history of arc formation and rifting before and during its accretion to Laurentia (van Staal and others, 2009). Avalonia (Kerr and others, 1995; Landing 1996; O'Brien and others, 1996; van Staal and others, 1998; Hibbard and others, 2007; Pollock and others, 2012), a peri-Gondwanan domain represented by the Caledonia terrane in southeastern New Brunswick, probably separated from West Africa or Amazonia (van Staal and others, 1996; McNamara and others, 2001; Murphy and others, 2002) in the Early Ordovician (Prigmore and others, 1997; van Staal and others, 1998; Murphy and others, 2004b) and was accreted to the southern margin of Ganderia. Multiple positions (and timings) have been proposed for sutures associated with Iapetus Ocean closure between Laurentia and Ganderia (e.g. McKerrow and Ziegler 1971; McKerrow, 1982; Bluck and others, 1992; van Staal and others, 1998).

Detrital zircon geochronology has been widely applied in the Appalachian-Caledonide orogen to constrain the timing of terrane juxtaposition resulting from plate convergence (e.g. Phillips and others, 2003; Waldron and others, 2008, 2012; Waldron and others, 2014a; Pothier and others, 2015). Accretion at a convergent plate boundary is typically accompanied by an influx of sediment from the upper plate onto the lower plate. Therefore, in convergent tectonic settings, analyzing the provenance of selected sediments can constrain the timing of terrane juxtaposition. In this paper, we use detrital zircon geochronology to provide new evidence for the timing of amalgamation between Laurentia and peri-Gondwanan terranes in New Brunswick during early Paleozoic orogenesis.

Figure 2.1. Lithotectonic divisions of the Appalachian-Caledonide orogen.
Pangean (pre-Mesozoic) reconstruction after Waldron and others (2014b) and references therein. Box encloses Figure 2.2. Lithotectonic divisions after van Staal and others (1998) and Hibbard and others (2006, 2007).

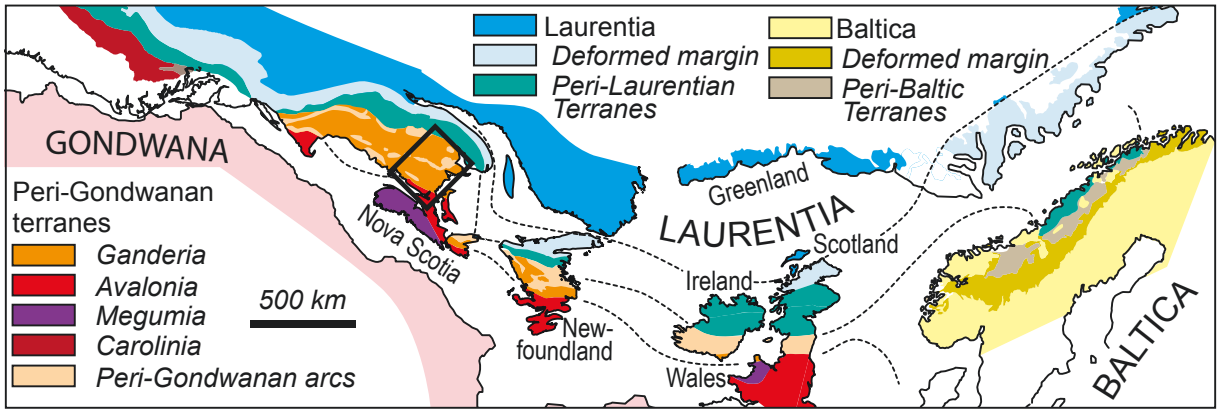

2. Geologic setting

2.1 Tectonic overview

Laurentia, the ancestral core of present-day North America, developed into an independent continent during the late Neoproterozoic Era following the break-up of Rodinia (Li and others, 2008). The Iapetus Ocean opened between Laurentia, Baltica, and Amazonia by ca. 570-550 Ma, leading to the development of a passive margin along the Laurentian boundary of Iapetus prior to the oldest drift sediments deposited at ca. 520-515 Ma (Williams and Hiscott, 1987; Cawood and others, 2001; timescale of Peng and others, 2012). The microcontinental domain Ganderia separated from Gondwana by about 505 Ma (White and others, 1994; Schulz and others, 2008; van Staal and others, 2009, 2012), though the mechanism of separation is uncertain; van Staal and others (2012) propose back-arc basin opening, potentially resulting from slab roll-back (van Staal and others, 2009), whereas Waldron and others (2014b) propose more oblique separation. Components of Ganderia (see below) collided with Laurentia beginning in the Early Ordovician in New England (Macdonald and others, 2014), or Late Ordovician in Newfoundland (van Staal and others, 2009), interpreted to result in the final phases of Taconic orogenesis (van Staal and others, 2009). Subsequent accretion of Ganderian material during the Silurian has been interpreted as the cause of Salinic orogenesis (van Staal and others, 2008, 2009), defined by a widespread Late Silurian unconformity in the Newfoundland Appalachians (Dunning and others, 1990), and extending to include multiple diachronous unconformities in New Brunswick (van Staal and de Roo 1995; Fyffe and others, 2011; Wilson and others, 2015). Avalonia separated from Gondwana by the Early Ordovician (Nance and others, 2002) and is interpreted to have collided with Laurentia during late Silurian to mid-Devonian Acadian orogenesis (van Staal and others, 2009).

In New Brunswick, Ganderia is represented by several terranes (Figure 2.2; Fyffe and others, 2011). North of the Fredericton Trough these include the Popelogan and Miramichi terranes (Figure 2.2). The Popelogan terrane (van Staal and others, 2016) is correlated with the

Figure 2.2. New Brunswick terranes and cover successions.

Map units after Smith (2005) and Smith and Fyffe (2006); see also Fyffe and others (2011). Locations of samples reported in this paper are shown. A: Digdeguash Formation. B: Flume Ridge Formation. C: Hayes Brook Formation. D: Burtts Corner Formation.

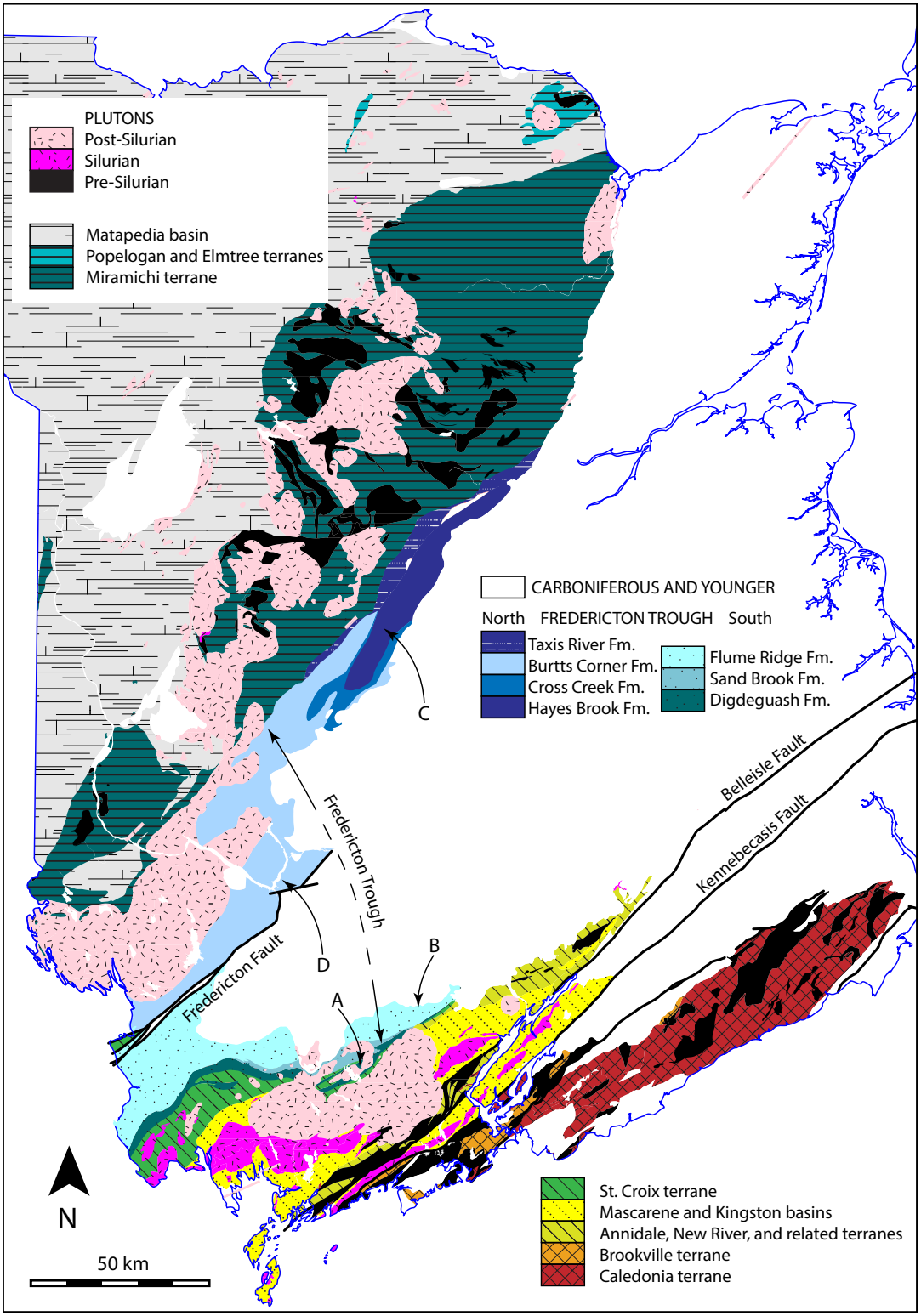

Victoria Arc of Newfoundland (van Staal and others, 1998) and the Bronson Hill Arc in New England, and is characterized by Late Ordovician chert and shale overlying Middle Ordovician mafic lapilli tuff and volcanics (Wilson, 2000, 2003). It is interpreted to have been accreted to Laurentia during the Late Ordovician (van Staal and others, 2009). The Elmtree terrane (Fyffe and others, 2011) represents an ensimatic basin to the southeast (present coordinates). Volcanic and sedimentary rocks of the Miramichi terrane characterize the Brunswick subduction complex (van Staal, 1994; van Staal and others, 2008), recording the accretion of Ganderian microcontinental material, accompanied by deformation and high-pressure/low-temperature metamorphism (van Staal and others, 2008), to Laurentia from the Late Ordovician to early Silurian.

The Annidale terrane includes rocks similar to the Miramichi terrane (Johnson and others, 2009; Fyffe and others, 2011; Johnson and others, 2012), but located south of the Fredericton Trough. Along strike to the southwest, the St. Croix terrane is characterized by the Cambrian to Upper Ordovician Cookson Group, comprising quartzose and lithic sandstone, shale, and minor pillow basalt (Ludman, 1987; Fyffe and Riva, 1990; Ludman, 1991), interpreted by Fyffe and others (2011) to have been deposited on a Ganderian passive margin. The Ganderian basement of these rocks may be represented (Fyffe and others, 2011) by the New River terrane (Johnson and McLeod, 1996), immediately south (Figure 2.2), consisting of several fault-bounded slices. These include Neoproterozoic to Cambrian arc and rift-related volcanics, with marine and volcanic sedimentary rocks (Johnson and others, 2009; Fyffe and others 2011).

The Fredericton Trough obscures the contact between the Miramichi terrane to the north and the St. Croix terrane to the south (Figure 2.2); it is filled by the Silurian Kingsclear Group, consisting mainly of turbiditic sandstone, siltstone, and shale, which sit disconformably upon the Cookson Group of the St. Croix terrane along the southern boundary of the trough (Fyffe and others, 2011). The trough is divided by the northeast-striking Fredericton Fault (Park and Whitehead, 2003). To the north of the fault, the Kingsclear Group is in contact with rocks of

the Miramichi terrane along the Bamford Brook - Hainesville Fault; its basement is locally unexposed. The trough was interpreted as the floor of the "Proto-Atlantic" or Iapetus Ocean by McKerrow and Ziegler (1971; see also McKerrow, 1982) but reinterpreted by Williams (1979) as a successor basin, isolated from the Iapetus Ocean. More recent interpretations have suggested it is a marine foredeep or foreland basin (van Staal and others, 1990; van Staal and de Roo, 1995; van Staal and others 1998) formed by tectonic loading of the Brunswick subduction complex upon the subducting Ganderian margin during Salinic orogenesis (Fyffe and others, 2011). The clastic sedimentary fill of the Fredericton Trough contrasts dramatically with Silurian volcanic successions that characterize the Mascarene Basin and the Kingston belt farther south in New Brunswick.

To the south of all these Silurian basins, the Brookville terrane (Figure 2.2) includes Meso-Neoproterozoic marble, quartzite, and siltstone; Neoproterozoic orthogneiss and paragneiss; Ediacaran rhyolite flows and tuffs; and various Neoproterozoic to early Cambrian plutonic rocks overlain by early Cambrian sandstones (White and Barr, 1996; Fyffe and others, 2011). Previous work (Barr and White, 1996; Barr and others, 2003) has demonstrated similarities with the New River terrane (Johnson and McLeod, 1996), allowing it to be assigned to Ganderia (Fyffe and others, 2009, 2011), though some previous workers (e.g. Williams, 1979) assigned the Brookville Terrane to Avalonia.

The Caledonia terrane (Figure 2.2) includes Ediacaran tuff and tuffaceous sedimentary rock, and comagmatic plutons (Fyffe and others, 2011). Their facies and geochemistry are consistent with Avalonia elsewhere in the northern Appalachians (Barr and White 1996; Barr and others, 2003). Overlying this basement is a Cambrian to Early Ordovician platformal sedimentary succession (Saint John Group), also characteristic of Avalonia (White and Barr, 1996; Fyffe and others, 2011).

Interpretations of the Ganderian domain variously regard it as a coherent microcontinent or a domain of many distinct slivers of lithosphere (Waldron and others, 2014a, 2014b; Pothier

and others, 2015). While the timing of accretion of the Popelogan and Miramichi terranes of Ganderia to the Laurentian margin has been relatively well constrained (e.g. van Staal, 1994; van Staal and others, 1998, 2008, 2016), the accretion of southern Ganderian components, particularly the St. Croix terrane (and its assumed New River basement) is less well known. Central to these issues is the timing of closure of the Iapetus Ocean. In the earliest tectonic models (e.g. McKerrow and Ziegler, 1971; McKerrow, 1982) the Fredericton Trough was regarded as marking a Silurian Iapetus suture correlative with that identified in the British Isles (Phillips and others, 1976; Leggett and others, 1983; Bluck and others, 1992). However Williams (1979) interpreted Iapetus closure in the Appalachians as Middle Ordovician; Late Ordovician and Silurian rocks including the Fredericton Trough were regarded as successor basins deposited across the accreted terranes. Later work (e.g. van Staal and others, 1998) in New Brunswick demonstrated the peri-Gondwanan affinities of the Popelogan and Miramichi terranes, suggesting that the Iapetus Ocean closed in the Late Ordovician with the accretion of the Ganderian Popelogan-Victoria arc to Laurentia along the Red Indian Line (Figure 2.1; van Staal and others, 1998). However, prior to this collision, Early Ordovician separation of this arc from the remainder of Ganderia had opened a wide Tetagouche-Exploits backarc basin (van Staal and others, 2009, 2012); this basin closed over the Late Ordovician to mid-Silurian (van Staal and others, 2009; Reusch and van Staal, 2012), ending with the accretion of the trailing Gander margin (including the St. Croix terrane and other southern components – *sensu* Reusch and van Staal, 2012), in the terminal event of Salinic orogenesis. In this model, the Fredericton Trough is interpreted as a marine foredeep basin built upon a Ganderian microcontinent and filled during the closure of the Tetagouche-Exploits backarc basin.

In the remainder of this paper we examine the provenance of sedimentary rocks in the Fredericton Trough to determine when a sedimentary connection was established across the trough and to shed light on the separation and collision of Ganderian fragments as remnants of the Iapetus Ocean closed.

2.2 Stratigraphy

The Fredericton Trough (Figure 2.2) is filled by the Silurian Kingsclear Group (Figure 2.3). At its southern margin, it sits unconformably upon rocks of the Late Ordovician Kendall Mountain Formation, belonging to the Cookson Group of the St. Croix terrane. The Kendall Mountain Formation bears Sandbian (ca. 455-453 Ma: timescale of Cooper and Sadler, 2012) graptolites of the *Climacograptus wilsoni* zone (Fyffe and Riva, 1990). To the north, the Fredericton Trough is in contact with rocks of the Miramichi terrane, separated from them by the Bamford Brook - Hainesville fault. The Fredericton Trough itself is divided by the Fredericton Fault, correlated with a segment of the Norumbega Fault Zone in Maine, which comprises an extensive system displaying up to 135 km of dextral offset beginning at ca. 380 Ma (Ludman and West, 1999; Ludman and others, 1999).

To the south of the fault, the Kingsclear Group includes the Digdeguash Formation, comprising medium-grained lithic and feldspathic wacke, quartz wacke, granule conglomerate, and grey to black shale, with commonly well-graded beds exhibiting Bouma sequences (Ruitenberg and Ludman, 1978). Fyffe and Riva (2001) recovered graptolites of the *Coronograptus cyphus* zone of the upper Rhuddanian stage (early Llandovery, ca. 441.6 to 440.8 Ma: Melchin and others, 2012).

The Sand Brook Formation conformably overlies the Digdeguash Formation, and pinches out to the west. It consists of greenish feldspathic wacke interlayered with green siltstone and mudstone (Fyffe, 1991). The age of the Sand Brook Formation is constrained as late Rhuddanian to Pridoli by its stratigraphic location above the Digdeguash and below the Flume Ridge Formation.

The youngest unit south of the fault, the Flume Ridge Formation, sits with apparent conformity upon both older units. It includes greyish-green calcareous and argillaceous sandstone, siltstone, and shale (Ruitenberg and Ludman, 1978). The Pocomoonshine pluton intrudes the Flume Ridge Formation in Maine, and has been dated by West and others (1992) at 422.7 ± 3 Ma, near the

Figure 2.3. Simplified stratigraphic chart for the Kingsclear Group.
Timescale from Cooper and Sadler (2012) and Melchin and others (2012); Pocomoonshine pluton age from West and others (1992).

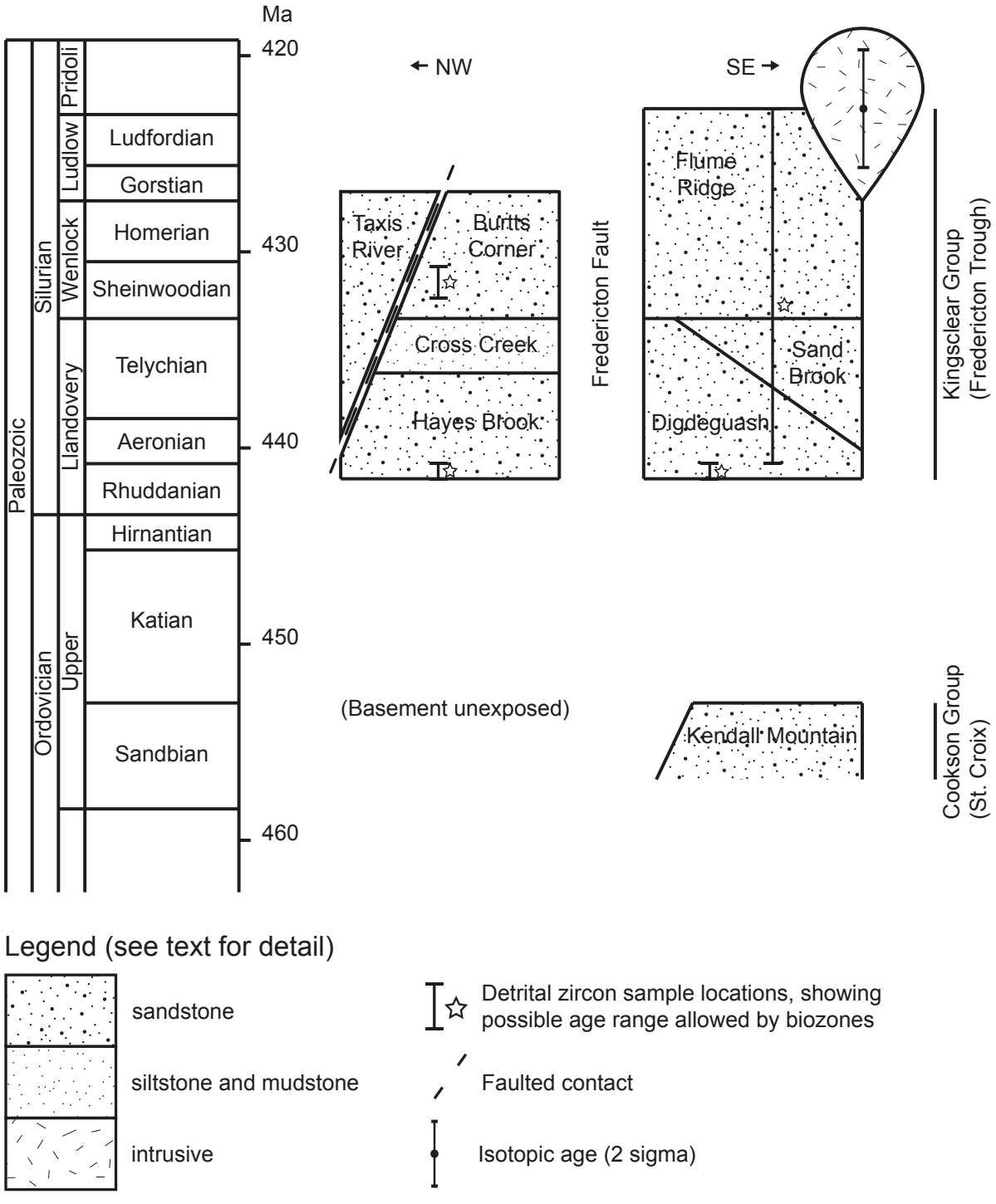

Ludlow-Pridoli boundary (Melchin and others, 2012).

North of the Fredericton Fault, the lowest unit in the Kingsclear Group is the Hayes Brook Formation, medium to thickly bedded greyish quartz wacke interlayered with thin grey-black shale (Poole, 1963). Its depositional age is constrained by upper Rhuddanian graptolites of the *Coronograptus cyphus* zone (formerly *Monograptus cyphus*; Cumming, 1960; Fyffe, 1995; Zalasiewicz and others, 2003), identical in age to those from the Digdeguash Formation to the south.

The Hayes Brook Formation is conformably overlain by green siltstone and shale of the Cross Creek Formation (Poole, 1963). Its depositional age is constrained by its stratigraphic position between the Hayes Brook and the conformably overlying Burtts Corner Formation.

The Burtts Corner Formation includes gray lithic wacke interlayed with dark grey siltstone and shale. Beds are well-graded with Bouma sequences, and show flute casts, climbing ripples, and soft-sediment deformation structures such as flames and convolute bedding (Fyffe, 1995; Park and Whitehead, 2003). Mid-Wenlock (ca. 432.4 to 430.5 Ma: timescale of Melchin and others, 2012) to early Ludlow (ca. 427.4 to 426.9 Ma) graptolites (*Cyrtograptus linnarssoni* and *M. nilssoni* zones, now respectively the *Cyrtograptus rigidus* and *Neodiversograptus nilssoni* zones; Zalasiewicz and others, 2009) have been recovered from the Burtts Corner Formation (Fyffe, 1995).

The Taxis River Formation, comprising grey lithic wacke and shale, was previously interpreted (Poole, 1963) to rest conformably upon the Burtts Corner Formation, but recent mapping (Smith and Fyffe, 2006 and references therein) suggests faulted contacts with bounding formations; its depositional age has not been determined, and it is not further considered here.

2.3 Structure

The northeast-trending belt of rocks comprising the Fredericton Trough shows multiple stages

of deformation (e.g. Smith, 2005; Smith and Fyffe, 2006), and only a few studies (e.g. Park and Whitehead, 2003) have examined their structural characteristics in detail. Structural characteristics of individual formations at their sampled locations are described later in this paper (see also Fyffe, 1995; Fyffe and others, 2001 and references therein). Rocks of the Fredericton Trough are interpreted by Park and Whitehead (2003) to record southeast-vergent Silurian thrusting and folding, documenting Salinic orogenesis, in which a low-angle, northwest-dipping thrust, a precursor to the Fredericton Fault, divided adjacent slices of the Kingsclear Group. Later dextral transpressive deformation may have resulted either in the steepening of this thrust (Park and Whitehead, 2003), or may have produced a new structure which reactivated or cut it. Ludman and others (1999) have documented an extensive history of activity on the correlative Norumbega Fault Zone to the southwest; the earliest dateable activity of this system is at ca. 380 Ma, and at present it has been interpreted to display up to 135 km of dextral offset. Additional work in correlating the New Brunswick Fredericton Trough with equivalents in Maine is in part hindered by an increasing Acadian metamorphic overprint (Ludman and others, 1999) to the southwest, and a paucity of fossils to provide depositional age constraint (Ludman and others, 1993).

3. Detrital zircon geochronology

3.1 Methods

Detrital zircon geochronology has been successfully applied in the Appalachian-Caledonide orogen to determining provenance and correlating terranes (Cawood and Nemchin, 2001; Cawood and others, 2003, 2004; Murphy and others, 2004b; Waldron and others, 2012; Macdonald and others, 2014; Waldron and others, 2014a). Previous work (e.g. Cawood and Nemchin, 2001; Waldron and others, 2014a) has demonstrated that Laurentian provenance is marked by an asymmetric peak at 1.0 to 1.1 Ga, with a tail of zircons typically extending to ca. 2.0 Ga, and a scarcity of zircons in the 2.0 to 2.4 Ga range. The population at 1.0 to 1.1

Ga is attributed to the Grenville orogen, which dominates the provenance of the Laurentian margin (Cawood and Nemchin, 2001; Waldron and others, 2014a). Peri-Gondwanan zircon signatures lack this distinctive asymmetric peak, and are distinguished by one or more large late Neoproterozoic populations, in the 550 to 650 Ma range. Within this range, peri-Gondwanan terranes of Avalonia and Ganderia may be distinguished by slightly older or younger peaks respectively (Murphy and others, 2004a; Fyffe and others, 2009; Pollock and others, 2009). Additionally, peri-Gondwanan detritus is frequently distinguished by zircon peaks from 2.0 – 2.2 Ga, often interpreted as representing derivation from the Eburnian or Trans-Amazonian orogens of West Africa or Amazonia respectively (Pollock and others, 2007; Waldron and others, 2009, 2011, 2014a). These distinguishing characteristics enable the differentiation between sources in Laurentia and the Ganderian terranes which converged with it during Salinic orogenesis (Waldron and others, 2014a). By examining the fill of the Fredericton Trough for these distinctive detrital zircon signatures, we can determine when southern components of Ganderia were juxtaposed with Laurentia, and investigate whether they were separated by a seaway, a possible remnant of the Iapetus Ocean.

Four samples from the Kingsclear Group were chosen, where possible, from known fossil localities to constrain depositional age. Samples of ~10 kg mass were selected from the coarser-grained sandstones representative of each formation, while avoiding any obvious weathering, alteration, or mineralization. These were disaggregated by crushing and milling, and dense minerals concentrated using a Wilfley table. The heavy mineral concentrate was sieved with a standard 70 size nylon mesh (approx. 210 μm) to remove remnant aggregate particles, and further processed with Frantz Isodynamic and Barrier separators (e.g. Rosenblum and Brownfield, 2000) to remove magnetic minerals. A final zircon concentrate was obtained by gravity separation with methylene iodide (specific gravity of 3.32). Obvious non-zircons (e.g. pyrite) were removed and the remaining portion then mounted in epoxy for LA-MC-ICP-MS U-Pb analysis. Zircons were not selected individually for analysis, to avoid bias towards easily recognizable zircon morphologies. Each zircon mount was polished to expose sections through

the grains, and imaged to reveal internal structure (zonation, inherited cores, altered rims, etc.) by backscattered electron and cathodoluminescence imaging utilizing a Zeiss EVO scanning electron microscope.

132 to 152 grains from each sample were analyzed at the Canadian Centre for Isotopic Microanalysis (CCIM) at the University of Alberta, using procedures modified from Simonetti and others (2005) for measuring U-Pb isotopic ratios by LA-MC-ICP-MS. Each zircon is typically represented by a single spot analysis, as restricted by physical grain size. When discrete cores and rims of different age can be distinguished, they are represented by separate analyses (ex. 001A and 001B within grain 001). Instrumentation consisted of a New Wave UP-213 laser ablation system interfaced with a Nu Plasma MC-ICP-MS, with three ion counters to measure Pb isotopes and twelve Faraday buckets measuring ^{238}U, ^{235}U, ^{205}Tl and ^{203}Tl. The laser was operated with a beam diameter of 30 microns, 4 Hz pulse frequency and fluence of ~3 J/cm^2. A He atmosphere was maintained in the ablation cell at a flow rate of 1 L/min. Output from this cell was combined with that from a standard Nu Instruments desolvating nebulizer (DSN). Unknowns from each sample were analyzed in groups of 10, with data collected statically in thirty 1 s integrations. Separating each set of analyses, on peak gas + acid blanks were measured over a duration of 30 s, and two zircon reference materials were analyzed to monitor U-Pb fractionation, reproducibility, and instrumental drift: LH94-15 (1830 ± 1 Ma; Ashton and others, 1999; Simonetti and others, 2005; Heaman, unpublished data) and GJ1-32 (606 Ma; Jackson and others, 2004; Elhlou and others, 2006; Heaman, unpublished data). Mass bias for Pb isotopes was corrected for by concurrently measuring $^{205}Tl/^{203}Tl$ from an aspirated 0.5 ppb Tl solution (NIST SRM 997), utilizing an exponential mass fractionation law and assuming a natural $^{205}Tl/^{203}Tl$ of 2.3871. Data were reduced using an offline Excel-based spreadsheet, in which sample (unknown) isotopic ratios were corrected based on standard analyses, using a cutoff value of $^{207}Pb/^{206}Pb$ = 0.0658 (800 Ma): young grains were normalized to GJ1-32, and old grains to LH94-15. This method of normalization allows unknowns to be corrected based on standards of a similar age; natural gaps in our data typically occur at 800 Ma, making this a convenient cutoff. Uncertainties

were reported using a quadratic combination of the standard error of the measured isotopic ratio, and the standard deviation of the standard means. Reproducibility of the zircon standards is estimated at ~1% ($^{207}Pb/^{206}Pb$) and 2% ($^{206}Pb/^{238}U$) (2σ). Sample measurements were discarded in the case of obvious inclusions that contributed to analysis (and could not be isolated), an extreme common Pb component, or analysis of non-zircons. Common Pb corrections after Simonetti and others (2005) were typically applied when measured ^{204}Pb exceeded ~400 cps. The software Isoplot (version 3.75: Ludwig, 2012) was employed to produce relative probability density plots for zircons 90% concordant or better. Concordia diagrams, weighted means, MSWD calculations, and other statistical analyses were prepared with the same software. Cumulative probability plots and Kolmogorov-Smirnov tests were calculated using analysis tools from the Arizona LaserChron Center (Gehrels and others, 2006).

3.2 Sampled units

Lithological observations (and classification after Dott, 1964) from each of the four sampled formations bear broadly similar characteristics (see below), and are consistent with their interpretation as polydeformed, turbiditic material deposited in a narrowing seaway. Zircon grains from each of the four formations also share similar characteristics (Figure 2.4). They vary from rounded to angular, with older zircons more frequently showing rounded shapes, and young zircons with the most angular shapes. Common textures include oscillatory zoning (with or without inherited cores), overgrowths, and various textures related to metasomatism, metamictization, or recrystallization.

3.2.1 Digdeguash Formation

The Digdeguash Formation was examined in the Digdeguash river where outcrops exhibit three generations of structures. The earliest fabric is a bedding-parallel S1 cleavage. F1 folds are not observed at outcrop scale. F2 folds gently plunge eastward and exhibit parasitic folding, and are refolded by F3 folds. These latest folds are open, with axial traces trending NNE-SSW.

Figure 2.4. CL (cathodoluminescent) images of selected zircons from four formations of the Fredericton Trough.

Circles show location of 30 micron laser ablation pits.

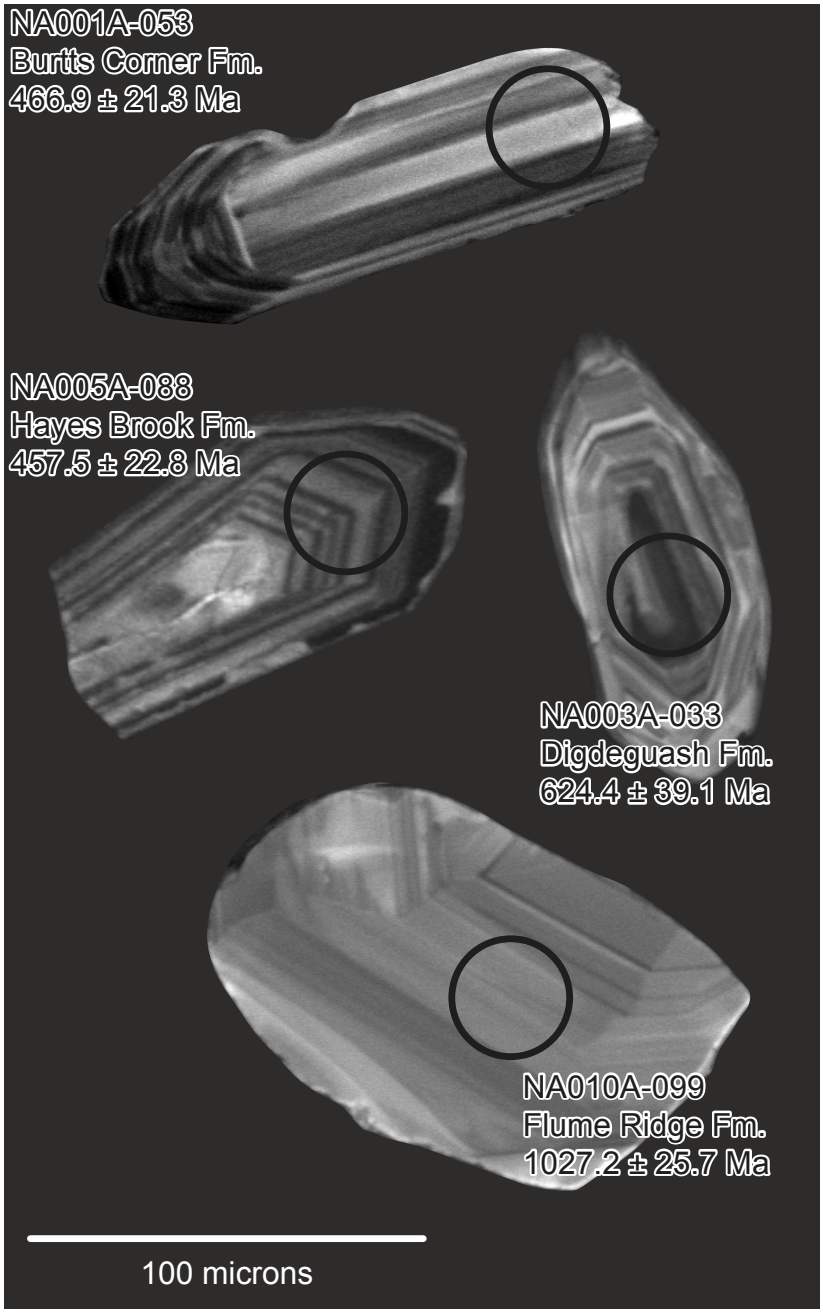

Because of the lack of fossils in the type section, the Digdeguash Formation was sampled at a known fossil locality (Upper Rhuddanian *Coronograptus cyphus* zone; Fyffe and Riva, 2001) southwest of Otter Lake (Figure 2.2). Thin section analysis (Figure 2.5) indicates the rock is a feldspathic wacke, with a relatively high amount of matrix (42%). Framework grains consist of quartz (52%, normalized to total QFL components; subgrain boundaries and polycrystalline quartz are particularly common) with a large amount of feldspar (42%, about two-thirds of which is alkali feldspar) and some lithic fragments (6%). Accessory phases include mainly biotite and opaque minerals. Framework grains are mainly subangular, and frequently show evidence of strain. Biotite comprises most of the matrix, along with a small amount of quartz and feldspar, and uncommon heavy minerals and opaques. A persistent foliation is present, approximately 60° to bedding, and is defined mainly by biotite, and to a lesser extent lath-shaped feldspars.

3.2.2 Flume Ridge Formation

The Flume Ridge Formation contains multiple generations of mapped folds (e.g. Smith, 2005), though these structures are frequently obscured in outcrop by abundant brittle fractures. The sampled section (Figure 2.2) is largely overturned, alternating with shorter intervals of upright beds, but the corresponding outcrop-scale fold closures themselves were not observed. Discrete, highly sheared intervals typically divide upright from overturned sections, and contain small folds, rare axial planar cleavage, and small duplexes (< 20 cm width).

The sampled rock (Figure 2.5) is a feldspathic wacke, including 60% matrix. Normalized QFL proportions are quartz (73%), feldspar (15%, mainly alkali feldspar) and lithic fragments (12%). Detrital accessory minerals include mainly muscovite, and smaller amounts of calcite, chlorite, opaques, and rare mafic minerals such as pyroxene. The matrix is composed mainly of calcite, muscovite, quartz and feldspar, with less common chlorite, opaques, and heavy minerals. Alteration is common, particularly of the matrix, and products include sericite, iron carbonate, and other iron-rich phases. A prominent foliation is defined by mostly muscovite and strained or

Figure 2.5. Representative thin section photomicrographs from sampled units of four formations of the Fredericton Trough.

PPL: plane polarized light, XPL: cross polarized light. A: Burtts Corner Formation, NA001A, PPL. B: Burtts Corner Formation, NA001A, XPL. C: Digdeguash Formation, NA003A, PPL. D: Digdeguash Formation, NA003A, XPL. E: Hayes Brook Formation, NA005A, PPL. F: Hayes Brook Formation, NA005A, XPL. G: Flume Ridge Formation, NA010A, PPL. H: Flume Ridge Formation, NA010A, XPL.

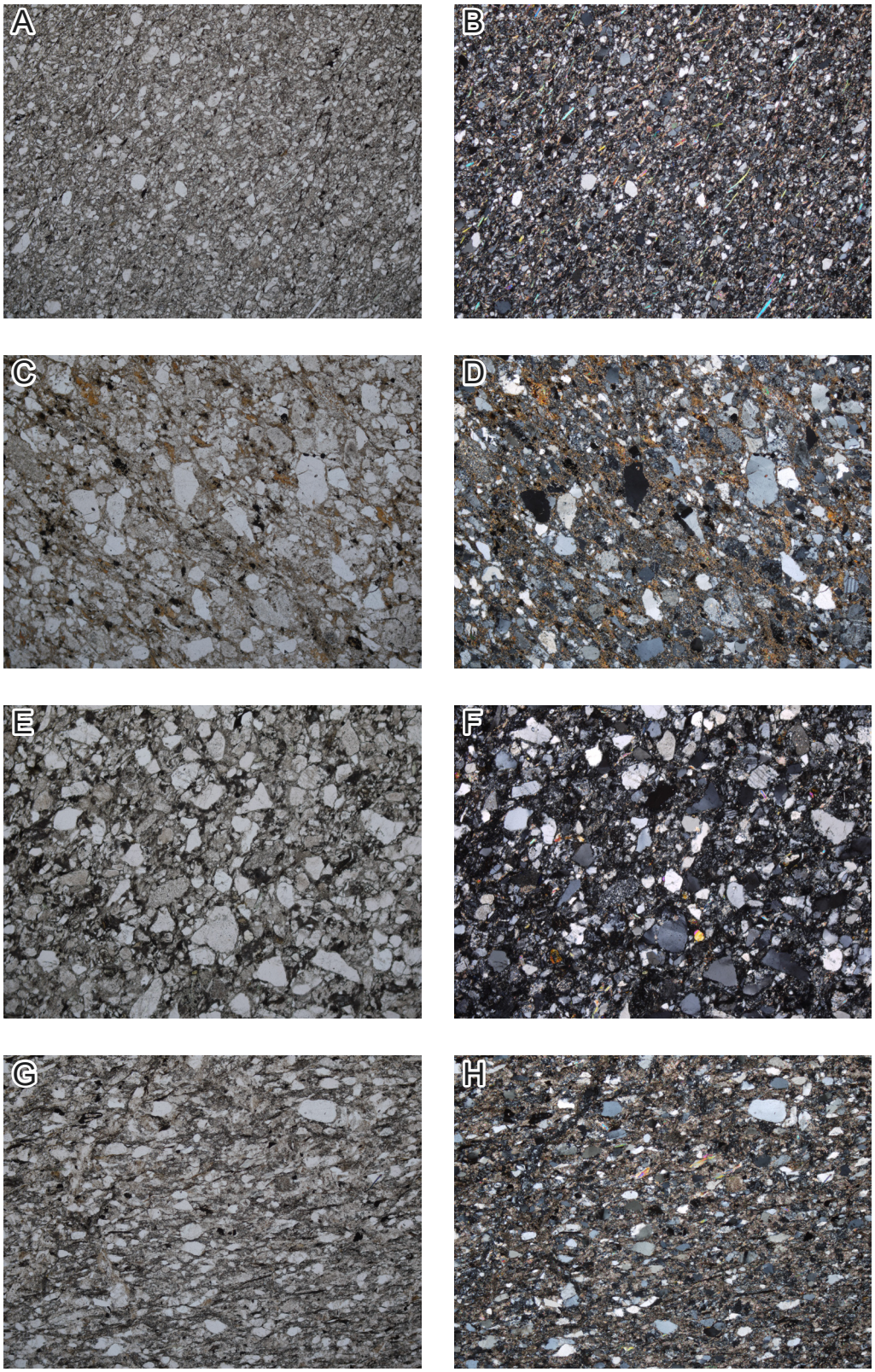
A
B
C
D
E
F
G
H
1 mm

recrystallized phases, and is about 60° to bedding.

3.2.3 Hayes Brook Formation

The Hayes Brook Formation shows multiple generations of map-scale folds (e.g. Smith and Fyffe, 2006), but may appear less deformed on outcrop scale relative to other sections of the Fredericton Trough. The sampled section, at a *Coronograptus cyphus* fossil locality (Figure 2.2; Cumming, 1960; Fyffe, 1995), contains consistently upright, steeply dipping beds striking NE (ex. 045/80). Visible cleavage is at a low angle to bedding, and is strictly limited to thin finer-grained beds between thickly bedded sandstones.

Thin section analysis (Figure 2.5) indicates the rock is a feldspathic wacke, comprising 43% matrix. Normalized framework grain proportions include quartz (53%), feldspar (38%, equally alkali and plagioclase feldspar), and lithic fragments (8%, including chert, volcanics, and granitoids). Mafic minerals (including pyroxene) make up a small portion of the detrital components. Framework grains are mainly subrounded to subangular. The matrix fraction of the rock includes quartz and feldspar, calcite, muscovite, and chlorite. There is no obvious or persistent fabric, despite the presence of orientable phases, in contrast to outcrop observations of bedding in coarser sandstone layers and cleavage in finer-grained siltstone and mudstone.

3.2.4 Burtts Corner Formation

Three distinct generations of folds have been identified in turbidites of the Burtts Corner Formation (Park and Whitehead, 2003). The most prominent are chevron-type, F2 folds locally exhibiting a well-developed axial planar cleavage. Interlimb angles tighten, from open to tight, with increasing proximity to the Fredericton Fault, while fold hinges become more curvilinear. These F2 folds plunge gently NE and SW, roughly parallel to the strike of the nearby Fredericton Fault. F1 fold closures have not been observed in outcrop, but limited occurrence is suggested by Park and Whitehead (2003). F3 structures reported by the same authors include kink bands, and

chevron folds with sub-horizontal axial planes and poorly developed axial planar cleavage. The sampled section (Figure 2.2), consisting of gray lithic wacke interbedded with dark gray siltstone and shale, bore graptolites of the *Cyrtograptus linnarssoni* (*rigidus*) zone (Fyffe, 1995).

In thin section (Figure 2.5), point counting allows the sampled rock to be classified as a feldspathic wacke, with a high proportion of matrix (53%). Framework grains consist of quartz (75%) with a significant amount of feldspar (22%, mainly alkali feldspar), and minor lithic fragments (3%). Major components are mainly subangular, and irregular grain boundaries are particularly common in quartz. Common accessories include muscovite and opaque minerals. Identifiable matrix consists mainly of calcite and white mica, with a small amount of chlorite. A strong foliation is defined primarily by white mica, and is about 50° to 60° from bedding.

3.3 Results

3.3.1 South of the Fredericton Fault

Detrital zircon probability density distributions are shown in Figure 2.6 for the four analyzed formations of the Kingsclear Group. To the south of the Fredericton Fault, the upper Rhuddanian Digdeguash Formation (Figure 2.6) shows a dominant statistical peak at ca. 615 Ma, consistent with sources in the peri-Gondwanan terranes of Ganderia and Avalonia. A scatter of other Proterozoic zircons range from 1.0 to 2.0 Ga, and a minor Cambrian peak (488.9 ± 7.1 Ma; MSWD of 0.63, probability of fit 0.71) is also observed. The overlying Flume Ridge Formation (Figure 2.6) shows a distinctly different zircon signature. A strong asymmetric latest Mesoproterozoic ("Grenville") peak, at about 1.0 Ga, is accompanied by a range of Proterozoic zircons up to 1.9 Ga, – a distribution closely resembling those from the Laurentian margin (Cawood and Nemchin, 2001; Waldron and others, 2008, 2014a) indicating Laurentian provenance. It bears a strong peak in the Ordovician (ca. 465 Ma), probably derived from an arc associated with Iapetan subduction. It contains only a single Neoproterozoic zircon (567.3 ± 26.1 Ma), in contrast to the abundant population in the underlying Digdeguash Formation, suggesting

Figure 2.6. Detrital zircon probability density plots (PDP) and cumulative probability distributions (CPD).

Horizontal axes from 0 to 4000 Ma; vertical scales arbitrary (PDP) or from 0.0 to 1.0 (CPD). All data <10% discordant. Analyses with $^{207}Pb/^{206}Pb$ ratios of less than 0.0658 are reported as $^{206}Pb/^{238}U$ ages; $^{207}Pb/^{206}Pb$ ages are reported otherwise. A: Digdeguash Formation. B: Flume Ridge Formation. C: Hayes Brook Formation. D: Burtts Corner Formation. Comparative data from Laurentia: E. Raeberry Castle Formation, Southern Uplands of Scotland (Waldron and others, 2014a). F: Birk Riggs Formation, English Lake District (Waldron and others, 2014a). Comparative data from Ganderia: G: Baskahegan Lake Formation, Miramichi Terrane (Fyffe and others, 2009). H: Martinon Formation, Brookville Terrane (Fyffe and others, 2009). I: Watch Hill Formation, English Lake District (Waldron and others, 2014a).

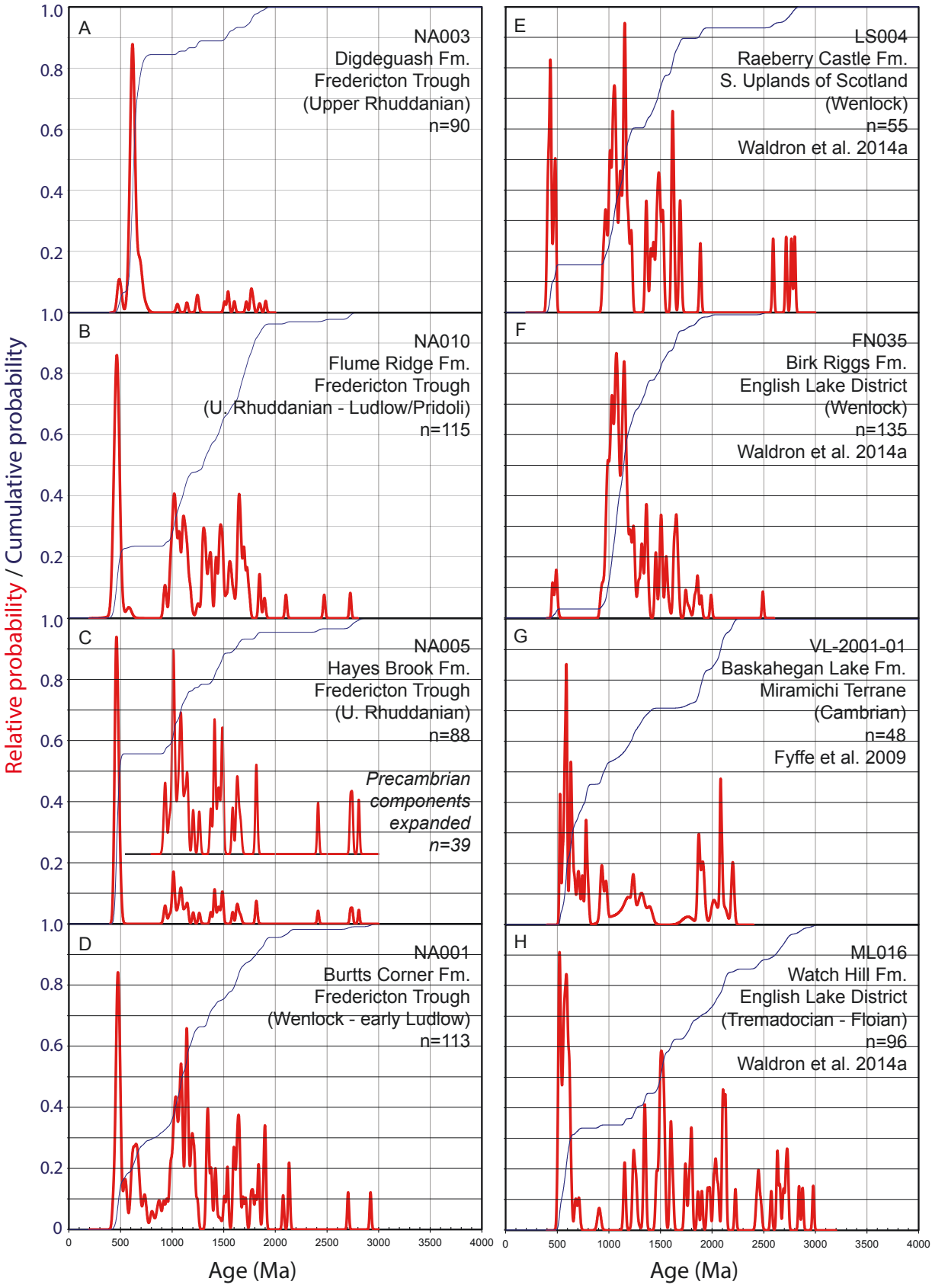
A
NA003
Digdeguash Fm.
Fredericton Trough
(Upper Rhuddanian)
n=90
B
NA010
Flume Ridge Fm.
Fredericton Trough
(U. Rhuddanian - Ludlow/Pridoli)
n=115
C
NA005
Hayes Brook Fm.
Fredericton Trough
(U. Rhuddanian)
n=88
Precambrian components expanded
n=39
D
NA001
Burtts Corner Fm.
Fredericton Trough
(Wenlock - early Ludlow)
n=113
E
LS004
Raeberry Castle Fm.
S. Uplands of Scotland
(Wenlock)
n=55
Waldron et al. 2014a
F
FN035
Birk Riggs Fm.
English Lake District
(Wenlock)
n=135
Waldron et al. 2014a
G
VL-2001-01
Baskahegan Lake Fm.
Miramichi Terrane
(Cambrian)
n=48
Fyffe et al. 2009
H
ML016
Watch Hill Fm.
English Lake District
(Tremadocian - Floian)
n=96
Waldron et al. 2014a
Relative probability / Cumulative probability
0
0.2
0.4
0.6
0.8
1.0
0
500
1000
1500
2000
2500
3000
3500
4000
Age (Ma)

that peri-Gondwanan sources are minor. Rare zircons from 2.1 to 2.8 Ga could also represent a combination of Laurentian and minor peri-Gondwanan sources.

3.3.2 North of the Fredericton Fault

North of the fault, the upper Rhuddanian Hayes Brook Formation (Figure 2.6) displays a strong Ordovician peak (ca. 465 Ma), probably representing a young arc. The majority of the remaining zircon is contained in an asymmetric "Grenville" peak at 1.0 Ga, accompanied by a range of Proterozoic zircons to 1.8 Ga, and a scatter of zircons from 2.4 to 2.8 Ga, indicating Laurentian sediment input. There are no zircons in the "Eburnean" (2.0 to 2.2 Ga) range, nor circa 600 Ma that would indicate peri-Gondwanan sources. The Burtts Corner Formation (Figure 2.6), sampled at a mid-Wenlock fossil locality, similarly displays an asymmetric "Grenville" peak at 1.0 to 1.1 Ga, suggesting Laurentian sources. However, the range of Mesoproterozoic and Paleoproterozoic zircons extends back to 2.2 Ga, overlapping the Eburnean range. In addition it displays a strong Neoproterozoic (~640 Ma) peak. These observations suggest a mixture of Laurentian and peri-Gondwanan sources. A peak in the Paleozoic (480 Ma) is similar in age to the youngest Penobscot volcanics (487 ± 3 Ma: Fyffe and others, 2011) and volcanism in the Annidale terrane (from 493 ± 2 Ma: McLeod and others, 1992; Ruitenberg and others, 1993; to 481 ± 1.7 Ma: Johnson and others, 2012), and probably indicates a contribution from Ordovician arc sources, as in the samples from the Flume Ridge and Hayes Brook Formations.

4. Discussion

4.1 Provenance of zircon

South of the Fredericton Fault our results show a distinct change in provenance through time. Although the early Llandovery Digdeguash Formation lacks the 2.0 – 2.2 Ga Eburnean zircons frequently present in peri-Gondwanan rocks (Pollock and others, 2007; Waldron and others, 2014a), its dominant late Neoproterozoic peak, and the scatter of Mesoproterozoic zircons

without a strong concentration at 1.0 Ga, are characteristic of peri-Gondwanan provenance (Fyffe and others, 2009; Waldron and others, 2014a). In contrast, the overlying Flume Ridge Formation shows a distinctive large and asymmetric Mesoproterozoic "Grenville" peak at 1.0 Ga, with a positive tail of older zircon extending to 1.9 Ga. These features indicate that by the time of deposition of the Flume Ridge Formation, Laurentian sources had overwhelmed Gondwanan sources in this part of the Fredericton Trough. Minor peaks in the Neoproterozoic and early Proterozoic suggest only a minor contribution of the peri-Gondwanan zircon that dominates the underlying Digdeguash Formation, or that might suggest exhumation of the Miramichi terrane to the north. Given our depositional age constraints for these formations, this brackets the arrival of Laurentian detritus in the southern Fredericton Trough between the late Rhuddanian (~441 Ma: Melchin and others, 2012) deposition of the Digdeguash Formation and intrusion of the Pocomoonshine pluton at 422.7 ±3 Ma (West and others, 1992), close to the Ludlow-Pridoli boundary (Melchin and others, 2012). Furthermore, the absence of material consistent with exhumed Miramichi terrane sources (seen in the Burtt Corner Formation by mid-Wenlock), suggests that the Flume Ridge sample predates this event: It is likely that the arrival of Laurentian detritus occurred no later than mid-Wenlock.

North of the fault, in the Hayes Brook Formation (contemporaneous with the Digdeguash Formation at the resolution of graptolite biostratigraphy; see Melchin and others, 2012), we record Laurentian detritus in the upper Rhuddanian, indicated by an asymmetric "Grenville" peak and tail similar to that in the Flume Ridge Formation. The conspicuous absence of peri-Gondwanan material suggests that the Miramichi terrane had not been exhumed at this time. The younger Burtts Corner Formation, in contrast, has a mixed zircon signature of both Laurentian and peri-Gondwanan elements, bearing both an asymmetric 1.0 Ga peak and tail, in addition to Neoproterozoic (ca. 660 Ma) and Eburnean (2.0 – 2.2 Ga) zircons typical of peri-Gondwanan terranes. Both samples indicate the presence of a significant Laurentian source; the additional components in the Burtts Corner Formation probably record exhumation of the peri-Gondwanan Miramichi terrane to the north, following its Late Ordovician to Llandovery metamorphism

under high P/T conditions in the Brunswick Subduction Complex (van Staal and others, 2008). Exhumation must have occurred by the Wenlock, consistent with the history proposed by van Staal and others (2008).

Large Ordovician (~465 to 480 Ma) peaks are characteristic of each of the three formations showing Laurentian zircon signatures, comprising 15 to 55% of their detrital zircon populations. The association of these young zircons with Laurentian detritus suggests that they probably represent peri-Laurentian arcs associated with Iapetan subduction.

4.2 Tectonic implications

McKerrow (1982) argued that the Iapetan suture in New Brunswick lies along the Fredericton Trough, the trough itself representing the floor of the Iapetus Ocean (McKerrow and Ziegler, 1971). However, Williams (1979) regarded the Iapetus suture as an Ordovician feature and interpreted the Fredericton Trough as a successor basin. Subsequent work (e.g. van Staal and de Roo, 1995 and references therein) confirmed peri-Gondwanan material north of the trough, and identified the main Iapetan suture along the Red Indian Line (van Staal and others, 1998), largely concealed as it passes through northwest New Brunswick. The Fredericton Trough was interpreted (e.g. van Staal and others, 2009) to record a part of the Tetagouche-Exploits backarc basin, which closed during Salinic orogenesis. The terminal Salinic suture, marking the final closure of this seaway, was drawn along the Bamford Brook - Hainesville fault in New Brunswick (Pollock and others, 2007; Reusch and van Staal 2012), which bounds the northern margin of the Fredericton Trough against rocks of the Miramichi terrane (Figure 2.2). The Tetagouche-Exploits seaway, though originating as a backarc basin, evolved into a seaway of significant width (van Staal and others, 2012), showing scarce volcanic input in its later (Silurian) history (van Staal and others, 2009). Recent reconstructions (Waldron and others, 2014a, 2014b) suggest that the Iapetus Ocean formed a large system comprising a number of seas separated by arcs and microcontinents. The Fredericton Trough, regarded as a part of this

larger system, records a remnant of the Iapetus Ocean in the New Brunswick Appalachians.

Contrasting detrital zircon signatures across the Fredericton Fault suggest that it marks the position of an earlier structure, possibly a suture or terrane boundary (McKerrow and Ziegler, 1971; McKerrow, 1982) dividing two distinct slices of the Fredericton foredeep as they were accreted to a composite Laurentia (Figure 2.7). An alternative hypothesis, that provenance differences could be produced from variable paleoflows in a small successor basin bounded by contrasting margins, is unlikely in the case of the Fredericton Trough. Previous work (e.g. Waldron and others, 2008, 2014a) clearly shows that Laurentian detritus is pervasively found throughout Silurian deepwater basins along the Laurentian margin, regardless of spatial and temporal fluctuations in paleocurrent direction. Thus, it is unlikely that interleaving turbiditic fans from different sources could preserve as clear a separation of distinct sediment sources as is seen in the contemporary Hayes Brook and Digdeguash Formations; reworking of sediment, and mixing of detrital zircon signatures, would be expected. It is therefore likely that provenance differences seen in the Fredericton Trough result from tectonic closure of a wider basin.

Structural observations (Park and Whitehead, 2003) indicate that the portion of the Fredericton Trough to the north of the Fredericton fault overrode those sediments to the south, juxtaposing the northern and southern portions of the basin in approximately their present configuration. The division of provenance across the fault records a seaway of significant width — a barrier to sedimentation — during deposition of the Hayes Brook and Digdeguash Formations, which are constrained to be approximately of the same late Rhuddanian depositional age. Contrasts in provenance between the Burtts Corner and Flume Ridge Formations may result from localization of exhumed Miramichi terrane sources along the Laurentian margin, either in time or space, or may indicate deposition of the Flume Ridge Formation sample prior to the exhumation of the Miramichi terrane, recorded in the Burtts Corner Formation sample. The seaway which divided the older Hayes Brook and Digdeguash Formations cannot have persisted after 422.7 ± 3 Ma, since by this time Laurentian detritus is clearly seen in the Flume Ridge Formation.

Figure 2.7. Schematic evolution of the Fredericton Trough and adjacent terranes during the Silurian Period.

A: Late Llandovery; B: Early Wenlock (before exhumation of the Brunswick subduction complex); C: Mid-Wenlock (after exhumation of the Brunswick subduction complex); D: Devonian, post-accretion. AV: Avalonia, BC: Burtts Corner Formation, BSC: Brunswick subduction complex, DG: Digdeguash Formation, FR: Flume Ridge Formation, HB: Hayes Brook Formation, KA: Kingston arc, LR: Laurentia, NR: New River terrane, PVA: Popelogan-Victoria arc, SC: St. Croix terrane. Arrows indicate the provenance of detritus.

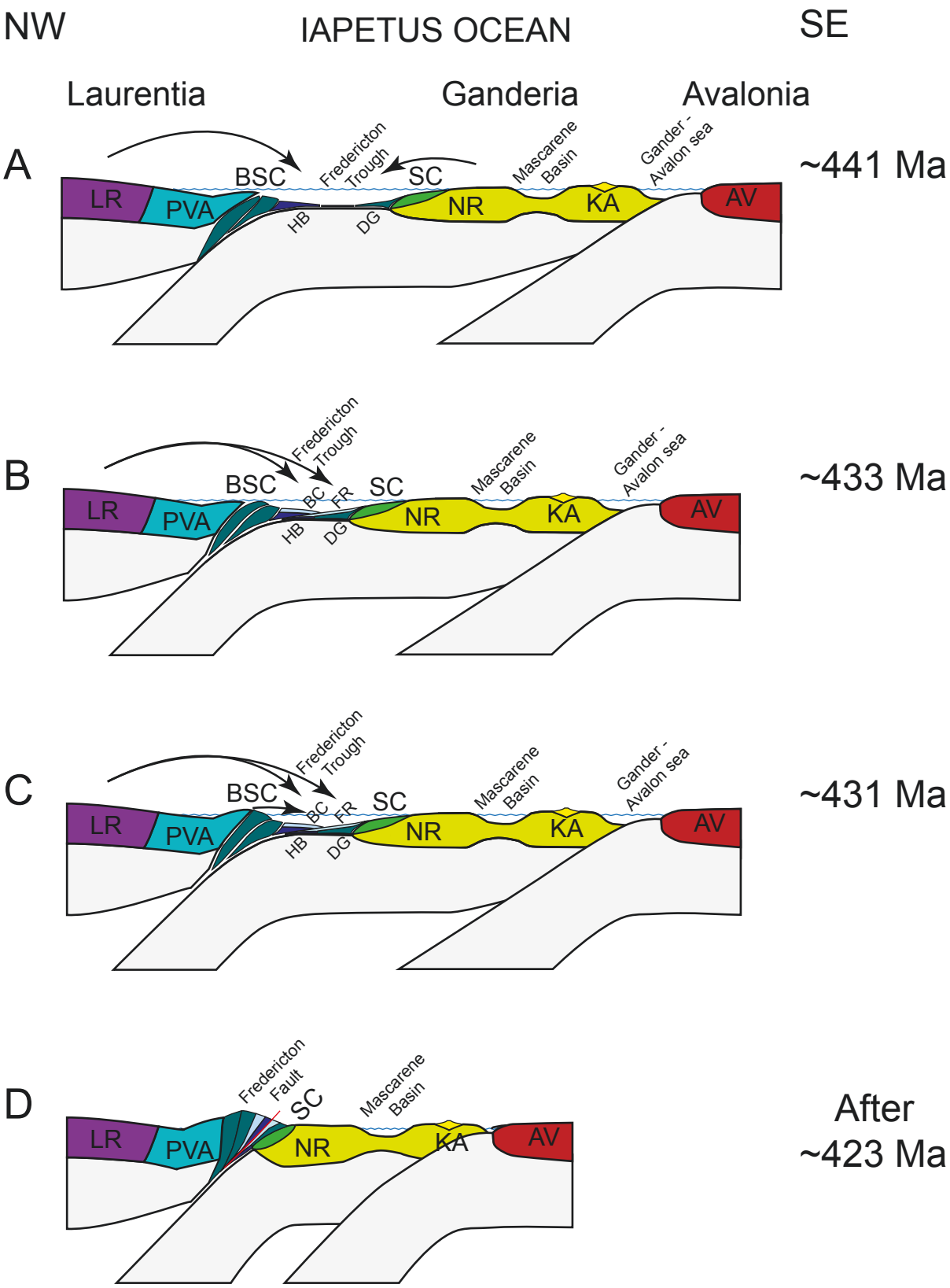
NW
IAPETUS OCEAN
SE
Laurentia
Ganderia
Avalonia
A
~441 Ma
BSC
Fredericton Trough
SC
Mascarene Basin
Gander - Avalon sea
LR
PVA
HB
DG
NR
KA
AV
B
~433 Ma
BC
FR
C
~431 Ma
D
Fredericton Fault
After
~423 Ma

Several locations have been proposed for the placement of the Salinic suture in New Brunswick. A position along the Bamford Brook – Hainesville faults (Figure 2.2; Reusch and van Staal, 2012) is not consistent with our results, particularly the evidence of Laurentian detritus in the late Rhuddanian Hayes Brook Formation, south of this proposed suture, prior to the closure of the Tetagouche-Exploits seaway. Based on detrital zircon provenance, the Fredericton Fault itself, though a later feature, approximates the position of the terminal Salinic suture in the New Brunswick Appalachians between the late Rhuddanian and 422.7 ± 3 Ma (late Ludlow - early Pridoli; West and others, 1992).

Traced to the northeast, this boundary corresponds to the Dog Bay Line in Newfoundland (Williams and others, 1993), where detrital zircon data and other work is consistent with a Silurian closure of the last vestige of Iapetus Ocean (Pollock and others, 2007). Farther northeast, in the British Isles, the equivalent Solway Line is commonly regarded as the Iapetan suture (Phillips and others, 1976; Leggett and others, 1983; Bluck and others, 1992), bounding the southern margin of the Southern Uplands terrane. Detrital zircon geochronology in the Caledonides (Waldron and others, 2014a) provides evidence for Ganderia-Laurentia collision in the Wenlock; however, there is no evidence for earlier Ordovician accretion of Ganderian fragments, as in the equivalent Canadian Appalachians.

The timing and nature of Ganderia-Avalonia juxtaposition is unclear, and is not further clarified by our detrital zircon data. However, work from Pothier and others (2015) in Wales has suggested that a portion of Ganderia was juxtaposed with Avalonia in the Early Ordovician Monian/Penobscot orogenic event, associated with sinistral movement along the Menai Strait Fault System. A similar scenario is possible in the New Brunswick Appalachians between southern Ganderian terranes and Avalonia, represented by the Caledonia terrane.

5. Conclusions

Detrital zircon U-Pb data from four formations of the Fredericton Trough contribute to resolving

several longstanding controversies in Appalachian geology:

1. A remnant of the Iapetus Ocean persisted into the mid-Silurian, and is recorded by the Fredericton Trough.

2. The closure of this seaway, and terminal Salinic convergence between northern and southern Ganderian components, is constrained by the arrival of Laurentian detritus within the Flume Ridge Formation: after the late Rhuddanian depositional age of the Digdeguash Formation, before intrusion of the Pocomoonshine pluton at 422.7 ± 3 Ma, and probably prior to the mid-Wenlock deposition of the Burtts Corner Formation.

3. The Miramichi terrane, including the Brunswick subduction complex, was exhumed by the mid-Silurian and shed detritus into the adjacent Fredericton Trough. Exhumation occurred after the late Rhuddanian Hayes Brook Formation, and had occurred by the mid-Wenlock deposition of the Burtts Corner Formation at the sampled locality.

4. The terminal Salinic suture in New Brunswick may be located close to the trace of the Fredericton Fault.

6. References

Ashton, K.E., Heaman, L.M., Lewry, J.F., Hartlaub, R.P., and Shi, R., 1999, Age and origin of the Jan Lake Complex: a glimpse at the buried Archean craton of the Trans-Hudson Orogen: Canadian Journal of Earth Sciences, v. 36, n. 2, p. 185-208.

Bluck, B.J., Gibbons, W., and Ingham, J.K., 1992, Terranes, *in* Cope, J.C.W., Ingham, J.K. and Rawson, P.F., editors, Atlas of palaeogeography and lithofacies: United Kingdom, Geological Society of London, Memoirs, v. 13, p. 1-4.

Cawood, P.A., and Nemchin, A.A., 2001, Paleogeographic development of the East Laurentian margin: constraints from U-Pb dating of detrital zircons in the Newfoundland Appalachians:

Geological Society of America Bulletin, v. 113, n. 9, p. 1234-1246.

Cawood, P.A., McCausland, P.J.A., and Dunning, G.R., 2001, Opening Iapetus: constraints from the Laurentian margin in Newfoundland: Geological Society of America Bulletin, v. 113, n. 4, p. 443-453.

Cawood, P.A., Nemchin, A.A., Smith, M., and Loewy, S., 2003, Source of the Dalradian Supergroup constrained by U-Pb dating of detrital zircon and implications for the East Laurentian margin: Journal of the Geological Society of London, v. 160, n. 2, p. 231-246.

Cawood, P.A., Nemchin, A.A., Strachan, R.A., Kinny, P.D., and Loewy, S., 2004, Laurentian provenance and an intracratonic tectonic setting for the Moine Supergroup, Scotland, constrained by detrital zircons from the Loch Eil and Glen Urquhart successions: Journal of the Geological Society of London, v. 161, n. 5, p. 861-874.

Cooper, R.A., and Sadler, P.M., 2012, The Ordovician Period, *in* Gradstein, F.M., Ogg, J.G., Schmitz, M.D. and Ogg, G.M., editors, The geologic time scale 2012: Oxford, Elsevier, p. 489-523.

Cumming, L.M., 1960, Report on fossils from the Hayesville and adjacent areas, New Brunswick. Submitted by Dr. W.H. Poole: Geological Survey of Canada, Report O-S-1-60/61-LMC, 2 p.

Dott, R.H., 1964, Wacke, graywacke and matrix—what approach to immature sandstone classification?: Journal of Sedimentary Research, v. 34, n. 3, p. 625-632.

Dunning, G.R., O'Brien, S.J., Colman-Sadd, S., Blackwood, R.F., Dickson, W.L., O'Neill, P.P., and Krogh, T.E., 1990, Silurian Orogeny in the Newfoundland Appalachians: The Journal of Geology, v. 98, n. 6, p. 895-913.

Elhlou, S., Belousova, E., Griffin, W.L., Pearson, N.J., and O'Reilly, S.Y., 2006, Trace element and isotopic composition of GJ-red zircon standard by laser ablation: Geochimica et

Cosmochimica Acta, v. 70, n. 18 supplement, p. A158.

Fyffe, L.R., 1991, Geology of the Flume Ridge-Kedron Stream map areas, Charlotte County, New Brunswick, *in* Abbott, S.A., editor, Project summaries for 1991, sixteenth annual review of activities: New Brunswick Department of Natural Resources and Energy, Mineral Resources, Information Circular 91-2, p. 12-20.

Fyffe, L.R., 1995, Fredericton Belt, *in* Williams, H., editor, Geology of the Appalachian-Caledonian Orogen in Canada and Greenland: Geological Survey of Canada, Geology of Canada, v. 6, p. 351-354.

Fyffe, L.R., and Riva, J., 1990, Revised stratigraphy of the Cookson Group of southwestern New Brunswick and adjacent Maine: Atlantic Geology, v. 26, n. 3, p. 271-275.

Fyffe, L.R., and Riva, J., 2001, Regional significance of graptolites from the Digdeguash Formation of southwestern New Brunswick, *in* Carroll, B.M.W., editor, Current Research 2000: New Brunswick Department of Natural Resources and Energy, Minerals and Energy Division, Mineral Resource Report 2001-4, p. 47-54.

Fyffe, L.R., Barr, S.M., Johnson, S.C., McLeod, M.J., McNicoll, V.J., Valverde Vaquero, P., van Staal, C.R., and White, C.E., 2009, Detrital zircon ages from Neoproterozoic and early Paleozoic conglomerate and sandstone units of New Brunswick and coastal Maine: implications for the tectonic evolution of Ganderia: Atlantic Geology, v. 45, p. 110-144.

Fyffe, L.R., Johnson, S.C., and van Staal, C.R., 2011, A review of Proterozoic to early Paleozoic lithotectonic terranes in the northeastern Appalachian Orogen of New Brunswick, Canada, and their tectonic evolution during Penobscot, Taconic, Salinic, and Acadian orogenesis: Atlantic Geology, v. 47, p. 211-248.

Gehrels, G., Valencia, V., and Pullen, A., 2006, Detrital zircon geochronology by laser-ablation multicollector ICPMS at the Arizona Laserchron Center, *in* Olszewski, T.D., editor,

Geochronology: Emerging Opportunities: Paleontological Society Papers, v. 12, p. 67-76.

Hibbard, J.P., van Staal, C.R., Rankin, D.W., and Williams, H., 2006, Lithotectonic map of the Appalachian Orogen, Canada-United States of America: Geological Survey of Canada, Map 2096A, scale 1:1,500,000.

Hibbard, J.P., van Staal, C.R., and Rankin, D.W., 2007, A comparative analysis of pre-Silurian crustal building blocks of the northern and the southern Appalachian Orogen: American Journal of Science, v. 307, n. 1, p. 23-45.

Jackson, S.E., Pearson, N.J., Griffin, W.L., and Belousova, E.A., 2004, The application of laser ablation-inductively coupled plasma-mass spectrometry to in situ U–Pb zircon geochronology: Chemical Geology, v. 211, n. 1–2, p. 47-69.

Johnson, S.C., McLeod, M.J., Fyffe, L.R., and Dunning, G.R., 2009, Stratigraphy, geochemistry, and geochronology of the Annidale and New River Belts, and the development of the Penobscot Arc in southern New Brunswick, *in* Martin, G.L., editor, Geological investigations in New Brunswick for 2008: New Brunswick Department of Natural Resources, Minerals, Policy, and Planning Division, Mineral Resource Report 2009-2, p. 141-218.

Johnson, S.C., Fyffe, L.R., McLeod, M.J., and Dunning, G.R., 2012, U–Pb ages, geochemistry, and tectonomagmatic history of the Cambro-Ordovician Annidale Group: a remnant of the Penobscot arc system in southern New Brunswick?: Canadian Journal of Earth Sciences, v. 49, n. 1, p. 166-188.

Kerr, A., Jenner, G.A., and Fryer, B.J., 1995, Sm–Nd isotopic geochemistry of Precambrian to Paleozoic granitoid suites and the deep-crustal structure of the southeast margin of the Newfoundland Appalachians: Canadian Journal of Earth Sciences, v. 32, n. 2, p. 224-245.

Landing, E., 1996, Avalon: Insular continent by the latest Precambrian, *in* Nance, R.D. and

Thompson, M.D., editors, Avalonian and related peri-Gondwanan terranes of the Circum-North Atlantic: Geological Society of America, Special Papers, v. 304, p. 29-63.

Leggett, J.K., McKerrow, W.S., and Soper, N.J., 1983, A model for the crustal evolution of southern Scotland: Tectonics, v. 2, n. 2, p. 187-210.

Li, Z.X., Bogdanova, S.V., Collins, A.S., Davidson, A., De Waele, B., Ernst, R.E., Fitzsimons, I.C.W., Fuck, R.A., Gladkochub, D.P., Jacobs, J., Karlstrom, K.E., Lu, S., Natapov, L.M., Pease, V., Pisarevsky, S.A., Thrane, K., and Vernikovsky, V., 2008, Assembly, configuration, and breakup history of Rodinia: a synthesis, *in* Bogdanova, S.V., Li, Z.X., Moores, E.M. and Pisaresvky, S.A., editors, Testing the Rodinia hypothesis: records in its building blocks: Precambrian Research, v. 160, n. 1-2, p. 179-210.

Ludman, A., 1987, Pre-Silurian stratigraphy and tectonic significance of the St. Croix Belt, southeastern Maine: Canadian Journal of Earth Sciences, v. 24, n. 12, p. 2459-2469.

Ludman, A., 1991, Revised stratigraphy of the Cookson Group in eastern Maine and southwestern New Brunswick: an alternative view: Atlantic Geology, v. 27, n. 1, p. 49-55.

Ludman, A., and West, D.P., Jr., editors, 1999, Norumbega fault system of the Northern Appalachians: Special Papers, v. 331, 202 p.

Ludman, A., Hopeck, J.T., and Brock, P.C., 1993, Nature of the Acadian Orogeny in eastern Maine, *in* Roy, D.C. and Skehan, J.W., editors, The Acadian Orogeny: recent studies in New England, Maritime Canada, and the autochthonous foreland: Special Paper - Geological Society of America, v. 275, p. 67-84.

Ludman, A., Lanzirotti, A., Lux, D., and Wang, C., 1999, Constraints on timing and displacement multistage shearing in the Norumbega fault system, eastern Maine, *in* Ludman, A. and West, D.P.,Jr., editors, Norumbega fault system of the Northern Appalachians: Geological Society of America, Special Papers, v. 331, p. 179-194.

Ludwig, K.R., 2012, User's manual for Isoplot 3.75: Berkeley Geochronology Center Special Publication, 5, 75 p.

Macdonald, F.A., Ryan-Davis, J., Coish, R.A., Crowley, J.L., and Karabinos, P., 2014, A newly identified Gondwanan terrane in the northern Appalachian mountains: implications for the Taconic orogeny and closure of the Iapetus Ocean: Geology, v. 42, n. 6, p. 539-542.

McKerrow, W.S., 1982, The northwest margin of the Iapetus Ocean during the early Paleozoic, *in* Watkins, J.S. and Drake, C.L., editors, Studies in continental margin geology: American Association of Petroleum Geologists, Memoirs, v. 34, p. 521-533.

McKerrow, W.S., and Ziegler, A.M., 1971, The lower Silurian paleogeography of New Brunswick and adjacent areas: Journal of Geology, v. 79, n. 6, p. 635-646.

McLeod, M.J., Ruitenburg, A.A., and Krogh, T.E., 1992, Geology and U-Pb geochronology of the Annidale Group, southern New Brunswick: Lower Ordovician volcanic and sedimentary rocks formed near the southeastern margin of Iapetus Ocean: Atlantic Geology, v. 28, n. 2, p. 181-192.

McNamara, A.K., Niocaill, C.M., van der Pluijm, B.A., and Van der Voo, R., 2001, West African proximity of the Avalon terrane in the latest Precambrian: Geological Society of America Bulletin, v. 113, n. 9, p. 1161-1170.

Melchin, M.J., Sadler, P.M., and Cramer, B.D., 2012, The Silurian Period, *in* Gradstein, F.M., Ogg, J.G., Schmitz, M.D. and Ogg, G.M., editors, The geologic time scale 2012: Oxford, Elsevier, p. 525-558.

Murphy, J.B., Nance, R.D., and Keppie, J.D., 2002, Discussion and reply: West African proximity of the Avalon terrane in the latest Precambrian: Geological Society of America Bulletin, v. 114, n. 8, p. 1049-1050.

Murphy, J.B., Fernandez-Suarez, J., Keppie, J.D., and Jeffries, T.E., 2004a, Contiguous rather

than discrete Paleozoic histories for the Avalon and Meguma Terranes based on detrital zircon data: Geology, v. 32, n. 7, p. 585-588.

Murphy, J.B., Pisarevsky, S.A., Nance, R.D., and Keppie, J.D., 2004b, Neoproterozoic—early Paleozoic evolution of peri-Gondwanan terranes: implications for Laurentia-Gondwana connections, *in* Doerr, W., Finger, F., Linnemann, U. and Zulauf, G., editors, The Avalonian-Cadomian Belt and related peri-Gondwanan terranes: International Journal of Earth Sciences, v. 93, n. 5, p. 659-682.

Nance, R.D., Murphy, J.B., and Keppie, J.D., 2002, A Cordilleran model for the evolution of Avalonia: Tectonophysics, v. 352, n. 1-2, p. 11-31.

Nance, R.D., Murphy, J.B., Strachan, R.A., Keppie, J.D., Gutierrez Alonso, G., Fernandez Suarez, J., Quesada, C., Linnemann, U., d'Lemos, R., and Pisarevsky, S.A., 2008, Neoproterozoic-early Palaeozoic tectonostratigraphy and palaeogeography of the peri-Gondwanan terranes: Amazonian v. West African connections, *in* Ennih, N. and Liegeois, J.P., editors, The boundaries of the West African Craton: Geological Society of London, Special Publications, v. 297, p. 345-383.

O'Brien, S.J., O'Brien, B.H., Dunning, G.R., and Tucker, R.D., 1996, Late Neoproterozoic Avalonian and related peri-Gondwanan rocks of the Newfoundland Appalachians, *in* Nance, R.D. and Thompson, M.D., editors, Avalonian and related peri-Gondwanan terranes of the Circum-North Atlantic: Geological Society of America, Special Papers, v. 304, p. 9-28.

Osberg, P.H., 1968, Stratigraphy, structural geology, and metamorphism of the Waterville-Vassalboro area, Maine: Maine Geological Survey, Bulletin 20, 64 p.

Park, A.F., and Whitehead, J., 2003, Structural transect through Silurian turbidites of the Fredericton Belt southwest of Fredericton, New Brunswick: the role of the Fredericton Fault in late Iapetus convergence: Atlantic Geology, v. 39, n. 3, p. 227-237.

Peng, S., Babcock, L.E., and Cooper, R.A., 2012, The Cambrian Period, *in* Gradstein, F.M., Ogg, J.G., Schmitz, M.D. and Ogg, G.M., editors, The geologic time scale 2012: Oxford, Elsevier, p. 437-488.

Phillips, E.R., Evans, J.A., Stone, P., Horstwood, M.S.A., Floyd, J.D., Smith, R.A., Akhurst, M.C., and Barron, H.F., 2003, Detrital Avalonian zircons in the Laurentian Southern Uplands terrane, Scotland: Geology, v. 31, n. 7, p. 625-628.

Phillips, W.E.A., Stillman, C.J., and Murphy, T., 1976, A Caledonian plate tectonic model: Journal of the Geological Society of London, v. 132, n. 6, p. 579-609.

Pollock, J.C., Wilton, D.H.C., van Staal, C.R., and Morrissey, K.D., 2007, U-Pb detrital zircon geochronological constraints on the Early Silurian collision of Ganderia and Laurentia along the Dog Bay Line: the terminal Iapetan suture in the Newfoundland Appalachians: American Journal of Science, v. 307, n. 2, p. 399-433.

Pollock, J.C., Hibbard, J.P., and Sylvester, P.J., 2009, Early Ordovician rifting of Avalonia and birth of the Rheic Ocean: U-Pb detrital zircon constraints from Newfoundland: Journal of the Geological Society of London, v. 166, n. 3, p. 501-515.

Pollock, J.C., Hibbard, J.P., and van Staal, C.R., 2012, A paleogeographical review of the peri-Gondwanan realm of the Appalachian Orogen: Canadian Journal of Earth Sciences, v. 49, n. 1, p. 259-288.

Poole, W.H., 1963, Geology, Hayesville, New Brunswick: Geological Survey of Canada, Map 6-1963, scale 1:63,360.

Pothier, H.D., Waldron, J.W.F., Schofield, D.I., and DuFrane, S.A., 2015, Peri-Gondwanan terrane interactions recorded in the Cambrian–Ordovician detrital zircon geochronology of North Wales: Gondwana Research, v. 28, n. 3, p. 987-1001.

Prigmore, J.K., Butler, A.J., and Woodcock, N.H., 1997, Rifting during separation of Eastern

Avalonia from Gondwana: Evidence from subsidence analysis: Geology, v. 25, n. 3, p. 203-206.

Reusch, D.N., and van Staal, C.R., 2012, The Dog Bay-Liberty Line and its significance for Silurian tectonics of the Northern Appalachian Orogen: Canadian Journal of Earth Sciences, v. 49, n. 1, p. 239-258.

Rosenblum, S., and Brownfield, I.K., 2000, Magnetic susceptibilities of minerals: United States Geological Survey, Open-File Report 99-529, 37 p.

Ruitenberg, A.A., and Ludman, A., 1978, Stratigraphy and tectonic setting of early Paleozoic sedimentary rocks of the Wirral-Big Lake area, southwestern New Brunswick and southeastern Maine: Canadian Journal of Earth Sciences, v. 15, n. 1, p. 22-32.

Ruitenberg, A.A., McLeod, M.J., and Krogh, T.E., 1993, Comparative metallogeny of Ordovician volcanic and sedimentary rocks in the Annidale-Shannon (New Brunswick) and Harborside-Blue Hill (Maine) areas: implications of new U-Pb age dates: Exploration and Mining Geology, v. 2, n. 4, p. 355-365.

Schulz, K.J., Stewart, D.B., Tucker, R.D., Pollock, J.C., and Ayuso, R.A., 2008, The Ellsworth terrane, coastal Maine: Geochronology, geochemistry, and Nd-Pb isotopic composition—Implications for the rifting of Ganderia: Geological Society of America Bulletin, v. 120, n. 9-10, p. 1134-1158.

Simonetti, A., Heaman, L., Hartlaub, R., Creaser, R., MacHattie, T., and Bohm, C., 2005, U-Pb zircon dating by laser ablation-MC-ICP-MS using a new multiple ion counting Faraday collector array: Journal of Analytical Atomic Spectrometry, v. 20, n. 8, p. 677-686.

Smith, E.A., 2005, Bedrock geology of southwestern New Brunswick (NTS 21 G, part of 21 B): New Brunswick Department of Natural Resources, Minerals, Policy, and Planning Division, Map NR-5 (Second Edition), scale 1:250000.

Smith, E.A., and Fyffe, L.R., 2006, Bedrock geology of central New Brunswick (NTS 21 J): New Brunswick Department of Natural Resources, Minerals, Policy, and Planning Division, Map NR-4 (Second Edition), scale 1:250000.

van Staal, C.R., 1994, Brunswick subduction complex in the Canadian Appalachians: record of the Late Ordovician to Late Silurian collision between Laurentia and the Gander margin of Avalon: Tectonics, v. 13, n. 4, p. 946-962.

van Staal, C.R., and de Roo, J.A., 1995, Mid-Paleozoic tectonic evolution of the Appalachian Central mobile belt in northern New Brunswick, Canada: collision, extensional collapse and dextral transpression, *in* Hibbard, J.P., van Staal, C.R. and Cawood, P.A., editors, Current perspectives in the Appalachian-Caledonian Orogen: Geological Association of Canada, Special Paper, v. 41, p. 367-389.

van Staal, C.R., Ravenhurst, C.E., Winchester, J.A., Roddick, J.C., and Langton, J.P., 1990, Post-Taconic blueschist suture in the Northern Appalachians of northern New Brunswick, Canada: Geology, v. 18, n. 11, p. 1073-1077.

van Staal, C.R., Sullivan, R.W., and Whalen, J.B., 1996, Provenance of tectonic history of the Gander Zone in the Caledonian/Appalachian Orogen: implications for the origin and assembly of Avalon, *in* Nance, R.D. and Thompson, M.D., editors, Avalonian and related peri-Gondwanan terranes of the Circum–North Atlantic: Geological Society of America, Special Papers, v. 304, p. 347-367.

van Staal, C.R., Dewey, J.F., Mac Niocaill, C., and McKerrow, W.S., 1998, The Cambrian-Silurian tectonic evolution of the Northern Appalachians and British Caledonides: history of a complex, west and southwest Pacific-type segment of Iapetus, *in* Blundell, D.J. and Scott, A.C., editors, Lyell: the Past is the Key to the Present: Geological Society of London, Special Publications, v. 143, p. 199-242.

van Staal, C.R., Wilson, R.A., Rogers, N., Fyffe, L.R., Langton, J.P., McCutcheon, S.R.,

McNicoll, V., and Ravenhurst, C.E., 2003, Geology and tectonic history of the Bathurst Supergroup, Bathurst mining camp, and its relationships to coeval rocks in southwestern New Brunswick and adjacent mine—a synthesis, *in* Goodfellow, W.D., McCutcheon, S.R. and Peter, J.M., editors, Massive sulfide deposits of the Bathurst mining camp, New Brunswick, and northern Maine: Economic Geology Monographs, v. 11, p. 37-60.

van Staal, C.R., Currie, K.L., Rowbotham, G., Rogers, N., and Goodfellow, W., 2008, Pressure-temperature paths and exhumation of Late Ordovician-Early Silurian blueschists and associated metamorphic nappes of the Salinic Brunswick subduction complex, Northern Appalachians: Geological Society of America Bulletin, v. 120, n. 11-12, p. 1455-1477.

van Staal, C.R., Whalen, J.B., Valverde-Vaquero, P., Zagorevski, A., and Rogers, N., 2009, Pre-Carboniferous, episodic accretion-related, orogenesis along the Laurentian margin of the Northern Appalachians, *in* Murphy, J.B., Keppie, J.D. and Hynes, A.J., editors, Ancient orogens and modern analogues: Geological Society of London, Special Publications, v. 327, p. 271-316.

van Staal, C.R., Barr, S.M., and Murphy, J.B., 2012, Provenance and tectonic evolution of Ganderia: constraints on the evolution of the Iapetus and Rheic Oceans: Geology, v. 40, n. 11, p. 987-990.

van Staal, C.R., Wilson, R.A., Kamo, S.L., McClelland, W.C., and McNicoll, V., 2016, Evolution of the Early to Middle Ordovician Popelogan Arc in New Brunswick, Canada, and adjacent Maine, USA: record of arc-trench migration and multiple phases of rifting: Geological Society of America Bulletin, v. 128, n. 1-2, p. 122-146.

Waldron, J.W.F., Floyd, J.D., Simonetti, A., and Heaman, L.M., 2008, Ancient Laurentian detrital zircon in the closing Iapetus Ocean, Southern Uplands terrane, Scotland: Geology, v. 36, n. 7, p. 527-530.

Waldron, J.W.F., White, C.E., Barr, S.M., Simonetti, A., and Heaman, L.M., 2009, Provenance

of the Meguma Terrane, Nova Scotia: rifted margin of early Paleozoic Gondwana: Canadian Journal of Earth Sciences, v. 46, n. 1, p. 1-8.

Waldron, J.W.F., Schofield, D.I., White, C.E., and Barr, S.M., 2011, Cambrian successions of the Meguma Terrane, Nova Scotia, and Harlech Dome, north Wales: dispersed fragments of a peri-Gondwanan basin?: Journal of the Geological Society of London, v. 168, n. 1, p. 83-98.

Waldron, J.W.F., McNicoll, V.J., and van Staal, C.R., 2012, Laurentia-derived detritus in the Badger Group of central Newfoundland: deposition during closing of the Iapetus Ocean: Canadian Journal of Earth Sciences, v. 49, n. 1, p. 207-221.

Waldron, J.W.F., Schofield, D.I., Dufrane, S.A., Floyd, J.D., Crowley, Q.G., Simonetti, A., Dokken, R.J., and Pothier, H.D., 2014a, Ganderia–Laurentia collision in the Caledonides of Great Britain and Ireland: Journal of the Geological Society of London, v. 171, n. 4, p. 555-569.

Waldron, J.W.F., Schofield, D.I., Murphy, J.B., and Thomas, C.W., 2014b, How was the Iapetus Ocean infected with subduction?: Geology, v. 42, n. 12, p. 1095-1098.

West, D.P., Jr., Ludman, A., and Lux, D.R., 1992, Silurian age for the Pocomoonshine Gabbro-Diorite, southeastern Maine and its regional tectonic implications: American Journal of Science, v. 292, n. 4, p. 253-273.

White, C.E., and Barr, S.M., 1996, Geology of the Brookville Terrane, southern New Brunswick, Canada, *in* Nance, R.D. and Thompson, M.D., editors, Avalonian and related peri-Gondwanan terranes of the Circum-North Atlantic: Geological Society of America, Special Papers, v. 304, p. 133-147.

White, C.E., Barr, S.M., Bevier, M.L., and Kamo, S., 1994, A revised interpretation of Cambrian and Ordovician rocks in the Bourinot Belt of central Cape Breton Island, Nova Scotia: Atlantic Geology, v. 30, n. 2, p. 123-142.

Williams, H., 1979, Appalachian Orogen in Canada: Canadian Journal of Earth Sciences, v. 16, n. 3, p. 792-807.

Williams, H., and Hiscott, R.N., 1987, Definition of the Iapetus rift-drift transition in western Newfoundland: Geology, v. 15, n. 11, p. 1044-1047.

Williams, H., Currie, K.L., and Piasecki, M.A.J., 1993, The Dog Bay Line: a major Silurian tectonic boundary in Northeast Newfoundland: Canadian Journal of Earth Sciences, v. 30, n. 12, p. 2481-2494.

Wilson, R.A., 2000, Geology of the Popelogan Lake-Lost Pine Lake area (NTS 21O/15a and b), Restigouche County, New Brunswick, *in* Carroll, B.M.W., editor, Current research 1999: New Brunswick Department of Natural Resources and Energy, Minerals and Energy Division, Mineral Resource Report 2000-4, p. 91-136.

Wilson, R.A., 2003, Geochemistry and petrogenesis of Ordovician arc-related mafic volcanic rocks in the Popelogan Inlier, northern New Brunswick: Canadian Journal of Earth Sciences, v. 40, n. 9, p. 1171-1189.

Wilson, R.A., van Staal, C.R., and McClelland, W.C., 2015, Synaccretionary sedimentary and volcanic rocks in the Ordovician Tetagouche backarc basin, New Brunswick, Canada: evidence for a transition from foredeep to forearc basin sedimentation: American Journal of Science, v. 315, n. 10, p. 958-1001.

Zalasiewicz, J.A., Williams, M., and Akhurst, M., 2003, An unlikely evolutionary lineage: the Rhuddanian (Silurian, Llandovery) graptolites Huttagraptus? praematurus and Coronograptus cyphus re-examined: Scottish Journal of Geology, v. 39, n. 1, p. 89-96.

Zalasiewicz, J.A., Taylor, L., Rushton, A.W.A., Loydell, D.K., Rickards, R.B., and Williams, M., 2009, Graptolites in British stratigraphy: Geological Magazine, v. 146, n. 6, p. 785-850.

Chapter 3: Detrital zircon geochronology of the Mascarene Group

Volcanic-sedimentary successions of the Mascarene Group, in present-day southwestern New Brunswick, were deposited across components of Ganderia from the Late Ordovician to late Silurian, contemporaneous with the convergence of the microcontinent Ganderia with a composite Laurentian continent across a narrowing remnant of the Iapetus Ocean. Samples were selected from three key formations of the Mascarene Group for detrital zircon geochronological analysis: the Waweig Formation, with a previously interpreted U-Pb zircon date from a felsic tuff suggesting a depositional age of 438 ± 4 Ma; the Back Bay Formation, of late Llandovery age indicated by brachiopods; and the Eastport Formation, bearing a felsic tuff dated at 423 ± 1 Ma. The Waweig Formation is found to contain almost entirely young zircon, ca. 430 Ma, slightly younger than the previously dated tuff outcrop 7 km away along strike. The Back Bay Formation displays significant proportions of zircon at about 610 Ma, with minor sources from 430 Ma, and suggests peri-Gondwanan provenance. The Eastport Formation, in addition to zircon peaks at about 425 Ma and 605 Ma, shows a range of zircon extending from 1.0 Ga to 1.7 Ga, similar to other distributions from Ganderia but also showing a resemblance to a distribution from the Fredericton Trough to the north, that shows mixed Laurentian and Ganderian provenance. The possible presence of Laurentian detritus in the Mascarene Basin, after the late Llandovery (Back Bay Formation) and by 423 ± 1 Ma (Eastport Formation), could constrain the time at which Ganderia was juxtaposed with Laurentia during their convergence and the associated closure of the Iapetus Ocean.

1. Introduction

The Appalachian Orogen (Figure 3.1) lies along the eastern edge of present day North America, and extends to include the correlative Caledonides in Greenland and the British Isles. Previous

Figure 3.1: Map of the Appalachian-Caledonide orogen showing lithotectonic divisions. Pangean (pre-Mesozoic) reconstruction after Waldron and others (2014b) and references therein. Box encloses Figure 3.2. Lithotectonic divisions after van Staal and others (1998) and Hibbard and others (2006, 2007).

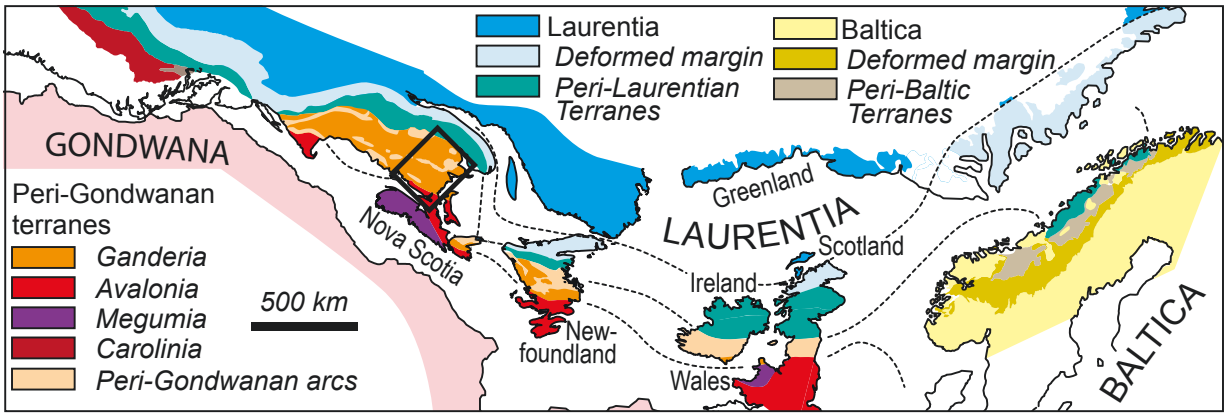

work (e.g. Williams, 1979; Hibbard and others, 2006, 2007) has detailed the various lithotectonic divisions which constitute the orogen, dividing them into terranes of Laurentian or Gondwanan origin (Figure 3.1). The Paleozoic convergence of peri-Gondwanan components, and Gondwana itself, with Laurentia is interpreted to have been a driving cause of Appalachian orogenesis.

Peri-Gondwanan components include Ganderia and Avalonia; the former is especially well represented in New Brunswick, Canada (Figure 3.2). Both Ganderia and Avalonia are interpreted to have originated from the margin of Gondwana, having rifted apart as domains of microcontinental material by the mid-Cambrian and Early Ordovician respectively (Nance and others, 2002; van Staal and others, 2012). Coinciding with the closure of the Iapetus Ocean (which divided Laurentia from Gondwana), these peri-Gondwanan components would converge with Laurentia in what have been interpreted as the Taconic, Salinic, and Acadian orogenies (van Staal and others, 2009).

Detrital zircon geochronology has been applied in key areas of the Appalachian-Caledonide orogen, enabling the determination of the provenance of various terranes, and using this knowledge to ascertain the timing of accretionary events (Cawood and Nemchin, 2001; Cawood and others, 2003, 2004; Waldron and others, 2012; Macdonald and others, 2014; Waldron and others, 2014a). Previous work has demonstrated that distinctive Laurentian detritus is pervasively found in basins formed within or upon terranes juxtaposed or accreted to Laurentia (Waldron and others, 2008, 2012, 2014a; Chapter 2). The presence of Laurentian detritus is typically indicated by a distinctive and prominent “Grenville” zircon population at 1.0 to 1.1 Ga, with an asymmetric tail of zircons typically extending to about 2.0 Ga, and a paucity of zircon populations in the 2.0 to 2.4 Ga range (Cawood and Nemchin, 2001; Waldron and others, 2014a). This is in contrast to the detrital zircon signatures typically found in peri-Gondwanan terranes, typically including a prominent Neoproterozoic peak from 550 to 650 Ma (Fyffe and others, 2009; Waldron and others, 2014a), and which lack Laurentian indicators.

The volcanic-sedimentary Mascarene Basin (Figure 3.2), a composite basin named by Fyffe and

Figure 3.2: Lithotectonic terrane map of New Brunswick.

After Smith (2005, 2006); see also Fyffe and others (2011). Sampled formations of the Mascarene Group are shown with arrows. A: Eastport Formation. B: Waweig Formation. C: Back Bay Formation.

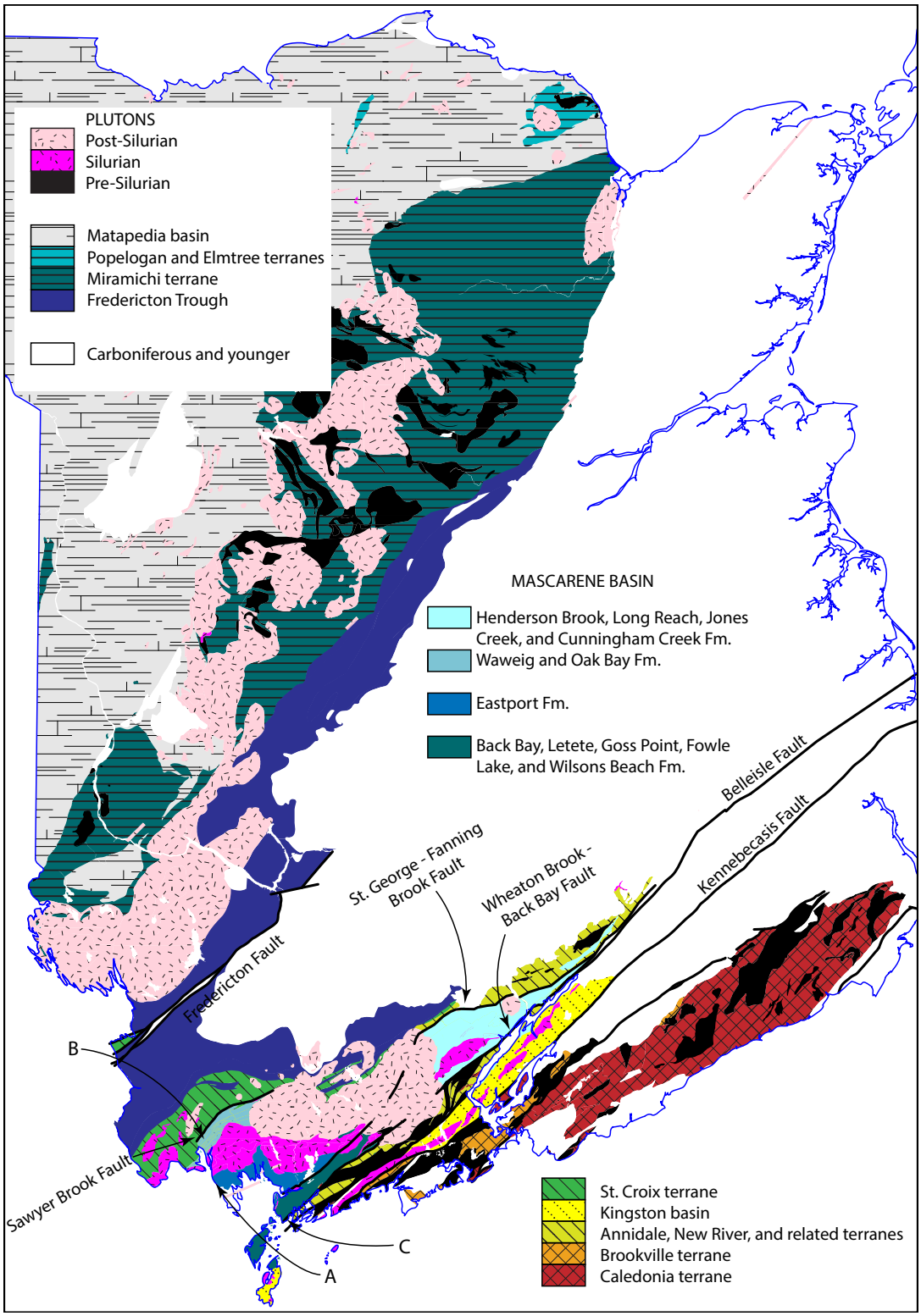

others (1999) after the Late Ordovician to late Silurian Mascarene Group, was deposited upon some of the last components of Ganderia to converge with the Laurentian continent (e.g. Fyffe and others, 2011). Its relatively constricted, extensional paleogeographic setting, and deposition during Salinic orogenesis, make it an ideal target to test this method of geochronology, and demonstrate if the methods used elsewhere in the orogen may be applied successfully within this basin. Based on the distinctive and contrasting indicators of Laurentian and peri-Gondwanan provenance, individual formations of the Mascarene Group can be studied to determine whether or not they were juxtaposed with Laurentia by the time of deposition. By suggesting when Laurentian detritus may first have arrived within the Mascarene Basin, we can provide constraints on the timing and nature of the accretion of Ganderia with Laurentia. Detrital zircon data have previously been reported from one formation of the Mascarene Group (Fyffe and others, 2009). The early Silurian Oak Bay Formation records only peri-Gondwanan sources; there has been no further detrital zircon study of other formations within the basin, and no record of Laurentian detritus.

2. Geologic Setting

2.1 Tectonic Overview

Laurentia took form as a discrete continent in the late Neoproterozoic, following the breakup of the supercontinent Rodinia (Li and others, 2008). The Iapetus Ocean opened by 570 – 550 Ma (Williams and Hiscott, 1987) between Laurentia, Baltica, and Amazonia, which led to the development of a Laurentian passive margin (Cawood and others, 2001) by 520 – 515 Ma (timescale of Peng and others, 2012).

The microcontinental domain Ganderia separated from Gondwana by 505 Ma (White and others, 1994; Schulz and others, 2008; van Staal and others, 2009, 2012); following this, components of Ganderia began to collide with Laurentia in the Early Ordovician in New England (Macdonald and others, 2014) and the Late Ordovician in Newfoundland (van Staal and others, 2008,

2009). Subsequent Salinic orogenesis is interpreted to have resulted from the accretion of other Ganderian components in the Silurian (van Staal and others 2008, 2009), and is defined by a late Silurian unconformity in west Newfoundland (Dunning and others, 1990), and multiple unconformities (Late Ordovician to late Silurian) in New Brunswick (van Staal and de Roo, 1995; Wilson and others, 2004; Fyffe and others, 2011; Wilson and Kamo, 2012; Wilson and others, 2015). The microcontinent Avalonia separated from Gondwana by the Early Ordovician (Nance and others, 2002). Its collision with Ganderia, which may have formed part of a composite Laurentian margin at the time, is interpreted to have resulted in late Silurian to mid-Devonian Acadian orogenesis (van Staal and others, 2009, 2014).

The Mascarene Basin overlies two Ganderian terranes (Figures 3.2, 3.3): the late Neoproterozoic to late Cambrian New River terrane (Johnson and McLeod, 1996; Johnson and others, 2009; Fyffe and others, 2011), and the late Neoproterozoic to Late Ordovician St. Croix terrane (Ludman, 1987; Fyffe and Riva, 1990; Ludman, 1991; Fyffe and others, 2011). The St. Croix terrane comprises a continental margin succession, at least part of which was deposited while Ganderia was still attached to Gondwana (Fyffe and others, 2011), and is overlain by a Salinic unconformity prior to deposition of the Mascarene Group. The New River terrane is itself the basement to the St. Croix terrane (Fyffe and others, 2011), and includes Late Neoproterozoic to Early Cambrian arc-related igneous rocks, overlain by thick Early Cambrian quartz-rich sediments typical of Ganderia, which are in turn overlain by volcanic rocks at the end of the Early Cambrian (Fyffe and others, 2011; Johnson and others, 2012).

The Mascarene Basin has been interpreted to have been deposited in an extensional, possibly back-arc setting (Van Wagoner and others 2001, 2002). Associated volcanic rocks are bimodal: basaltic rocks are probably derived from partial melting of the mantle, modified by both crustal contamination and mantle metasomatism from a subduction event; rhyolitic rocks are crustal melts probably driven by underplating of continental crust (Van Wagoner and others, 2002). These rocks are consistent with, and have been interpreted as resulting from the convergence of

Figure 3.3: Stratigraphic columns of the Mascarene Group and related formations. Timescales of Cooper and Sadler (2012), Melchin and others (2012), and Peng and others (2012).

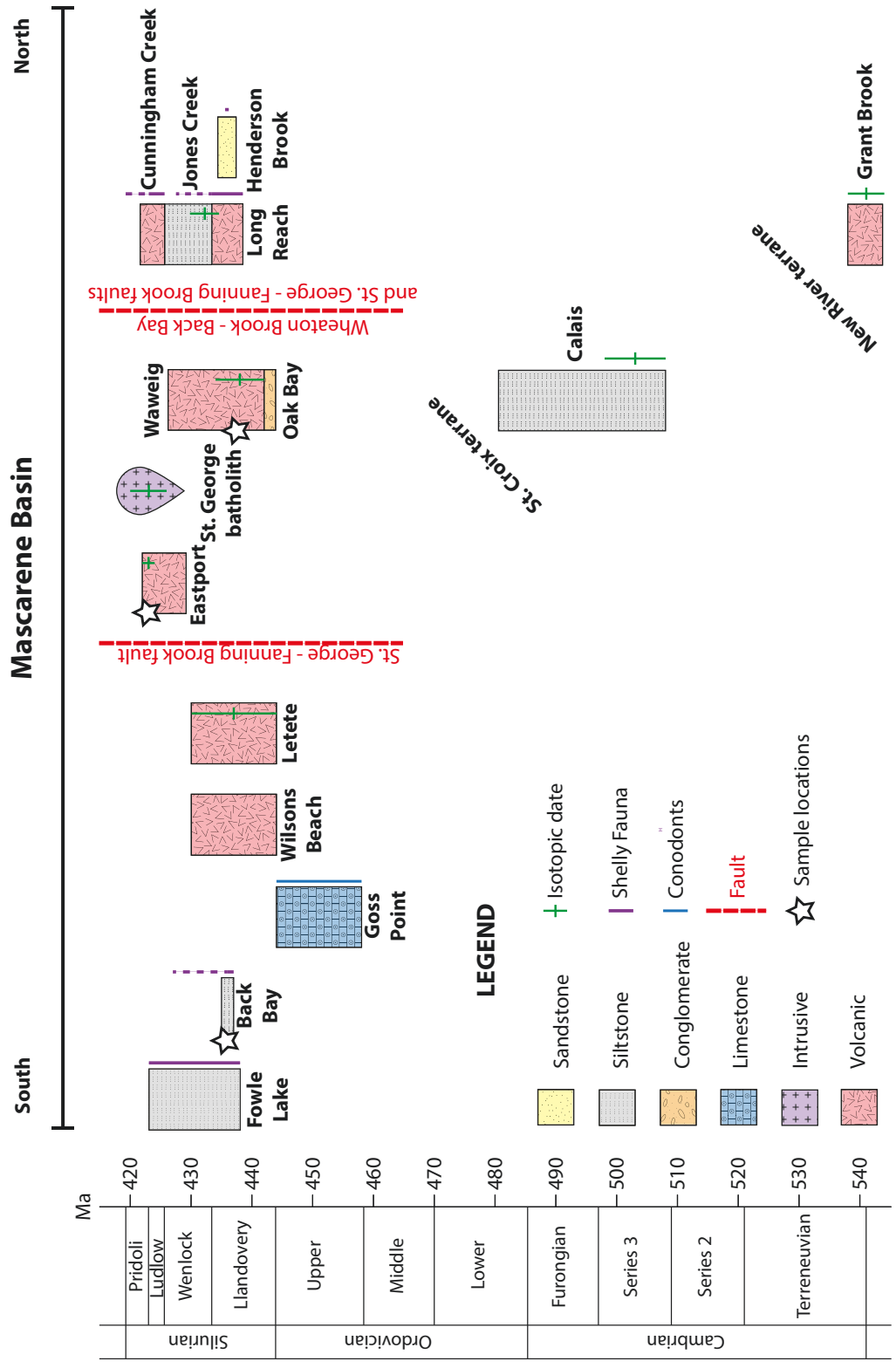

Avalonia with Ganderia, along a northerly-dipping subduction zone beneath Ganderia's southern margin (Fyffe and others, 1999; Van Wagoner and others, 2001, 2002; Fyffe and others, 2011; van Staal and others, 2014). In this hypothesis the Mascarene Basin is interpreted as Silurian back-arc basin fill, associated with volcanic and intrusive rocks of the Kingston arc to the southeast (Figure 3.2).

Coinciding with the deposition of the Mascarene Basin in the Silurian, the Fredericton Trough to the northwest was filled, deposited along the margins of a closing Iapetus Ocean, and sharing in part the same St. Croix terrane basement as the Mascarene Basin (Fyffe, 1995). Previous study (Chapter 2) has demonstrated the arrival of Laurentian detritus within the Fredericton Trough between the late Rhuddanian and mid-Wenlock, providing evidence that this part of Ganderia accreted to Laurentia during this time. Although these two basins share the same basement terrane, post-depositional faulting and differing lithologies (notably the paucity of volcanic input in the Fredericton Trough) suggest separated depositional settings, and a more complex convergent scenario. There are few existing constraints on when the Mascarene Basin, and southernmost Ganderian terranes, converged with a composite Laurentia, which this detrital zircon study attempts to address.

2.2 Stratigraphy

The Mascarene Basin (Fyffe and others, 1999) is filled by Late Ordovician to late Silurian bimodal volcanic-sedimentary rocks of the Mascarene Group (Figure 3.3). The basin is filled by ca. 2 to 3 km of mixed sedimentary and volcanic rocks (King and Barr, 2004) overstepping the boundary between its St. Croix terrane basement to the north, and New River terrane basement to the south (Figure 3.2). However, the basin is a composite of lithologically similar successions with similar faunal assemblages (Fyffe and others, 1999), which are divided by many faults; few formations within the basin are in stratigraphic contact with one another. The Mascarene Basin is correlated with the Coastal Volcanic Belt in Maine, and is coeval with arc-related igneous rocks

of the Kingston terrane to the south.

Numerous formations are considered part of the Mascarene Group in New Brunswick (Figures 3.2, 3.3), found in four main fault-bounded sequences (Miller and Fyffe, 2002). The Oak Bay Formation, unconformably overlain by the Waweig Formation, is composed of polymictic conglomerate interbedded with sandstone; brachiopods in a limestone clast suggest an early Silurian age (Cumming, 1967). The Waweig Formation consists of sandstone interbedded with mudstone and tuff; U-Pb zircon dating (TIMS) of a tuff within the formation yielded a Llandovery age of 438 ± 4 Ma (Miller and Fyffe, 2002). The St. George batholith intrudes the Waweig Formation and obscures its contact with the Eastport Formation; however, mapping relationships suggest that the latter may be conformable upon the Waweig Formation (Fyffe and others, 2011; Johnson and others, 2012). The Eastport Formation bears a felsic tuff dated at 423 ± 1 Ma (Dadd and Van Wagoner, 2001; van Wagoner and others, 2001), and includes bimodal volcanic rocks interbedded with an increasing proportion of sandstone, siltstone, and mudstone towards the upper portion of the unit. The Goss Point Formation is composed mainly of limestone interbedded with quartzite and tuff, with conodonts indicating a Late Ordovician (Caradoc to Ashgill, ca. 458 to 444 Ma: Cooper and Sadler, 2012) age (Nowlan and others, 1997). Shale, siltstone, and sandstone of the Fowle Lake Formation bears a diverse fossil assemblage indicating a Llandovery (C3, ca. 438 Ma: Cocks and others, 1970; Melchin and others, 2012) to Ludlow age (Johnson and McLeod, 1996). The Letete Formation is composed of bimodal volcanics, quartz wacke, mudstone, siltstone, and tuff, with a U-Pb zircon age from a felsic tuff of 437 ± 7 Ma (Miller and Fyffe, 2002). The lithologically similar Wilsons Beach Formation is correlated to the Letete Formation (McLeod and others, 2001), and has no additional age control. The Back Bay Formation includes sandstone, grey to green siltstone and mudstone, conglomerate, and volcanic rock, and bears fossils suggesting a Late Llandovery age (Boucot and others, 1966). The Henderson Brook Formation is of similar age and lithology, consisting of polymictic conglomerate, volcanic rock, sandstone and other clastic rock, and bears fossils suggesting a Llandovery (C5, ca. 436 Ma: Cocks and others, 1970; Melchin and

others, 2012) age (McCutcheon and Boucot, 1984). An outlier of Henderson Brook Formation sits unconformably on the Grant Brook Formation of the New River terrane, dated at 541 ± 3 Ma from zircons in its type locality (Johnson and others, 2009). The Long Reach Formation is composed mainly of volcanic rocks, sandstone and siltstone, and bears brachiopods suggesting a late Llandovery to Wenlock age (Boucot and others, 1966; Berry and Boucot, 1970). Its depositional age is further constrained by the conformably (McCutcheon and Ruitenberg, 1987) overlying Jones Creek Formation, which bears an interlayered dacite dated at 432.2 ± 2.4 Ma (Dadd and Van Wagoner, 2001). The Jones Creek Formation consists of feldspathic arenite, wacke, siltstone and volcanic rock. The Cunningham Creek Formation conformably (Johnson, 2000) overlies the Jones Creek Formation, and consists of mudstone, siltstone, tuff, and other volcanic rocks. It contains fossil assemblages suggesting a late Ludlow to Pridoli age (Turner, 1986; others).

Within this complex basin, three formations were selected for detrital zircon analysis based on the most robust depositional age constraints, and lithologies likely to yield detrital zircon from basement source rocks. Those selected are the Waweig, Back Bay, and Eastport Formations. The Waweig Formation is located in southwestern New Brunswick, striking northeast from Oak Bay past the Digdeguash River along the northern margin of the St. George batholith (Figure 3.2). The formation includes, from oldest to youngest: volcaniclastic conglomerate and sandstone of the Campbell Point Member; interbedded mudstone and tuff of the Sawyer Brook Member; and sandstone, mudstone, and tuff of the Simpson Corner Member (Fyffe and others, 1999). The latter member is up to 3000 m thick, while the others are about 600 m each, for a total formation thickness of about 4200 m over a belt 5 km wide. The Waweig Formation conformably overlies the early Silurian Oak Bay Formation; a detrital zircon study by Fyffe and others (2009) reported only peri-Gondwanan sources within this formation. The Oak Bay Formation in turn unconformably overlies the Ordovician Cookson Group of the St. Croix terrane (Fyffe and others, 1999, 2011). The Waweig Formation is intruded by the Early Devonian Magaguadavic Granite in the east (Fyffe, 2005; McLeod and others, 2005a), and the probably late Silurian

(based on a coeval relationship with the Utopia Granite: McLeod, 1990) Bocabec Gabbro to the south (Fyffe, 2005). Brachiopods were previously interpreted to indicate a late Ludlow to Pridoli age (ca. 424 to 419 Ma: Melchin and others, 2012) for the Simpson Corner Member (Boucot and others, 1966; Pickerill, 1976). However, analysis by Miller and Fyffe (2002) of a felsic tuff from the Campbell Point Member provided a U-Pb zircon age of 438 ± 4 Ma (Llandovery); from this and other data, the authors subsequently questioned the validity of assigning late Silurian ages based specifically on the occurrence of *Salopina* sp., but allow that the thickness of the Waweig Formation may mean that it extends to the Ludlow. The upper age limit is constrained by the intrusion into the Simpson Corner Member (Fyffe and others, 1999) of the Bocabec Gabbro in the late Silurian: the Utopia Granite, coeval with the Bocabec Gabbro, has been dated at 423 ± 3 Ma (U-Pb age) (McLeod, 1990; McLaughlin and others, 2003). The Waweig Formation may be conformably overlain by the Eastport Formation to the south (Fyffe and others, 2011).

The Back Bay Formation, extending several hundred meters along the shore of Back Bay near the village of the same name (Figure 3.2), consists of shale, slate, quartz wacke and arenite, and volcanic wacke. It has a thickness of about 300 m and a relatively limited extent. The formation is in faulted contact with adjacent units (McLeod and others, 2005b), including the Letete Formation and igneous rocks of the New River terrane. The Back Bay Formation has a late Llandovery (C4-C5, or about 437-436 Ma: Cocks and others, 1970; Melchin and others, 2012) depositional age based on the occurrence of the brachiopod *Pentamerus* sp. (Boucot and others, 1966). Other fossils are consistent with a late Llandovery to Wenlock age (Boucot and others, 1966), corresponding to approximately 437-427 Ma in the timescale of Melchin and others (2012).

The Eastport Formation is present along the shore of Passamaquoddy Bay, and extends northeast past Utopia Lake and southeast into Maine (Figure 3.2). It is composed of interbedded mafic and felsic flows, red sandstone and siltstone, and dips gently south (Fyffe and others, 2011). The formation is intruded by the late Silurian Utopia Granite (423 ±3 Ma U-Pb age) and Bocabec

Gabbro (McLeod, 1990; McLaughlin and others, 2003) and the Mesozoic Ministers Island Dyke (Dunn and Stringer, 1990). A felsic tuff within the Eastport Formation yielded an age of 423 ± 1 Ma (Dadd and Van Wagoner, 2001; van Wagoner and others, 2001), approximately at the Ludlow-Pridoli boundary, although fossil assemblages previously suggested the Early Devonian (Pickerill and Pajari, 1976). It is unconformably overlain by the Late Devonian Perry Formation. The formation is up to 4000 m thick in the Passamaquoddy Bay area, and consists of four cycles of bimodal volcanic-sedimentary rocks, including the dated felsic tuff (Dadd and Van Wagoner, 2001; van Wagoner and others, 2001, 2002). The Eastport Formation may conformably overlie the Waweig Formation, in which case it would probably overstep the St. Croix-New River boundary in the subsurface (Fyffe and others, 2011).

2.3 Structure

The Mascarene Basin consists of four main fault-bounded successions of similar age and lithology, with few stratigraphic contacts. The four sequences include (Figure 3.3): 1) Oak Bay and Waweig Formations. 2) Eastport Formation, and other formations in the Coastal Volcanic Belt in Maine. 3) Goss Point, Back Bay, Fowle Lake, Letete, and Wilsons Beach Formations. 4) Henderson Brook, Long Reach, Jones Creek, and Cunningham Creek Formations. Correlative formations in Maine may include the Quoddy, Dennys, Edmunds, Hersey, and Leighton Formations (Miller and Fyffe, 2002).

The northern margin of the Mascarene Basin is bounded by the Sawyer Brook Fault (Figure 3.2), which juxtaposes Oak Bay against the Calais and Kendall Mountain Formations of the St. Croix terrane (Fyffe and others, 2011). However, the contact is an angular unconformity between the Oak Bay and Calais Formations (Fyffe and others, 1999, 2011). The faulting, where present, between the Calais and Oak Bay Formations has been interpreted to mark the initiation of rifting or opening of the Mascarene Basin (Fyffe and others, 1999, 2011). Rocks of the Mascarene Group are also juxtaposed (at its northern margin) against the New River terrane by the St.

George – Fanning Brook Fault, which becomes an internal fault within the Mascarene Basin to the west of the St. George Batholith (Fyffe and others, 2011). The southern contact of the Mascarene Basin, also against the New River terrane, is marked by the Wheaton Brook – Back Bay Fault (Fyffe and others, 2011; Johnson and others, 2012).

The contrasting lithologies of the Mascarene Basin and the Fredericton Trough suggest that, though sharing the same Ganderian St. Croix terrane basement, the two were not juxtaposed in their present position until after deposition. In addition, the study of faults separating the basins (Fyffe and others, 1999; Park and Whitehead, 2003; Park and others, 2008), and the unique tectonic setting of the Fredericton Trough (Chapter 2), suggest a more complex scenario of convergence, where the St. Croix terrane basement may not have been continuous between the two basins.

3. Detrital zircon geochronology

3.1 Sampled units

The Waweig Formation (Figure 3.2; Figure 3.3) was sampled from the Campbell Point Member (Fyffe and others, 1999; Johnson and others, 2007) at a road cut along New Brunswick Route 1. About 400 m northwest lies the northeast-southwest trending contact with the Oak Bay Formation. Approximately 7 km northeast, along strike, felsic tuff from the Campbell Point Member has been sampled and dated at 438 ± 4 Ma (Miller and Fyffe, 2002). A detrital zircon sample was obtained from a bed about 20 cm thick, a fine-grained, volcaniclastic, quartz-rich and feldspathic sandstone. It is a well-indurated, grey weathering rock, surrounded by other similar beds along with reworked and welded tuffs. Surrounding beds have a laminated texture in finer-grained portions and are locally calcareous. The unit strikes to the northeast, and dips moderately to steeply southeast.

Thin section analysis of the sample (Figure 3.4) indicates the rock is a feldspathic wacke

Figure 3.4: Thin section photomicrographs from three sampled formations of the Mascarene Group.

A: Eastport Formation (plane-polarized light, ppl). B: Eastport Formation (cross-polarized light, xpl). C: Waweig Formation (ppl). D: Waweig Formation (xpl). E: Back Bay Formation (ppl). F: Back Bay Formation (xpl).

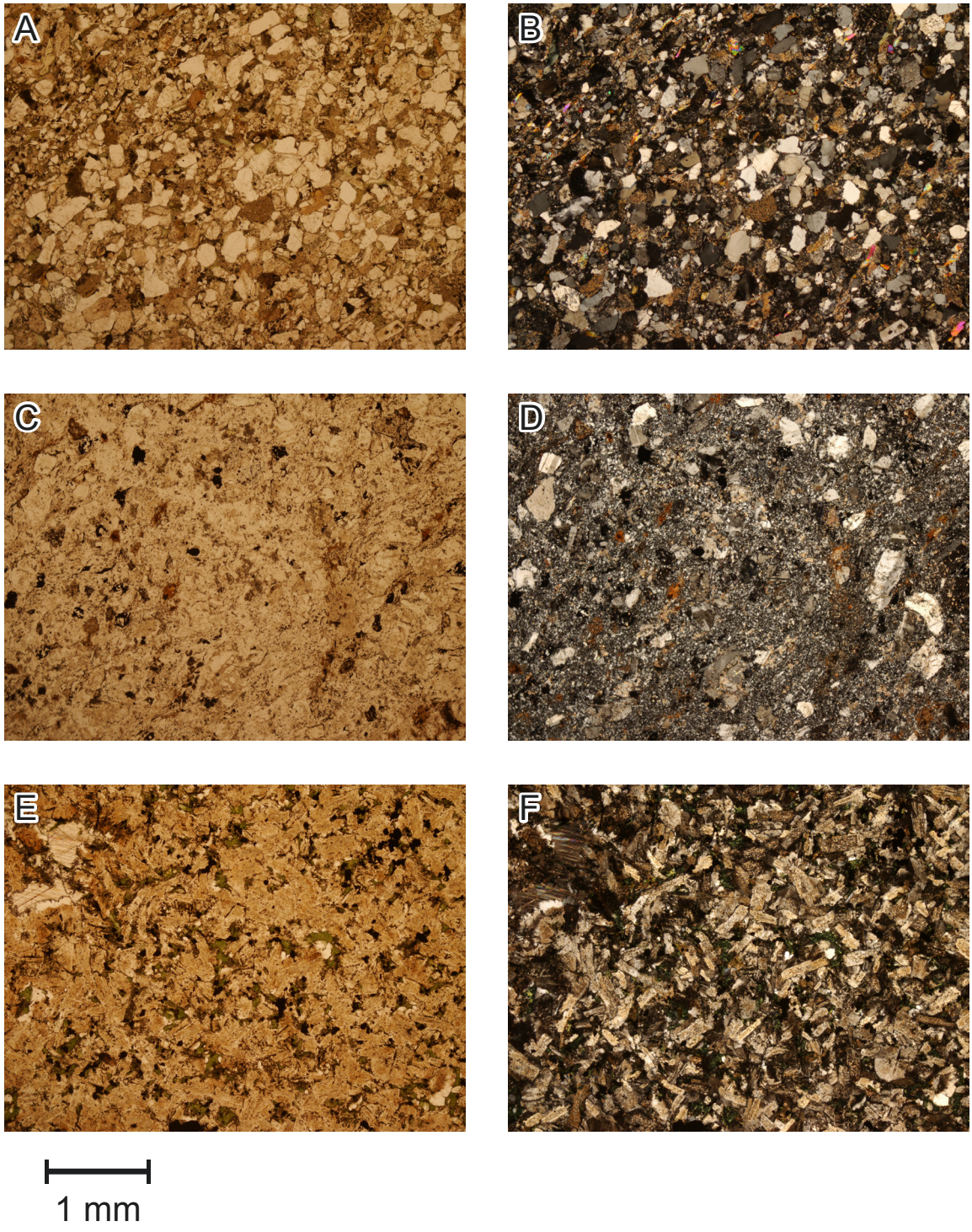

(classifications are after Dott, 1964), with a very high proportion of matrix (68%). Framework grains are feldspar-rich, and typically sub-angular to sub-rounded. Normalized to total QFL (quartz, feldspar, lithic fragment) components, they include 27% quartz, 68% feldspar, and 5% lithic fragments. The feldspar is about two-thirds potassium feldspar, and one-third plagioclase. Veins are commonly parallel to bedding, and filled by opaque minerals and clays. The section is locally very calcareous, and includes recrystallized calcite. Alteration is common in both the framework grains and the matrix, including calcite, white mica, chlorite, and glauconite. While the largest clasts may range up to 1 mm, the average framework grain size is about 220 microns, or fine sand. The section has no obvious foliation, but bedding is readily observed. Overall, the sample is very texturally immature. Cathodoluminescence (CL) imaging (Figure 3.5) of selected zircons from this sample shows that they tend to be sub-angular in shape, and frequently display oscillatory zoning. Inherited cores and crystal overgrowths are also observed.

The Back Bay Formation (Figure 3.3) was sampled at a *Pentamerus* fossil locality (Boucot and others, 1966) along the shore of Back Bay, south of the town of Back Bay, about 500 m west of Douglas Island (Figure 3.2). The sampled bed, about 15 cm thick, is grey-green, fine-grained, quartz-rich sandstone, and is surrounded by beds of similar lithology and thicknesses ranging from a few centimeters to several meters. The rock is highly fractured, and bedding is typically unclear. A second common lithology in the vicinity includes pink to green, fine to medium-grained volcaniclastic sandstone with abundant euhedral feldspar laths up to 5 mm long. Less commonly, dark brown volcanic clasts are also present, accompanied by brown haloes in surrounding rock. A third lithology is locally interlayered with the first, and consists of green mudstone layers from 2 to 5 cm thick. This rock type is highly veined and fractured, with volcanic interbeds. The mudstones are cleaved at a low angle to bedding, and many veins are bedding parallel. Bedding is clearer here than in other lithologies, particularly along contacts with the coarser beds of the first lithology, and strikes north-northeast, dipping steeply.

Thin section analysis (Figure 3.4) of the sampled rock from this formation indicates it is a

Figure 3.5: Representative cathodoluminescence images of zircons from sampled formations of the Mascarene Group.

Circles show location of 30 micron laser ablation spots.

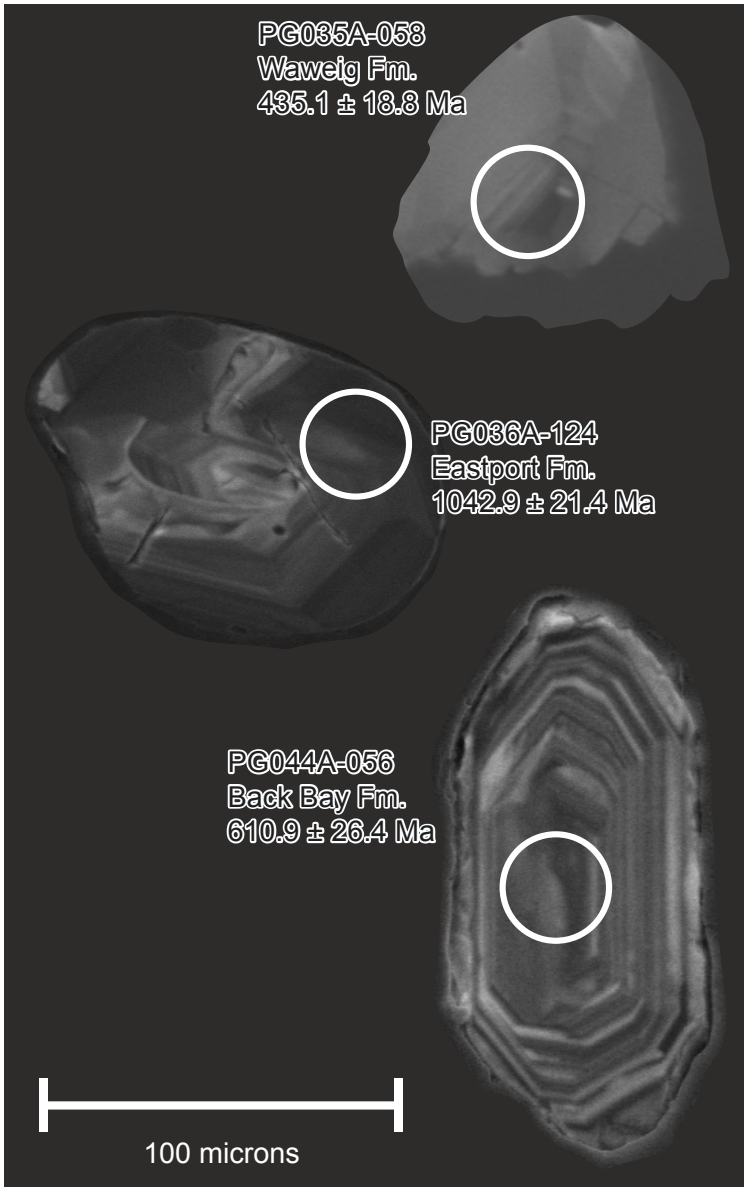

feldspathic wacke with about 21% matrix, and includes 15% quartz and 85% feldspar (75% of which is potassium feldspar), normalized to total QFL components. Accessory phases include chlorite and opaque minerals. Both chlorite and calcite are present as cement, but the rock appears to be more matrix-supported. The matrix includes chlorite, quartz, feldspar, opaque minerals, and calcite. The rock is very texturally immature and tuffaceous, with no obvious bedding or other fabric. While feldspars are typically angular, quartz grains may be more rounded. Framework grains tend to have poorly defined grain boundaries, whether resulting from heavy alteration, or reflecting their depositional setting. Large feldspar laths range up to 2 mm in length, but framework grain size in general is much smaller, averaging about 200 microns (fine sand). CL imaging of zircon studied from this sample (Figure 3.5) shows both sub-rounded and sub-angular shapes. Larger, more rounded grains frequently correspond to older zircons, while smaller, angular grains, often with oscillatory zoning, have younger ages. Both types may show overgrowths, inherited cores, and textures suggestive of metamictization or recrystallization.

The Eastport Formation (Figure 3.3) was sampled along the northwest shore of Bayside, about 1 km northeast of St. Croix Island (Figure 3.2). It is mapped as the youngest part of the formation, Cycle 4 (Van Wagoner and others, 2002). A felsic tuff from the Eastport Formation in the Passamaquoddy Bay area has been dated as 423 ± 1 Ma (Dadd and Van Wagoner, 2001; Van Wagoner and others, 2001). The sampled bed, about 20 cm thick, is a fine-grained, grey-green, quartz-rich, micaceous and feldspathic sandstone. It is part of a continuous shoreline outcrop showing little deformation, apart from some near-vertical jointing. The beds locally strike north, and dip sub-horizontally eastward. Other lithologies in the exposure include cleaved mudstones and vesicular basaltic flows.

Thin section analysis (Figure 3.4) indicates that the sampled rock is a feldspathic wacke, composed of 63% quartz, 31% feldspar, and 6% lithic fragments (QFL normalized), and including about 40% matrix. Many quartz grains are polycrystalline, or show subgrain boundaries. Feldspar is about one third plagioclase, and two thirds potassium feldspar. Lithic

fragments are mainly chert. Accessory phases include white mica, chlorite, pyroxene, and opaque minerals. In comparison to the previous sampled formations, framework grains of the Eastport Formation are much less altered. The rock is also more mature in appearance, and clasts are sub-angular to sub-rounded. Bedding is observable in thin section, but no other fabric is present. CL imaging of selected zircon from this sample (Figure 3.5) shows an assortment of zircon morphologies, from rounded to more angular forms. As seen in previous samples, larger zircons tend to be more rounded, and typically correspond to the older zircons of the sample. Smaller zircons tend to be more angular, typically show oscillatory zoning, and often have young ages. Oscillatory zoning is very common, as are overgrowths and inherited cores, and various textures or amorphous internal structures suggest recrystallization or metamictization.

3.2 Methods

Previous work has established the efficacy of detrital zircon geochronology in solving geological problems in the Appalachian-Caledonide orogen (Cawood and Nemchin, 2001; Cawood and others, 2003, 2004; Murphy and others, 2004; Waldron and others, 2012; Macdonald and others, 2014; Waldron and others, 2014a). This and other research has established that Laurentian provenance is indicated by a dominant zircon peak at 1.0 to 1.1 Ga (attributed to the Grenville orogen), with an asymmetric tail extending up to 2.0 Ga (representing other Meso- and Paleoproterozoic orogens in the Canadian Shield); this is typically accompanied by a lack of grains in the 2.0 to 2.4 Ga range (Cawood and Nemchin, 2001; Waldron and others, 2014a). In contrast, rocks of peri-Gondwanan provenance, such as those found in terranes not yet linked to Laurentia, lack the conspicuous Laurentian “Grenville” peak, and typically bear one or more prominent zircon peaks in the 550 to 650 Ma range (Fyffe and others, 2009). Different peri-Gondwanan terranes may differ slightly: Avalonia normally displays slightly older populations in this Neoproterozoic range, and typical Ganderian populations fall within the younger part of the range (Pollock and others, 2007). Early Cambrian (ca. 540 to 510 Ma) populations are also indicative of Ganderia, being very rare in Avalonia and absent in Laurentia (Pollock and

others, 2007). Also characteristic of peri-Gondwanan terranes are zircon peaks in the 2.0 to 2.2 Ga range (normally absent in rocks of Laurentian provenance), possibly indicating derivation from the Eburnean orogen of West Africa or the Trans-Amazonian orogen of Amazonia (Pollock and others, 2007; Waldron and others, 2009, 2011, 2014a). A diverse range of Mesoproterozoic zircon may also be present, particularly in Ganderian rocks, suggesting sources from Amazonia (Pollock and others, 2007).

Three formations of the Mascarene Group were chosen for analysis by detrital zircon geochronology. The depositional age of each formation was constrained by either fossil control (the Back Bay Formation) or previously published U-Pb zircon geochronology of felsic tuffs (the Waweig and Eastport Formations). Samples ranging from 10 to 20 kg were taken from the coarsest sandstone layers of each unit, avoiding obvious volcanogenic horizons (which would tend to yield high proportions of contemporary volcanic zircon, and under-representative proportions of detrital zircon derived from source terrane basement, critical to provenance determination). Weathered, veined, mineralized, or otherwise altered parts of the sampled formations were also avoided. Each rock sample was individually crushed and milled, using a jaw crusher and disk mill, to release individual minerals from the rock matrix. Samples were then processed using a Wilfley water table to concentrate heavy minerals (including zircon, pyrite, and others). The heavy fraction of each sample was then sieved with a standard 70 size nylon mesh (approximately 210 μm) to remove uncrushed or aggregate particles. The coarse fractions were inspected to ensure that they did not contain discrete heavy mineral crystals. The sieved heavy portions were then processed using a Frantz Isodynamic separator (model L-1) in freefall operation to remove highly magnetic material, and with a Frantz Barrier Laboratory separator (model LB-1) to remove other magnetically susceptible minerals (e.g. Rosenblum and Brownfield, 2000). The non-magnetic portions of each sample were then processed using methylene iodide (specific gravity of 3.32) in a standard separatory funnel, producing a final heavy mineral concentrate from the sinking fraction. These final portions consisted primarily of zircon and pyrite; if large proportions of pyrite overwhelmed any zircon present, the sample

was lastly treated with a nitric acid solution to dissolve pyrite and leave only the most refractory minerals, effectively concentrating zircon. Otherwise, pyrite (and other obvious non-zircon) was simply picked aside in a clean culture dish. To keep zircon selection as random as possible, and avoid introducing bias towards particular zircon populations, grains were not individually selected for analysis. Instead, the remaining zircon-rich portions were mounted in epoxy. Each mount was then polished to expose the interior of the grains, and imaged by energy-dispersive X-ray spectroscopy to identify zircon (and non-zircon) in each sample. Further backscattered electron and/or cathodoluminescent imaging were used to reveal crystal structure and other features (such as igneous zonation, inherited cores, and altered rims).

128 to 329 zircon grains from each mount were analyzed at the Canadian Centre for Isotopic Microanalysis (CCIM) at the University of Alberta, using procedures modified from Simonetti and others (2005) for measuring for U-Pb isotopic data using LA-MC-ICP-MS. Each zircon is typically represented by a single spot analysis, due to physical grain size restrictions and the need to avoid bias by over-representing an age. When discrete cores and rims can be distinguished, they are represented by separate analyses (ex. 001A and 001B within grain 001). Sample PG036A (the Eastport Formation) was additionally analyzed a second time via LA-Q-ICP-MS at the same facility. The multi-collector instrumentation consisted of a New Wave UP-213 laser ablation system interfaced with a Nu Plasma MC-ICP-MS, with three ion counters to measure Pb isotopes and twelve Faraday buckets measuring ^{238}U, ^{235}U, ^{205}Tl, and ^{203} Tl. The laser was operated with a beam diameter of 30 microns, 4 Hz pulse frequency and fluence of ~3 J/cm^2. A He atmosphere was maintained in the ablation cell at a flow rate of 1 L/min. Output from this cell was combined with that from a standard Nu Instruments desolvating nebulizer (DSN). Sampled unknown zircon grains were analyzed in groups of 10, with data collected statically in thirty 1 s integrations. Separating each set of analyses, on peak gas + acid blanks were measured over a duration of 30 s, and two zircon reference materials were analyzed to monitor U-Pb fractionation, reproducibility, and instrumental drift: LH94-15 (1830 ± 1 Ma; Ashton and others, 1999; Simonetti and others, 2005; Heaman, unpublished data) and GJ1-32 (606 Ma; Jackson and

others, 2004; Elhlou and others, 2006; Heaman, unpublished data). Mass bias for Pb isotopes was corrected for by concurrently measuring $^{205}Tl/^{203}Tl$ from an aspirated 0.5 ppb Tl solution (NIST SRM 997), utilizing an exponential mass fractionation law and assuming a natural $^{205}Tl/^{203}Tl$ of 2.3871. Data were reduced using an offline Excel-based spreadsheet, in which sample (unknown) isotopic ratios were corrected based on standard analyses, using a cutoff value of $^{207}Pb/^{206}Pb = 0.0658$ (800 Ma): young grains were normalized to GJ1-32, and old grains to LH94-15. This ensures unknowns are normalized to standards of a similar age; natural gaps in our data often occur at 800 Ma, making this a convenient choice of cutoff. Uncertainties were reported using a quadratic combination of the standard error of the measured isotopic ratio, and the standard deviation of the standard means. Reproducibility of the zircon standards is estimated at about ~1% ($^{207}Pb/^{206}Pb$) and 2% ($^{206}Pb/^{238}U$) (2σ). Sample measurements were discarded in the case of obvious inclusions that contributed to analysis (and could not be isolated), an extreme common Pb component, or analysis of non-zircons. Common Pb corrections after Simonetti and others (2005) were typically applied when measured ^{204}Pb exceeded ~400 cps.

The quadrupole instrumentation employed in additional analysis of the Eastport Formation consisted of a New Wave UP-213 laser ablation system interfaced with a Thermo Scientific ICAP-Q. The laser was operated with a beam diameter of 40 microns, at a frequency of 5 Hz and fluence of ~3-4 J/cm^2. A He atmosphere in the ablation cell was maintained at a flow rate of 0.5 L/min. Output from this cell was combined with an Ar make-up gas line (0.55 L/min) and an N_2 line (4 mls/min) prior to entering the injector. The instrument was auto-tuned by ablating NIST 612, and manually adjusting the Ar make-up gas to achieve a U/Th ratio of about ~1.05. Data were collected in time-resolved mode with each analysis taking about 70 s, including a 25 s blank, and with a 30-45 s washout between analyses. Dwell times were 50 ms for masses 238, 235, 232, and 208, and 80 ms for masses 207, 206, 204, 202, for an estimated duty cycle of about 550 ms. Zircon reference materials GJ1-32 and LH94-15 were measured as before, between sets of 10-20 analyses. Data were reduced offline using the program Iolite and the visual-age data reduction scheme (DRS). A cutoff of $^{207}Pb/^{206}Pb = 0.0658$ was likewise applied:

young zircons were normalized to GJ1-32 as the primary standard, and older zircons to LH94-15. Reported uncertainties are a quadratic combination of the internal measurement precision and the reproducibility of the standards analyzed during the session. Analyses containing significant amounts of common Pb were corrected after the method of Anderson (2002).

The resulting data (combining, in the Eastport Formation, the results of both analytical sessions) were studied with the use of Isoplot (version 3.75: Ludwig, 2012), utilizing concordia diagrams, weighted means, MSWD calculations, probability density plots, and other standard methods. Other analysis tools from the Arizona LaserChron Center (Gehrels and others, 2006) were used to produce cumulative probability plots, and perform Kolmogorov-Smirnov tests, which test the null hypothesis that two distributions could represent the same population.

3.3 Results

Analyses of 140 zircons of the Waweig Formation (Figures 3.6, 3.7) produced almost entirely contemporary zircon: rejecting grains with worse than 10% discordancy (as with all reported data, unless noted), this population ranges from 402.8 ± 25.3 Ma to 469.1 ± 20.8 Ma (analyses with $^{207}Pb/^{206}Pb$ ratios less than 0.0658, or 800 Ma, are reported as $^{206Pb}/^{238}U$ ages, with 2-sigma errors; $^{207}Pb/^{206}Pb$ ages are reported otherwise). A weighted mean calculation for this entire population of 70 concordant grains yields a mean of 429.9 ± 3.4 Ma at 95% confidence; however, the range is overscattered with an MSWD of 2.1 and a very low probability of fit of 0.00000025. A possible break in the population separates grains younger than approximately 450 Ma; this 60 grain subset yields a mean of 426.0 ± 2.4 Ma at 95% confidence, with an MSWD of 0.98 and a probability of fit of 0.52. The remaining older subset of 10 grains then gives a mean of 459.1 ± 6.6 Ma, MSWD of 0.28, probability of fit 0.98. However, given the relatively high continuity in the contemporary zircon population, and the error associated with each measurement, it is difficult to be certain whether these are two discrete populations. The previous radiometric age (TIMS) for this locality is 438 ± 4 Ma (Miller and Fyffe, 2002), significantly older than the mean

of 426.0 ± 2.4 Ma for the youngest subset, and slightly outside of overlapping the 429.9 ± 3.4 Ma mean calculated for the entire population of young zircon. In addition to this near-contemporary zircon, two other grains (less than 10% discordant) were analyzed, at 675.7 ± 32.6 Ma and 1749.2 ± 19.5 Ma.

Analyses of 129 zircons of the Back Bay Formation (Figures 3.6, 3.7) display a prominent zircon peak at ca. 610 Ma, a relatively continuous range of 67 zircons from 550 Ma to 680 Ma. A secondary peak, of 6 zircons, has a mean of 431.7 ± 7.7 Ma, MSWD of 0.80, probability of fit 0.55. This is within error of a late Llandovery depositional age suggested by Boucot and others (1966) based on the occurrence of *Pentamerus* sp. Remaining concordant grains (5 zircons) are scattered throughout the 1.0 to 1.9 Ga range, at: 1069.5 ± 22.3 Ma, 1114.8 ± 27.2 Ma, 1722.3 ± 20.9 Ma, 1870.7 ± 34.3 Ma, and 1874.4 ± 19.4 Ma.

The Eastport Formation (Figures 3.6, 3.7), of which 329 zircons were analysed in two sessions, bears a large portion of zircon near-contemporary with the depositional age, including a population of 25 concordant grains at 424.1 ± 3.0 Ma, with an MSWD of 1.3 and probability of fit of 0.14. This is within error of a felsic tuff dated at 423 ± 1 Ma (Dadd and Van Wagoner, 2001; van Wagoner and others, 2001). About 18 other early Paleozoic zircons range from the latest Silurian to mid-Cambrian, ca. 440 Ma to 515 Ma. A range of about 21 zircons spans the late Neoproterozoic from about 550 Ma to 670 Ma, including an over-scattered peak of 12 zircons at 606.2 ± 8.5 Ma, MSWD 2.3 and probability of fit 0.007. An additional 4 grains populate the early Neoproterozoic from ca. 815 Ma to 890 Ma. Remaining zircon is largely concentrated in the 1.0 to 1.7 Ga range (44 grains), including 9 grains forming a double peak in the late Mesoproterozoic (ca. 1.00 to 1.07 Ga). Remaining older grains are at 2152.6 ± 18.3 Ma, 2155.9 ± 17.9 Ma, 2213.5 ± 17.7 Ma, and 2667.8 ± 16.6 Ma.

4. Discussion

Results from the Waweig Formation are broadly consistent with its previous (Llandovery)

Figure 3.6: Detrital zircon probability density plots and cumulative probability plots for sampled formations of the Mascarene Group, and other formations for comparison. Plots consist of ages <10% discordant. Analyses with $^{207}Pb/^{206}Pb$ ratios of less than 0.0658 are reported as $^{206}Pb/^{238}U$ ages; $^{207}Pb/^{206}Pb$ ages are reported otherwise. A: Eastport Formation. B: Waweig Formation. C: Back Bay Formation. D: Oak Bay Formation (Fyffe and others, 2009). E: Calais Formation, St. Croix terrane (Fyffe and others, 2009). F: Matthews Lake Formation, New River terrane (Fyffe and others, 2009). G: Burtts Corner Formation, Fredericton Trough (Chapter 2). H: Hayes Brook Formation, Fredericton Trough (Chapter 2). Note that the data reported by Fyffe and others (2009) is replotted here with a 10% discordance filter.

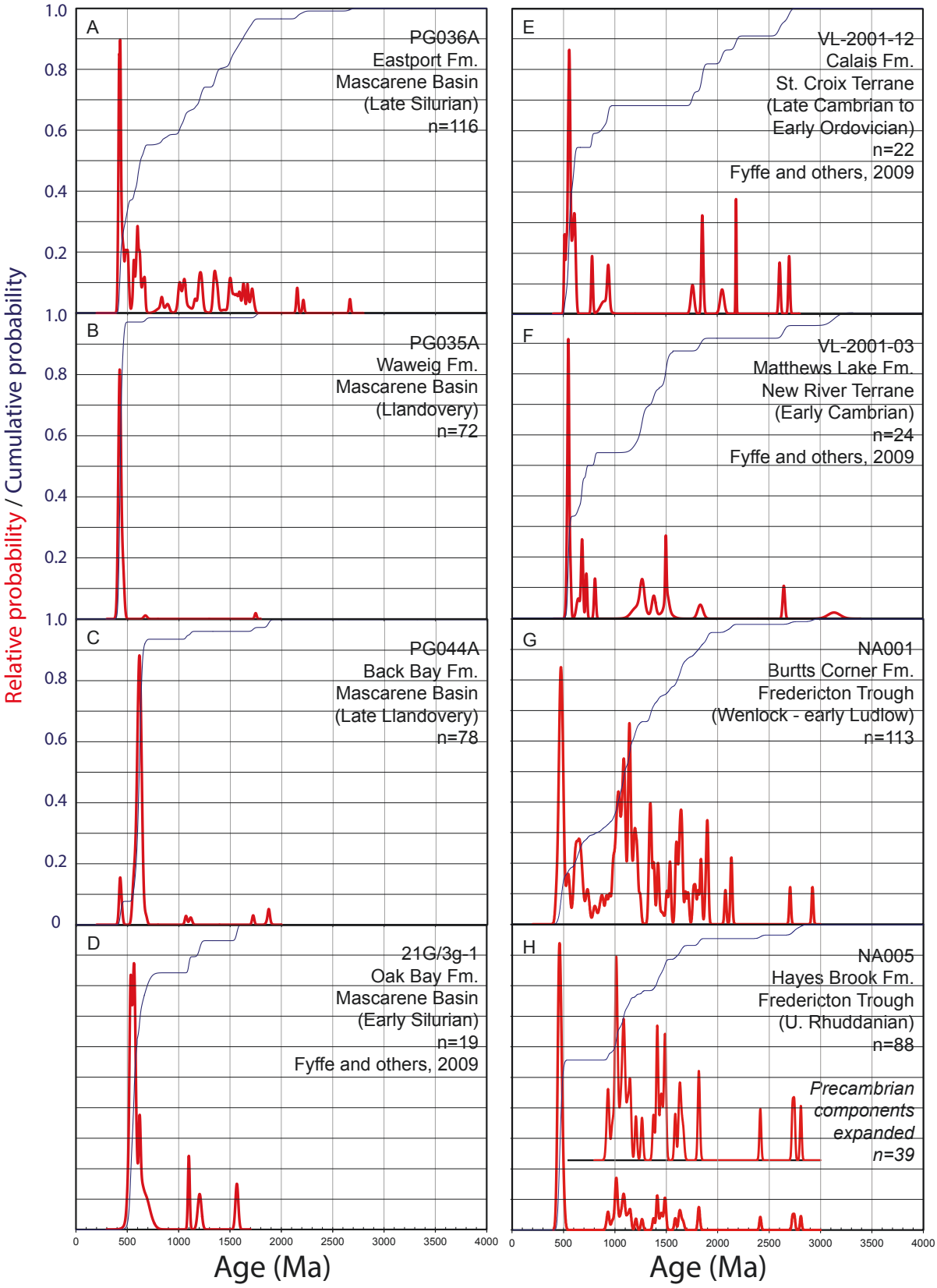
Relative probability / Cumulative probability
1.0
0.8
0.6
0.4
0.2
0
A
PG036A
Eastport Fm.
Mascarene Basin
(Late Silurian)
n=116
B
PG035A
Waweig Fm.
Mascarene Basin
(Llandovery)
n=72
C
PG044A
Back Bay Fm.
Mascarene Basin
(Late Llandovery)
n=78
D
21G/3g-1
Oak Bay Fm.
Mascarene Basin
(Early Silurian)
n=19
Fyffe and others, 2009
E
VL-2001-12
Calais Fm.
St. Croix Terrane
(Late Cambrian to
Early Ordovician)
n=22
Fyffe and others, 2009
F
VL-2001-03
Matthews Lake Fm.
New River Terrane
(Early Cambrian)
n=24
Fyffe and others, 2009
G
NA001
Burtts Corner Fm.
Fredericton Trough
(Wenlock - early Ludlow)
n=113
H
NA005
Hayes Brook Fm.
Fredericton Trough
(U. Rhuddanian)
n=88
Precambrian
components
expanded
n=39
0
500
1000
1500
2000
2500
3000
3500
4000
Age (Ma)

Figure 3.7: Selected weighted means and MSWDs for sampled formations of the Mascarene Group.

See text for discussion. Plots consist of $^{206}Pb/^{238}U$ ages <10% discordant. A: Waweig Formation, n=70. 429.9 ± 3.4 Ma. MSWD: 2.1, probability of fit: 0.00000025. B: Waweig Formation, n=60. 426.0 ± 2.4 Ma. MSWD: 0.98, probability of fit: 0.52. C: Waweig Formation, n=10. 459.1 ± 6.6 Ma. MSWD: 0.28, probability of fit: 0.98. D: Back Bay Formation, n= 6. 431.7 ± 7.7 Ma. MSWD: 0.80, probability of fit: 0.55. E: Eastport Formation, n=25. 424.1 ± 3.0 Ma. MSWD: 1.3, probability of fit: 0.14. F: Eastport Formation, n=12. 606.2 ± 8.5 Ma. MSWD: 2.3, probability of fit: 0.007.

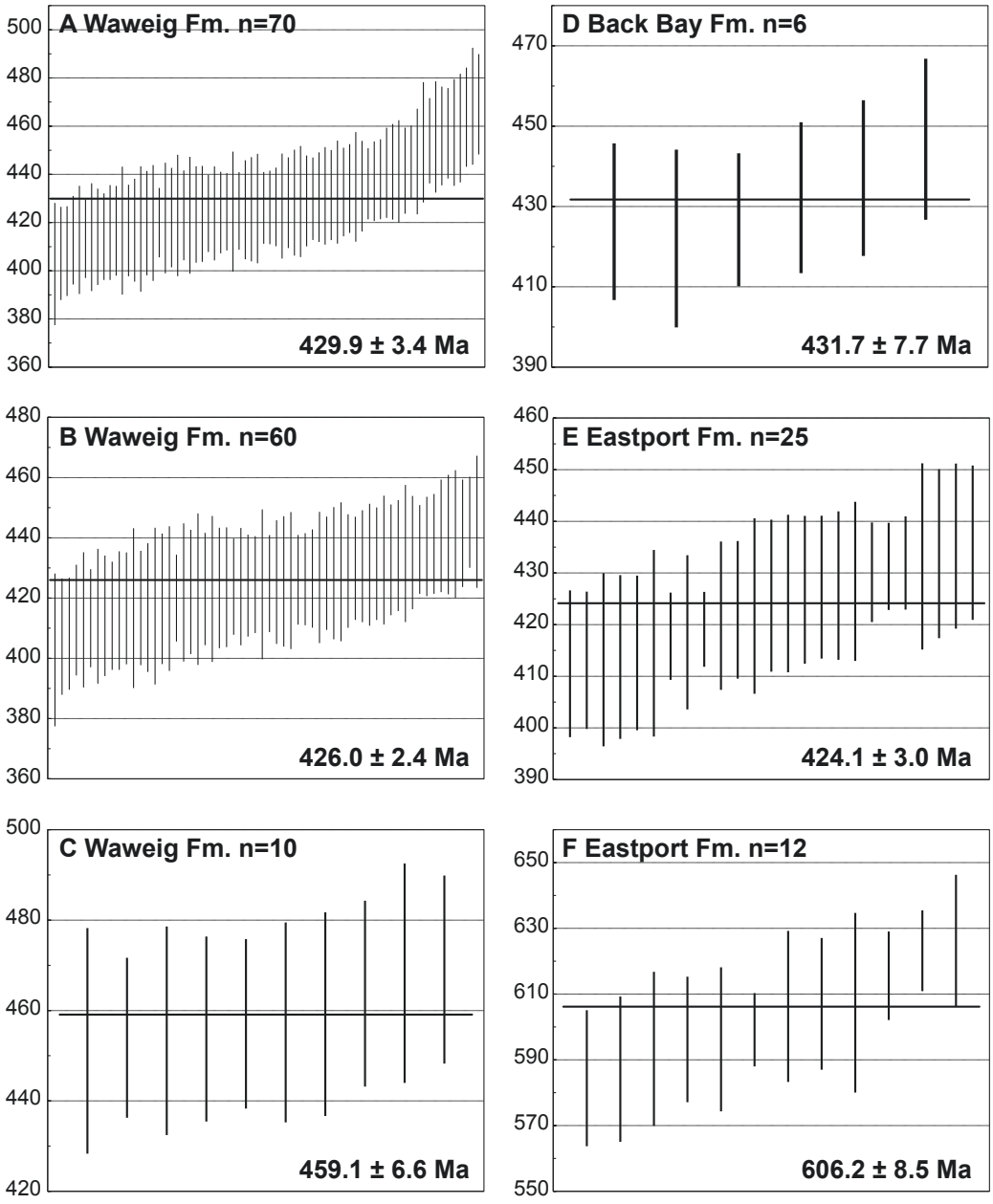

radiometric age of 438 ± 4 Ma (Miller and Fyffe, 2002). However, the weighted mean and MSWD calculations may suggest two populations at 426.0 ± 2.4 Ma and 459.1 ± 6.6 Ma. These uncertainties are probably underestimated due to the large number of analyses; uncertainties of ~2-3% are more likely. The continuity of the populations, and the conflict of the younger population with the previously determined radiometric age, suggest that this is a single population at about 429.9 ± 3.4 Ma with excess scatter. Isoplot calculations suggest an additional constant external error of 4.7% in this scenario, though the scatter could be geological as well (representing a prolonged period of volcanism). An alternative explanation, that the 426.0 ± 2.4 Ma age accurately reflects the depositional age range of the 600 m thick Campbell Point Member, would require that the sampled unit is significantly younger than the dated tuff, possible due to unexposed stratigraphic and/or structural complications in the 7 km along-strike interval between the locations. The remaining two grains from this sample are insufficient to determine provenance. Future work may seek other horizons in the formation that are more likely to yield detrital zircon from source terranes, closer to dated units. Additionally, more precise (TIMS) dating of young grains in the existing sample may provide better constraints on its depositional age.

The early Silurian Back Bay Formation, dominated by Neoproterozoic zircon and lacking any distinctive Laurentian signature, is consistent with peri-Gondwanan provenance. Available fossil evidence, particularly the occurrence of *Pentamerus* sp. (Boucot and others, 1966), indicates a late Llandovery depositional age for the Back Bay Formation (C4-C5, or about 437-436 Ma: Cocks and others, 1970; Melchin and others, 2012), which is consistent with our youngest zircons at 431.7 ± 7.7 Ma. These results are corroborated by detrital zircon study of the early Silurian Oak Bay Formation (Fyffe and others, 2009), which bears a continuous range of zircons from about 490 to 700 Ma, with peaks reported at 548 ± 8 Ma, 619 ± 15 Ma, and 680 ± 26 Ma, and a few Mesoproterozoic zircons at 1097 ± 12 Ma, 1178 ± 30 Ma, 1568 ± 37 Ma. The Neoproterozoic peaks are similarly suggestive of peri-Gondwanan sources, and the late Neoproterozoic/earliest Cambrian peak may suggest Ganderia specifically. This suggests that,

Figure 3.8: Schematic tectonic setting of the Mascarene Group.
A: Early Silurian (Late Llandovery) setting of the Oak Bay and Back Bay Formations. B: Late Silurian (Ludlow-Pridoli) setting of the Eastport Formation. Arrows show extent of Laurentian or peri-Gondawnan detritus. AV: Avalonia. BB: Back Bay Formation. BSC: Brunswick subduction complex. EP: Eastport Formation. KA: Kingston arc. LR: Laurentia. NR: New River terrane. OB: Oak Bay Formation. PVA: Popelogan-Victoria arc. SC: St. Croix terrane.

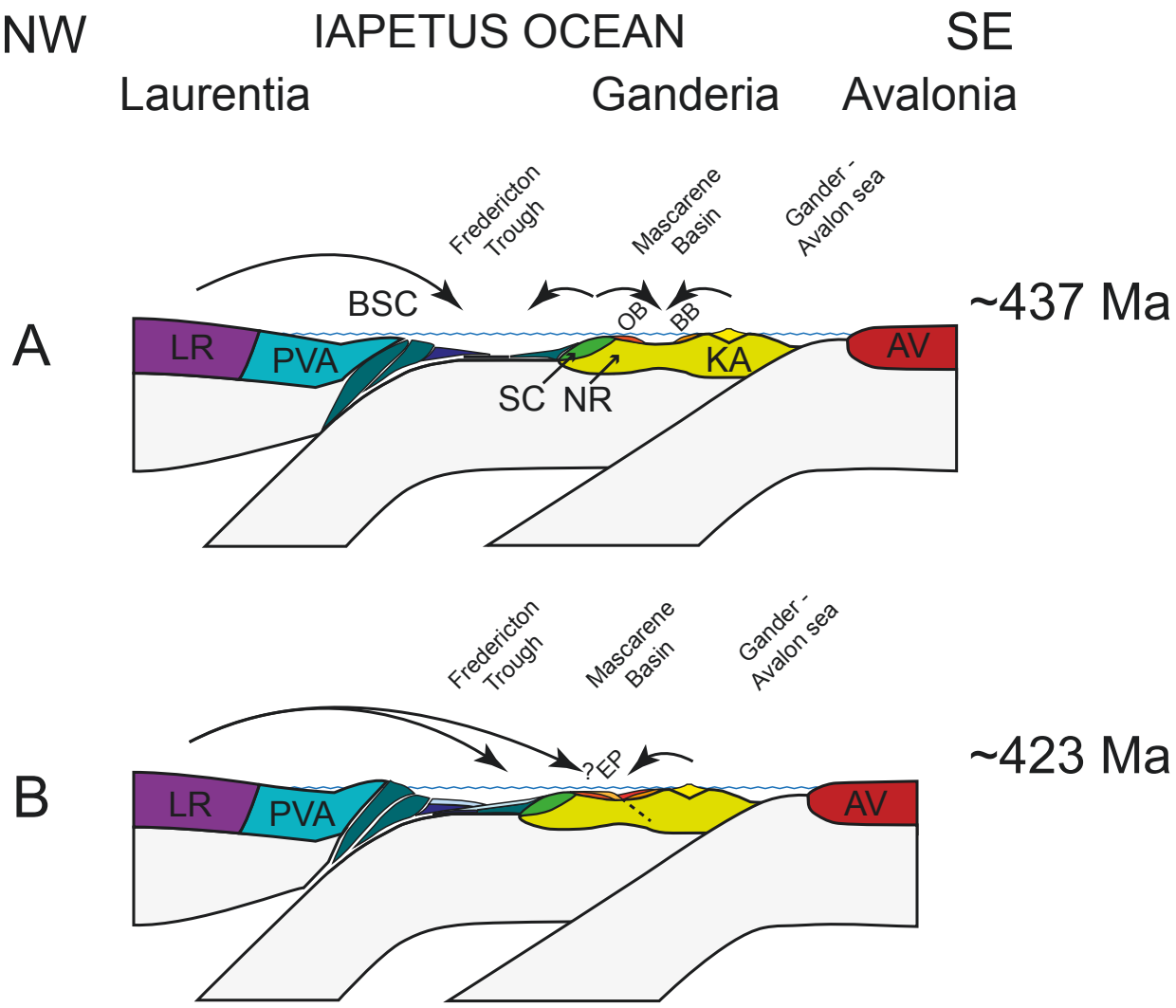

during the late Llandovery, part or all of the Mascarene Basin was separated from the Laurentian margin (Figure 3.8). This likely indicates that a remnant of the Iapetus Ocean persisted until this time, or that Ganderian basement to the north formed a barrier to detritus from Laurentia, or some combination of the two. The persistence of an Iapetan seaway, forming a barrier to otherwise ubiquitous and pervasive Laurentian detritus, is supported by analogous detrital zircon studies in the Fredericton Trough (Chapter 2).

The late Silurian Eastport Formation bears a mixed detrital zircon signature, and is clearly different than the older Back Bay Formation. The Neoproterozoic (ca. 605 Ma) zircon population is typical of peri-Gondwanan samples, and the presence of Cambrian zircon may suggest Ganderia specifically (Pollock and others, 2007). The Mesoproterozoic zircon, while contrasting with the older Back Bay Formation, is more ambiguous. It spans the "Grenville" range (1.0 to 1.1 Ga) typical of Laurentian provenance, but not as the prominent asymmetric peak we see in more typical Laurentian samples (Chapter 2, Waldron and others, 2014a), nor in great proportions relative to other Meso-Paleoproterozoic zircon. K-S testing (Figure 3.9) points out the similarity of the Eastport Formation with the Hayes Brook Formation (Fredericton Trough, New Brunswick: see Chapter 2), showing Laurentian provenance. When Paleozoic zircon is excluded (to compare only the pre-Paleozoic history of the samples), similarity is shown with the Burtts Corner Formation (Fredericton Trough, New Brunswick: see Chapter 2), which was interpreted as showing a mixed provenance of both Laurentian and peri-Gondwanan sources. One of the lowest D-values reported is for these two samples, suggesting that similarity is independent of sample size. However, the same testing shows it is decidedly dissimilar from the Flume Ridge Formation (Fredericton Trough, New Brunswick: see Chapter 2), interpreted as having Laurentian provenance. Additional comparison suggests similarity between the Eastport Formation and a number of Ganderian terranes (Fyffe and others, 2009), including the Calais Formation and Matthews Lake Formation, from the St. Croix and New River terranes respectively, basement to the Mascarene Basin. These results allow the possibility that the Eastport Formation received detritus from both Laurentian and peri-Gondwanan sources. This

Figure 3.9: Kolmogorov-Smirnov test results.

K-S tests comparing samples of the Mascarene Group to formations of the Fredericton Trough (Chapter 2), other samples from the Mascarene Basin and Ganderian terranes (Fyffe and others, 2009). Testing compares only age data <10% discordant. P-values and D-values were calculated using errors in the cumulative density function. P-values less than 0.05 are probably from different populations (at a confidence level of 95%). P-values greater than 0.05 are highlighted, and are unlikely to be from different populations. Note that very small sample sizes may not produce meaningful comparisons (the Waweig Fm. in B, n=2, is greyed out).

A: All age data **K-S P-values using error in the CDF** **D-values using error in the CDF**

	Eastport Fm. PG036A (n=116)	Waweig Fm. PG035A (n=72)	Back Bay Fm. PG044A (n=78)	Oak Bay Fm. 21G/3g-1 (n=19)	Calais Fm. VL-2001-12 (n=22)	Matthews Lake Fm. VL-2001-03 (n=24)	Burtts Corner Fm. NA001A (n=113)	Hayes Brook Fm. NA005A (n=88)	Flume Ridge Fm. NA010A (n=115)	Digdeguash Fm. NA003A (n=90)
Eastport Fm.		0.000	0.000	**0.069**	0.028	0.010	0.000	**0.053**	0.000	0.000
Waweig Fm.	0.000		0.000	0.000	0.000	0.000	0.000	0.000	0.000	0.000
Back Bay Fm.	0.000	0.000		0.046	0.011	0.000	0.000	0.000	0.000	0.039
Oak Bay Fm.	**0.069**	0.000	0.046		**0.253**	**0.078**	0.000	0.001	0.000	0.006
Calais Fm.	0.028	0.000	0.011	**0.253**		**0.753**	0.027	0.000	0.007	**0.093**
Matthews Lake Fm.	0.010	0.000	0.000	**0.078**	**0.753**		**0.203**	0.000	**0.105**	0.020
Burtts Corner Fm.	0.000	0.000	0.000	0.000	0.027	**0.203**		0.000	**0.502**	0.000
Hayes Brook Fm.	**0.053**	0.000	0.000	0.001	0.000	0.000	0.000		0.000	0.000
Flume Ridge Fm.	0.000	0.000	0.000	0.000	0.007	**0.105**	**0.502**	0.000		0.000
Digdeguash Fm.	0.000	0.000	0.039	0.006	**0.093**	0.020	0.000	0.000	0.000	

	Eastport Fm. PG036A (n=116)	Waweig Fm. PG035A (n=72)	Back Bay Fm. PG044A (n=78)	Oak Bay Fm. 21G/3g-1 (n=19)	Calais Fm. VL-2001-12 (n=22)	Matthews Lake Fm. VL-2001-03 (n=24)	Burtts Corner Fm. NA001A (n=113)	Hayes Brook Fm. NA005A (n=88)	Flume Ridge Fm. NA010A (n=115)	Digdeguash Fm. NA003A (n=90)
Eastport Fm.		0.661	0.384	0.321	0.339	0.364	0.289	0.190	0.314	0.314
Waweig Fm.	0.661		0.895	0.961	0.972	0.972	0.879	0.702	0.792	0.944
Back Bay Fm.	0.384	0.895		0.352	0.390	0.543	0.666	0.478	0.667	0.217
Oak Bay Fm.	0.321	0.961	0.352		0.318	0.391	0.547	0.512	0.573	0.428
Calais Fm.	0.339	0.972	0.390	0.318		0.199	0.342	0.530	0.392	0.295
Matthews Lake Fm.	0.364	0.972	0.543	0.391	0.199		0.240	0.551	0.273	0.349
Burtts Corner Fm.	0.289	0.879	0.666	0.547	0.342	0.240		0.394	0.109	0.551
Hayes Brook Fm.	0.190	0.702	0.478	0.512	0.530	0.551	0.394		0.300	0.492
Flume Ridge Fm.	0.314	0.792	0.667	0.573	0.392	0.273	0.109	0.300		0.575
Digdeguash Fm.	0.314	0.944	0.217	0.428	0.295	0.349	0.551	0.492	0.575	

B: Pre-Paleozoic age data only

	Eastport Fm. PG036A (n=73)	Waweig Fm. PG035A (n=2)	Back Bay Fm. PG044A (n=72)	Oak Bay Fm. 21G/3g-1 (n=14)	Calais Fm. VL-2001-12 (n=20)	Matthews Lake Fm. VL-2001-03 (n=22)	Burtts Corner Fm. NA001A (n=94)	Hayes Brook Fm. NA005A (n=39)	Flume Ridge Fm. NA010A (n=85)	Digdeguash Fm. NA003A (n=84)
Eastport Fm.		0.866	0.000	0.007	**0.107**	**0.448**	**0.179**	0.006	0.000	0.000
Waweig Fm.	0.866		0.131	0.498	0.763	0.969	0.955	0.728	0.740	0.462
Back Bay Fm.	0.000	0.131		**0.373**	0.006	0.000	0.000	0.000	0.000	0.032
Oak Bay Fm.	0.007	0.498	**0.373**		**0.265**	**0.183**	0.000	0.000	0.000	**0.124**
Calais Fm.	**0.107**	0.763	0.006	**0.265**		**0.725**	0.003	0.000	0.000	**0.062**
Matthews Lake Fm.	**0.448**	0.969	0.000	**0.183**	**0.725**		0.032	0.002	0.000	0.011
Burtts Corner Fm.	**0.179**	0.955	0.000	0.000	0.003	0.032		**0.334**	**0.059**	0.000
Hayes Brook Fm.	0.006	0.728	0.000	0.000	0.000	0.002	**0.334**		**0.910**	0.000
Flume Ridge Fm.	0.000	0.740	0.000	0.000	0.000	0.000	**0.059**	**0.910**		0.000
Digdeguash Fm.	0.000	0.462	0.032	**0.124**	**0.062**	0.011	0.000	0.000	0.000	

	Eastport Fm. PG036A (n=73)	Waweig Fm. PG035A (n=2)	Back Bay Fm. PG044A (n=72)	Oak Bay Fm. 21G/3g-1 (n=14)	Calais Fm. VL-2001-12 (n=20)	Matthews Lake Fm. VL-2001-03 (n=22)	Burtts Corner Fm. NA001A (n=94)	Hayes Brook Fm. NA005A (n=39)	Flume Ridge Fm. NA010A (n=85)	Digdeguash Fm. NA003A (n=84)
Eastport Fm.		0.429	0.643	0.491	0.305	0.210	0.171	0.336	0.326	0.541
Waweig Fm.	0.429		0.836	0.627	0.496	0.364	0.366	0.500	0.488	0.610
Back Bay Fm.	0.643	0.836		0.267	0.431	0.593	0.811	0.931	0.919	0.231
Oak Bay Fm.	0.491	0.627	0.267		0.350	0.374	0.633	0.786	0.774	0.340
Calais Fm.	0.305	0.496	0.431	0.350		0.214	0.445	0.593	0.611	0.328
Matthews Lake Fm.	0.210	0.364	0.593	0.374	0.214		0.340	0.500	0.488	0.385
Burtts Corner Fm.	0.171	0.366	0.811	0.633	0.445	0.340		0.180	0.198	0.683
Hayes Brook Fm.	0.336	0.500	0.931	0.786	0.593	0.500	0.180		0.109	0.833
Flume Ridge Fm.	0.326	0.488	0.919	0.774	0.611	0.488	0.198	0.109		0.822
Digdeguash Fm.	0.541	0.610	0.231	0.340	0.328	0.385	0.683	0.833	0.822	

would require that by the time of deposition of this part of the Eastport Formation (423 ± 1 Ma: Dadd and Van Wagoner, 2001; Van Wagoner and others, 2001), the Mascarene Basin had been juxtaposed to and in sedimentary communication with the Laurentian margin (Figure 3.8). The greater proportion of peri-Gondwanan detritus, relative to that from Laurentia, would probably have resulted from the unique depositional setting of the Eastport Formation, farther outboard relative to the Laurentian margin and its accreted terranes, and more proximal to peri-Gondwanan sources. These observations may also have resulted from receiving detritus from a Burtts Corner Formation-like source of mixed provenance to the north, further diluted in the Eastport Formation by proximal peri-Gondwanan sources.

The provenance contrast between the early Silurian Back Bay and late Silurian Eastport Formations indicates new, more diverse sources of detritus in the Mascarene Basin over time. It may, additionally, suggest the arrival time of Laurentian detritus within the Mascarene Basin, requiring the juxtaposition of its Ganderian basement with Laurentia by this time, due to the associated closure of the Iapetus Ocean. If this were the case, then this accretion must have been after the late Llandovery (ca. 437-436 Ma) depositional age of the Back Bay Formation, but before the 423 ± 1 Ma age of the Eastport Formation (approximately at the Ludlow-Pridoli boundary). A remnant of the Iapetus Ocean, dividing the composite Laurentian continent from these southern components of Ganderia, must have persisted until at least the late Llandovery, and had essentially closed by the Ludlow-Pridoli boundary.

This scenario is consistent with that suggested by detrital zircon analysis of the Fredericton Trough (see Chapter 2), a Silurian basin to the north of the Mascarene Group, deposited along the margins of a closing Iapetus. The Fredericton Trough is divided by the northeast trending Fredericton Fault. Formations south of this fault unconformably overlie Ganderian (St. Croix terrane) basement, and formations north of the fault do not have exposed basement relationships (though they are currently in faulted contact with the Ganderian Miramichi terrane at its northern edge). Upper Rhuddanian (early Llandovery) formations of the Fredericton Trough, north

and south of the fault, bear distinctly contrasting detrital zircon signatures that indicate the persistence of the Iapetus Ocean at this time. This ocean probably closed by the mid-Wenlock, indicated by the appearance of Laurentian detritus in the youngest formation south of the Fredericton Fault. This closure juxtaposed Laurentia with southern components of Ganderia, including the St. Croix terrane basement. These combined results suggest that Laurentian detritus progressively encroached upon successively accreted terranes: the Fredericton Trough by the mid-Wenlock, and the Mascarene Basin by the Ludlow-Pridoli boundary. However, limited depositional age constraints of the formations in question prevent us from resolving the difference in timing between the arrival of Laurentian detritus in the Fredericton Trough and the Mascarene Basin. Additionally, the ambiguous sources in the Eastport Formation allow a different scenario: that Laurentian sediment did not reach the Eastport Formation until after its deposition (423 ± 1 Ma). This hiatus after the arrival of Laurentian detritus in the Fredericton Trough could indicate a barrier to sedimentation, such as an oceanic remnant or an uplifted basement block, or suggest different paleogeographic settings.

The paleogeography of these basins — the Mascarene Basin and the Fredericton Trough — introduces a further complication, as the two were probably not juxtaposed until after their deposition. As a result, their supposedly shared St. Croix terrane basement is ambiguous: they may have been distinct pieces of Ganderia, or in different settings. Similarly, post-depositional faulting within the Mascarene Basin itself could have juxtaposed formations that may have been separated before.

5. Conclusions

Three selected formations of the Mascarene Basin, in southern New Brunswick, were studied by means of detrital zircon geochronology, and have contributed to an understanding of Appalachian orogenesis:

1. A remnant of the Iapetus Ocean, dividing Laurentia from southern components of Gan-

deria, persisted until at least the late Llandovery, as recorded in the Back Bay Formation, and corroborated by previous study of the early Silurian Oak Bay Formation.

2. The juxtaposition of Laurentia with southern components of Ganderia, accompanied by the closure of the Iapetus Ocean, is a scenario suggested by the possible presence of Laurentian detritus within the Eastport Formation. This event would then have taken place after the Late Llandovery depositional age of the Back Bay Formation, and by the time of the deposition of the Eastport Formation at 423 ± 1 Ma.

3. This model is consistent with detrital zircon results from the Fredericton Trough, which records the arrival of Laurentian detritus after the Upper Rhuddanian (early Llandovery) and before the mid-Wenlock. However, due to the ambiguous sources within the Eastport Formation, further study is required before suggesting this as the most probable model.

4. The deposition of the Waweig Formation at about 429.9 ± 3.4 Ma is broadly consistent with the previously reported age of 438 ± 4 Ma from a tuff 7 km away along strike; the overscattered zircon population is insufficient to suggest a different depositional age.

6. References

Anderson, T., 2002, Correction of common lead in U-Pb analyses that do not report ^{204}Pb, Chemical Geology, v. 192, 59-79.

Ashton, K.E., Heaman, L.M., Lewry, J.F., Hartlaub, R.P., and Shi, R., 1999, Age and origin of the Jan Lake Complex: a glimpse at the buried Archean craton of the Trans-Hudson Orogen: Canadian Journal of Earth Sciences, v. 36, n. 2, p. 185-208.

Berry, W.B.N., and Boucot, A.J., editors, 1970, Correlation of the North American Silurian rocks: Geological Society of America, Special Papers, v. 102, 289 p.

Boucot, A.J., Johnson, J.G., Harper, C., and Walmsley, V.G., 1966, Silurian brachiopods and

gastropods of southern New Brunswick: Geological Survey Canada, Bulletin 140, 45 p.

Cawood, P.A., and Nemchin, A.A., 2001, Paleogeographic development of the East Laurentian margin: constraints from U-Pb dating of detrital zircons in the Newfoundland Appalachians: Geological Society of America Bulletin, v. 113, n. 9, p. 1234-1246.

Cawood, P.A., McCausland, P.J.A., and Dunning, G.R., 2001, Opening Iapetus: constraints from the Laurentian margin in Newfoundland: Geological Society of America Bulletin, v. 113, n. 4, p. 443-453.

Cawood, P.A., Nemchin, A.A., Smith, M., and Loewy, S., 2003, Source of the Dalradian Supergroup constrained by U-Pb dating of detrital zircon and implications for the East Laurentian margin: Journal of the Geological Society of London, v. 160, n. 2, p. 231-246.

Cawood, P.A., Nemchin, A.A., Strachan, R.A., Kinny, P.D., and Loewy, S., 2004, Laurentian provenance and an intracratonic tectonic setting for the Moine Supergroup, Scotland, constrained by detrital zircons from the Loch Eil and Glen Urquhart successions: Journal of the Geological Society of London, v. 161, n. 5, p. 861-874.

Cocks, L.R.M., Toghill, P., and Ziegler, A.M., 1970, Stage names within the Llandovery series: Geological Magazine, v. 107, n. 1, p. 79-87.

Cooper, R.A., and Sadler, P.M., 2012, The Ordovician Period, *in* Gradstein, F.M., Ogg, J.G., Schmitz, M.D. and Ogg, G.M., editors, The geologic time scale 2012: Oxford, Elsevier, p. 489-523.

Cumming, L.M., 1967, Geology of the Passamaquoddy Bay region, Charlotte County, New Brunswick: Geological Survey of Canada, Paper 65-29, 36 p.

Dadd, K.A., and Van Wagoner, N.A., 2001, Physical volcanology of the Silurian CVB rocks of Passamaquoddy Bay, southwestern New Brunswick, *in* Pickerill, R.K. and Lentz, D.R., editors, Guidebook to field trips in New Brunswick and western Maine: New England

Intercollegiate Geological Conference, Department of Geology, University of New Brunswick, Fredericton, New Brunswick, v. 93, p. C2.1-C2.13.

Dott, R.H., 1964, Wacke, graywacke and matrix—what approach to immature sandstone classification?: Journal of Sedimentary Research, v. 34, n. 3, p. 625-632.

Dunn, T., and Stringer, P., 1990, Petrology and petrogenesis of the Ministers Island Dike, Southwest New Brunswick, Canada: Contributions to Mineralogy and Petrology, v. 105, n. 1, p. 55-65.

Dunning, G.R., O'Brien, S.J., Colman-Sadd, S., Blackwood, R.F., Dickson, W.L., O'Neill, P.P., and Krogh, T.E., 1990, Silurian Orogeny in the Newfoundland Appalachians: The Journal of Geology, v. 98, n. 6, p. 895-913.

Elhlou, S., Belousova, E., Griffin, W.L., Pearson, N.J., and O'Reilly, S.Y., 2006, Trace element and isotopic composition of GJ-red zircon standard by laser ablation: Geochimica et Cosmochimica Acta, v. 70, n. 18 supplement, p. A158.

Fyffe, L.R., 1995, Fredericton Belt, *in* Williams, H., editor, Geology of the Appalachian-Caledonian Orogen in Canada and Greenland: Geological Survey of Canada, Geology of Canada, v. 6, p. 351-354.

Fyffe, L.R., 2005, Bedrock geology of the Rollingdam area (NTS 21 G/06), Charlotte County, New Brunswick: New Brunswick Department of Natural Resources, Minerals, Policy, and Planning Division, Plate 2005-29, scale 1:50000.

Fyffe, L.R., and Riva, J., 1990, Revised stratigraphy of the Cookson Group of southwestern New Brunswick and adjacent Maine: Atlantic Geology, v. 26, n. 3, p. 271-275.

Fyffe, L.R., Pickerill, R.K., and Stringer, P., 1999, Stratigraphy, sedimentology and structure of the Oak Bay and Waweig formations, Mascarene Basin; implications for the paleotectonic evolution of southwestern New Brunswick: Atlantic Geology, v. 35, n. 1; 1, p. 59-84.

Fyffe, L.R., Barr, S.M., Johnson, S.C., McLeod, M.J., McNicoll, V.J., Valverde Vaquero, P., van Staal, C.R., and White, C.E., 2009, Detrital zircon ages from Neoproterozoic and early Paleozoic conglomerate and sandstone units of New Brunswick and coastal Maine: implications for the tectonic evolution of Ganderia: Atlantic Geology, v. 45, p. 110-144.

Fyffe, L.R., Johnson, S.C., and van Staal, C.R., 2011, A review of Proterozoic to early Paleozoic lithotectonic terranes in the northeastern Appalachian Orogen of New Brunswick, Canada, and their tectonic evolution during Penobscot, Taconic, Salinic, and Acadian orogenesis: Atlantic Geology, v. 47, p. 211-248.

Gehrels, G., Valencia, V., and Pullen, A., 2006, Detrital zircon geochronology by laser-ablation multicollector ICPMS at the Arizona Laserchron Center, *in* Olszewski, T.D., editor, Geochronology: Emerging Opportunities: Paleontological Society Papers, v. 12, p. 67-76.

Hibbard, J.P., van Staal, C.R., Rankin, D.W., and Williams, H., 2006, Lithotectonic map of the Appalachian Orogen, Canada-United States of America: Geological Survey of Canada, Map 2096A, scale 1:1,500,000.

Hibbard, J.P., van Staal, C.R., and Rankin, D.W., 2007, A comparative analysis of pre-Silurian crustal building blocks of the northern and the southern Appalachian Orogen: American Journal of Science, v. 307, n. 1, p. 23-45.

Jackson, S.E., Pearson, N.J., Griffin, W.L., and Belousova, E.A., 2004, The application of laser ablation-inductively coupled plasma-mass spectrometry to in situ U–Pb zircon geochronology: Chemical Geology, v. 211, n. 1–2, p. 47-69.

Johnson, S.C., 2000, Bedrock geology of the Long Reach area (parts of NTS 21G/08a,b,g and h), southern New Brunswick: New Brunswick Department of Natural Resources and Energy, Minerals and Energy Division, Plate 2000-17.

Johnson, S.C., and McLeod, M.J., 1996, The New River Belt: a unique segment along the

western margin of the Avalon composite terrane, southern New Brunswick, Canada, *in* Nance, R.D. and Thompson, M.D., editors, Avalonian and related peri-Gondwanan terranes of the Circum-North Atlantic: Geological Society of America, Special Papers, v. 304, p. 149-164.

Johnson, S.C., McLeod, M.J., Fyffe, L.R., and Dunning, G.R., 2009, Stratigraphy, geochemistry, and geochronology of the Annidale and New River Belts, and the development of the Penobscot Arc in southern New Brunswick, *in* Martin, G.L., editor, Geological investigations in New Brunswick for 2008: New Brunswick Department of Natural Resources, Minerals, Policy, and Planning Division, Mineral Resource Report 2009-2, p. 141-218.

Johnson, S.C., McLeod, M.J., Fyffe, L.R., Thorne, K.G., Barr, S.M., and White, C.E., 2007, Southern New Brunswick field trip – June 20-22, 2007: New Brunswick Department of Natural Resources, Unpublished Field Guide, 30 p.

Johnson, S.C., McLeod, M.J., Barr, S.M., White, C.E., van Staal, C.R., Fyffe, L.R., and Thorne, K.G., 2012, Tectonic evolution of peri-Gondwanan terranes in southwestern New Brunswick, Canada: New Brunswick Department of Natural Resources, Lands, Minerals, and Petroleum Division, Field Guide No. 4, 62 p.

King, M.S., and Barr, S.M., 2004, Magnetic and gravity models across terrane boundaries in southern New Brunswick, Canada: Canadian Journal of Earth Sciences, v. 41, n. 9; 9, p. 1027-1047.

Li, Z.X., Bogdanova, S.V., Collins, A.S., Davidson, A., De Waele, B., Ernst, R.E., Fitzsimons, I.C.W., Fuck, R.A., Gladkochub, D.P., Jacobs, J., Karlstrom, K.E., Lu, S., Natapov, L.M., Pease, V., Pisarevsky, S.A., Thrane, K., and Vernikovsky, V., 2008, Assembly, configuration, and breakup history of Rodinia: a synthesis, *in* Bogdanova, S.V., Li, Z.X., Moores, E.M. and Pisaresvky, S.A., editors, Testing the Rodinia hypothesis: records in its building blocks:

Precambrian Research, v. 160, n. 1-2, p. 179-210.

Ludman, A., 1987, Pre-Silurian stratigraphy and tectonic significance of the St. Croix Belt, southeastern Maine: Canadian Journal of Earth Sciences, v. 24, n. 12, p. 2459-2469.

Ludman, A., 1991, Revised stratigraphy of the Cookson Group in eastern Maine and southwestern New Brunswick: an alternative view: Atlantic Geology, v. 27, n. 1, p. 49-55.

Ludwig, K.R., 2012, User's manual for Isoplot 3.75: Berkeley Geochronology Center Special Publication, 5, 75 p.

Macdonald, F.A., Ryan-Davis, J., Coish, R.A., Crowley, J.L., and Karabinos, P., 2014, A newly identified Gondwanan terrane in the northern Appalachian mountains: implications for the Taconic orogeny and closure of the Iapetus Ocean: Geology, v. 42, n. 6, p. 539-542.

McCutcheon, S.R., and Boucot, A.J., 1984, A new Lower Silurian fossil locality in the northeastern Mascarene-Nerepis Belt, southern New Brunswick: Maritime Sediments and Atlantic Geology, v. 20, n. 3, p. 121-126.

McCutcheon, S.R., and Ruitenberg, A.A., 1987, Geology and mineral deposits, Annidale-Nerepis area, New Brunswick, New Brunswick Department of Natural Resources and Energy, Mineral Resources Division, Memoir 2, 141 p.

McLaughlin, K.J., Barr, S.M., Hill, M.D., Thompson, M.D., Ramezani, J., and Reynolds, P.H., 2003, The Moosehorn plutonic suite, southeastern Maine and southwestern New Brunswick: age, petrochemistry, and tectonic setting: Atlantic Geology, v. 39, n. 2, p. 123-146.

McLeod, M.J., 1990, Geology, Geochemistry, and Related Mineral Deposits of the Saint George Batholith; Charlotte, Queens, and Kings Counties, New Brunswick: New Brunswick Department of Natural Resources and Energy, Mineral Resources, Mineral Resource Report 5, 169 p.

McLeod, M.J., and Pickerill, R.K., 2001, Bedrock geology of Campobello Island; remnants of a Silurian arc and back-arc complex in southwestern New Brunswick, *in* Pickerill, R.K. and Lentz, D.R., editors, Guidebook to field trips in New Brunswick and western Maine: New England Intercollegiate Geological Conference, Department of Geology, University of New Brunswick, Fredericton, New Brunswick, v. 93, p. B4.1-B4.20.

McLeod, M.J., Fyffe, L.R., and McCutcheon, S.R., 2005a, Bedrock geology of the McDougall Lake area (NTS 21 G/07), Charlotte County, New Brunswick: New Brunswick Department of Natural Resources, Minerals, Policy, and Planning Division, Plate 2005-30, scale 1:50000.

McLeod, M.J., Johnson, S.C., Barr, S.M., and White, C.E., 2005b, Bedrock geology of the St. George area (NTS 21 G/02), Charlotte County, New Brunswick: New Brunswick Department of Natural Resources, Minerals, Policy, and Planning Division, Plate 2005-27, scale 1:50000.

Melchin, M.J., Sadler, P.M., and Cramer, B.D., 2012, The Silurian Period, *in* Gradstein, F.M., Ogg, J.G., Schmitz, M.D. and Ogg, G.M., editors, The geologic time scale 2012: Oxford, Elsevier, p. 525-558.

Miller, B.V., and Fyffe, L.R., 2002, Geochronology of the Letete and Waweig Formations, Mascarene Group, southwestern New Brunswick: Atlantic Geology, v. 38, n. 1, p. 29-36.

Murphy, J.B., Pisarevsky, S.A., Nance, R.D., and Keppie, J.D., 2004, Neoproterozoic—early Paleozoic evolution of peri-Gondwanan terranes: implications for Laurentia-Gondwana connections, *in* Doerr, W., Finger, F., Linnemann, U. and Zulauf, G., editors, The Avalonian-Cadomian Belt and related peri-Gondwanan terranes: International Journal of Earth Sciences, v. 93, n. 5, p. 659-682.

Nance, R.D., Murphy, J.B., and Keppie, J.D., 2002, A Cordilleran model for the evolution of Avalonia: Tectonophysics, v. 352, n. 1-2, p. 11-31.

Nowlan, G.S., McCracken, A.D., and McLeod, M.J., 1997, Tectonic and paleogeographic significance of Late Ordovician conodonts in the Canadian Appalachians: Canadian Journal of Earth Sciences, v. 34, n. 11, p. 1521-1537.

Park, A.F., and Whitehead, J., 2003, Structural transect through Silurian turbidites of the Fredericton Belt southwest of Fredericton, New Brunswick: the role of the Fredericton Fault in late Iapetus convergence: Atlantic Geology, v. 39, n. 3, p. 227-237.

Park, A.F., Lentz, D.R., and Thorne, K.G., 2008, Deformation and structural controls on gold mineralization in the Clarence Stream shear zone, southwestern New Brunswick, Canada, *in* Thorne, K.G. and Castonguay, S., editors, Metallogeny and setting of gold systems in southern New Brunswick: implications for exploration in the Northern Appalachians: Exploration and Mining Geology, v. 17, n. 1-2, p. 51-66.

Peng, S., Babcock, L.E., and Cooper, R.A., 2012, The Cambrian Period, *in* Gradstein, F.M., Ogg, J.G., Schmitz, M.D. and Ogg, G.M., editors, The geologic time scale 2012: Oxford, Elsevier, p. 437-488.

Pickerill, R.K., 1976, Significance of a new fossil locality containing a Salopina community in the Waweig Formation (Silurian-uppermost Ludlow/Pridoli) of Southwest New Brunswick: Canadian Journal of Earth Sciences, v. 13, n. 9, p. 1328-1331.

Pickerill, R.K., and Pajari, G.E., J., 1976, The Eastport Formation (lower Devonian) in the northern Passamaquoddy Bay area, Southwest New Brunswick: Canadian Journal of Earth Sciences, v. 13, n. 2, p. 266-270.

Pollock, J.C., Wilton, D.H.C., van Staal, C.R., and Morrissey, K.D., 2007, U-Pb detrital zircon geochronological constraints on the Early Silurian collision of Ganderia and Laurentia along the Dog Bay Line: the terminal Iapetan suture in the Newfoundland Appalachians: American Journal of Science, v. 307, n. 2, p. 399-433.

Rosenblum, S., and Brownfield, I.K., 2000, Magnetic susceptibilities of minerals: United States Geological Survey, Open-File Report 99-529, 37 p.

Schulz, K.J., Stewart, D.B., Tucker, R.D., Pollock, J.C., and Ayuso, R.A., 2008, The Ellsworth terrane, coastal Maine: Geochronology, geochemistry, and Nd-Pb isotopic composition—Implications for the rifting of Ganderia: Geological Society of America Bulletin, v. 120, n. 9-10, p. 1134-1158.

Simonetti, A., Heaman, L., Hartlaub, R., Creaser, R., MacHattie, T., and Bohm, C., 2005, U-Pb zircon dating by laser ablation-MC-ICP-MS using a new multiple ion counting Faraday collector array: Journal of Analytical Atomic Spectrometry, v. 20, n. 8, p. 677-686.

Smith, E.A., 2005, Bedrock geology of southwestern New Brunswick (NTS 21 G, part of 21 B): New Brunswick Department of Natural Resources, Minerals, Policy, and Planning Division, Map NR-5 (Second Edition), scale 1:250000.

Smith, E.A., 2006, Bedrock geology of southeastern New Brunswick (NTS 21 H): New Brunswick Department of Natural Resources, Minerals, Policy, and Planning Division, Map NR-6 (Second Edition), 1:250000.

Turner, S., 1986, *Thelodus macintoshi* Stetson 1928, the largest known thelodont (Agnatha: Thelodonti): Breviora, v. 486, p. 1-18.

van Staal, C.R., and de Roo, J.A., 1995, Mid-Paleozoic tectonic evolution of the Appalachian Central mobile belt in northern New Brunswick, Canada: collision, extensional collapse and dextral transpression, *in* Hibbard, J.P., van Staal, C.R. and Cawood, P.A., editors, Current perspectives in the Appalachian-Caledonian Orogen: Geological Association of Canada, Special Paper, v. 41, p. 367-389.

van Staal, C.R., Currie, K.L., Rowbotham, G., Rogers, N., and Goodfellow, W., 2008, Pressure-temperature paths and exhumation of Late Ordovician-Early Silurian blueschists and

associated metamorphic nappes of the Salinic Brunswick subduction complex, Northern Appalachians: Geological Society of America Bulletin, v. 120, n. 11-12, p. 1455-1477.

van Staal, C.R., Whalen, J.B., Valverde-Vaquero, P., Zagorevski, A., and Rogers, N., 2009, Pre-Carboniferous, episodic accretion-related, orogenesis along the Laurentian margin of the Northern Appalachians, *in* Murphy, J.B., Keppie, J.D. and Hynes, A.J., editors, Ancient orogens and modern analogues: Geological Society of London, Special Publications, v. 327, p. 271-316.

van Staal, C.R., Barr, S.M., and Murphy, J.B., 2012, Provenance and tectonic evolution of Ganderia: constraints on the evolution of the Iapetus and Rheic Oceans: Geology, v. 40, n. 11, p. 987-990.

van Staal, C.R., Zagorevski, A., McNicoll, V.J., and Rogers, N., 2014, Time-transgressive Salinic and Acadian orogenesis, magmatism and Old Red Sandstone sedimentation in Newfoundland: Geoscience Canada, v. 41, n. 2, p. 138-164.

Van Wagoner, N.A., Leybourne, M.I., Dadd, K.A., and Huskins, M.L.A., 2001, The Silurian(?) Passamaquoddy Bay mafic dyke swarm, New Brunswick: petrogenesis and tectonic implications: Canadian Journal of Earth Sciences, v. 38, n. 11, p. 1565-1578.

Van Wagoner, N.A., Leybourne, M.I., Dadd, K.A., Baldwin, D.K., and McNeil, W., 2002, Late Silurian bimodal volcanism of southwestern New Brunswick, Canada: products of continental extension: Geological Society of America Bulletin, v. 114, n. 4, p. 400-418.

Waldron, J.W.F., Floyd, J.D., Simonetti, A., and Heaman, L.M., 2008, Ancient Laurentian detrital zircon in the closing Iapetus Ocean, Southern Uplands terrane, Scotland: Geology, v. 36, n. 7, p. 527-530.

Waldron, J.W.F., White, C.E., Barr, S.M., Simonetti, A., and Heaman, L.M., 2009, Provenance of the Meguma Terrane, Nova Scotia: rifted margin of early Paleozoic Gondwana: Canadian

Journal of Earth Sciences, v. 46, n. 1, p. 1-8.

Waldron, J.W.F., Schofield, D.I., White, C.E., and Barr, S.M., 2011, Cambrian successions of the Meguma Terrane, Nova Scotia, and Harlech Dome, north Wales; dispersed fragments of a peri-Gondwanan basin?: Journal of the Geological Society of London, v. 168, n. 1; 1, p. 83-98.

Waldron, J.W.F., McNicoll, V.J., and van Staal, C.R., 2012, Laurentia-derived detritus in the Badger Group of central Newfoundland: deposition during closing of the Iapetus Ocean: Canadian Journal of Earth Sciences, v. 49, n. 1, p. 207-221.

Waldron, J.W.F., Schofield, D.I., Dufrane, S.A., Floyd, J.D., Crowley, Q.G., Simonetti, A., Dokken, R.J., and Pothier, H.D., 2014a, Ganderia–Laurentia collision in the Caledonides of Great Britain and Ireland: Journal of the Geological Society, v. 171, n. 4, p. 555-569.

Waldron, J.W.F., Schofield, D.I., Murphy, J.B., and Thomas, C.W., 2014b, How was the Iapetus Ocean infected with subduction?: Geology, v. 42, n. 12, p. 1095-1098.

White, C.E., Barr, S.M., Bevier, M.L., and Kamo, S., 1994, A revised interpretation of Cambrian and Ordovician rocks in the Bourinot Belt of central Cape Breton Island, Nova Scotia: Atlantic Geology, v. 30, n. 2, p. 123-142.

Williams, H., 1979, Appalachian Orogen in Canada: Canadian Journal of Earth Sciences, v. 16, n. 3, p. 792-807.

Williams, H., and Hiscott, R.N., 1987, Definition of the Iapetus rift-drift transition in western Newfoundland: Geology, v. 15, n. 11, p. 1044-1047.

Wilson, R.A., and Kamo, S.L., 2012, The Salinic Orogeny in northern New Brunswick: geochronological constraints and implications for Silurian stratigraphic nomenclature: Canadian Journal of Earth Sciences, v. 49, n. 1, p. 222-238.

Wilson, R.A., Burden, E.T., Bertrand, R., Asselin, E., and McCracken, A.D., 2004, Stratigraphy and tectono-sedimentary evolution of the Late Ordovician to Middle Devonian Gaspe Belt in northern New Brunswick: evidence from the Restigouche area: Canadian Journal of Earth Sciences, v. 41, n. 5, p. 527-551.

Wilson, R.A., van Staal, C.R., and McClelland, W.C., 2015, Synaccretionary sedimentary and volcanic rocks in the Ordovician Tetagouche backarc basin, New Brunswick, Canada: evidence for a transition from foredeep to forearc basin sedimentation: American Journal of Science, v. 315, n. 10, p. 958-1001.

Chapter 4: Conclusions

1. Fredericton Trough

The Fredericton Trough, New Brunswick, was filled by turbidites of the Silurian Kingsclear Group during closure of the Iapetus Ocean (Chapter 2). Deposited proximal to the shores of both the continent Laurentia and the microcontinental domain Ganderia, it is ideally situated to constrain when Ganderia converged with Laurentia, and determine the timing of closure of the associated Iapetus Ocean.

The upper Rhuddanian (ca. 441.6 to 440.8 Ma: Cumming, 1960; Fyffe, 1995; timescale of Melchin and others, 2012) Hayes Brook Formation, north of the present-day Fredericton Fault, records detrital zircon signatures which indicate the prominence of Laurentian detritus within this part of the basin. This formation was juxtaposed with the Laurentian margin at this time. In contrast, the Digdeguash Formation, of identical age (Fyffe and Riva, 2001) but located south of the Fredericton Fault, contains no indication of Laurentian detritus. It was clearly separated from the Laurentian margin at this time. The Ganderian St. Croix terrane, basement to the Digdeguash Formation, was therefore also separated from Laurentia by the last vestige of the Iapetus Ocean, the Tetagouche-Exploits seaway (Figure 4.1).

Later in the Silurian, the Burtts Corner Formation, north of the Fredericton Fault, records the persistence of Laurentian detritus in this part of the basin, with the addition of new sources of peri-Gondwanan detritus, interpreted to result from the uplift of the Miramichi and related terranes to the north. This uplift must have occurred by the mid-Wenlock depositional age of the sampled Burtts Corner Formation, ca. 432.4 to 430.5 Ma (Melchin and others, 2012). South of the fault, the mid-Silurian Flume Ridge Formation records the arrival of Laurentian detritus. The lack of peri-Gondwanan detrital zircon suggests this probably occurred before the mid-Wenlock deposition of the Burtts Corner Formation. It must have also occurred prior to the intrusion of the Flume Ridge Formation by the Pocomoonshine Pluton at 422.7 ± 3 Ma (West and others,

Figure 4.1: Schematic tectonic diagram of the Fredericton Trough and Mascarene Basin.
A: Early Llandovery. Laurentian detritus recorded in the Hayes Brook Formation. Peri-Gondwanan detritus recorded in the Digdeguash Formation.
B: Late Llandovery. Peri-Gondwanan detritus recorded in the Oak Bay and Back Bay Formations.
C: Early Wenlock. Laurentian detritus recorded in the Flume Ridge Formation.
D: Ludlow-Pridoli. Laurentian detritus may arrive in the Eastport Formation. Peri-Gondwanan sources contribute to the Eastport Formation. Mixed detritus recorded in the Burtts Corner Formation by the mid-Wenlock, due to exhumation of the Brunswick subduction complex.
E: Devonian, post-accretion.
Arrows show extent and provenance of detritus. AV: Avalonia. BB: Back Bay Formation. BC: Burtts Corner Formation. BSC: Brunswick subduction complex. DG: Digdeguash Formation. EP: Eastport Formation. FR: Flume Ridge Formation. HB: Hayes Brook Formation. KA: Kingston arc. LR: Laurentia. NR: New River terrane. OB: Oak Bay Formation. PVA: Popelogan-Victoria arc. SC: St. Croix terrane.

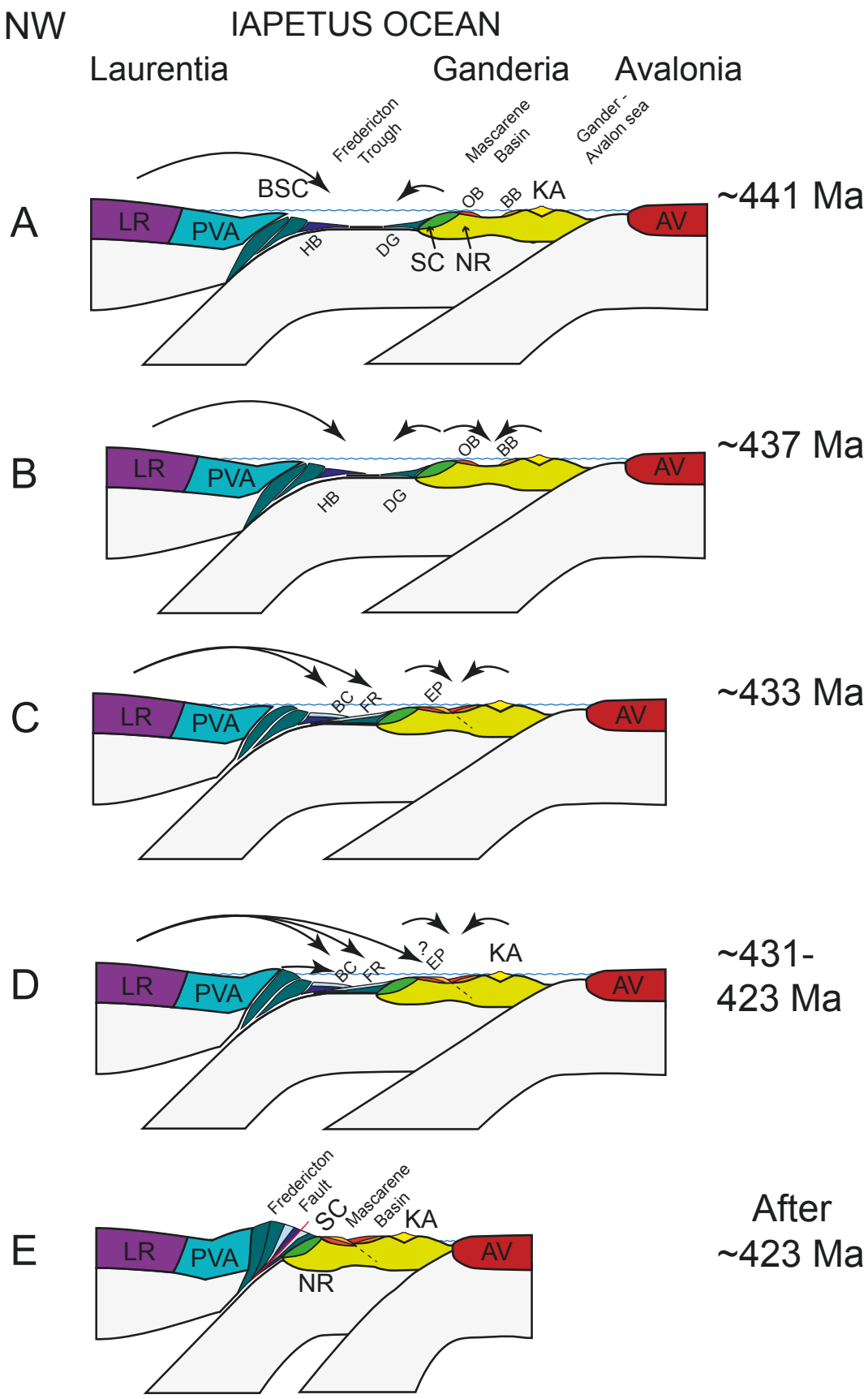
NW
IAPETUS OCEAN
Laurentia
Ganderia
Avalonia
A
B
C
D
E
LR
PVA
AV
BSC
Fredericton Trough
Mascarene Basin
Gander - Avalon sea
OB
BB
KA
HB
DG
SC
NR
BC
FR
EP
?
Fredericton Fault
~441 Ma
~437 Ma
~433 Ma
~431-423 Ma
After ~423 Ma

1992). The clear contrast between detrital zircon provenance of the Digdeguash and Flume Ridge Formations constrains the timing of juxtaposition of this part of Ganderia with Laurentia (Figure 4.1), and approximately coincides with the closure of the last remnant of the Iapetus Ocean. This juxtaposition must have occurred after deposition of the Digdeguash Formation (ca. 441 Ma) and probably prior to deposition of the Burtts Corner Formation (ca. 431 Ma).

Provenance contrasts across the Fredericton Fault, particularly between formations of an identical depositional age, suggests that it marks the position of an earlier suture or terrane boundary (McKerrow and Ziegler, 1971; McKerrow, 1982). The terminal Salinic suture, or Dog Bay Line (Reusch and van Staal, 2012), marks the closure of the last remnant of the Iapetus Ocean, the Tetagouche-Exploits seaway. It has previously been drawn along the northernmost faulted contact of the Fredericton Trough with rocks of the Miramichi terrane, already a part of composite Laurentia at this time. However, the clear juxtaposition of the Hayes Brook Formation with Laurentia prior to final Iapetan closure indicates that this suture must lie farther south, approximately along the trace of the Fredericton Fault.

2. Mascarene Basin

The Mascarene Basin, a fault-bounded composite basin of volcanic-sedimentary successions, has been interpreted as Silurian back-arc basin fill within the southernmost Ganderian terranes (Van Wagoner and others 2001, 2002; van Staal and others, 2014), located to the south of the Fredericton Trough, and sharing St. Croix terrane basement at its northern margin. Multiple formations of the Mascarene Basin were studied to test a model of successive terrane accretion at the Laurentian margin (Chapter 3), which would result in the progressively increasing extent of Laurentian detritus across juxtaposed terranes.

The early Silurian Waweig Formation, bearing a felsic tuff dated at 438 ± 4 Ma (Miller and Fyffe, 2002), contains mainly contemporary zircon, with only a few older zircons insufficient to suggest provenance. The Back Bay Formation, with fossils indicating a late Llandovery C4-C5

depositional age (ca. 437.2 – 436.5 Ma: Melchin and others, 2012), records peri-Gondwanan sources, with no indication of Laurentian detritus at this time. This corroborates previous study of the early Silurian Oak Bay Formation (Fyffe and others, 2009), with comparable detrital zircon signatures. Notably, these two formations span nearly the present-day width of the Mascarene Basin: the Oak Bay Formation at its northern margin, on Ganderian St. Croix terrane basement; and the Back Bay Formation near its southern margin. This suggests that the Mascarene Basin was not juxtaposed with Laurentia at this time (Figure 4.1), or that there was a barrier to receiving detritus from sources to the north.

The late Silurian Eastport Formation, with a felsic tuff dated at 423 ± 1 Ma (Dadd and Van Wagoner, 2001; van Wagoner and others, 2001), records new sources of detritus, in contrast to the older Back Bay Formation. Although these sources are not clearly of Laurentian affinity, K-S tests show that they do share some similarities, suggesting the possibility that the Mascarene Basin was juxtaposed to and in communication with the Laurentian margin by the time of deposition of the Eastport Formation at 423 ± 1 Ma (Figure 4.1).

3. Synthesis

Previous work in the Appalachians has proposed a model of orogenesis resulting from successive terrane accretion at the Laurentian margin of the Iapetus Ocean, opposite Gondwana (Williams and Hatcher, 1982, 1983; van Staal and others, 1998, 2009). The timing of terrane juxtaposition has been studied by means of detrital zircon geochronology, which searches for signs of Laurentian detritus within basins deposited upon accreted terranes (Waldron and others, 2014).

Results from the Fredericton Trough and Mascarene Basin demonstrate the progressive spread of Laurentian detritus over Ganderian terranes in southern New Brunswick (Figure 4.2). The northern margin of the Fredericton Trough was clearly juxtaposed with Laurentia by about 441 Ma, its southern portion by about 431 Ma, and the Mascarene Basin may have been juxtaposed by 423 Ma. The closure of a remnant of the Iapetus Ocean, approximated by the coinciding

Figure 4.2: Progressive extent of Laurentian detritus in New Brunswick through the Silurian.

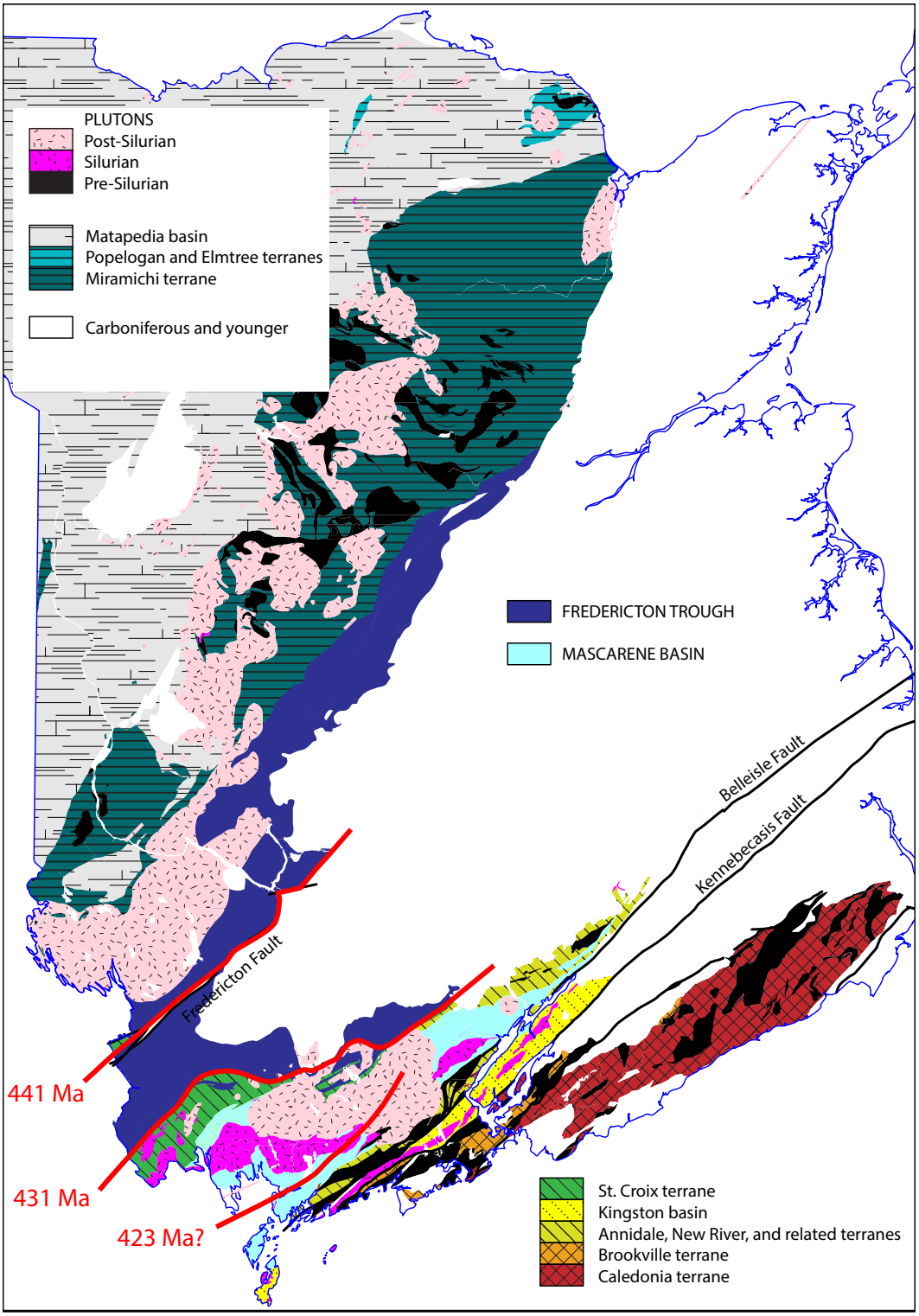

convergence of Laurentia with southernmost terranes of Ganderia, took place after the upper Rhuddanian and by the mid-Wenlock (between ca. 441 to 431 Ma), as indicated by the changing provenance of the Fredericton Trough. In the Mascarene Basin, sharing the same Ganderian basement as the Fredericton Trough, the Back Bay Formation records only peri-Gondwanan detrital zircon signatures in the late Llandovery, at about 437 Ma. This suggests a narrower constraint on the time of juxtaposition of these last components of Ganderia with Laurentia, between about 437 to 431 Ma.

However, this inference is complicated by the detrital zircon record of the Eastport Formation, at about 423 Ma, or 8 Ma after the terrane juxtaposition recorded by the Flume Ridge Formation. Laurentian detritus, if present in the Eastport Formation, is ambiguously diluted by other sources, with the result that no published detrital zircon samples from the Mascarene Basin show unequivocal indication of Laurentian detritus.

This requires the consideration of at least two alternative scenarios. First, that the Mascarene Basin did not receive Laurentian detritus by ca. 423 Ma, despite the closure of the Fredericton Trough about 8 Ma earlier. This might suggest along-strike differences in the depositional settings of the Fredericton Trough and Mascarene Basin; for example, a model of oblique convergence, or a ribbon-like Ganderian microcontinent that converged at an angle to the Laurentian margin. The Fredericton Trough, in this scenario, would record early terrane juxtaposition in the narrow neck of Iapetus Ocean, while the Mascarene Basin, and its Ganderian basement, was still separated by a substantial seaway. Previous estimates of the rate of convergence of this portion of Ganderia are approximately 5 cm/yr (van Staal and others, 2012), or up to 400 km over the 8 Ma period between the juxtaposition of the Fredericton Trough, and the deposition of the Eastport Formation. If this rate were constant through this period, this would require the Mascarene Basin (and its Ganderian basement) to have trailed substantially behind that of the Fredericton Trough. Additionally, this may suggest that the supposedly shared Ganderian basement of the two Silurian basins is not the same terrane, but distinct and separated

portions of Ganderia. Northern Ganderian terranes have already been shown to have arrived in many distinct pieces (van Staal and others, 2008, 2009; Waldron and others, 2017), and the predominantly faulted margins of the Mascarene Basin make this a plausible explanation.

A last consideration is the unique depositional setting of the Mascarene Basin, compared to previous detrital zircon studies. Previous work, demonstrating the pervasive extent of Laurentian detritus in accreted terranes, has sampled basins deposited in settings such as foredeeps or foreland basins (Waldron and others, 2014, 2017). In these settings, Laurentian detritus may be deposited without hindrance, and spread pervasively. However, the Mascarene Basin, interpreted as a back-arc within microcontinental material, is a distinctly different setting. Abundant proximal volcanic sources could easily overwhelm more distal sources, and in this setting, Ganderian basement to the north may have formed a barrier to detritus. These complications point out the limits of detrital zircon study in the Appalachian orogen.

4. Future Work

Correlating detrital zircon provenance between the Fredericton Trough and Mascarene Basin is complicated by ambiguous basement relationships. In the Fredericton Trough, the Digdeguash Formation has been interpreted to unconformably overlie rocks of the St. Croix terrane (Fyffe and others, 2011); however, this contact may also be faulted (Ruitenberg, 1967; Ludman 1987, 1991). Similarly, the locally unconformable contact of the Mascarene Oak Bay Formation over St. Croix basement is also elsewhere faulted (Fyffe and others, 1999, 2011). Faults have also been mapped within the St. Croix terrane itself. Further study of the structural relationships between and within these Silurian basins is essential in understanding their tectonic evolution; specifically, whether they were each deposited on Ganderian basement represented by the St. Croix terrane, and whether this terrane itself may be formed of distinct pieces of Ganderia.

Further detrital zircon work is also required in other formations of the Mascarene Basin, with several goals. This will further constrain provenance changes across faults, and demonstrate

whether or not they mark the positions of earlier, significant structures during basin evolution. Similarly, this will demonstrate any provenance changes across intrusions, which may obscure contacts and correlations between units. The abundant volcanic components in the Mascarene Basin also introduce a complication in detrital zircon analysis, and further work can suggest which formations and lithologies minimize these contemporary volcanic sources. Further work will also show any provenance changes across the width of the basin, and through time, demonstrating how provenance may have changed during Silurian convergence. Lastly, further detrital zircon work may show if the arrival of Laurentian detritus can be unequivocally recorded in the unique depositional setting of the Mascarene Basin, as it has in other parts of the orogen.

Correlative Silurian basins along the length of the orogen may also be studied. The Fredericton Trough continues southwest into the Merrimack-Fredericton belt of Maine, and preliminary detrital zircon work has suggested the presence of Laurentian sources by about 430 Ma (Ludman and others, 2014). However, the absence of fossils in this part of the trough severely limits depositional age constraints (Ludman and others, 1993), and therefore poorly constrains the timing of ocean closure and terrane juxtaposition. The Mascarene Basin is correlative to the Aspy terrane of Nova Scotia, La Poile basin of Newfoundland, and Coastal Volcanic Belt of Maine (van Staal and others, 2009), from which no detrital zircon data have been reported.

Sm-Nd, Hf isotope, or other geochemical work may also be used to help distinguish a Laurentian source (Murphy and others, 1996, 2004; Willner and others, 2014). Paleoflow indicators would also be helpful, but probably insufficient in the case of the Mascarene Basin specifically, since a source to the northwest could suggest Ganderian basement as easily as Laurentia. Methods of analysis which are able to clearly distinguish Laurentian sources in formations of mixed provenance would be very useful in complicated basins such as the Mascarene Basin.

5. References

Cumming, L.M., 1960, Report on fossils from the Hayesville and adjacent areas, New

Brunswick. Submitted by Dr. W.H. Poole: Geological Survey of Canada, Report O-S-1-60/61-LMC, 2 p.

Dadd, K.A., and Van Wagoner, N.A., 2001, Physical volcanology of the Silurian CVB rocks of Passamaquoddy Bay, southwestern New Brunswick, *in* Pickerill, R.K. and Lentz, D.R., editors, Guidebook to field trips in New Brunswick and western Maine: New England Intercollegiate Geological Conference, Department of Geology, University of New Brunswick, Fredericton, New Brunswick, v. 93, p. C2.1-C2.13.

Fyffe, L.R., 1995, Fredericton Belt, in Williams, H., editor, Geology of the Appalachian-Caledonian Orogen *in* Canada and Greenland: Geological Survey of Canada, Geology of Canada, v. 6, p. 351-354.

Fyffe, L.R., and Riva, J., 2001, Regional significance of graptolites from the Digdeguash Formation of southwestern New Brunswick, *in* Carroll, B.M.W., editor, Current Research 2000: New Brunswick Department of Natural Resources and Energy, Minerals and Energy Division, Mineral Resource Report 2001-4, p. 47-54.

Fyffe, L.R., Pickerill, R.K., and Stringer, P., 1999, Stratigraphy, sedimentology and structure of the Oak Bay and Waweig formations, Mascarene Basin; implications for the paleotectonic evolution of southwestern New Brunswick: Atlantic Geology, v. 35, n. 1; 1, p. 59-84.

Fyffe, L.R., Barr, S.M., Johnson, S.C., McLeod, M.J., McNicoll, V.J., Valverde Vaquero, P., van Staal, C.R., and White, C.E., 2009, Detrital zircon ages from Neoproterozoic and early Paleozoic conglomerate and sandstone units of New Brunswick and coastal Maine: implications for the tectonic evolution of Ganderia: Atlantic Geology, v. 45, p. 110-144.

Fyffe, L.R., Johnson, S.C., and van Staal, C.R., 2011, A review of Proterozoic to early Paleozoic lithotectonic terranes in the northeastern Appalachian Orogen of New Brunswick, Canada, and their tectonic evolution during Penobscot, Taconic, Salinic, and Acadian orogenesis: Atlantic Geology, v. 47, p. 211-248.

Ludman, A., 1987, Pre-Silurian stratigraphy and tectonic significance of the St. Croix Belt, southeastern Maine: Canadian Journal of Earth Sciences, v. 24, n. 12, p. 2459-2469.

Ludman, A., 1991, Revised stratigraphy of the Cookson Group in eastern Maine and southwestern New Brunswick: an alternative view: Atlantic Geology, v. 27, n. 1, p. 49-55.

Ludman, A., Hopeck, J.T., and Brock, P.C., 1993, Nature of the Acadian Orogeny in eastern Maine, *in* Roy, D.C. and Skehan, J.W., editors, The Acadian Orogeny: recent studies in New England, Maritime Canada, and the autochthonous foreland: Special Paper - Geological Society of America, v. 275, p. 67-84.

Ludman, A., Aleinikoff, J.N., Hopeck, J., and Berry, H.N., IV, 2014, Shrimp U-Pb geochronology of pre-Acadian Silurian basins of central and east-central Maine and the Pocomoonshine Pluton: diverse sources, rapid sedimentation, tectonism, and intrusion: Geological Society of America, Abstracts with Programs, v. 46, n. 2, p. 122-122.

McKerrow, W.S., 1982, The northwest margin of the Iapetus Ocean during the early Paleozoic, *in* Watkins, J.S. and Drake, C.L., editors, Studies in continental margin geology: American Association of Petroleum Geologists, Memoirs, v. 34, p. 521-533.

McKerrow, W.S., and Ziegler, A.M., 1971, The lower Silurian paleogeography of New Brunswick and adjacent areas: Journal of Geology, v. 79, n. 6, p. 635-646.

Melchin, M.J., Sadler, P.M., and Cramer, B.D., 2012, The Silurian Period, *in* Gradstein, F.M., Ogg, J.G., Schmitz, M.D. and Ogg, G.M., editors, The geologic time scale 2012: Oxford, Elsevier, p. 525-558.

Miller, B.V., and Fyffe, L.R., 2002, Geochronology of the Letete and Waweig Formations, Mascarene Group, southwestern New Brunswick: Atlantic Geology, v. 38, n. 1, p. 29-36.

Murphy, J.B., Keppie, J.D., Dostal, J., Waldron, J.W.F., and Cude, M.P., 1996, Geochemical and isotopic characteristics of Early Silurian clastic sequences in Antigonish Highlands, Nova

Scotia, Canada: constraints on the accretion of Avalonia in the Appalachian-Caledonide Orogen: Canadian Journal of Earth Sciences, v. 33, n. 3, p. 379-388.

Murphy, J.B., Fernandez-Suarez, J., and Jeffries, T.E., 2004, Lithogeochemical and Sm-Nd and U-Pb isotope data from the Silurian-Lower Devonian Arisaig Group clastic rocks, Avalon Terrane, Nova Scotia: a record of terrane accretion in the Appalachian-Caledonide Orogen: Geological Society of America Bulletin, v. 116, n. 9-10, p. 1183-1201.

Reusch, D.N., and van Staal, C.R., 2012, The Dog Bay-Liberty Line and its significance for Silurian tectonics of the Northern Appalachian Orogen: Canadian Journal of Earth Sciences, v. 49, n. 1, p. 239-258.

Ruitenberg, A.A., 1967, Stratigraphy, structure and metallization Piskahegan-Rolling Dam area (northern Appalachians, New Brunswick, Canada): Leidse Geologische Mededelingen, v. 40, p. 79-120.

Smith, E.A., 2005, Bedrock geology of southwestern New Brunswick (NTS 21 G, part of 21 B): New Brunswick Department of Natural Resources, Minerals, Policy, and Planning Division, Map NR-5 (Second Edition), scale 1:250000.

van Staal, C.R., Dewey, J.F., Mac Niocaill, C., and McKerrow, W.S., 1998, The Cambrian-Silurian tectonic evolution of the Northern Appalachians and British Caledonides: history of a complex, west and southwest Pacific-type segment of Iapetus, *in* Blundell, D.J. and Scott, A.C., editors, Lyell: the Past is the Key to the Present: Geological Society of London, Special Publications, v. 143, p. 199-242.

van Staal, C.R., Currie, K.L., Rowbotham, G., Rogers, N., and Goodfellow, W., 2008, Pressure-temperature paths and exhumation of Late Ordovician-Early Silurian blueschists and associated metamorphic nappes of the Salinic Brunswick subduction complex, Northern Appalachians: Geological Society of America Bulletin, v. 120, n. 11-12, p. 1455-1477.

van Staal, C.R., Whalen, J.B., Valverde-Vaquero, P., Zagorevski, A., and Rogers, N., 2009, Pre-Carboniferous, episodic accretion-related, orogenesis along the Laurentian margin of the Northern Appalachians, *in* Murphy, J.B., Keppie, J.D. and Hynes, A.J., editors, Ancient orogens and modern analogues: Geological Society of London, Special Publications, v. 327, p. 271-316.

van Staal, C.R., Barr, S.M., and Murphy, J.B., 2012, Provenance and tectonic evolution of Ganderia: constraints on the evolution of the Iapetus and Rheic Oceans: Geology, v. 40, n. 11, p. 987-990.

van Staal, C.R., Zagorevski, A., McNicoll, V.J., and Rogers, N., 2014, Time-transgressive Salinic and Acadian orogenesis, magmatism and Old Red Sandstone sedimentation in Newfoundland: Geoscience Canada, v. 41, n. 2, p. 138-164.

Van Wagoner, N.A., Leybourne, M.I., Dadd, K.A., and Huskins, M.L.A., 2001, The Silurian(?) Passamaquoddy Bay mafic dyke swarm, New Brunswick: petrogenesis and tectonic implications: Canadian Journal of Earth Sciences, v. 38, n. 11, p. 1565-1578.

Van Wagoner, N.A., Leybourne, M.I., Dadd, K.A., Baldwin, D.K., and McNeil, W., 2002, Late Silurian bimodal volcanism of southwestern New Brunswick, Canada: products of continental extension: Geological Society of America Bulletin, v. 114, n. 4, p. 400-418.

Waldron, J.W.F., Schofield, D.I., Dufrane, S.A., Floyd, J.D., Crowley, Q.G., Simonetti, A., Dokken, R.J., and Pothier, H.D., 2014, Ganderia–Laurentia collision in the Caledonides of Great Britain and Ireland: Journal of the Geological Society of London, v. 171, n. 4, p. 555-569.

Waldron, J.W.F., Schofield, D.I., Murphy, J.B., 2017 (in review), Diachronous Palaeozoic accretion of peri-Gondwanan terranes at the Laurentian margin: Geological Society of London, Special Publications.

West, D.P., Jr., Ludman, A., and Lux, D.R., 1992, Silurian age for the Pocomoonshine Gabbro-Diorite, southeastern Maine and its regional tectonic implications: American Journal of Science, v. 292, n. 4, p. 253-273.

Williams, H., and Hatcher, R.D., Jr., 1982, Suspect terranes and accretionary history of the Appalachian Orogen: Geology, v. 10, n. 10, p. 530-536.

Williams, H., and Hatcher, R.D., Jr., 1983, Appalachian suspect terranes, *in* Hatcher, R.D., Jr., Williams, H. and Zietz, I., editors, Contributions to the tectonics and geophysics of mountain chains: Geological Society of America, Memoirs, v. 158, p. 33-53.

Willner, A., Gerdes, A., Massonne, H., van Staal, C.R., Zagorevski, A., 2014, Crustal Evolution of the Northeast Laurentian Margin and the Peri-Gondwanan Microcontinent Ganderia Prior to and During Closure of the Iapetus Ocean: Detrital Zircon U–Pb and Hf Isotope Evidence from Newfoundland: Geoscience Canada, v. 41, n. 3, p. 345-364.

Bibliography

Ashton, K.E., Heaman, L.M., Lewry, J.F., Hartlaub, R.P., and Shi, R., 1999, Age and origin of the Jan Lake Complex: a glimpse at the buried Archean craton of the Trans-Hudson Orogen: Canadian Journal of Earth Sciences, v. 36, n. 2, p. 185-208.

Berry, W.B.N., and Boucot, A.J., editors, 1970, Correlation of the North American Silurian rocks: Geological Society of America, Special Papers, v. 102, 289 p.

Bird, J.M., and Dewey, J.F., 1970, Lithosphere plate-continental margin tectonics and the evolution of the Appalachian orogen: Geological Society of America Bulletin, v. 81, n. 4, p. 1031-1059.

Bluck, B.J., Gibbons, W., and Ingham, J.K., 1992, Terranes, *in* Cope, J.C.W., Ingham, J.K. and Rawson, P.F., editors, Atlas of palaeogeography and lithofacies: United Kingdom, Geological Society of London, Memoirs, v. 13, p. 1-4.

Boucot, A.J., Johnson, J.G., Harper, C., and Walmsley, V.G., 1966, Silurian brachiopods and gastropods of southern New Brunswick: Geological Survey Canada, Bulletin 140, 45 p.

Cawood, P.A., and Nemchin, A.A., 2001, Paleogeographic development of the East Laurentian margin: constraints from U-Pb dating of detrital zircons in the Newfoundland Appalachians: Geological Society of America Bulletin, v. 113, n. 9, p. 1234-1246.

Cawood, P.A., McCausland, P.J.A., and Dunning, G.R., 2001, Opening Iapetus: constraints from the Laurentian margin in Newfoundland: Geological Society of America Bulletin, v. 113, n. 4, p. 443-453.

Cawood, P.A., Nemchin, A.A., Smith, M., and Loewy, S., 2003, Source of the Dalradian Supergroup constrained by U-Pb dating of detrital zircon and implications for the East Laurentian margin: Journal of the Geological Society of London, v. 160, n. 2, p. 231-246.

Cawood, P.A., Nemchin, A.A., Strachan, R.A., Kinny, P.D., and Loewy, S., 2004, Laurentian provenance and an intracratonic tectonic setting for the Moine Supergroup, Scotland, constrained by detrital zircons from the Loch Eil and Glen Urquhart successions: Journal of the Geological Society of London, v. 161, n. 5, p. 861-874.

Cocks, L.R.M., Toghill, P., and Ziegler, A.M., 1970, Stage names within the Llandovery series: Geological Magazine, v. 107, n. 1, p. 79-87.

Cooper, R.A., and Sadler, P.M., 2012, The Ordovician Period, *in* Gradstein, F.M., Ogg, J.G., Schmitz, M.D. and Ogg, G.M., editors, The geologic time scale 2012: Oxford, Elsevier, p. 489-523.

Cumming, L.M., 1960, Report on fossils from the Hayesville and adjacent areas, New Brunswick. Submitted by Dr. W.H. Poole: Geological Survey of Canada, Report O-S-1-60/61-LMC, 2 p.

Cumming, L.M., 1967, Geology of the Passamaquoddy Bay region, Charlotte County, New Brunswick: Geological Survey of Canada, Paper 65-29, 36 p.

Dadd, K.A., and Van Wagoner, N.A., 2001, Physical volcanology of the Silurian CVB rocks of Passamaquoddy Bay, southwestern New Brunswick, *in* Pickerill, R.K. and Lentz, D.R., editors, Guidebook to field trips in New Brunswick and western Maine: New England Intercollegiate Geological Conference, Department of Geology, University of New Brunswick, Fredericton, New Brunswick, v. 93, p. C2.1-C2.13.

Dana, J.D., 1873, On some results of the earth's contraction from cooling including a discussion of the origin of mountains and the nature of the earth's interior: American Journal of Science, v. 5, n. 30, p. 423-443.

Dewey, J.F., 1969, Evolution of the Appalachian/Caledonian orogen: Nature, v. 222, n. 5189, p. 124-129.

Dewey, J.F., and Mange, M., 1999, Petrography of Ordovician and Silurian sediments in the western Irish Caledonides; tracers of a short-lived Ordovician continent-arc collision orogeny and the evolution of the Laurentian Appalachian-Caledonian margin: Geological Society of London, Special Publications, v. 164, p. 55-107.

Dickin, A.P., 2005, Radiogenic isotope geology: United Kingdom, Cambridge University Press, 492 p.

Dott, R.H., 1964, Wacke, graywacke and matrix—what approach to immature sandstone classification?: Journal of Sedimentary Research, v. 34, n. 3, p. 625-632.

Dunn, T., and Stringer, P., 1990, Petrology and petrogenesis of the Ministers Island Dike, Southwest New Brunswick, Canada: Contributions to Mineralogy and Petrology, v. 105, n. 1, p. 55-65.

Dunning, G.R., O'Brien, S.J., Colman-Sadd, S., Blackwood, R.F., Dickson, W.L., O'Neill, P.P., and Krogh, T.E., 1990, Silurian Orogeny in the Newfoundland Appalachians: The Journal of Geology, v. 98, n. 6, p. 895-913.

Elhlou, S., Belousova, E., Griffin, W.L., Pearson, N.J., and O'Reilly, S.Y., 2006, Trace element and isotopic composition of GJ-red zircon standard by laser ablation: Geochimica et Cosmochimica Acta, v. 70, n. 18 supplement, p. A158.

Eriksson, K., Campbell, I., Palin, J., and Allen, C., 2003, Predominance of Grenvillian Magmatism Recorded in Detrital Zircons from Modern Appalachian Rivers: The Journal of Geology, v. 111, n. 6, p. 707-717.

Fyffe, L.R., 1991, Geology of the Flume Ridge-Kedron Stream map areas, Charlotte County, New Brunswick, *in* Abbott, S.A., editor, Project summaries for 1991, sixteenth annual review of activities: New Brunswick Department of Natural Resources and Energy, Mineral Resources, Information Circular 91-2, p. 12-20.

Fyffe, L.R., 1995, Fredericton Belt, *in* Williams, H., editor, Geology of the Appalachian-Caledonian Orogen in Canada and Greenland: Geological Survey of Canada, Geology of Canada, v. 6, p. 351-354.

Fyffe, L.R., 2005, Bedrock geology of the Rollingdam area (NTS 21 G/06), Charlotte County, New Brunswick: New Brunswick Department of Natural Resources, Minerals, Policy, and Planning Division, Plate 2005-29, scale 1:50000.

Fyffe, L.R., and Riva, J., 1990, Revised stratigraphy of the Cookson Group of southwestern New Brunswick and adjacent Maine: Atlantic Geology, v. 26, n. 3, p. 271-275.

Fyffe, L.R., and Riva, J., 2001, Regional significance of graptolites from the Digdeguash Formation of southwestern New Brunswick, *in* Carroll, B.M.W., editor, Current Research 2000: New Brunswick Department of Natural Resources and Energy, Minerals and Energy Division, Mineral Resource Report 2001-4, p. 47-54.

Fyffe, L.R., Pickerill, R.K., and Stringer, P., 1999, Stratigraphy, sedimentology and structure of the Oak Bay and Waweig formations, Mascarene Basin; implications for the paleotectonic evolution of southwestern New Brunswick: Atlantic Geology, v. 35, n. 1; 1, p. 59-84.

Fyffe, L.R., Barr, S.M., Johnson, S.C., McLeod, M.J., McNicoll, V.J., Valverde Vaquero, P., van Staal, C.R., and White, C.E., 2009, Detrital zircon ages from Neoproterozoic and early Paleozoic conglomerate and sandstone units of New Brunswick and coastal Maine: implications for the tectonic evolution of Ganderia: Atlantic Geology, v. 45, p. 110-144.

Fyffe, L.R., Johnson, S.C., and van Staal, C.R., 2011, A review of Proterozoic to early Paleozoic lithotectonic terranes in the northeastern Appalachian Orogen of New Brunswick, Canada, and their tectonic evolution during Penobscot, Taconic, Salinic, and Acadian orogenesis: Atlantic Geology, v. 47, p. 211-248.

Gehrels, G., 2013, U-Pb geochronology and Hf isotope geochemistry applied to detrital minerals:

Geological Society of America, Annual Meeting, Short Course 521, 216 p.

Gehrels, G., Valencia, V., and Pullen, A., 2006, Detrital zircon geochronology by laser-ablation multicollector ICPMS at the Arizona Laserchron Center, *in* Olszewski, T.D., editor, Geochronology: Emerging Opportunities: Paleontological Society Papers, v. 12, p. 67-76.

Guynn, J., and Gehrels, G., 2010, Comparison of detrital zircon age distributions using the K-S test: University of Arizona, Department of Geosciences, 16 p.

Hall, J., 1883, Contributions to the geological history of the American continent: American Association for the Advancement of Science, Proceedings, p. 29-69.

Harland, W.B., and Gayer, R.A., 1972, The Arctic Caledonides and earlier Oceans: Geological Magazine, v. 109, n. 4, p. 289-314.

Hibbard, J.P., van Staal, C.R., Rankin, D.W., and Williams, H., 2006, Lithotectonic map of the Appalachian Orogen, Canada-United States of America: Geological Survey of Canada, Map 2096A, scale 1:1,500,000.

Hibbard, J.P., van Staal, C.R., and Rankin, D.W., 2007, A comparative analysis of pre-Silurian crustal building blocks of the northern and the southern Appalachian Orogen: American Journal of Science, v. 307, n. 1, p. 23-45.

Jackson, S.E., Pearson, N.J., Griffin, W.L., and Belousova, E.A., 2004, The application of laser ablation-inductively coupled plasma-mass spectrometry to in situ U–Pb zircon geochronology: Chemical Geology, v. 211, n. 1–2, p. 47-69.

Johnson, S.C., 2000, Bedrock geology of the Long Reach area (parts of NTS 21G/08a,b,g and h), southern New Brunswick: New Brunswick Department of Natural Resources and Energy, Minerals and Energy Division, Plate 2000-17.

Johnson, S.C., and McLeod, M.J., 1996, The New River Belt: a unique segment along the

western margin of the Avalon composite terrane, southern New Brunswick, Canada, *in* Nance, R.D. and Thompson, M.D., editors, Avalonian and related peri-Gondwanan terranes of the Circum-North Atlantic: Geological Society of America, Special Papers, v. 304, p. 149-164.

Johnson, S.C., McLeod, M.J., Fyffe, L.R., and Dunning, G.R., 2009, Stratigraphy, geochemistry, and geochronology of the Annidale and New River Belts, and the development of the Penobscot Arc in southern New Brunswick, *in* Martin, G.L., editor, Geological investigations in New Brunswick for 2008: New Brunswick Department of Natural Resources, Minerals, Policy, and Planning Division, Mineral Resource Report 2009-2, p. 141-218.

Johnson, S.C., McLeod, M.J., Fyffe, L.R., Thorne, K.G., Barr, S.M., and White, C.E., 2007, Southern New Brunswick field trip – June 20-22, 2007: New Brunswick Department of Natural Resources, Unpublished Field Guide, 30 p.

Johnson, S.C., Fyffe, L.R., McLeod, M.J., and Dunning, G.R., 2012, U–Pb ages, geochemistry, and tectonomagmatic history of the Cambro-Ordovician Annidale Group: a remnant of the Penobscot arc system in southern New Brunswick?: Canadian Journal of Earth Sciences, v. 49, n. 1, p. 166-188.

Johnson, S.C., McLeod, M.J., Barr, S.M., White, C.E., van Staal, C.R., Fyffe, L.R., and Thorne, K.G., 2012, Tectonic evolution of peri-Gondwanan terranes in southwestern New Brunswick, Canada: New Brunswick Department of Natural Resources, Lands, Minerals, and Petroleum Division, Field Guide No. 4, 62 p.

Kay, M., 1951, North American geosynclines: Geological Society of America, Memoirs, v. 48, p. 1-132.

Kerr, A., Jenner, G.A., and Fryer, B.J., 1995, Sm–Nd isotopic geochemistry of Precambrian to Paleozoic granitoid suites and the deep-crustal structure of the southeast margin of the

Newfoundland Appalachians: Canadian Journal of Earth Sciences, v. 32, n. 2, p. 224-245.

King, M.S., and Barr, S.M., 2004, Magnetic and gravity models across terrane boundaries in southern New Brunswick, Canada: Canadian Journal of Earth Sciences, v. 41, n. 9; 9, p. 1027-1047.

Landing, E., 1996, Avalon: Insular continent by the latest Precambrian, *in* Nance, R.D. and Thompson, M.D., editors, Avalonian and related peri-Gondwanan terranes of the Circum-North Atlantic: Geological Society of America, Special Papers, v. 304, p. 29-63.

Leggett, J.K., McKerrow, W.S., and Soper, N.J., 1983, A model for the crustal evolution of southern Scotland: Tectonics, v. 2, n. 2, p. 187-210.

Li, Z.X., Bogdanova, S.V., Collins, A.S., Davidson, A., De Waele, B., Ernst, R.E., Fitzsimons, I.C.W., Fuck, R.A., Gladkochub, D.P., Jacobs, J., Karlstrom, K.E., Lu, S., Natapov, L.M., Pease, V., Pisarevsky, S.A., Thrane, K., and Vernikovsky, V., 2008, Assembly, configuration, and breakup history of Rodinia: a synthesis, *in* Bogdanova, S.V., Li, Z.X., Moores, E.M. and Pisaresvky, S.A., editors, Testing the Rodinia hypothesis: records in its building blocks: Precambrian Research, v. 160, n. 1-2, p. 179-210.

Ludman, A., 1987, Pre-Silurian stratigraphy and tectonic significance of the St. Croix Belt, southeastern Maine: Canadian Journal of Earth Sciences, v. 24, n. 12, p. 2459-2469.

Ludman, A., 1991, Revised stratigraphy of the Cookson Group in eastern Maine and southwestern New Brunswick: an alternative view: Atlantic Geology, v. 27, n. 1, p. 49-55.

Ludman, A., and West, D.P., Jr., editors, 1999, Norumbega fault system of the Northern Appalachians: Special Papers, v. 331, 202 p.

Ludman, A., Hopeck, J.T., and Brock, P.C., 1993, Nature of the Acadian Orogeny in eastern Maine, *in* Roy, D.C. and Skehan, J.W., editors, The Acadian Orogeny: recent studies in New England, Maritime Canada, and the autochthonous foreland: Special Paper - Geological

Society of America, v. 275, p. 67-84.

Ludman, A., Lanzirotti, A., Lux, D., and Wang, C., 1999, Constraints on timing and displacement multistage shearing in the Norumbega fault system, eastern Maine, *in* Ludman, A. and West, D.P.,Jr., editors, Norumbega fault system of the Northern Appalachians: Geological Society of America, Special Papers, v. 331, p. 179-194.

Ludman, A., Aleinikoff, J.N., Hopeck, J., and Berry, H.N., IV, 2014, Shrimp U-Pb geochronology of pre-Acadian Silurian basins of central and east-central Maine and the Pocomoonshine Pluton: diverse sources, rapid sedimentation, tectonism, and intrusion: Geological Society of America, Abstracts with Programs, v. 46, n. 2, p. 122-122.

Ludwig, K.R., 2012, User's manual for Isoplot 3.75: Berkeley Geochronology Center Special Publication, 5, 75 p.

Macdonald, F.A., Ryan-Davis, J., Coish, R.A., Crowley, J.L., and Karabinos, P., 2014, A newly identified Gondwanan terrane in the northern Appalachian mountains: implications for the Taconic orogeny and closure of the Iapetus Ocean: Geology, v. 42, n. 6, p. 539-542.

McCutcheon, S.R., and Boucot, A.J., 1984, A new Lower Silurian fossil locality in the northeastern Mascarene-Nerepis Belt, southern New Brunswick: Maritime Sediments and Atlantic Geology, v. 20, n. 3, p. 121-126.

McCutcheon, S.R., and Ruitenberg, A.A., 1987, Geology and mineral deposits, Annidale-Nerepis area, New Brunswick, New Brunswick Department of Natural Resources and Energy, Mineral Resources Division, Memoir 2, 141 p.

McKerrow, W.S., 1982, The northwest margin of the Iapetus Ocean during the early Paleozoic, *in* Watkins, J.S. and Drake, C.L., editors, Studies in continental margin geology: American Association of Petroleum Geologists, Memoirs, v. 34, p. 521-533.

McKerrow, W.S., and Ziegler, A.M., 1971, The lower Silurian paleogeography of New

Brunswick and adjacent areas: Journal of Geology, v. 79, n. 6, p. 635-646.

McKerrow, W.S., Mac Niocaill, C., and Dewey, J.F., 2000, The Caledonian Orogeny redefined: Journal of the Geological Society of London, v. 157, n. 6, p. 1149-1154.

McLaughlin, K.J., Barr, S.M., Hill, M.D., Thompson, M.D., Ramezani, J., and Reynolds, P.H., 2003, The Moosehorn plutonic suite, southeastern Maine and southwestern New Brunswick: age, petrochemistry, and tectonic setting: Atlantic Geology, v. 39, n. 2, p. 123-146.

McLeod, M.J., 1990, Geology, Geochemistry, and Related Mineral Deposits of the Saint George Batholith; Charlotte, Queens, and Kings Counties, New Brunswick: New Brunswick Department of Natural Resources and Energy, Mineral Resources, Mineral Resource Report 5, 169 p.

McLeod, M.J., and Pickerill, R.K., 2001, Bedrock geology of Campobello Island; remnants of a Silurian arc and back-arc complex in southwestern New Brunswick, *in* Pickerill, R.K. and Lentz, D.R., editors, Guidebook to field trips in New Brunswick and western Maine: New England Intercollegiate Geological Conference, Department of Geology, University of New Brunswick, Fredericton, New Brunswick, v. 93, p. B4.1-B4.20.

McLeod, M.J., Ruitenburg, A.A., and Krogh, T.E., 1992, Geology and U-Pb geochronology of the Annidale Group, southern New Brunswick: Lower Ordovician volcanic and sedimentary rocks formed near the southeastern margin of Iapetus Ocean: Atlantic Geology, v. 28, n. 2, p. 181-192.

McLeod, M.J., Fyffe, L.R., and McCutcheon, S.R., 2005, Bedrock geology of the McDougall Lake area (NTS 21 G/07), Charlotte County, New Brunswick: New Brunswick Department of Natural Resources, Minerals, Policy, and Planning Division, Plate 2005-30, scale 1:50000.

McLeod, M.J., Johnson, S.C., Barr, S.M., and White, C.E., 2005, Bedrock geology of the

St. George area (NTS 21 G/02), Charlotte County, New Brunswick: New Brunswick Department of Natural Resources, Minerals, Policy, and Planning Division, Plate 2005-27, scale 1:50000.

McNamara, A.K., Niocaill, C.M., van der Pluijm, B.A., and Van der Voo, R., 2001, West African proximity of the Avalon terrane in the latest Precambrian: Geological Society of America Bulletin, v. 113, n. 9, p. 1161-1170.

Melchin, M.J., Sadler, P.M., and Cramer, B.D., 2012, The Silurian Period, *in* Gradstein, F.M., Ogg, J.G., Schmitz, M.D. and Ogg, G.M., editors, The geologic time scale 2012: Oxford, Elsevier, p. 525-558.

Miller, B.V., and Fyffe, L.R., 2002, Geochronology of the Letete and Waweig Formations, Mascarene Group, southwestern New Brunswick: Atlantic Geology, v. 38, n. 1, p. 29-36.

Moecher, D.P., and Samson, S.D., 2006, Differential zircon fertility of source terranes and natural bias in the detrital zircon record: Implications for sedimentary provenance analysis: Earth and Planetary Science Letters, v. 247, n. 3–4, p. 252-266.

Murphy, J.B., Nance, R.D., and Keppie, J.D., 2002, Discussion and reply: West African proximity of the Avalon terrane in the latest Precambrian: Geological Society of America Bulletin, v. 114, n. 8, p. 1049-1050.

Murphy, J.B., Fernandez-Suarez, J., Keppie, J.D., and Jeffries, T.E., 2004, Contiguous rather than discrete Paleozoic histories for the Avalon and Meguma Terranes based on detrital zircon data: Geology, v. 32, n. 7, p. 585-588.

Murphy, J.B., Fernandez-Suarez, J., and Jeffries, T.E., 2004, Lithogeochemical and Sm-Nd and U-Pb isotope data from the Silurian-Lower Devonian Arisaig Group clastic rocks, Avalon Terrane, Nova Scotia: a record of terrane accretion in the Appalachian-Caledonide Orogen: Geological Society of America Bulletin, v. 116, n. 9-10, p. 1183-1201.

Murphy, J.B., Pisarevsky, S.A., Nance, R.D., and Keppie, J.D., 2004, Neoproterozoic—early Paleozoic evolution of peri-Gondwanan terranes: implications for Laurentia-Gondwana connections, *in* Doerr, W., Finger, F., Linnemann, U. and Zulauf, G., editors, The Avalonian-Cadomian Belt and related peri-Gondwanan terranes: International Journal of Earth Sciences, v. 93, n. 5, p. 659-682.

Nance, R.D., Murphy, J.B., and Keppie, J.D., 2002, A Cordilleran model for the evolution of Avalonia: Tectonophysics, v. 352, n. 1-2, p. 11-31.

Nance, R.D., Murphy, J.B., Strachan, R.A., Keppie, J.D., Gutierrez Alonso, G., Fernandez Suarez, J., Quesada, C., Linnemann, U., d'Lemos, R., and Pisarevsky, S.A., 2008, Neoproterozoic-early Palaeozoic tectonostratigraphy and palaeogeography of the peri-Gondwanan terranes: Amazonian v. West African connections, *in* Ennih, N. and Liegeois, J.P., editors, The boundaries of the West African Craton: Geological Society of London, Special Publications, v. 297, p. 345-383.

Nowlan, G.S., McCracken, A.D., and McLeod, M.J., 1997, Tectonic and paleogeographic significance of Late Ordovician conodonts in the Canadian Appalachians: Canadian Journal of Earth Sciences, v. 34, n. 11, p. 1521-1537.

O'Brien, S.J., O'Brien, B.H., Dunning, G.R., and Tucker, R.D., 1996, Late Neoproterozoic Avalonian and related peri-Gondwanan rocks of the Newfoundland Appalachians, *in* Nance, R.D. and Thompson, M.D., editors, Avalonian and related peri-Gondwanan terranes of the Circum-North Atlantic: Geological Society of America, Special Papers, v. 304, p. 9-28.

Osberg, P.H., 1968, Stratigraphy, structural geology, and metamorphism of the Waterville-Vassalboro area, Maine: Maine Geological Survey, Bulletin 20, 64 p.

Park, A.F., and Whitehead, J., 2003, Structural transect through Silurian turbidites of the Fredericton Belt southwest of Fredericton, New Brunswick: the role of the Fredericton Fault in late Iapetus convergence: Atlantic Geology, v. 39, n. 3, p. 227-237.

Park, A.F., Lentz, D.R., and Thorne, K.G., 2008, Deformation and structural controls on gold mineralization in the Clarence Stream shear zone, southwestern New Brunswick, Canada, *in* Thorne, K.G. and Castonguay, S., editors, Metallogeny and setting of gold systems in southern New Brunswick: implications for exploration in the Northern Appalachians: Exploration and Mining Geology, v. 17, n. 1-2, p. 51-66.

Peng, S., Babcock, L.E., and Cooper, R.A., 2012, The Cambrian Period, *in* Gradstein, F.M., Ogg, J.G., Schmitz, M.D. and Ogg, G.M., editors, The geologic time scale 2012: Oxford, Elsevier, p. 437-488.

Phillips, E.R., Evans, J.A., Stone, P., Horstwood, M.S.A., Floyd, J.D., Smith, R.A., Akhurst, M.C., and Barron, H.F., 2003, Detrital Avalonian zircons in the Laurentian Southern Uplands terrane, Scotland: Geology, v. 31, n. 7, p. 625-628.

Phillips, W.E.A., Stillman, C.J., and Murphy, T., 1976, A Caledonian plate tectonic model: Journal of the Geological Society of London, v. 132, n. 6, p. 579-609.

Pickerill, R.K., 1976, Significance of a new fossil locality containing a Salopina community in the Waweig Formation (Silurian-uppermost Ludlow/Pridoli) of Southwest New Brunswick: Canadian Journal of Earth Sciences, v. 13, n. 9, p. 1328-1331.

Pickerill, R.K., and Pajari, G.E., J., 1976, The Eastport Formation (lower Devonian) in the northern Passamaquoddy Bay area, Southwest New Brunswick: Canadian Journal of Earth Sciences, v. 13, n. 2, p. 266-270.

Pollock, J.C., Wilton, D.H.C., van Staal, C.R., and Morrissey, K.D., 2007, U-Pb detrital zircon geochronological constraints on the Early Silurian collision of Ganderia and Laurentia along the Dog Bay Line: the terminal Iapetan suture in the Newfoundland Appalachians: American Journal of Science, v. 307, n. 2, p. 399-433.

Pollock, J.C., Hibbard, J.P., and Sylvester, P.J., 2009, Early Ordovician rifting of Avalonia and

birth of the Rheic Ocean: U-Pb detrital zircon constraints from Newfoundland: Journal of the Geological Society of London, v. 166, n. 3, p. 501-515.

Pollock, J.C., Hibbard, J.P., and van Staal, C.R., 2012, A paleogeographical review of the peri-Gondwanan realm of the Appalachian Orogen: Canadian Journal of Earth Sciences, v. 49, n. 1, p. 259-288.

Poole, W.H., 1963, Geology, Hayesville, New Brunswick: Geological Survey of Canada, Map 6-1963, scale 1:63,360.

Pothier, H.D., Waldron, J.W.F., Schofield, D.I., and DuFrane, S.A., 2015, Peri-Gondwanan terrane interactions recorded in the Cambrian–Ordovician detrital zircon geochronology of North Wales: Gondwana Research, v. 28, n. 3, p. 987-1001.

Prigmore, J.K., Butler, A.J., and Woodcock, N.H., 1997, Rifting during separation of Eastern Avalonia from Gondwana: Evidence from subsidence analysis: Geology, v. 25, n. 3, p. 203-206.

Reusch, D.N., and van Staal, C.R., 2012, The Dog Bay-Liberty Line and its significance for Silurian tectonics of the Northern Appalachian Orogen: Canadian Journal of Earth Sciences, v. 49, n. 1, p. 239-258.

Rosenblum, S., and Brownfield, I.K., 2000, Magnetic susceptibilities of minerals: United States Geological Survey, Open-File Report 99-529, 37 p.

Ruitenberg, A.A., 1967, Stratigraphy, structure and metallization Piskahegan-Rolling Dam area (northern Appalachians, New Brunswick, Canada): Leidse Geologische Mededelingen, v. 40, p. 79-120.

Ruitenberg, A.A., and Ludman, A., 1978, Stratigraphy and tectonic setting of early Paleozoic sedimentary rocks of the Wirral-Big Lake area, southwestern New Brunswick and southeastern Maine: Canadian Journal of Earth Sciences, v. 15, n. 1, p. 22-32.

Ruitenberg, A.A., McLeod, M.J., and Krogh, T.E., 1993, Comparative metallogeny of Ordovician volcanic and sedimentary rocks in the Annidale-Shannon (New Brunswick) and Harborside-Blue Hill (Maine) areas: implications of new U-Pb age dates: Exploration and Mining Geology, v. 2, n. 4, p. 355-365.

Schoene, B., 2014, U–Th–Pb Geochronology, *in* Holland, H.D. and Turekian, K.K., editors, Treatise on Geochemistry (Second Edition): Oxford, Elsevier, p. 341-378.

Schulz, K.J., Stewart, D.B., Tucker, R.D., Pollock, J.C., and Ayuso, R.A., 2008, The Ellsworth terrane, coastal Maine: Geochronology, geochemistry, and Nd-Pb isotopic composition—Implications for the rifting of Ganderia: Geological Society of America Bulletin, v. 120, n. 9-10, p. 1134-1158.

Simonetti, A., Heaman, L., Hartlaub, R., Creaser, R., MacHattie, T., and Bohm, C., 2005, U-Pb zircon dating by laser ablation-MC-ICP-MS using a new multiple ion counting Faraday collector array: Journal of Analytical Atomic Spectrometry, v. 20, n. 8, p. 677-686.

Smith, E.A., 2005, Bedrock geology of southwestern New Brunswick (NTS 21 G, part of 21 B): New Brunswick Department of Natural Resources, Minerals, Policy, and Planning Division, Map NR-5 (Second Edition), scale 1:250000.

Smith, E.A., 2006, Bedrock geology of southeastern New Brunswick (NTS 21 H): New Brunswick Department of Natural Resources, Minerals, Policy, and Planning Division, Map NR-6 (Second Edition), 1:250000.

Smith, E.A., and Fyffe, L.R., 2006, Bedrock geology of central New Brunswick (NTS 21 J): New Brunswick Department of Natural Resources, Minerals, Policy, and Planning Division, Map NR-4 (Second Edition), scale 1:250000.

Soper, N.J., Ryan, P.D., and Dewey, J.F., 1999, Age of the Grampian Orogeny in Scotland and Ireland: Journal of the Geological Society of London, v. 156, n. 6, p. 1231-1236.

Tera, F., and Wasserburg, G.J., 1972a, U-Th-Pb systematics in lunar highland samples from the Luna 20 and Apollo 16 missions: Earth and Planetary Science Letters, v. 17, n. 1, p. 36-51.

Tera, F., and Wasserburg, G.J., 1972b, U-Th-Pb systematics in three Apollo 14 basalts and the problem of initial Pb in lunar rocks: Earth and Planetary Science Letters, v. 14, n. 3, p. 281-304.

Turner, S., 1986, *Thelodus macintoshi* Stetson 1928, the largest known thelodont (Agnatha: Thelodonti): Breviora, v. 486, p. 1-18.

van Staal, C.R., 1994, Brunswick subduction complex in the Canadian Appalachians: record of the Late Ordovician to Late Silurian collision between Laurentia and the Gander margin of Avalon: Tectonics, v. 13, n. 4, p. 946-962.

van Staal, C.R., and de Roo, J.A., 1995, Mid-Paleozoic tectonic evolution of the Appalachian Central mobile belt in northern New Brunswick, Canada: collision, extensional collapse and dextral transpression, *in* Hibbard, J.P., van Staal, C.R. and Cawood, P.A., editors, Current perspectives in the Appalachian-Caledonian Orogen: Geological Association of Canada, Special Paper, v. 41, p. 367-389.

van Staal, C.R., Ravenhurst, C.E., Winchester, J.A., Roddick, J.C., and Langton, J.P., 1990, Post-Taconic blueschist suture in the Northern Appalachians of northern New Brunswick, Canada: Geology, v. 18, n. 11, p. 1073-1077.

van Staal, C.R., Sullivan, R.W., and Whalen, J.B., 1996, Provenance of tectonic history of the Gander Zone in the Caledonian/Appalachian Orogen: implications for the origin and assembly of Avalon, *in* Nance, R.D. and Thompson, M.D., editors, Avalonian and related peri-Gondwanan terranes of the Circum–North Atlantic: Geological Society of America, Special Papers, v. 304, p. 347-367.

van Staal, C.R., Dewey, J.F., Mac Niocaill, C., and McKerrow, W.S., 1998, The Cambrian-

Silurian tectonic evolution of the Northern Appalachians and British Caledonides: history of a complex, west and southwest Pacific-type segment of Iapetus, *in* Blundell, D.J. and Scott, A.C., editors, Lyell: the Past is the Key to the Present: Geological Society of London, Special Publications, v. 143, p. 199-242.

van Staal, C.R., Wilson, R.A., Rogers, N., Fyffe, L.R., Langton, J.P., McCutcheon, S.R., McNicoll, V., and Ravenhurst, C.E., 2003, Geology and tectonic history of the Bathurst Supergroup, Bathurst mining camp, and its relationships to coeval rocks in southwestern New Brunswick and adjacent mine—a synthesis, *in* Goodfellow, W.D., McCutcheon, S.R. and Peter, J.M., editors, Massive sulfide deposits of the Bathurst mining camp, New Brunswick, and northern Maine: Economic Geology Monographs, v. 11, p. 37-60.

van Staal, C.R., Currie, K.L., Rowbotham, G., Rogers, N., and Goodfellow, W., 2008, Pressure-temperature paths and exhumation of Late Ordovician-Early Silurian blueschists and associated metamorphic nappes of the Salinic Brunswick subduction complex, Northern Appalachians: Geological Society of America Bulletin, v. 120, n. 11-12, p. 1455-1477.

van Staal, C.R., Whalen, J.B., Valverde-Vaquero, P., Zagorevski, A., and Rogers, N., 2009, Pre-Carboniferous, episodic accretion-related, orogenesis along the Laurentian margin of the Northern Appalachians, *in* Murphy, J.B., Keppie, J.D. and Hynes, A.J., editors, Ancient orogens and modern analogues: Geological Society of London, Special Publications, v. 327, p. 271-316.

van Staal, C.R., Barr, S.M., and Murphy, J.B., 2012, Provenance and tectonic evolution of Ganderia: constraints on the evolution of the Iapetus and Rheic Oceans: Geology, v. 40, n. 11, p. 987-990.

van Staal, C.R., Zagorevski, A., McNicoll, V.J., and Rogers, N., 2014, Time-transgressive Salinic and Acadian orogenesis, magmatism and Old Red Sandstone sedimentation in Newfoundland: Geoscience Canada, v. 41, n. 2, p. 138-164.

van Staal, C.R., Wilson, R.A., Kamo, S.L., McClelland, W.C., and McNicoll, V., 2016, Evolution of the Early to Middle Ordovician Popelogan Arc in New Brunswick, Canada, and adjacent Maine, USA: record of arc-trench migration and multiple phases of rifting: Geological Society of America Bulletin, v. 128, n. 1-2, p. 122-146.

Van Wagoner, N.A., Leybourne, M.I., Dadd, K.A., and Huskins, M.L.A., 2001, The Silurian(?) Passamaquoddy Bay mafic dyke swarm, New Brunswick: petrogenesis and tectonic implications: Canadian Journal of Earth Sciences, v. 38, n. 11, p. 1565-1578.

Van Wagoner, N.A., Leybourne, M.I., Dadd, K.A., Baldwin, D.K., and McNeil, W., 2002, Late Silurian bimodal volcanism of southwestern New Brunswick, Canada: products of continental extension: Geological Society of America Bulletin, v. 114, n. 4, p. 400-418.

Vermeesch, P., 2004, How many grains are needed for a provenance study?: Earth and Planetary Science Letters, v. 224, n. 3-4, p. 441-451.

Vermeesch, P., 2012, On the visualisation of detrital age distributions: Chemical Geology, v. 312-313, p. 190-194.

Waldron, J.W.F., Floyd, J.D., Simonetti, A., and Heaman, L.M., 2008, Ancient Laurentian detrital zircon in the closing Iapetus Ocean, Southern Uplands terrane, Scotland: Geology, v. 36, n. 7, p. 527-530.

Waldron, J.W.F., White, C.E., Barr, S.M., Simonetti, A., and Heaman, L.M., 2009, Provenance of the Meguma Terrane, Nova Scotia: rifted margin of early Paleozoic Gondwana: Canadian Journal of Earth Sciences, v. 46, n. 1, p. 1-8.

Waldron, J.W.F., Schofield, D.I., White, C.E., and Barr, S.M., 2011, Cambrian successions of the Meguma Terrane, Nova Scotia, and Harlech Dome, north Wales: dispersed fragments of a peri-Gondwanan basin?: Journal of the Geological Society of London, v. 168, n. 1, p. 83-98.

Waldron, J.W.F., McNicoll, V.J., and van Staal, C.R., 2012, Laurentia-derived detritus in the

Badger Group of central Newfoundland: deposition during closing of the Iapetus Ocean: Canadian Journal of Earth Sciences, v. 49, n. 1, p. 207-221.

Waldron, J.W.F., Schofield, D.I., Dufrane, S.A., Floyd, J.D., Crowley, Q.G., Simonetti, A., Dokken, R.J., and Pothier, H.D., 2014a, Ganderia–Laurentia collision in the Caledonides of Great Britain and Ireland: Journal of the Geological Society of London, v. 171, n. 4, p. 555-569.

Waldron, J.W.F., Schofield, D.I., Murphy, J.B., and Thomas, C.W., 2014b, How was the Iapetus Ocean infected with subduction?: Geology, v. 42, n. 12, p. 1095-1098.

Waldron, J.W.F., Schofield, D.I., Murphy, J.B., 2017 (in review), Diachronous Palaeozoic accretion of peri-Gondwanan terranes at the Laurentian margin: Geological Society of London, Special Publications.

West, D.P., Jr., Ludman, A., and Lux, D.R., 1992, Silurian age for the Pocomoonshine Gabbro-Diorite, southeastern Maine and its regional tectonic implications: American Journal of Science, v. 292, n. 4, p. 253-273.

Wetherill, G.W., 1956, Discordant uranium-lead ages: Transaction of the American Geophysical Union, v. 37, p. 320-326.

White, C.E., and Barr, S.M., 1996, Geology of the Brookville Terrane, southern New Brunswick, Canada, *in* Nance, R.D. and Thompson, M.D., editors, Avalonian and related peri-Gondwanan terranes of the Circum-North Atlantic: Geological Society of America, Special Papers, v. 304, p. 133-147.

White, C.E., Barr, S.M., Bevier, M.L., and Kamo, S., 1994, A revised interpretation of Cambrian and Ordovician rocks in the Bourinot Belt of central Cape Breton Island, Nova Scotia: Atlantic Geology, v. 30, n. 2, p. 123-142.

Williams, H., 1979, Appalachian Orogen in Canada: Canadian Journal of Earth Sciences, v. 16,

n. 3, p. 792-807.

Williams, H., 1995, Introduction, *in* Geology of the Appalachian-Caledonian Orogen in Canada and Greenland: Geological Survey of Canada, Geology of Canada, v. 6, p. 3-19.

Williams, H., and Hatcher, R.D., Jr., 1982, Suspect terranes and accretionary history of the Appalachian Orogen: Geology, v. 10, n. 10, p. 530-536.

Williams, H., and Hatcher, R.D., Jr., 1983, Appalachian suspect terranes, *in* Hatcher, R.D., Jr., Williams, H. and Zietz, I., editors, Contributions to the tectonics and geophysics of mountain chains: Geological Society of America, Memoirs, v. 158, p. 33-53.

Williams, H., and Hiscott, R.N., 1987, Definition of the Iapetus rift-drift transition in western Newfoundland: Geology, v. 15, n. 11, p. 1044-1047.

Williams, H., Currie, K.L., and Piasecki, M.A.J., 1993, The Dog Bay Line: a major Silurian tectonic boundary in Northeast Newfoundland: Canadian Journal of Earth Sciences, v. 30, n. 12, p. 2481-2494.

Willner, A., Gerdes, A., Massonne, H., van Staal, C.R., Zagorevski, A., 2014, Crustal Evolution of the Northeast Laurentian Margin and the Peri-Gondwanan Microcontinent Ganderia Prior to and During Closure of the Iapetus Ocean: Detrital Zircon U–Pb and Hf Isotope Evidence from Newfoundland: Geoscience Canada, v. 41, n. 3, p. 345-364.

Wilson, J.T., 1966, Did the Atlantic close and then re-open?: Nature, v. 211, n. 5050, p. 676-681.

Wilson, R.A., 2000, Geology of the Popelogan Lake-Lost Pine Lake area (NTS 21O/15a and b), Restigouche County, New Brunswick, *in* Carroll, B.M.W., editor, Current research 1999: New Brunswick Department of Natural Resources and Energy, Minerals and Energy Division, Mineral Resource Report 2000-4, p. 91-136.

Wilson, R.A., 2003, Geochemistry and petrogenesis of Ordovician arc-related mafic volcanic

rocks in the Popelogan Inlier, northern New Brunswick: Canadian Journal of Earth Sciences, v. 40, n. 9, p. 1171-1189.

Wilson, R.A., and Kamo, S.L., 2012, The Salinic Orogeny in northern New Brunswick: geochronological constraints and implications for Silurian stratigraphic nomenclature: Canadian Journal of Earth Sciences, v. 49, n. 1, p. 222-238.

Wilson, R.A., Burden, E.T., Bertrand, R., Asselin, E., and McCracken, A.D., 2004, Stratigraphy and tectono-sedimentary evolution of the Late Ordovician to Middle Devonian Gaspe Belt in northern New Brunswick: evidence from the Restigouche area: Canadian Journal of Earth Sciences, v. 41, n. 5, p. 527-551.

Wilson, R.A., van Staal, C.R., and McClelland, W.C., 2015, Synaccretionary sedimentary and volcanic rocks in the Ordovician Tetagouche backarc basin, New Brunswick, Canada: evidence for a transition from foredeep to forearc basin sedimentation: American Journal of Science, v. 315, n. 10, p. 958-1001.

Woodcock, N.H., and Soper, N.J., 2006, The Acadian Orogeny: the Mid-Devonian phase of deformation that formed slate belts in England and Wales, *in* Brenchley, P.J. and Rawson, P.F., editors, The geology of England and Wales: p. 131-146.

York, D., 1969, Least squares fitting of a straight line with correlated errors: Earth and Planetary Science Letters, v. 5, n. 5, p. 320-324.

Zalasiewicz, J.A., Williams, M., and Akhurst, M., 2003, An unlikely evolutionary lineage: the Rhuddanian (Silurian, Llandovery) graptolites Huttagraptus? praematurus and Coronograptus cyphus re-examined: Scottish Journal of Geology, v. 39, n. 1, p. 89-96.

Zalasiewicz, J.A., Taylor, L., Rushton, A.W.A., Loydell, D.K., Rickards, R.B., and Williams, M., 2009, Graptolites in British stratigraphy: Geological Magazine, v. 146, n. 6, p. 785-850.

Appendix A: Fredericton Trough detrital zircon data and diagrams

Notes to appendix:

[1]Percent discordance between $^{206}Pb/^{238}U$ and $^{207}Pb/^{206}Pb$, as per the following formula:

$$[(e^{0.000155125 \times 207Pb/206Pb\ age} - 1) - {}^{207}Pb/^{206}Pb\ ratio] \times 100 / [(e^{0.000155125 \times 207Pb/206Pb\ age} - 1)]$$

[2] $^{207}Pb/^{206}Pb$ ages are reported for $^{207}Pb/^{206}Pb$ ratios greater than 0.0658 (800 Ma); $^{206}Pb/^{238}U$ ages reported otherwise.

Samples in *italics* are corrected for common lead. A discordance cutoff of 10% is applied: analyses which fall outside of the -10% to +10% range are greyed out.

Concordia diagrams do not exclude discordant analyses.

Correlation coefficients (ρ) calculated by the following formula:

$$[(2\sigma^{207}Pb/^{235}U / {}^{207}Pb/^{235}U)^2 + (2\sigma^{206}Pb/^{238}U / {}^{206}Pb/^{238}U)^2 - (2\sigma^{207}Pb/^{206}Pb / {}^{207}Pb/^{206}Pb)^2] / [(2)(2\sigma^{206}Pb/^{238}U / {}^{206}Pb/^{238}U)(2\sigma^{207}Pb/^{235}U /^{207}Pb/^{235}U)]$$

$^{207}Pb/^{235}U$ ratios are calculated as $137.88 \times {}^{206}Pb/^{238}U \times {}^{207}Pb/^{206}Pb$.

Histograms and KDEs were generated using DensityPlotter 7.3 (Vermeesch, 2012), and concordia diagrams with Isoplot 3.75 (Ludwig, 2012).

Burtts Corner Fm. (NA001A)

sample name	^{206}Pb (cps)	^{204}Pb (cps)	^{207}Pb/^{206}Pb	2 σ	^{207}Pb/^{235}U	2 σ	^{206}Pb/^{238}U	2 σ	ρ	age (Ma) ^{207}Pb/^{206}Pb	error (Ma) 2 σ	age (Ma) ^{207}Pb/^{235}U	error (Ma) 2 σ	age (Ma) ^{206}Pb/^{238}U	error (Ma) 2 σ	discordance[1] %	reported age[2] (Ma)	2 σ
NA001A-001	161231	56	0.06486	0.00160	0.94860	0.05799	0.10608	0.00594	0.915	770	51	677	30	650	35	16.3	650	35
NA001A-002	86915	32	0.07371	0.00093	1.54231	0.08498	0.15175	0.00814	0.973	1034	25	947	33	911	45	12.7	1034	25
NA001A-003	235024	36	0.06173	0.00123	0.85774	0.04658	0.10077	0.00509	0.930	665	42	629	25	619	30	7.2	619	30
NA001A-004	272467	7152	0.40895	0.03892	7.49725	0.97810	0.13296	0.01186	0.684	3942	136	2173	111	805	67	84.2	3942	136
NA001A-005	69125	79	0.06383	0.00145	1.06075	0.06050	0.12052	0.00631	0.917	736	47	734	29	734	36	0.4	734	36
NA001A-006	31906	70	0.07293	0.00134	1.70842	0.09394	0.16989	0.00880	0.942	1012	37	1012	35	1011	48	0.1	1012	37
NA001A-007	242104	106	0.07518	0.00132	1.55112	0.09788	0.14965	0.00907	0.961	1073	35	951	38	899	51	17.4	1073	35
NA001A-008	139034	102	0.10085	0.00114	3.98138	0.22056	0.28631	0.01553	0.979	1640	21	1630	44	1623	77	1.2	1640	21
NA001A-009	66206	64	0.05604	0.00128	0.59012	0.03584	0.07638	0.00430	0.926	454	50	471	23	474	26	-4.7	474	26
NA001A-010	166800	79	0.08654	0.00094	2.71653	0.14476	0.22766	0.01188	0.979	1350	21	1333	39	1322	62	2.3	1350	21
NA001A-011	266175	34	0.05753	0.00114	0.64071	0.03478	0.08077	0.00408	0.931	512	43	503	21	501	24	2.3	501	24
NA001A-012	12355	37	0.06847	0.00223	1.58962	0.09762	0.16839	0.00877	0.848	883	66	966	38	1003	48	-14.7	883	66
NA001A-013	653476	70	0.09259	0.00098	2.71900	0.15981	0.21297	0.01231	0.984	1480	20	1334	43	1245	65	17.5	1480	20
NA001A-014	26383	40	0.05229	0.00196	0.48982	0.03231	0.06794	0.00368	0.822	298	83	405	22	424	22	-43.6	424	22
NA001A-015	57551	41	0.07979	0.00102	2.13634	0.11915	0.19418	0.01054	0.973	1192	25	1161	38	1144	57	4.4	1192	25
NA001A-016	324743	61	0.10975	0.00135	3.04297	0.23846	0.20108	0.01556	0.988	1795	22	1418	58	1181	83	37.4	1795	22
NA001A-017	246187	59	0.11225	0.00117	4.82753	0.25945	0.31193	0.01645	0.981	1836	19	1790	44	1750	80	5.3	1836	19
NA001A-018	98382	44	0.08018	0.00100	2.16004	0.11659	0.19538	0.01026	0.973	1201	24	1168	37	1150	55	4.6	1201	24
NA001A-019	148966	60	0.06966	0.00080	1.49896	0.08048	0.15606	0.00818	0.977	918	24	930	32	935	45	-1.9	918	24
NA001A-020	241907	58	0.12832	0.00132	6.57839	0.36375	0.37181	0.02020	0.982	2075	18	2056	48	2038	94	2.1	2075	18
NA001A-021	68449	39	0.05845	0.00127	0.61774	0.03305	0.07665	0.00375	0.914	547	47	488	21	476	22	13.4	476	22
NA001A-022	145851	112	0.10006	0.00259	3.39424	0.20779	0.24602	0.01365	0.906	1625	47	1503	47	1418	70	14.2	1625	47
NA001A-023	55324	66	0.06408	0.00151	0.86057	0.04876	0.09740	0.00502	0.909	744	49	630	26	599	29	20.4	599	29
NA001A-024	783096	43	0.07791	0.00080	2.12882	0.11484	0.19818	0.01049	0.982	1144	20	1158	37	1166	56	-2.0	1144	20
NA001A-025	49528	42	0.05795	0.00132	0.62994	0.03597	0.07884	0.00413	0.917	528	49	496	22	489	25	7.6	489	25
NA001A-026	136968	81	0.11620	0.00128	5.28256	0.29560	0.32973	0.01809	0.980	1898	20	1866	47	1837	87	3.7	1898	20
NA001A-027	64117	40	0.05856	0.00134	0.64813	0.03786	0.08027	0.00432	0.921	551	49	507	23	498	26	10.0	498	26
NA001A-028	52629	68	0.05979	0.00155	0.64683	0.03513	0.07846	0.00375	0.879	596	55	507	21	487	22	19.0	487	22
NA001A-029	142554	49	0.10489	0.00114	4.15142	0.22126	0.28705	0.01498	0.979	1712	20	1664	43	1627	75	5.7	1712	20
NA001A-030	705819	72	0.06115	0.00121	0.88099	0.04651	0.10450	0.00512	0.927	644	42	642	25	641	30	0.6	641	30
NA001A-031	156214	115	0.13260	0.00142	6.72387	0.39733	0.36776	0.02137	0.983	2133	19	2076	51	2019	100	6.2	2133	19
NA001A-032	570090	210	0.06372	0.00135	0.94139	0.05407	0.10715	0.00572	0.929	732	44	674	28	656	33	10.9	656	33
NA001A-033	55811	129	0.07642	0.00101	1.88147	0.10416	0.17857	0.00960	0.971	1106	26	1075	36	1059	52	4.6	1106	26
NA001A-034	14125	119	0.08004	0.00238	1.74298	0.11341	0.15794	0.00914	0.890	1198	58	1025	41	945	51	22.7	1198	58
NA001A-035	71425	141	0.05945	0.00126	0.67128	0.03741	0.08189	0.00422	0.925	584	45	521	22	507	25	13.6	507	25
NA001A-036	195703	178	0.07230	0.00082	1.62299	0.09720	0.16281	0.00957	0.982	994	23	979	37	972	53	2.4	994	23
NA001A-037	222612	137	0.07823	0.00083	2.09941	0.11445	0.19465	0.01041	0.981	1153	21	1149	37	1146	56	0.6	1153	21
NA001A-038	394252	135	0.06459	0.00128	1.18341	0.05880	0.13288	0.00606	0.917	761	41	793	27	804	34	-6.0	804	34
NA001A-039	274946	118	0.07381	0.00079	1.82609	0.10363	0.17944	0.01000	0.982	1036	22	1055	37	1064	54	-2.9	1036	22
NA001A-040	141324	113	0.07785	0.00086	2.04997	0.10553	0.19097	0.00960	0.977	1143	22	1132	35	1127	52	1.6	1143	22
NA001A-041	282157	55	0.09389	0.00099	3.33289	0.18458	0.25746	0.01400	0.982	1506	20	1489	42	1477	71	2.2	1506	20
NA001A-042	47607	68	0.05632	0.00143	0.59826	0.03592	0.07704	0.00419	0.906	465	55	476	23	478	25	-3.0	478	25
NA001A-043	60207	53	0.05603	0.00129	0.56477	0.03378	0.07311	0.00404	0.923	453	50	455	22	455	24	-0.3	455	24
NA001A-044	48249	52	0.07971	0.00108	2.16543	0.11295	0.19703	0.00993	0.966	1190	26	1170	36	1159	53	2.8	1190	26
NA001A-045	29547	30	0.05582	0.00180	0.61604	0.04192	0.08005	0.00479	0.880	445	70	487	26	496	29	-12.0	496	29
NA001A-046	21422	34	0.05257	0.00154	0.56244	0.03311	0.07760	0.00396	0.867	310	65	453	21	482	24	-57.4	482	24
NA001A-047	33722	29	0.06769	0.00133	1.40389	0.07872	0.15042	0.00790	0.936	859	40	891	33	903	44	-5.5	859	40
NA001A-048	280159	9	0.10792	0.00113	4.55803	0.26544	0.30633	0.01755	0.984	1765	19	1742	47	1723	86	2.7	1765	19

Burtts Corner Fm. (NA001A)

										age (Ma)	error (Ma)	age (Ma)	error (Ma)	age (Ma)	error (Ma)	discordance[1]	reported age[2]	
sample name	^{206}Pb (cps)	^{204}Pb (cps)	^{207}Pb/^{206}Pb	2 σ	^{207}Pb/^{235}U	2 σ	^{206}Pb/^{238}U	2 σ	ρ	^{207}Pb/^{206}Pb	2 σ	^{207}Pb/^{235}U	2 σ	^{206}Pb/^{238}U	2 σ	%	(Ma)	2 σ
NA001A-049	824725	49	0.09904	0.00104	3.52285	0.21475	0.25797	0.01549	0.985	1606	20	1532	47	1479	79	8.8	1606	20
NA001A-050	304338	26	0.07532	0.00083	1.86906	0.10267	0.17997	0.00969	0.980	1077	22	1070	36	1067	53	1.0	1077	22
NA001A-051	156048	1	0.07529	0.00088	1.79116	0.09836	0.17254	0.00926	0.977	1076	23	1042	35	1026	51	5.0	1076	23
NA001A-052	265459	0	0.10033	0.00103	3.89627	0.20984	0.28166	0.01489	0.982	1630	19	1613	43	1600	74	2.1	1630	19
NA001A-053	179799	4	0.05733	0.00121	0.59379	0.03084	0.07511	0.00356	0.913	504	46	473	19	467	21	7.7	467	21
NA001A-054	60731	119	0.05670	0.00153	0.58420	0.03680	0.07473	0.00425	0.903	480	59	467	23	465	25	3.3	465	25
NA001A-055	363070	170	0.09999	0.00118	3.81121	0.21063	0.27644	0.01493	0.977	1624	22	1595	44	1573	75	3.5	1624	22
NA001A-056	366090	151	0.05695	0.00118	0.60235	0.03872	0.07671	0.00467	0.947	490	45	479	24	476	28	2.8	476	28
NA001A-057	395223	136	0.09836	0.00108	3.56699	0.23783	0.26301	0.01730	0.986	1593	20	1542	52	1505	88	6.2	1593	20
NA001A-058	121438	99	0.05677	0.00116	0.57483	0.03455	0.07343	0.00415	0.940	483	45	461	22	457	25	5.6	457	25
NA001A-059	218791	78	0.09141	0.00249	2.94897	0.21544	0.23398	0.01586	0.928	1455	51	1395	54	1355	82	7.6	1455	51
NA001A-060	375351	79	0.11241	0.00118	4.89718	0.29747	0.31596	0.01890	0.985	1839	19	1802	50	1770	92	4.3	1839	19
NA001A-061	287070	33	0.08656	0.00091	2.67460	0.16630	0.22410	0.01373	0.985	1351	20	1321	45	1304	72	3.9	1351	20
NA001A-062	786279	43	0.08581	0.00095	2.64849	0.15509	0.22385	0.01287	0.982	1334	21	1314	42	1302	67	2.6	1334	21
NA001A-063	364332	24	0.07323	0.00077	1.64905	0.08863	0.16332	0.00861	0.981	1020	21	989	33	975	48	4.8	1020	21
NA001A-064	127034	21	0.05532	0.00117	0.54984	0.03264	0.07208	0.00400	0.935	425	46	445	21	449	24	-5.7	449	24
NA001A-065	190825	25	0.13261	0.00139	6.79370	0.40166	0.37157	0.02162	0.984	2133	18	2085	51	2037	101	5.2	2133	18
NA001A-066	150682	35	0.07458	0.00094	1.81015	0.10705	0.17603	0.01017	0.977	1057	25	1049	38	1045	56	1.2	1057	25
NA001A-066-B	400697	34	0.05631	0.00113	0.61437	0.03720	0.07913	0.00452	0.944	465	44	486	23	491	27	-5.9	491	27
NA001A-067	94125	32	0.05427	0.00119	0.51732	0.03234	0.06913	0.00405	0.936	382	49	423	21	431	24	-13.1	431	24
NA001A-068	151701	39	0.06008	0.00125	0.88421	0.04793	0.10674	0.00535	0.924	606	44	643	26	654	31	-8.2	654	31
NA001A-069	5436	36	0.02396	0.01199	0.33431	0.16870	0.10121	0.00638	0.125	-1912	1278	293	121	621	37	139.4	621	37
NA001A-070	138509	50	0.06229	0.00126	0.95566	0.05289	0.11127	0.00573	0.931	684	43	681	27	680	33	0.6	680	33
NA001A-071	95934	44	0.05543	0.00121	0.57510	0.03157	0.07525	0.00379	0.918	430	48	461	20	468	23	-9.2	468	23
NA001A-072	166508	38	0.10341	0.00110	4.02909	0.22007	0.28259	0.01514	0.981	1686	19	1640	43	1604	76	5.5	1686	19
NA001A-073	71706	28	0.05256	0.00121	0.51395	0.03640	0.07092	0.00475	0.946	310	51	421	24	442	29	-44.0	442	29
NA001A-074	71105	25	0.06838	0.00110	1.39815	0.08519	0.14829	0.00872	0.965	880	33	888	35	891	49	-1.4	880	33
NA001A-075	87070	46	0.05254	0.00119	0.50665	0.03055	0.06993	0.00391	0.927	309	51	416	20	436	24	-42.3	436	24
NA001A-076	392298	13	0.10169	0.00106	3.92633	0.27583	0.28003	0.01946	0.989	1655	19	1619	55	1592	97	4.3	1655	19
NA001A-077	946428	44	0.07179	0.00073	1.60132	0.09868	0.16177	0.00983	0.986	980	21	971	38	967	54	1.5	980	21
NA001A-078A	136859	17	0.05853	0.00122	0.80640	0.05041	0.09992	0.00589	0.942	550	45	600	28	614	34	-12.2	614	34
NA001A-078B	87908	25	0.05714	0.00125	0.81140	0.04861	0.10299	0.00574	0.931	497	48	603	27	632	33	-28.5	632	33
NA001A-079	246492	19	0.07410	0.00084	1.85248	0.10221	0.18130	0.00979	0.979	1044	23	1064	36	1074	53	-3.1	1044	23
NA001A-080	159138	110	0.06266	0.00167	0.67316	0.04244	0.07792	0.00445	0.906	697	56	523	25	484	27	31.7	484	27
NA001A-081	70726	10	0.06023	0.00126	0.82126	0.04909	0.09890	0.00554	0.937	612	45	609	27	608	32	0.7	608	32
NA001A-082	221241	23	0.05659	0.00118	0.62054	0.03391	0.07953	0.00402	0.925	476	45	490	21	493	24	-3.8	493	24
NA001A-083	129081	37	0.06015	0.00150	0.73524	0.04452	0.08865	0.00489	0.911	609	53	560	26	548	29	10.5	548	29
NA001A-084	48921	41	0.07622	0.00117	1.94444	0.11547	0.18503	0.01061	0.966	1101	30	1097	39	1094	57	0.6	1101	30
NA001A-085	62615	59	0.05764	0.00179	0.64023	0.04036	0.08056	0.00442	0.870	516	67	502	25	499	26	3.4	499	26
NA001A-086	459751	35	0.07585	0.00077	1.86573	0.11245	0.17840	0.01060	0.986	1091	20	1069	39	1058	58	3.3	1091	20
NA001A-087	416914	16	0.08089	0.00083	2.28078	0.12373	0.20449	0.01089	0.982	1219	20	1206	38	1199	58	1.7	1219	20
NA001A-088	329512	30	0.10102	0.00107	3.87635	0.19829	0.27829	0.01393	0.978	1643	20	1609	40	1583	70	4.1	1643	20
NA001A-089	170933	21	0.21210	0.00219	15.89050	0.91925	0.54338	0.03093	0.984	2922	17	2870	54	2798	128	5.2	2922	17
NA001A-090	380547	22	0.06073	0.00120	0.89546	0.05263	0.10694	0.00592	0.942	630	42	649	28	655	34	-4.2	655	34
NA001A-091	94081	14	0.07366	0.00091	1.67117	0.09766	0.16454	0.00940	0.977	1032	25	998	36	982	52	5.3	1032	25
NA001A-092	374724	14	0.09849	0.00102	3.72485	0.21698	0.27430	0.01573	0.984	1596	19	1577	46	1563	79	2.3	1596	19
NA001A-093	996156	6	0.08788	0.00090	2.89534	0.17576	0.23894	0.01430	0.986	1380	20	1381	45	1381	74	-0.1	1380	20
NA001A-094	539507	7	0.11654	0.00119	5.40098	0.30453	0.33613	0.01864	0.983	1904	18	1885	47	1868	89	2.2	1904	18

Burtts Corner Fm. (NA001A)

sample name	^{206}Pb (cps)	^{204}Pb (cps)	^{207}Pb/^{206}Pb	2 σ	^{207}Pb/^{235}U	2 σ	^{206}Pb/^{238}U	2 σ	ρ	age (Ma) ^{207}Pb/^{206}Pb	error (Ma) 2 σ	age (Ma) ^{207}Pb/^{235}U	error (Ma) 2 σ	age (Ma) ^{206}Pb/^{238}U	error (Ma) 2 σ	discordance[1] %	reported age[2] (Ma)	2 σ
NA001A-095	584145	23	0.07584	0.00083	1.95887	0.12578	0.18734	0.01185	0.985	1091	22	1101	42	1107	64	-1.6	1091	22
NA001A-096	281946	24	0.06228	0.00129	0.93118	0.05291	0.10843	0.00574	0.931	684	44	668	27	664	33	3.1	664	33
NA001A-097	405625	6	0.07759	0.00080	2.01005	0.12065	0.18789	0.01111	0.985	1136	20	1119	40	1110	60	2.5	1136	20
NA001A-098	46453	6	0.05496	0.00142	0.60187	0.03763	0.07942	0.00452	0.911	411	57	478	24	493	27	-20.7	493	27
NA001A-099	2167303	225	0.09993	0.00103	3.19930	0.17610	0.23220	0.01256	0.982	1623	19	1457	42	1346	65	18.9	1623	19
NA001A-100	321964	13	0.08599	0.00089	2.69988	0.14212	0.22772	0.01175	0.981	1338	20	1328	38	1323	61	1.3	1338	20
NA001A-101	439308	21	0.11526	0.00128	5.19969	0.28811	0.32717	0.01776	0.980	1884	20	1853	46	1825	86	3.6	1884	20
NA001A-102	34211	24	0.05549	0.00177	0.58020	0.03721	0.07583	0.00422	0.867	432	70	465	24	471	25	-9.4	471	25
NA001A-103	190834	32	0.10148	0.00112	3.75327	0.21543	0.26824	0.01511	0.981	1651	20	1583	45	1532	76	8.1	1651	20
NA001A-104	204884	71	0.08769	0.00096	2.78408	0.15416	0.23026	0.01250	0.980	1376	21	1351	41	1336	65	3.2	1376	21
NA001A-105	188353	31	0.08817	0.00099	2.56821	0.17357	0.21126	0.01408	0.986	1386	21	1292	48	1236	75	11.9	1386	21
NA001A-106	1166414	33	0.18568	0.00188	12.17228	0.61194	0.47546	0.02341	0.979	2704	17	2618	46	2507	101	8.8	2704	17
NA001A-107	130697	30	0.08639	0.00098	2.75083	0.16220	0.23094	0.01336	0.981	1347	22	1342	43	1339	70	0.6	1347	22
NA001A-108	284767	35	0.08983	0.00098	2.98299	0.18758	0.24083	0.01492	0.985	1422	21	1403	47	1391	77	2.4	1422	21
NA001A-109	338222	56	0.07924	0.00092	1.95692	0.11014	0.17911	0.00986	0.978	1178	23	1101	37	1062	54	10.7	1178	23
NA001A-110	189813	61	0.07361	0.00103	1.72991	0.09402	0.17044	0.00895	0.966	1031	28	1020	34	1015	49	1.7	1031	28
NA001A-111	284964	15	0.07488	0.00079	1.77778	0.10055	0.17220	0.00957	0.982	1065	21	1037	36	1024	52	4.2	1065	21
NA001A-112	63308	43	0.06211	0.00180	0.74446	0.04561	0.08694	0.00469	0.880	678	61	565	26	537	28	21.6	537	28
NA001A-113	60966	58	0.05788	0.00123	0.70457	0.04083	0.08828	0.00476	0.931	525	46	542	24	545	28	-4.0	545	28
NA001A-114	108860	103	0.10206	0.00120	3.52020	0.21529	0.25016	0.01502	0.981	1662	22	1532	47	1439	77	14.9	1662	22
NA001A-115	191106	60	0.07067	0.00083	1.42078	0.08018	0.14581	0.00805	0.978	948	24	898	33	877	45	8.0	948	24
NA001A-116	314282	63	0.09533	0.00099	3.48306	0.18845	0.26500	0.01407	0.982	1535	19	1523	42	1515	71	1.4	1535	19
NA001A-117	725460	60	0.07872	0.00081	2.14760	0.12428	0.19786	0.01127	0.984	1165	20	1164	39	1164	60	0.1	1165	20
NA001A-118	301064	210	0.07561	0.00082	1.80754	0.10013	0.17338	0.00942	0.981	1085	22	1048	36	1031	52	5.4	1085	22
NA001A-119	95350	173	0.06245	0.00135	0.95984	0.06094	0.11146	0.00666	0.941	690	45	683	31	681	38	1.3	681	38
NA001A-120	603633	97	0.11061	0.00116	4.84937	0.24305	0.31797	0.01558	0.978	1809	19	1794	41	1780	76	1.9	1809	19
NA001A-121	53489	30	0.05724	0.00126	0.67654	0.04247	0.08572	0.00504	0.937	501	48	525	25	530	30	-6.1	530	30
NA001A-122	111329	34	0.07747	0.00084	1.98381	0.10922	0.18572	0.01003	0.981	1133	21	1110	37	1098	54	3.4	1133	21
NA001A-123	129686	141	0.05741	0.00126	0.60983	0.03332	0.07704	0.00386	0.916	507	47	483	21	478	23	5.9	478	23
NA001A-124	103721	65	0.07959	0.00101	2.16625	0.12036	0.19740	0.01068	0.973	1187	25	1170	38	1161	57	2.4	1187	25
NA001A-125	28228	41	0.06641	0.00185	1.37977	0.09244	0.15068	0.00918	0.909	819	57	880	39	905	51	-11.2	819	57
NA001A-126	179325	35	0.08953	0.00098	2.91410	0.16571	0.23606	0.01317	0.981	1416	21	1386	42	1366	68	3.9	1416	21
NA001A-127	65458	83	0.07436	0.00107	1.81137	0.10059	0.17667	0.00947	0.966	1051	29	1050	36	1049	52	0.3	1051	29
NA001A-128	358777	59	0.07797	0.00082	2.01462	0.10799	0.18741	0.00985	0.981	1146	21	1120	36	1107	53	3.7	1146	21
NA001A-129	1252270	643	0.10442	0.00128	3.47331	0.19714	0.24124	0.01337	0.976	1704	22	1521	44	1393	69	20.3	1704	22
NA001A-130	107530	180	0.07593	0.00112	1.84658	0.09941	0.17638	0.00913	0.962	1093	29	1062	35	1047	50	4.6	1093	29
NA001A-131	220137	7	0.06072	0.00122	0.85493	0.04733	0.10212	0.00527	0.932	629	43	627	26	627	31	0.4	627	31
NA001A-132	48007	5	0.05665	0.00130	0.67549	0.04011	0.08648	0.00473	0.922	478	50	524	24	535	28	-12.4	535	28
NA001A-133	7550	12	0.06117	0.00527	1.42939	0.14953	0.16947	0.01007	0.568	645	175	901	61	1009	55	-61.0	1009	55
NA001A-134	219892	12	0.07707	0.00083	1.79424	0.11703	0.16884	0.01086	0.986	1123	21	1043	42	1006	60	11.3	1123	21
NA001A-135	106509	5	0.08071	0.00096	2.20762	0.13664	0.19837	0.01205	0.981	1214	23	1183	42	1167	64	4.3	1214	23
NA001A-136	163315	34	0.05894	0.00120	0.73239	0.04244	0.09012	0.00489	0.936	565	44	558	25	556	29	1.6	556	29
NA001A-137	709777	901	0.11566	0.00298	4.31133	0.26942	0.27035	0.01539	0.911	1890	46	1696	50	1543	78	20.7	1890	46
NA001A-138	403826	55	0.10903	0.00113	4.51907	0.23996	0.30062	0.01566	0.981	1783	19	1734	43	1694	77	5.7	1783	19
NA001A-139	79015	12	0.05566	0.00136	0.53051	0.03347	0.06913	0.00402	0.922	439	54	432	22	431	24	1.8	431	24
NA001A-140	231477	13	0.05615	0.00115	0.60207	0.03266	0.07777	0.00391	0.926	458	45	479	20	483	23	-5.5	483	23
NA001A-141	129546	12	0.06090	0.00126	0.83194	0.05521	0.09908	0.00625	0.950	636	44	615	30	609	37	4.4	609	37
NA001A-142	235366	17	0.07752	0.00082	1.97181	0.10317	0.18448	0.00945	0.980	1135	21	1106	35	1091	51	4.1	1135	21

Burtts Corner Fm. (NA001A)

										age (Ma)	error (Ma)	age (Ma)	error (Ma)	age (Ma)	error (Ma)	discordance[1]	reported age[2]	
sample name	^{206}Pb (cps)	^{204}Pb (cps)	^{207}Pb/^{206}Pb	2 σ	^{207}Pb/^{235}U	2 σ	^{206}Pb/^{238}U	2 σ	ρ	^{207}Pb/^{206}Pb	2 σ	^{207}Pb/^{235}U	2 σ	^{206}Pb/^{238}U	2 σ	%	(Ma)	2 σ
NA001A-143	136898	11	0.08198	0.00090	2.28067	0.13437	0.20176	0.01168	0.982	1245	21	1206	41	1185	62	5.3	1245	21
NA001A-144	472020	7	0.06400	0.00127	1.06492	0.05816	0.12068	0.00614	0.932	742	41	736	28	734	35	1.0	734	35
NA001A-145	387002	30	0.09547	0.00101	3.44538	0.18468	0.26175	0.01375	0.980	1537	20	1515	41	1499	70	2.8	1537	20
NA001A-146	100872	23	0.07780	0.00096	2.02353	0.11815	0.18864	0.01076	0.977	1142	24	1123	39	1114	58	2.6	1142	24
NA001A-147	105668	63	0.08691	0.00130	2.09578	0.11599	0.17489	0.00932	0.963	1359	29	1147	37	1039	51	25.4	1359	29
NA001A-148	36331	8	0.07199	0.00162	1.61484	0.10329	0.16269	0.00974	0.936	986	45	976	39	972	54	1.5	986	45
NA001A-149	181463	12	0.07290	0.00080	1.60343	0.08349	0.15953	0.00812	0.978	1011	22	972	32	954	45	6.1	1011	22
NA001A-150	692730	14	0.11620	0.00119	5.17133	0.28730	0.32278	0.01762	0.983	1899	18	1848	46	1803	85	5.7	1899	18

Concordia diagrams for NA001A, Burtts Corner Fm.

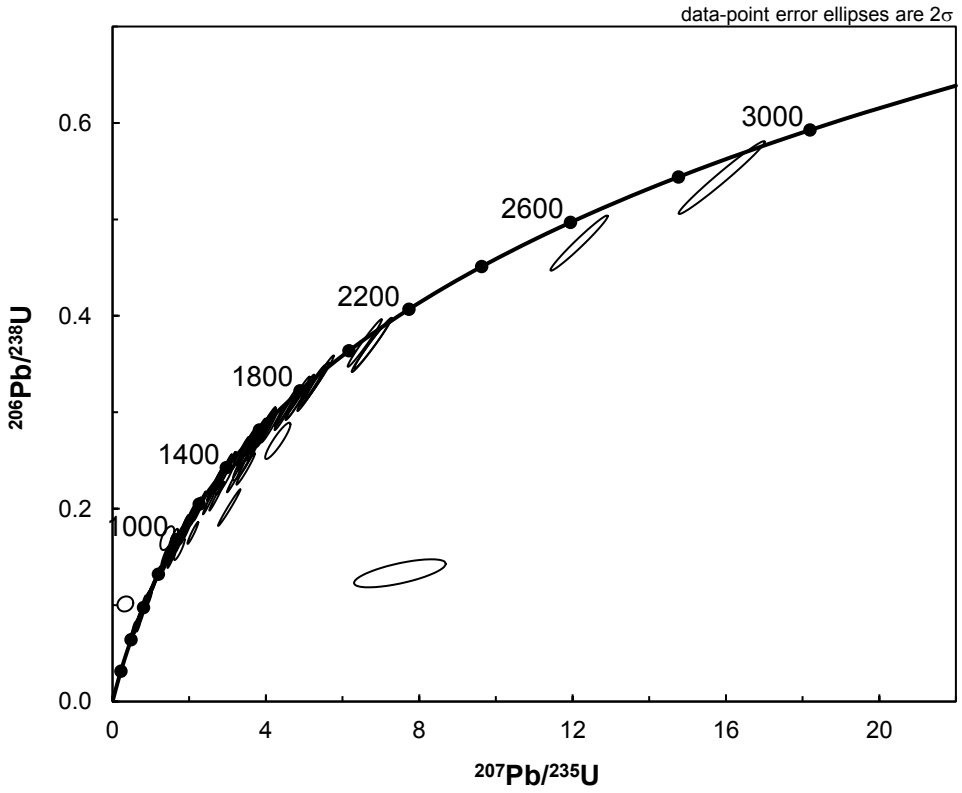

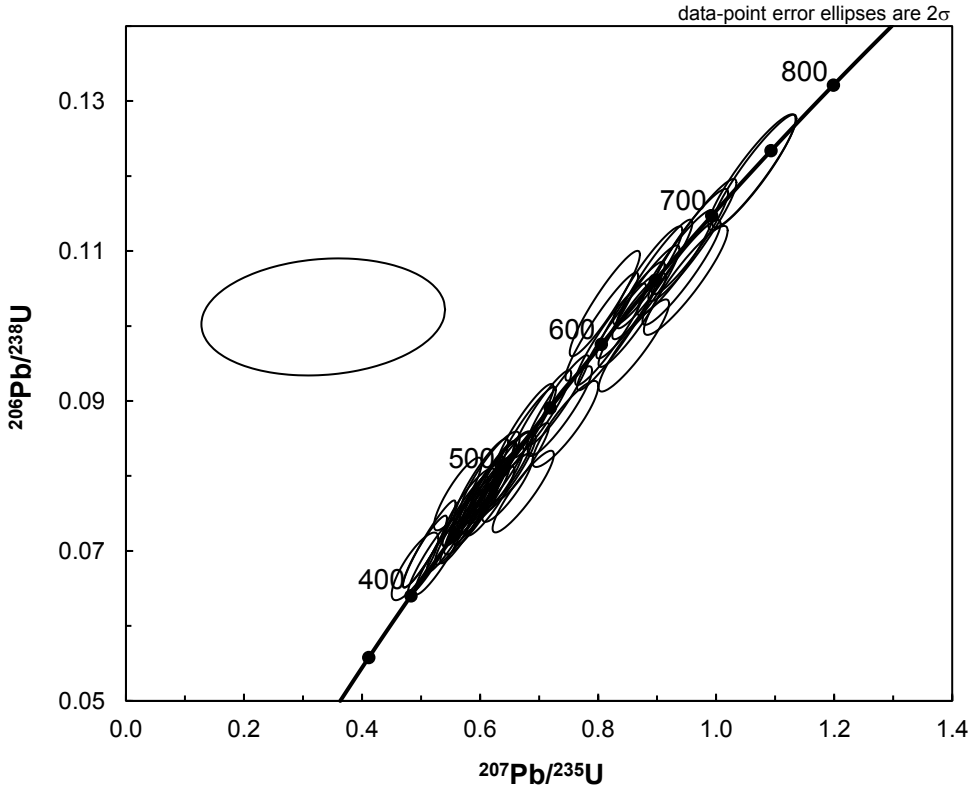

Histogram and kernel density plot for NA001A, Burtts Corner Fm. Bandwidth and bin width is equal to median 2σ, 22.1 Ma.

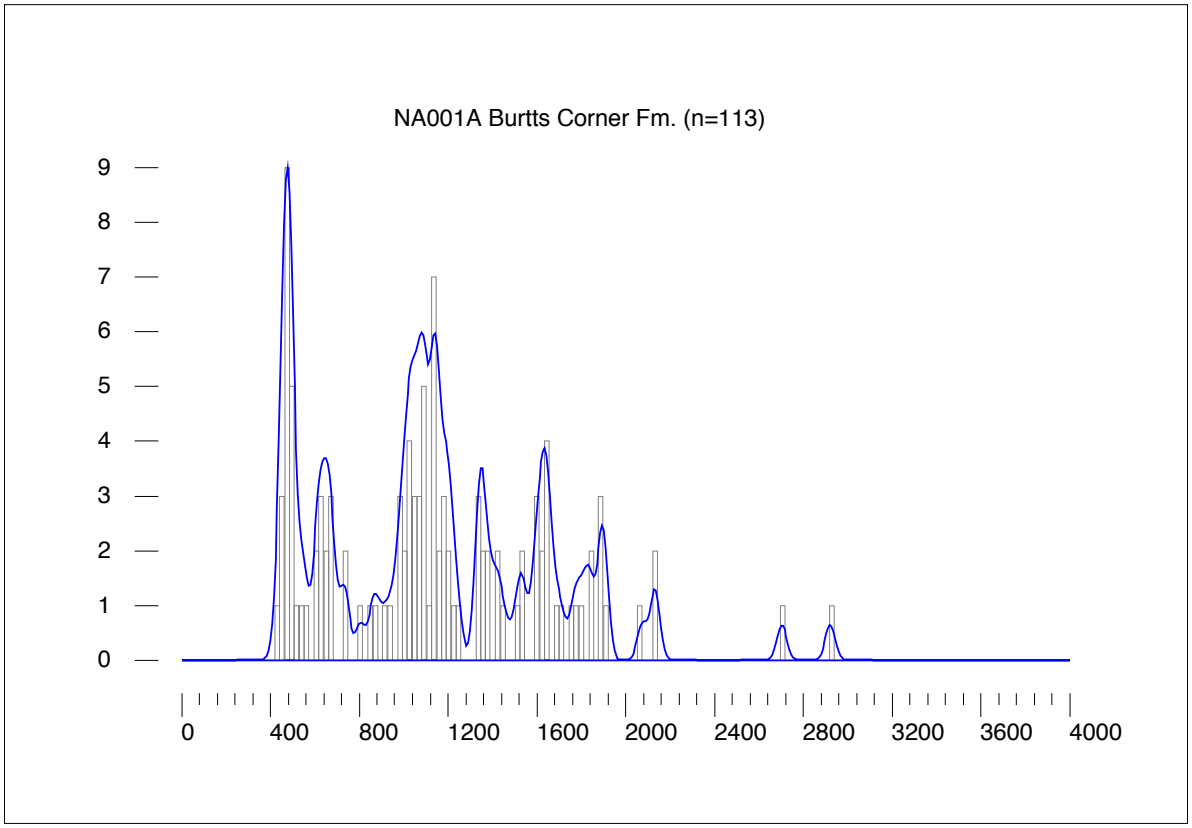

Digdeguash Fm. (NA003A)

										age (Ma)	error (Ma)	age (Ma)	error (Ma)	age (Ma)	error (Ma)	discordance[1]	reported age[2]	
sample name	^{206}Pb (cps)	^{204}Pb (cps)	^{207}Pb/^{206}Pb	2 σ	^{207}Pb/^{235}U	2 σ	^{206}Pb/^{238}U	2 σ	ρ	^{207}Pb/^{206}Pb	2 σ	^{207}Pb/^{235}U	2 σ	^{206}Pb/^{238}U	2 σ	%	(Ma)	2 σ
NA003A-001	152041	172	0.06127	0.00065	0.84231	0.05621	0.09970	0.00657	0.987	649	23	620	31	613	38	5.8	613	38
NA003A-002	63385	160	0.06189	0.00081	0.84860	0.05749	0.09944	0.00661	0.981	670	28	624	31	611	39	9.3	611	39
NA003A-003	80685	212	0.06147	0.00076	0.83114	0.05464	0.09806	0.00633	0.982	656	26	614	30	603	37	8.4	603	37
NA003A-004	61206	204	0.06202	0.00089	0.84203	0.05750	0.09847	0.00658	0.978	675	30	620	31	605	38	10.8	605	38
NA003A-005	148125	218	0.06118	0.00066	0.88302	0.05796	0.10468	0.00678	0.986	646	23	643	31	642	39	0.6	642	39
NA003A-006	27213	204	0.05834	0.00098	0.62358	0.04214	0.07752	0.00508	0.969	543	36	492	26	481	30	11.7	481	30
NA003A-007	328550	250	0.06264	0.00067	0.97817	0.06566	0.11326	0.00751	0.987	696	23	693	33	692	43	0.7	692	43
NA003A-008	49145	240	0.05824	0.00078	0.64972	0.04376	0.08091	0.00534	0.980	539	29	508	27	502	32	7.2	502	32
NA003A-009	71682	240	0.06194	0.00068	0.86299	0.05645	0.10105	0.00652	0.986	672	23	632	30	621	38	8.0	621	38
NA003A-010	234641	269	0.06206	0.00067	0.99482	0.06800	0.11625	0.00785	0.987	676	23	701	34	709	45	-5.1	709	45
NA003A-011	120447	250	0.06156	0.00067	0.85131	0.05710	0.10030	0.00664	0.987	659	23	625	31	616	39	6.8	616	39
NA003A-012	303091	284	0.06101	0.00067	0.87067	0.05913	0.10350	0.00694	0.987	640	24	636	32	635	40	0.8	635	40
NA003A-013	117635	240	0.06279	0.00068	0.97647	0.06816	0.11279	0.00778	0.988	701	23	692	34	689	45	1.8	689	45
NA003A-014	90638	275	0.05772	0.00063	0.61844	0.04072	0.07771	0.00504	0.986	519	24	489	25	482	30	7.3	482	30
NA003A-015	23862	231	0.06322	0.00091	0.83073	0.05444	0.09531	0.00609	0.976	716	30	614	30	587	36	18.8	587	36
NA003A-016	63223	237	0.06176	0.00075	0.83793	0.05675	0.09839	0.00656	0.984	666	26	618	31	605	38	9.6	605	38
NA003A-017	155856	247	0.06128	0.00067	0.82690	0.05460	0.09786	0.00637	0.986	649	23	612	30	602	37	7.6	602	37
NA003A-018	408306	235	0.09884	0.00109	3.51590	0.22963	0.25800	0.01661	0.986	1602	20	1531	50	1480	85	8.6	1602	20
NA003A-019	40057	218	0.06151	0.00080	0.83577	0.05584	0.09855	0.00646	0.981	657	28	617	30	606	38	8.1	606	38
NA003A-020	122989	469	0.05966	0.00122	0.63874	0.04429	0.07765	0.00515	0.956	591	44	502	27	482	31	19.2	482	31
NA003A-021	44875	163	0.06426	0.00085	0.94358	0.06583	0.10649	0.00729	0.982	750	28	675	34	652	42	13.7	652	42
NA003A-022	63599	166	0.06178	0.00072	0.84645	0.05631	0.09937	0.00651	0.984	667	25	623	31	611	38	8.8	611	38
NA003A-023	24598	182	0.06165	0.00097	0.82667	0.05548	0.09726	0.00634	0.972	662	33	612	30	598	37	10.1	598	37
NA003A-024	99376	155	0.09561	0.00111	3.28920	0.21552	0.24952	0.01609	0.984	1540	22	1479	50	1436	82	7.5	1540	22
NA003A-025	94578	162	0.06142	0.00070	0.86444	0.05655	0.10208	0.00658	0.985	654	24	633	30	627	38	4.4	627	38
NA003A-026	178097	179	0.05998	0.00227	0.80632	0.06373	0.09750	0.00676	0.878	603	80	600	35	600	40	0.5	600	40
NA003A-027	61501	190	0.05812	0.00075	0.65003	0.04580	0.08112	0.00562	0.983	534	28	508	28	503	33	6.1	503	33
NA003A-028	60817	150	0.10797	0.00126	4.24516	0.28747	0.28515	0.01902	0.985	1766	21	1683	54	1617	95	9.5	1766	21
NA003A-029	81445	150	0.06142	0.00070	0.84802	0.05944	0.10014	0.00693	0.987	654	24	624	32	615	40	6.2	615	40
NA003A-030	104738	159	0.06351	0.00076	0.96798	0.06378	0.11054	0.00716	0.983	725	25	687	32	676	41	7.2	676	41
NA003A-031	98621	202	0.06424	0.00135	0.85763	0.05716	0.09683	0.00613	0.949	749	44	629	31	596	36	21.5	596	36
NA003A-032	83595	179	0.06142	0.00074	0.85603	0.05844	0.10108	0.00679	0.984	654	26	628	31	621	40	5.3	621	40
NA003A-033	226627	172	0.06178	0.00082	0.86638	0.05827	0.10171	0.00671	0.980	666	28	634	31	624	39	6.6	624	39
NA003A-034	47271	180	0.06518	0.00084	1.02469	0.06818	0.11402	0.00744	0.981	780	27	716	34	696	43	11.4	696	43
NA003A-035	59059	166	0.06194	0.00079	0.83831	0.05546	0.09816	0.00637	0.981	672	27	618	30	604	37	10.7	604	37
NA003A-036	58099	134	0.05794	0.00070	0.61386	0.04075	0.07684	0.00501	0.983	528	26	486	25	477	30	9.9	477	30
NA003A-037	235240	175	0.06073	0.00064	0.84934	0.05632	0.10143	0.00664	0.987	630	23	624	30	623	39	1.2	623	39
NA003A-038	153738	203	0.06058	0.00067	0.85208	0.05625	0.10200	0.00664	0.986	625	24	626	30	626	39	-0.3	626	39
NA003A-039	145991	215	0.07785	0.00090	2.01546	0.13386	0.18775	0.01228	0.985	1143	23	1121	44	1109	66	3.2	1143	23
NA003A-040	79343	234	0.06063	0.00069	0.84164	0.05582	0.10068	0.00658	0.985	626	24	620	30	618	38	1.3	618	38
NA003A-041	40106	253	0.06222	0.00084	0.81859	0.05425	0.09541	0.00619	0.979	682	29	607	30	587	36	14.5	587	36
NA003A-042	38025	270	0.05877	0.00078	0.62977	0.04246	0.07772	0.00514	0.980	559	29	496	26	483	31	14.1	483	31
NA003A-043	305408	257	0.08171	0.00093	2.35999	0.15000	0.20947	0.01310	0.984	1239	22	1231	44	1226	69	1.1	1239	22
NA003A-044	68242	261	0.06136	0.00073	0.85690	0.05782	0.10129	0.00673	0.984	652	25	628	31	622	39	4.8	622	39
NA003A-045	96521	290	0.06134	0.00078	0.86584	0.05890	0.10238	0.00684	0.982	651	27	633	32	628	40	3.7	628	40
NA003A-046	163930	307	0.06098	0.00069	0.83558	0.05549	0.09939	0.00650	0.985	638	24	617	30	611	38	4.5	611	38
NA003A-047	46162	298	0.06411	0.00085	0.96817	0.06444	0.10953	0.00714	0.980	745	28	688	33	670	41	10.6	670	41
NA003A-048	65107	294	0.05854	0.00072	0.60520	0.04050	0.07498	0.00493	0.983	550	26	481	25	466	30	15.8	466	30

Digdeguash Fm. (NA003A)

sample name	^{206}Pb (cps)	^{204}Pb (cps)	$^{207}Pb/^{206}Pb$	2 σ	$^{207}Pb/^{235}U$	2 σ	$^{206}Pb/^{238}U$	2 σ	ρ	age (Ma) $^{207}Pb/^{206}Pb$	error (Ma) 2 σ	age (Ma) $^{207}Pb/^{235}U$	error (Ma) 2 σ	age (Ma) $^{206}Pb/^{238}U$	error (Ma) 2 σ	discordance[1] %	reported age[2] (Ma)	2 σ
NA003A-049	46580	279	0.06492	0.00077	0.93058	0.06052	0.10397	0.00665	0.983	772	25	668	31	638	39	18.2	638	39
NA003A-050	19874	301	0.06903	0.00148	1.06212	0.07296	0.11160	0.00728	0.950	900	44	735	35	682	42	25.5	900	44
NA003A-051	157625	293	0.10529	0.00119	4.23078	0.28192	0.29142	0.01914	0.986	1719	21	1680	53	1649	95	4.7	1719	21
NA003A-052	23256	299	0.05945	0.00096	0.61741	0.04354	0.07533	0.00517	0.973	583	35	488	27	468	31	20.5	468	31
NA003A-053	39093	261	0.06200	0.00091	0.81540	0.05619	0.09539	0.00642	0.977	674	31	605	31	587	38	13.5	587	38
NA003A-054	58228	294	0.06244	0.00075	0.84968	0.05777	0.09870	0.00660	0.984	689	25	624	31	607	39	12.5	607	39
NA003A-055	77699	266	0.06071	0.00071	0.78857	0.05444	0.09421	0.00641	0.986	629	25	590	30	580	38	8.1	580	38
NA003A-056	56030	265	0.06245	0.00090	0.83062	0.05669	0.09646	0.00644	0.978	690	30	614	31	594	38	14.6	594	38
NA003A-057	51623	271	0.06138	0.00079	0.81356	0.05379	0.09613	0.00624	0.981	653	27	604	30	592	37	9.8	592	37
NA003A-058	151152	284	0.06090	0.00070	0.82253	0.05530	0.09796	0.00649	0.985	636	24	609	30	602	38	5.5	602	38
NA003A-059	81060	259	0.06129	0.00073	0.87312	0.05769	0.10332	0.00672	0.984	649	25	637	31	634	39	2.5	634	39
NA003A-060	30839	274	0.06415	0.00087	0.95298	0.06540	0.10774	0.00725	0.980	747	28	680	33	660	42	12.3	660	42
NA003A-061	611397	548	0.06895	0.00118	1.04132	0.06918	0.10954	0.00703	0.966	897	35	725	34	670	41	26.6	897	35
NA003A-062	100830	235	0.06240	0.00117	0.85759	0.05815	0.09968	0.00650	0.961	688	39	629	31	613	38	11.5	613	38
NA003A-063	55523	204	0.06195	0.00086	0.84769	0.05802	0.09924	0.00665	0.979	672	30	623	31	610	39	9.7	610	39
NA003A-064	89135	218	0.06333	0.00079	0.98990	0.06732	0.11336	0.00758	0.983	719	26	699	34	692	44	4.0	692	44
NA003A-065	151224	228	0.06127	0.00069	0.87458	0.05952	0.10353	0.00695	0.986	649	24	638	32	635	40	2.2	635	40
NA003A-066	153322	240	0.06100	0.00067	0.87286	0.05918	0.10378	0.00694	0.987	639	24	637	32	637	40	0.4	637	40
NA003A-067	91156	194	0.06099	0.00069	0.86636	0.05850	0.10303	0.00686	0.986	639	24	634	31	632	40	1.1	632	40
NA003A-068	117027	209	0.06137	0.00075	0.82412	0.06051	0.09739	0.00705	0.986	652	26	610	33	599	41	8.5	599	41
NA003A-069	60802	212	0.05754	0.00068	0.63805	0.04261	0.08043	0.00529	0.984	512	26	501	26	499	31	2.7	499	31
NA003A-070	35987	496	0.16258	0.00734	2.34008	0.18880	0.10439	0.00698	0.829	2483	74	1225	56	640	41	77.8	2483	74
NA003A-071	123229	255	0.06337	0.00080	0.77435	0.05660	0.08863	0.00638	0.985	721	27	582	32	547	38	25.1	547	38
NA003A-072	23036	186	0.06415	0.00106	0.85743	0.05881	0.09694	0.00645	0.971	747	34	629	32	596	38	21.1	596	38
NA003A-073	81591	207	0.06157	0.00076	0.83208	0.05941	0.09802	0.00689	0.985	659	26	615	32	603	40	9.0	603	40
NA003A-074	46481	208	0.06132	0.00079	0.84684	0.05845	0.10016	0.00679	0.983	650	27	623	32	615	40	5.7	615	40
NA003A-075	145090	242	0.06124	0.00071	0.88466	0.06114	0.10478	0.00714	0.986	648	25	643	32	642	42	0.8	642	42
NA003A-076	679810	290	0.06071	0.00063	0.92995	0.06172	0.11110	0.00728	0.988	629	22	668	32	679	42	-8.4	679	42
NA003A-077	77245	268	0.06064	0.00161	0.79873	0.07367	0.09554	0.00844	0.958	626	56	596	41	588	49	6.4	588	49
NA003A-078	112356	250	0.06111	0.00066	0.84685	0.05626	0.10051	0.00659	0.987	643	23	623	30	617	38	4.2	617	38
NA003A-079	327175	317	0.06276	0.00090	0.88392	0.05869	0.10215	0.00662	0.976	700	30	643	31	627	39	11.0	627	39
NA003A-080	74316	247	0.06079	0.00071	0.85448	0.05805	0.10195	0.00682	0.985	632	25	627	31	626	40	1.0	626	40
NA003A-081	369766	256	0.06238	0.00067	1.05751	0.06872	0.12295	0.00788	0.986	687	23	733	33	748	45	-9.3	748	45
NA003A-082	278691	283	0.11752	0.00133	4.66815	0.34057	0.28809	0.02076	0.988	1919	20	1762	59	1632	103	16.9	1919	20
NA003A-083	95952	250	0.06128	0.00070	0.87315	0.05804	0.10334	0.00677	0.985	649	24	637	31	634	39	2.5	634	39
NA003A-084	47942	232	0.06108	0.00074	0.84678	0.05662	0.10054	0.00661	0.984	642	26	623	31	618	39	4.0	618	39
NA003A-085	38660	223	0.06124	0.00081	0.84915	0.05725	0.10057	0.00665	0.981	648	28	624	31	618	39	4.8	618	39
NA003A-086	188426	236	0.06081	0.00066	0.84321	0.05493	0.10057	0.00646	0.986	633	23	621	30	618	38	2.5	618	38
NA003A-087	180309	244	0.10797	0.00122	4.61577	0.30031	0.31005	0.01986	0.985	1765	21	1752	53	1741	97	1.6	1765	21
NA003A-088	198763	262	0.06034	0.00063	0.84693	0.05540	0.10180	0.00657	0.987	616	22	623	30	625	38	-1.5	625	38
NA003A-089	14432	256	0.06239	0.00118	0.90972	0.06282	0.10575	0.00702	0.962	688	40	657	33	648	41	6.0	648	41
NA003A-090	86179	255	0.06490	0.00123	0.88854	0.05986	0.09930	0.00642	0.960	771	39	646	32	610	38	21.8	610	38
NA003A-091	20425	325	0.05936	0.00093	0.63582	0.04339	0.07768	0.00516	0.973	580	34	500	27	482	31	17.5	482	31
NA003A-092	116516	278	0.06159	0.00074	0.87273	0.05885	0.10278	0.00682	0.984	660	26	637	31	631	40	4.6	631	40
NA003A-093	93148	325	0.06787	0.00111	1.00936	0.06663	0.10786	0.00690	0.969	865	34	709	33	660	40	24.8	865	34
NA003A-094	49368	259	0.05827	0.00077	0.62801	0.04250	0.07817	0.00519	0.981	540	29	495	26	485	31	10.5	485	31
NA003A-095	37083	261	0.06569	0.00103	0.85981	0.05573	0.09493	0.00597	0.970	797	32	630	30	585	35	27.8	585	35
NA003A-096	191240	257	0.08224	0.00092	2.27265	0.14728	0.20043	0.01279	0.985	1251	22	1204	45	1178	68	6.4	1251	22

Digdeguash Fm. (NA003A)

sample name	^{206}Pb (cps)	^{204}Pb (cps)	^{207}Pb/^{206}Pb	2 σ	^{207}Pb/^{235}U	2 σ	^{206}Pb/^{238}U	2 σ	ρ	age (Ma) ^{207}Pb/^{206}Pb	error (Ma) 2 σ	age (Ma) ^{207}Pb/^{235}U	error (Ma) 2 σ	age (Ma) ^{206}Pb/^{238}U	error (Ma) 2 σ	discordance[1] %	reported age[2] (Ma)	2 σ
NA003A-097	145828	238	0.08415	0.00143	1.83455	0.12841	0.15812	0.01074	0.970	1296	33	1058	45	946	59	29.0	1296	33
NA003A-098	92300	252	0.06323	0.00072	0.97838	0.06437	0.11223	0.00727	0.985	716	24	693	33	686	42	4.4	686	42
NA003A-099	70917	227	0.06170	0.00069	0.82008	0.05533	0.09640	0.00641	0.986	664	24	608	30	593	38	11.1	593	38
NA003A-100	713322	261	0.11667	0.00127	5.55441	0.35745	0.34529	0.02190	0.986	1906	19	1909	54	1912	104	-0.4	1906	19
NA003A-101	49789	202	0.05874	0.00068	0.62323	0.04085	0.07695	0.00496	0.984	558	25	492	25	478	30	14.8	478	30
NA003A-102	199868	175	0.06302	0.00067	0.98048	0.06490	0.11284	0.00737	0.987	709	22	694	33	689	43	2.9	689	43
NA003A-103	172265	164	0.06088	0.00091	0.82467	0.06616	0.09825	0.00775	0.983	635	32	611	36	604	45	5.1	604	45
NA003A-104	100248	159	0.06299	0.00071	0.95439	0.06357	0.10989	0.00721	0.986	708	24	680	32	672	42	5.3	672	42
NA003A-105	89250	176	0.06189	0.00101	0.83384	0.05782	0.09771	0.00658	0.972	670	35	616	32	601	39	10.9	601	39
NA003A-106	339357	142	0.06033	0.00065	0.83336	0.05558	0.10019	0.00659	0.987	615	23	615	30	616	39	0.0	616	39
NA003A-107	349441	139	0.06065	0.00063	0.86819	0.05641	0.10382	0.00666	0.987	627	22	635	30	637	39	-1.6	637	39
NA003A-108	131760	130	0.06252	0.00066	0.96927	0.06367	0.11245	0.00729	0.987	692	22	688	32	687	42	0.7	687	42
NA003A-109	127939	134	0.10911	0.00124	4.62671	0.29486	0.30755	0.01929	0.984	1785	21	1754	52	1729	94	3.6	1785	21
NA003A-110	89113	133	0.06100	0.00070	0.82451	0.05410	0.09803	0.00633	0.985	639	24	611	30	603	37	5.9	603	37
NA003A-111	35286	109	0.06256	0.00098	0.84250	0.05600	0.09767	0.00631	0.972	693	33	621	30	601	37	14.0	601	37
NA003A-112	21810	120	0.05898	0.00094	0.59676	0.04033	0.07338	0.00482	0.972	566	34	475	25	457	29	20.1	457	29
NA003A-113	61207	127	0.06019	0.00080	0.71744	0.04895	0.08644	0.00578	0.981	611	29	549	29	534	34	13.0	534	34
NA003A-114	34932	136	0.06184	0.00083	0.81508	0.05457	0.09560	0.00627	0.980	669	28	605	30	589	37	12.5	589	37
NA003A-115	173119	146	0.06466	0.00073	1.04859	0.07221	0.11762	0.00799	0.987	763	24	728	35	717	46	6.4	717	46
NA003A-116	453545	178	0.11142	0.00123	4.50817	0.28597	0.29345	0.01833	0.985	1823	20	1732	51	1659	91	10.2	1823	20
NA003A-117	23072	172	0.05886	0.00124	0.61152	0.04289	0.07535	0.00504	0.954	562	45	485	27	468	30	17.3	468	30
NA003A-118	56094	139	0.05788	0.00071	0.61078	0.04034	0.07654	0.00497	0.983	525	26	484	25	475	30	9.8	475	30
NA003A-119	3120	316	0.82957	0.01841	198.75024	########	1.73760	2.07923	1.000	4973	31	5379	796	6492	3642	-49.4	4973	31
NA003A-120	37465	156	0.06124	0.00083	0.72319	0.04953	0.08565	0.00575	0.980	648	29	553	29	530	34	18.9	530	34
NA003A-121	82582	200	0.06165	0.00070	0.83726	0.05449	0.09850	0.00631	0.985	662	24	618	30	606	37	8.9	606	37
NA003A-122	78381	197	0.06179	0.00069	0.83665	0.05543	0.09821	0.00641	0.986	667	24	617	30	604	38	9.9	604	38
NA003A-123	63835	230	0.05781	0.00079	0.60161	0.03993	0.07548	0.00490	0.978	522	30	478	25	469	29	10.6	469	29
NA003A-124	72141	197	0.06047	0.00075	0.74402	0.05061	0.08924	0.00597	0.983	620	26	565	29	551	35	11.6	551	35
NA003A-125	98609	223	0.06223	0.00075	0.79794	0.05307	0.09300	0.00608	0.984	682	25	596	30	573	36	16.7	573	36
NA003A-126	145145	220	0.06149	0.00066	0.87271	0.05664	0.10293	0.00659	0.986	656	23	637	30	632	38	4.0	632	38
NA003A-127	180680	220	0.06110	0.00071	0.84276	0.05753	0.10003	0.00673	0.985	643	25	621	31	615	39	4.6	615	39
NA003A-128	1978019	401	0.11294	0.00155	4.67464	0.31329	0.30019	0.01969	0.979	1847	25	1763	55	1692	97	9.5	1847	25
NA003A-129	100204	241	0.06062	0.00076	0.83884	0.05510	0.10036	0.00647	0.982	626	27	619	30	617	38	1.6	617	38
NA003A-130	29500	231	0.05851	0.00102	0.62009	0.04299	0.07687	0.00516	0.968	549	38	490	27	477	31	13.5	477	31
NA003A-131	113112	5520	0.29999	0.02079	8.79306	5.08967	0.21258	0.12216	0.993	3470	103	2317	425	1243	619	70.2	3470	103
NA003A-132	43447	194	0.06166	0.00108	0.82523	0.05540	0.09707	0.00629	0.965	662	37	611	30	597	37	10.3	597	37
NA003A-133	55301	181	0.06146	0.00084	0.83897	0.05674	0.09901	0.00656	0.979	655	29	619	31	609	38	7.5	609	38
NA003A-134	30301	161	0.06247	0.00104	0.84320	0.05720	0.09789	0.00644	0.969	690	35	621	31	602	38	13.4	602	38
NA003A-135	206336	171	0.08810	0.00118	2.21343	0.15726	0.18222	0.01272	0.982	1385	25	1185	49	1079	69	24.0	1385	25
NA003A-136	11170	146	0.05942	0.00116	0.68185	0.04729	0.08322	0.00554	0.959	583	42	528	28	515	33	12.0	515	33
NA003A-137	47224	122	0.06155	0.00074	0.81034	0.05405	0.09549	0.00627	0.984	658	25	603	30	588	37	11.2	588	37
NA003A-138	535352	137	0.09581	0.00106	3.44132	0.22217	0.26051	0.01657	0.985	1544	21	1514	50	1492	84	3.7	1544	21
NA003A-139	152170	117	0.09397	0.00104	3.24202	0.20904	0.25022	0.01589	0.985	1508	21	1467	49	1440	81	5.0	1508	21
NA003A-140	69197	104	0.06110	0.00077	0.79570	0.05437	0.09445	0.00634	0.983	643	27	594	30	582	37	9.9	582	37
NA003A-141	189740	111	0.06102	0.00065	0.85444	0.05827	0.10156	0.00684	0.988	640	23	627	31	624	40	2.7	624	40
NA003A-142-X	42112	87	0.05852	0.00081	0.59353	0.03986	0.07356	0.00484	0.979	549	30	473	25	458	29	17.3	458	29
NA003A-143	169443	103	0.09325	0.00106	2.89983	0.19893	0.22555	0.01526	0.986	1493	21	1382	51	1311	80	13.4	1493	21
NA003A-144	95791	562	0.10041	0.00584	1.32920	0.11913	0.09601	0.00655	0.761	1632	104	859	51	591	38	66.7	1632	104

Digdeguash Fm. (NA003A)

										age (Ma)	error (Ma)	age (Ma)	error (Ma)	age (Ma)	error (Ma)	discordance[1]	reported age[2]	
sample name	^{206}Pb (cps)	^{204}Pb (cps)	$^{207}Pb/^{206}Pb$	2 σ	$^{207}Pb/^{235}U$	2 σ	$^{206}Pb/^{238}U$	2 σ	ρ	$^{207}Pb/^{206}Pb$	2 σ	$^{207}Pb/^{235}U$	2 σ	$^{206}Pb/^{238}U$	2 σ	%	(Ma)	2 σ
NA003A-145	55511	81	0.07437	0.00101	1.64734	0.11558	0.16066	0.01106	0.981	1051	27	989	43	960	61	9.3	1051	27
NA003A-146	132491	746	0.06662	0.00275	0.82817	0.06519	0.09016	0.00605	0.852	826	84	613	36	556	36	34.0	826	84
NA003A-147	74521	75	0.06074	0.00074	0.82775	0.05828	0.09883	0.00685	0.985	630	26	612	32	608	40	3.8	608	40
NA003A-148	535862	73	0.10848	0.00126	3.84526	0.24955	0.25709	0.01641	0.984	1774	21	1602	51	1475	84	18.8	1774	21
NA003A-149	59325	62	0.06079	0.00076	0.81439	0.05483	0.09717	0.00643	0.982	632	27	605	30	598	38	5.6	598	38
NA003A-150	397988	81	0.08376	0.00102	2.11059	0.15077	0.18276	0.01286	0.985	1287	24	1152	48	1082	70	17.3	1287	24

Concordia diagrams for NA003A, Digdeguash Fm.

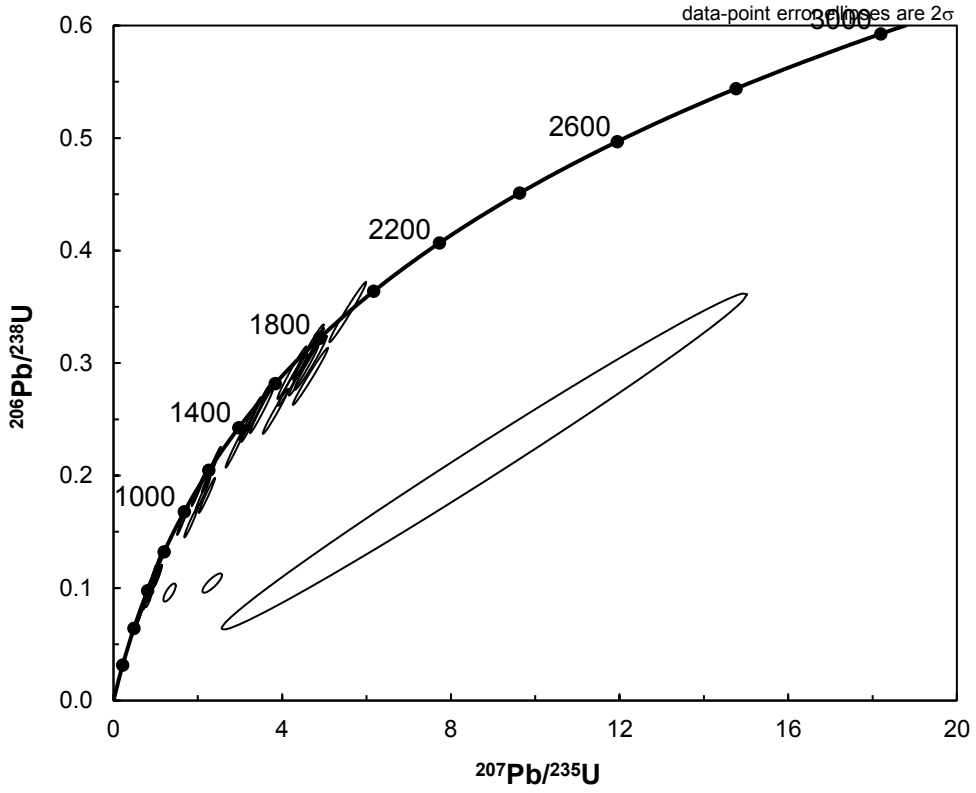

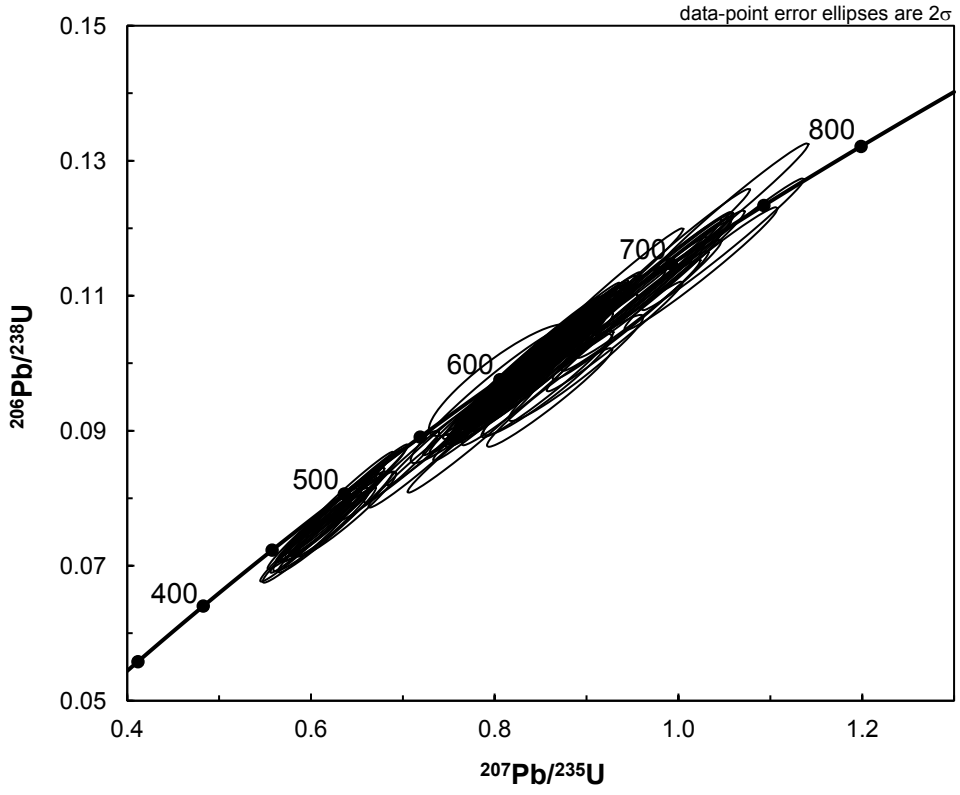

Histogram and kernel density plot for NA003A, Digdeguash Fm. Bandwidth and bin width is equal to median 2σ, 38.6 Ma.

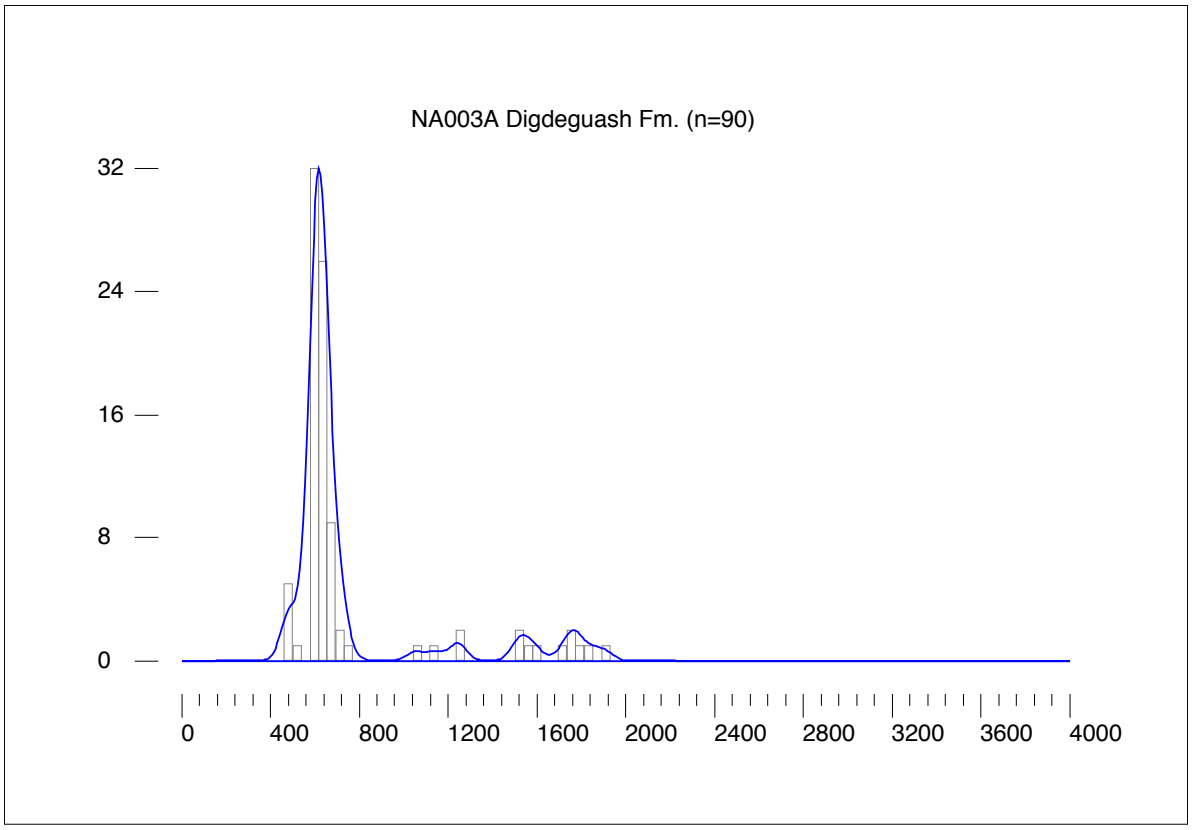

Hayes Brook Fm. (NA005A)

sample name	^{206}Pb (cps)	^{204}Pb (cps)	^{207}Pb/^{206}Pb	2 σ	^{207}Pb/^{235}U	2 σ	^{206}Pb/^{238}U	2 σ	ρ	age (Ma) ^{207}Pb/^{206}Pb	error (Ma) 2 σ	age (Ma) ^{207}Pb/^{235}U	error (Ma) 2 σ	age (Ma) ^{206}Pb/^{238}U	error (Ma) 2 σ	discordance[1] %	reported age[2] (Ma)	2 σ
NA005A-001	35548	23	0.05711	0.00128	0.60882	0.03414	0.07732	0.00397	0.917	496	49	483	21	480	24	3.2	480	24
NA005A-002	28480	11	0.05631	0.00127	0.58114	0.03293	0.07485	0.00389	0.917	465	49	465	21	465	23	-0.1	465	23
NA005A-003	89974	11	0.05721	0.00083	0.61022	0.03327	0.07736	0.00407	0.964	500	32	484	21	480	24	4.0	480	24
NA005A-004	257277	14	0.05703	0.00073	0.64116	0.03319	0.08153	0.00409	0.969	493	28	503	20	505	24	-2.6	505	24
NA005A-005	201825	21	0.05749	0.00088	0.59012	0.03063	0.07445	0.00369	0.956	510	33	471	19	463	22	9.6	463	22
NA005A-006	183269	7	0.07025	0.00074	1.51758	0.07658	0.15667	0.00773	0.978	936	21	938	30	938	43	-0.3	936	21
NA005A-007	184695	9	0.05658	0.00084	0.61754	0.03291	0.07916	0.00405	0.960	475	33	488	20	491	24	-3.5	491	24
NA005A-008	152569	26	0.07162	0.00094	1.53598	0.11164	0.15555	0.01112	0.983	975	27	945	44	932	62	4.8	975	27
NA005A-009	80558	12	0.05656	0.00150	0.60973	0.03672	0.07819	0.00423	0.898	474	57	483	23	485	25	-2.4	485	25
NA005A-010	250181	7	0.05595	0.00074	0.60471	0.03176	0.07838	0.00398	0.967	451	29	480	20	486	24	-8.3	486	24
NA005A-011	74981	47	0.05760	0.00085	0.59715	0.03074	0.07519	0.00371	0.958	514	32	475	19	467	22	9.5	467	22
NA005A-012	111030	65	0.05871	0.00097	0.62450	0.03318	0.07715	0.00389	0.950	556	36	493	21	479	23	14.4	479	23
NA005A-013	167437	53	0.05714	0.00084	0.61214	0.03768	0.07770	0.00464	0.971	497	32	485	23	482	28	3.0	482	28
NA005A-014	136514	42	0.05716	0.00090	0.64060	0.03394	0.08129	0.00411	0.955	498	34	503	21	504	24	-1.3	504	24
NA005A-015	68858	38	0.05738	0.00098	0.60295	0.03542	0.07622	0.00428	0.957	506	37	479	22	473	26	6.7	473	26
NA005A-016	284284	47	0.07564	0.00080	1.88751	0.09842	0.18099	0.00924	0.979	1086	21	1077	34	1072	50	1.3	1086	21
NA005A-017	266937	101	0.05981	0.00131	0.59305	0.03325	0.07192	0.00371	0.920	597	47	473	21	448	22	25.8	448	22
NA005A-018	120318	39	0.05721	0.00105	0.58925	0.03454	0.07470	0.00416	0.950	500	40	470	22	464	25	7.3	464	25
NA005A-019	952316	54	0.08929	0.00093	2.97364	0.14527	0.24154	0.01153	0.977	1410	20	1401	36	1395	60	1.2	1410	20
NA005A-020	128513	52	0.07441	0.00093	1.74132	0.08681	0.16973	0.00819	0.968	1053	25	1024	32	1011	45	4.3	1053	25
NA005A-021	304802	33	0.05631	0.00071	0.61305	0.03183	0.07896	0.00398	0.970	464	28	485	20	490	24	-5.7	490	24
NA005A-022	84849	53	0.05595	0.00100	0.58953	0.03183	0.07642	0.00390	0.944	450	39	471	20	475	23	-5.6	475	23
NA005A-023	161813	25	0.09286	0.00098	3.21965	0.16639	0.25148	0.01272	0.979	1485	20	1462	39	1446	65	2.9	1485	20
NA005A-024	154588	49	0.05672	0.00082	0.60445	0.03231	0.07729	0.00398	0.962	481	32	480	20	480	24	0.2	480	24
NA005A-025	355630	56	0.08764	0.00091	2.88534	0.14167	0.23877	0.01146	0.977	1375	20	1378	36	1380	59	-0.5	1375	20
NA005A-026	242341	49	0.05595	0.00073	0.56935	0.02935	0.07380	0.00368	0.968	450	29	458	19	459	22	-2.0	459	22
NA005A-027	149982	61	0.05633	0.00078	0.55888	0.03081	0.07196	0.00384	0.968	465	30	451	20	448	23	3.8	448	23
NA005A-028	141139	76	0.07783	0.00088	2.03649	0.10085	0.18978	0.00915	0.974	1142	22	1128	33	1120	49	2.1	1142	22
NA005A-029	544164	93	0.09078	0.00095	3.04602	0.15793	0.24335	0.01236	0.980	1442	20	1419	39	1404	64	2.9	1442	20
NA005A-030	68414	292	0.10589	0.00713	1.12097	0.09240	0.07678	0.00365	0.577	1730	119	763	43	477	22	75.1	1730	119
NA005A-031	247380	369	0.10153	0.00520	3.15766	0.25337	0.22556	0.01393	0.770	1652	92	1447	60	1311	73	22.8	1652	92
NA005A-032	393786	31	0.05610	0.00071	0.60187	0.03018	0.07781	0.00378	0.968	456	28	478	19	483	23	-6.1	483	23
NA005A-033	43954	29	0.05286	0.00096	0.56261	0.03009	0.07720	0.00388	0.940	323	41	453	19	479	23	-50.4	479	23
NA005A-034	215147	24	0.05644	0.00077	0.57361	0.03034	0.07370	0.00377	0.966	470	30	460	19	458	23	2.5	458	23
NA005A-035	87320	22	0.07266	0.00085	1.60775	0.07802	0.16049	0.00756	0.971	1004	23	973	30	960	42	4.8	1004	23
NA005A-036	775037	31	0.07056	0.00098	1.37704	0.07505	0.14154	0.00746	0.967	945	28	879	32	853	42	10.3	945	28
NA005A-037	64531	11	0.05765	0.00088	0.60716	0.03294	0.07639	0.00398	0.960	516	33	482	21	475	24	8.4	475	24
NA005A-038	154948	18	0.05665	0.00077	0.57108	0.02952	0.07312	0.00365	0.965	478	30	459	19	455	22	5.0	455	22
NA005A-039	94732	32	0.07523	0.00124	1.75800	0.09046	0.16948	0.00826	0.948	1075	33	1030	33	1009	45	6.6	1075	33
NA005A-040	643166	25	0.10003	0.00103	3.57101	0.20817	0.25893	0.01485	0.984	1625	19	1543	45	1484	76	9.7	1625	19
NA005A-041	285909	5	0.08543	0.00096	2.27769	0.12508	0.19337	0.01039	0.979	1325	22	1205	38	1140	56	15.3	1325	22
NA005A-042	77603	12	0.05560	0.00089	0.53738	0.02866	0.07010	0.00356	0.954	436	35	437	19	437	21	-0.1	437	21
NA005A-043	73578	8	0.05802	0.00181	0.57533	0.03618	0.07192	0.00393	0.869	530	67	461	23	448	24	16.1	448	24
NA005A-044	165172	96	0.07102	0.00174	0.80086	0.05487	0.08178	0.00523	0.934	958	49	597	30	507	31	49.0	958	49
NA005A-045	514302	51	0.05724	0.00076	0.59979	0.03142	0.07599	0.00385	0.968	501	29	477	20	472	23	5.9	472	23
NA005A-046	66962	8	0.05622	0.00110	0.56673	0.03030	0.07311	0.00364	0.930	461	43	456	19	455	22	1.4	455	22
NA005A-047	763713	6	0.09275	0.00095	3.00065	0.14726	0.23464	0.01126	0.978	1483	19	1408	37	1359	59	9.3	1483	19
NA005A-048	262020	3	0.08630	0.00090	2.07032	0.10314	0.17399	0.00848	0.978	1345	20	1139	34	1034	46	25.0	1345	20

Hayes Brook Fm. (NA005A)

										age (Ma)	error (Ma)	age (Ma)	error (Ma)	age (Ma)	error (Ma)	discordance[1]	reported age[2]	
sample name	^{206}Pb (cps)	^{204}Pb (cps)	^{207}Pb/^{206}Pb	2 σ	^{207}Pb/^{235}U	2 σ	^{206}Pb/^{238}U	2 σ	ρ	^{207}Pb/^{206}Pb	2 σ	^{207}Pb/^{235}U	2 σ	^{206}Pb/^{238}U	2 σ	%	(Ma)	2 σ
NA005A-049	103189	4	0.05564	0.00090	0.55967	0.02968	0.07296	0.00369	0.953	438	35	451	19	454	22	-3.8	454	22
NA005A-050	191104	4	0.15607	0.00163	9.12672	0.50001	0.42412	0.02281	0.982	2414	18	2351	49	2279	102	6.6	2414	18
NA005A-051	125783	2	0.08274	0.00090	2.31863	0.11236	0.20324	0.00960	0.974	1263	21	1218	34	1193	51	6.1	1263	21
NA005A-052	92668	17	0.09712	0.00134	2.01561	0.10799	0.15051	0.00779	0.966	1570	26	1121	36	904	44	45.4	1570	26
NA005A-053	533771	2	0.05577	0.00071	0.53874	0.02845	0.07006	0.00359	0.971	443	28	438	19	437	22	1.6	437	22
NA005A-054	438010	3	0.19778	0.00201	13.55700	0.66074	0.49715	0.02370	0.978	2808	17	2719	45	2602	101	8.9	2808	17
NA005A-055	920981	19	0.07613	0.00115	1.80829	0.10027	0.17228	0.00919	0.962	1098	30	1048	36	1025	50	7.3	1098	30
NA005A-056	84627	4	0.05380	0.00082	0.54637	0.02857	0.07366	0.00368	0.956	363	34	443	19	458	22	-27.3	458	22
NA005A-057	65265	1	0.05311	0.00095	0.51273	0.02811	0.07002	0.00363	0.945	333	40	420	19	436	22	-31.9	436	22
NA005A-058	29333	4	0.06441	0.00144	1.35252	0.07826	0.15230	0.00813	0.922	755	47	869	33	914	45	-22.6	914	45
NA005A-059	1171289	10	0.09799	0.00103	3.39877	0.16292	0.25155	0.01177	0.976	1586	19	1504	37	1446	60	9.8	1586	19
NA005A-060	199114	47	0.06120	0.00174	0.62472	0.03587	0.07403	0.00369	0.869	646	60	493	22	460	22	29.8	460	22
NA005A-061	389032	38	0.05671	0.00072	0.57501	0.03047	0.07353	0.00378	0.970	480	28	461	19	457	23	5.0	457	23
NA005A-062	2210728	67	0.05643	0.00070	0.57358	0.02918	0.07372	0.00364	0.970	469	27	460	19	459	22	2.4	459	22
NA005A-063	28857	45	0.06021	0.00156	0.73469	0.04384	0.08849	0.00476	0.901	611	55	559	25	547	28	11.0	547	28
NA005A-064	112395	40	0.05922	0.00121	0.59882	0.03372	0.07334	0.00385	0.931	575	44	476	21	456	23	21.4	456	23
NA005A-065	555433	55	0.05692	0.00072	0.59948	0.03150	0.07639	0.00390	0.971	488	28	477	20	475	23	2.9	475	23
NA005A-066	21017	36	0.07323	0.00142	1.44903	0.07940	0.14351	0.00735	0.935	1020	39	909	32	864	41	16.3	1020	39
NA005A-067	49834	36	0.05734	0.00108	0.55399	0.03019	0.07007	0.00358	0.939	505	41	448	20	437	22	14.0	437	22
NA005A-068	69681	48	0.05708	0.00088	0.59315	0.03125	0.07537	0.00380	0.956	495	34	473	20	468	23	5.5	468	23
NA005A-069	67601	49	0.05654	0.00101	0.58493	0.03052	0.07503	0.00368	0.939	474	39	468	19	466	22	1.6	466	22
NA005A-070	77747	47	0.07586	0.00094	1.80443	0.09560	0.17252	0.00888	0.972	1091	25	1047	34	1026	49	6.5	1091	25
NA005A-071	73861	37	0.07546	0.00138	1.67067	0.08548	0.16057	0.00767	0.934	1081	36	997	32	960	42	12.0	1081	36
NA005A-072A	140177	15	0.05691	0.00077	0.55119	0.03016	0.07024	0.00372	0.969	488	30	446	20	438	22	10.7	438	22
NA005A-072B	439129	23	0.09325	0.00097	3.15146	0.15693	0.24512	0.01194	0.978	1493	20	1445	38	1413	62	5.9	1493	20
NA005A-073	41160	14	0.07299	0.00137	1.54711	0.08081	0.15373	0.00749	0.933	1014	38	949	32	922	42	9.7	1014	38
NA005A-074	75646	12	0.05647	0.00080	0.56024	0.02936	0.07196	0.00363	0.963	471	31	452	19	448	22	5.0	448	22
NA005A-075	91964	295	0.11158	0.00270	1.08711	0.05926	0.07066	0.00345	0.896	1825	43	747	28	440	21	78.4	1825	43
NA005A-076	69768	9	0.05620	0.00085	0.58355	0.03151	0.07530	0.00390	0.960	460	33	467	20	468	23	-1.7	468	23
NA005A-077	560691	255	0.06395	0.00091	0.70965	0.04244	0.08048	0.00468	0.971	740	30	545	25	499	28	33.9	499	28
NA005A-078	591686	8	0.07290	0.00077	1.58054	0.08348	0.15724	0.00814	0.980	1011	21	963	32	941	45	7.4	1011	21
NA005A-079	52725	43	0.05937	0.00341	0.59882	0.04521	0.07315	0.00358	0.648	581	120	476	28	455	21	22.4	455	21
NA005A-080	241334	1	0.05645	0.00079	0.57819	0.02968	0.07428	0.00367	0.962	470	31	463	19	462	22	1.8	462	22
NA005A-081	141642	11	0.05605	0.00079	0.56556	0.02894	0.07319	0.00360	0.961	454	31	455	19	455	22	-0.2	455	22
NA005A-082	1472376	6	0.11085	0.00112	4.82462	0.24168	0.31568	0.01549	0.979	1813	18	1789	41	1769	75	2.8	1813	18
NA005A-083	93690	12	0.05884	0.00094	0.60760	0.03098	0.07490	0.00363	0.949	561	35	482	19	466	22	17.6	466	22
NA005A-084	255758	18	0.11119	0.00127	5.06831	0.26310	0.33060	0.01674	0.976	1819	21	1831	43	1841	81	-1.4	1819	21
NA005A-085	81418	11	0.05538	0.00092	0.57362	0.03107	0.07513	0.00387	0.952	427	37	460	20	467	23	-9.6	467	23
NA005A-086A	95927	15	0.05531	0.00094	0.57017	0.03073	0.07477	0.00383	0.949	425	37	458	20	465	23	-9.8	465	23
NA005A-086B	21771	5	0.05073	0.00148	0.50354	0.02930	0.07198	0.00362	0.865	229	66	414	20	448	22	-99.3	448	22
NA005A-087	301449	4	0.08940	0.00096	2.90089	0.15057	0.23534	0.01195	0.978	1413	20	1382	38	1362	62	4.0	1413	20
NA005A-088	113054	4	0.05656	0.00104	0.57360	0.03148	0.07355	0.00380	0.943	475	40	460	20	458	23	3.7	458	23
NA005A-089	281736	5	0.05610	0.00075	0.57343	0.03079	0.07413	0.00386	0.969	456	29	460	20	461	23	-1.0	461	23
NA005A-090	39383	2	0.05530	0.00210	0.58011	0.03902	0.07608	0.00423	0.826	424	82	465	25	473	25	-11.8	473	25
NA005A-091	51741	2	0.05399	0.00097	0.53370	0.03062	0.07169	0.00391	0.950	371	40	434	20	446	23	-21.1	446	23
NA005A-092	393321	43	0.05926	0.00094	0.60271	0.03163	0.07377	0.00369	0.954	577	34	479	20	459	22	21.1	459	22
NA005A-093	149993	2	0.19031	0.00196	13.28314	0.63638	0.50623	0.02369	0.977	2745	17	2700	44	2641	101	4.6	2745	17
NA005A-094	204179	3	0.07708	0.00082	1.93246	0.09711	0.18184	0.00893	0.977	1123	21	1092	33	1077	49	4.5	1123	21

Hayes Brook Fm. (NA005A)

										age (Ma)	error (Ma)	age (Ma)	error (Ma)	age (Ma)	error (Ma)	discordance[1]	reported age[2]	
sample name	^{206}Pb (cps)	^{204}Pb (cps)	^{207}Pb/^{206}Pb	2 σ	^{207}Pb/^{235}U	2 σ	^{206}Pb/^{238}U	2 σ	ρ	^{207}Pb/^{206}Pb	2 σ	^{207}Pb/^{235}U	2 σ	^{206}Pb/^{238}U	2 σ	%	(Ma)	2 σ
NA005A-095	257359	1	0.07301	0.00076	1.67985	0.08490	0.16688	0.00825	0.979	1014	21	1001	32	995	45	2.0	1014	21
NA005A-096	155287	12	0.10194	0.00143	3.89377	0.19531	0.27702	0.01334	0.960	1660	26	1612	40	1576	67	5.7	1660	26
NA005A-097	37164	4	0.05264	0.00193	0.54297	0.03704	0.07481	0.00430	0.843	313	81	440	24	465	26	-50.1	465	26
NA005A-098	240428	8	0.05659	0.00075	0.56124	0.02911	0.07193	0.00361	0.967	476	29	452	19	448	22	6.1	448	22
NA005A-099	49596	2	0.05385	0.00105	0.54571	0.02969	0.07350	0.00373	0.934	365	43	442	19	457	22	-26.2	457	22
NA005A-100	67181	17	0.06360	0.00219	0.65801	0.04003	0.07504	0.00376	0.824	728	71	513	24	466	23	37.3	466	23
NA005A-101	456343	205	0.06132	0.00122	0.66131	0.03656	0.07822	0.00404	0.933	651	42	515	22	485	24	26.3	485	24
NA005A-102	103666	88	0.05804	0.00098	0.62151	0.03350	0.07766	0.00398	0.950	531	37	491	21	482	24	9.6	482	24
NA005A-103	328885	67	0.08028	0.00084	2.17581	0.10639	0.19657	0.00939	0.977	1204	20	1173	33	1157	50	4.3	1204	20
NA005A-104	264433	125	0.05971	0.00133	0.60402	0.03314	0.07337	0.00368	0.914	593	48	480	21	456	22	23.9	456	22
NA005A-105	231104	71	0.10071	0.00108	3.99496	0.21346	0.28770	0.01506	0.979	1637	20	1633	42	1630	75	0.5	1637	20
NA005A-106	272400	37	0.07815	0.00083	1.95920	0.09729	0.18181	0.00882	0.977	1151	21	1102	33	1077	48	7.0	1151	21
NA005A-107	172538	39	0.07516	0.00088	1.81698	0.09005	0.17533	0.00844	0.972	1073	23	1052	32	1041	46	3.2	1073	23
NA005A-108	185511	37	0.05622	0.00075	0.56192	0.03015	0.07249	0.00377	0.968	461	29	453	19	451	23	2.3	451	23
NA005A-109	109348	39	0.05672	0.00089	0.56200	0.02816	0.07187	0.00342	0.950	480	34	453	18	447	21	7.1	447	21
NA005A-110	122250	50	0.05760	0.00090	0.58702	0.03146	0.07392	0.00379	0.956	515	34	469	20	460	23	11.0	460	23
NA005A-111	123253	17	0.05702	0.00083	0.56539	0.03054	0.07192	0.00374	0.963	492	32	455	20	448	22	9.4	448	22
NA005A-112	168000	37	0.05684	0.00076	0.54474	0.02811	0.06950	0.00346	0.965	485	29	442	18	433	21	11.1	433	21
NA005A-113	1237313	110	0.07338	0.00085	1.57467	0.07601	0.15564	0.00729	0.971	1024	23	960	30	933	41	9.6	1024	23
NA005A-114	73044	66	0.07621	0.00142	1.74641	0.11980	0.16619	0.01097	0.963	1101	37	1026	43	991	60	10.7	1101	37
NA005A-115	334422	24	0.08931	0.00094	2.81561	0.14359	0.22866	0.01141	0.979	1411	20	1360	38	1327	60	6.5	1411	20
NA005A-116	50776	20	0.08670	0.00145	2.45497	0.12304	0.20536	0.00970	0.943	1354	32	1259	36	1204	52	12.1	1354	32
NA005A-117	98541	16	0.05572	0.00079	0.53513	0.02795	0.06966	0.00350	0.963	441	31	435	18	434	21	1.7	434	21
NA005A-118	69240	9	0.06992	0.00088	1.36894	0.06847	0.14201	0.00687	0.968	926	26	876	29	856	39	8.1	926	26
NA005A-119	182399	21	0.05813	0.00088	0.56894	0.02908	0.07098	0.00347	0.955	535	33	457	19	442	21	17.9	442	21
NA005A-120	71953	18	0.05906	0.00175	0.57690	0.03251	0.07084	0.00339	0.850	569	63	462	21	441	20	23.3	441	20
NA005A-121	1569333	272	0.17277	0.00181	9.31759	0.50443	0.39115	0.02078	0.981	2585	17	2370	48	2128	96	20.7	2585	17
NA005A-122	275222	19	0.05623	0.00071	0.56797	0.02876	0.07326	0.00359	0.968	461	28	457	18	456	22	1.2	456	22
NA005A-123	469960	12	0.09154	0.00095	3.03208	0.15361	0.24023	0.01191	0.979	1458	20	1416	38	1388	62	5.3	1458	20
NA005A-124	118739	9	0.07294	0.00080	1.62809	0.08114	0.16189	0.00787	0.975	1012	22	981	31	967	44	4.8	1012	22
NA005A-125	228791	103	0.06466	0.00101	0.65408	0.03415	0.07337	0.00366	0.954	763	33	511	21	456	22	41.6	456	22
NA005A-126	49712	13	0.05570	0.00097	0.55122	0.02987	0.07177	0.00368	0.947	441	38	446	19	447	22	-1.5	447	22
NA005A-127	70848	12	0.05554	0.00100	0.55400	0.03069	0.07235	0.00379	0.945	434	40	448	20	450	23	-3.9	450	23
NA005A-128	183598	21	0.18830	0.00197	13.19534	0.66755	0.50824	0.02516	0.978	2727	17	2694	47	2649	107	3.5	2727	17
NA005A-129	242530	28	0.05896	0.00106	0.59195	0.03050	0.07281	0.00352	0.937	566	39	472	19	453	21	20.6	453	21
NA005A-130	42501	6	0.05467	0.00087	0.53776	0.02824	0.07134	0.00357	0.953	399	35	437	18	444	21	-11.8	444	21

Concordia diagrams for NA005A, Hayes Brook Fm.

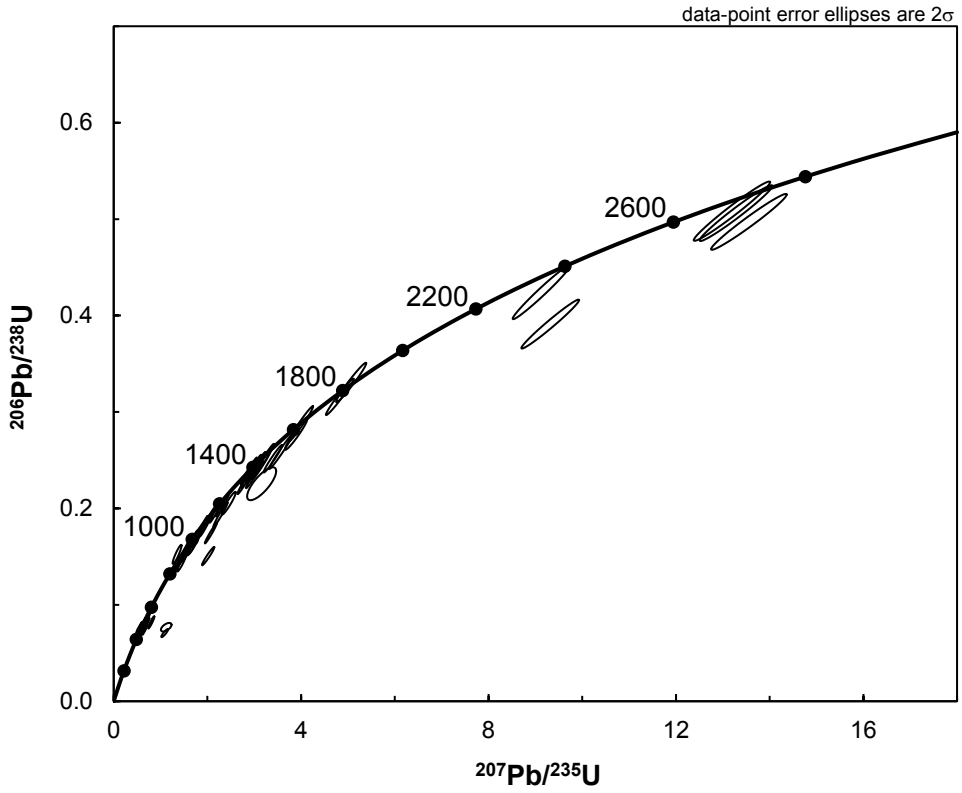

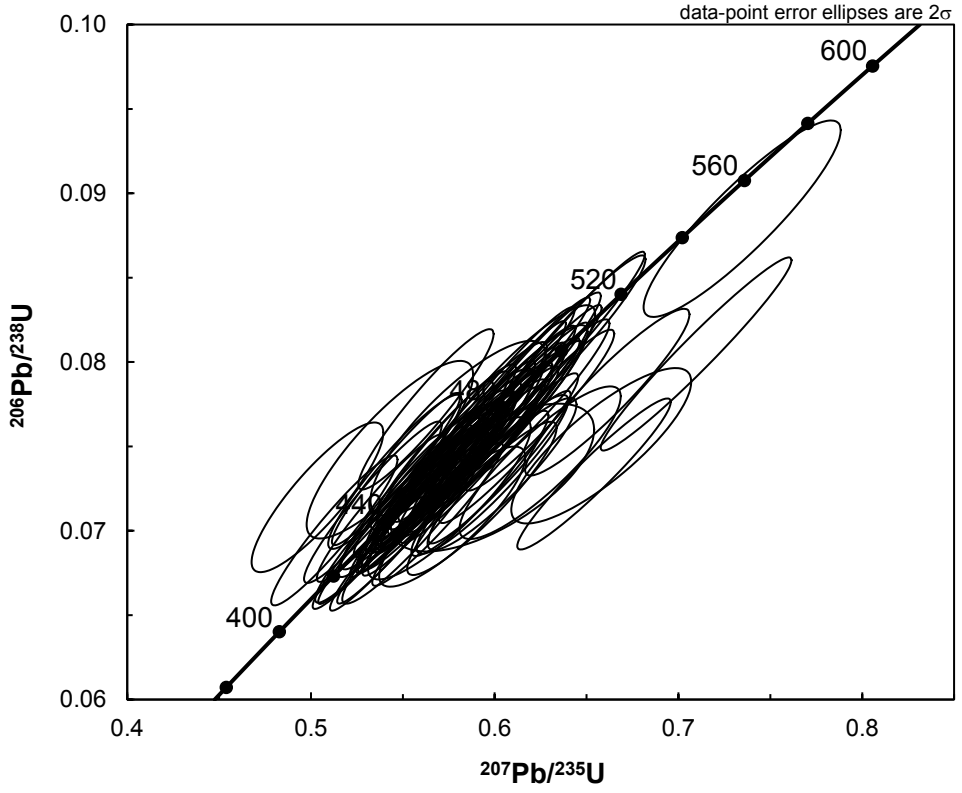

Histogram and kernel density plot for NA005A, Hayes Brook Fm. Bandwidth and bin width is equal to median 2σ, 22.2 Ma.

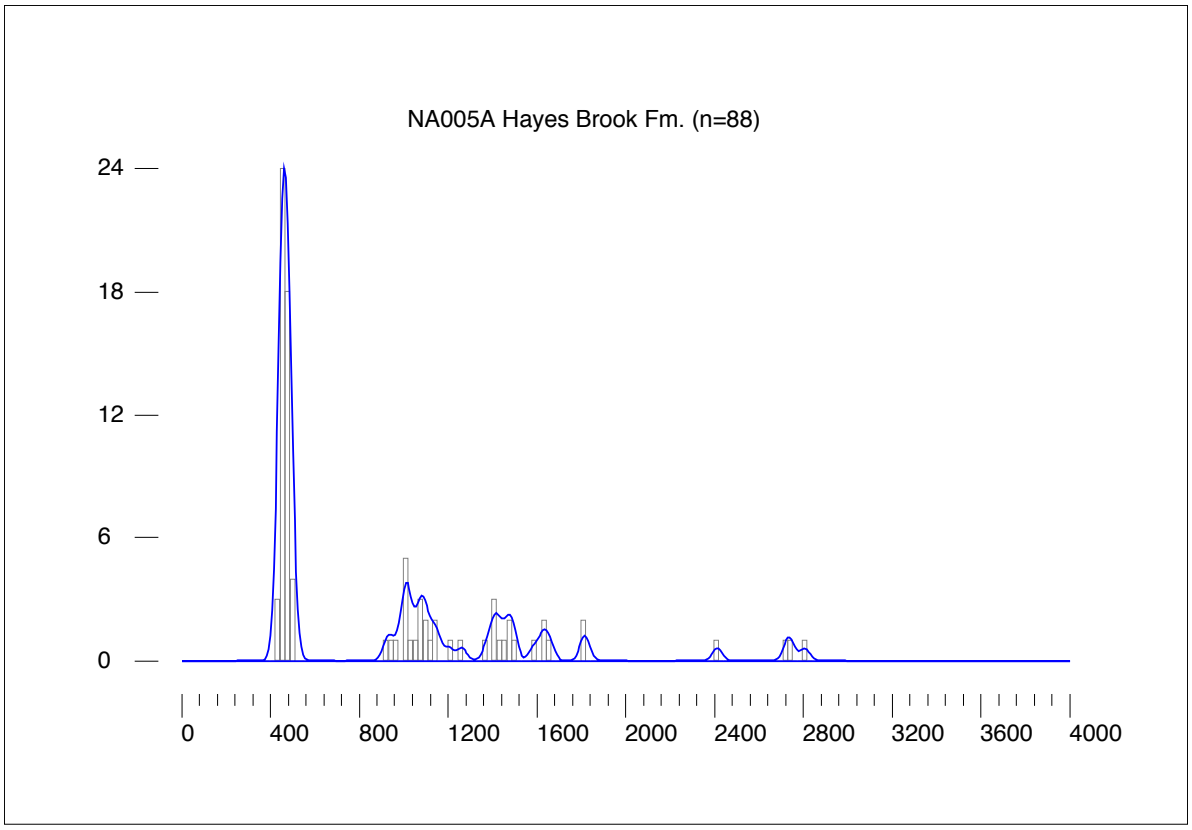

Flume Ridge Fm. (NA010A)

										age (Ma)	error (Ma)	age (Ma)	error (Ma)	age (Ma)	error (Ma)	discordance[1]	reported age[2]	
sample name	^{206}Pb (cps)	^{204}Pb (cps)	^{207}Pb/^{206}Pb	2 σ	^{207}Pb/^{235}U	2 σ	^{206}Pb/^{238}U	2 σ	ρ	^{207}Pb/^{206}Pb	2 σ	^{207}Pb/^{235}U	2 σ	^{206}Pb/^{238}U	2 σ	%	(Ma)	2 σ
NA010A-001	58406	173	0.05982	0.00113	0.63832	0.05359	0.07739	0.00633	0.974	597	40	501	33	480	38	20.3	480	38
NA010A-002	209441	171	0.05683	0.00093	0.58408	0.04815	0.07454	0.00602	0.980	485	36	467	30	463	36	4.6	463	36
NA010A-003	169222	233	0.07662	0.00122	1.97887	0.13808	0.18730	0.01272	0.973	1111	32	1108	46	1107	69	0.5	1111	32
NA010A-004	676632	207	0.08781	0.00102	2.95579	0.20113	0.24413	0.01637	0.985	1378	22	1396	50	1408	84	-2.4	1378	22
NA010A-005	153568	194	0.09477	0.00113	3.66860	0.24441	0.28076	0.01840	0.984	1524	22	1565	52	1595	92	-5.3	1524	22
NA010A-006	574423	230	0.07499	0.00091	1.91600	0.12651	0.18531	0.01203	0.983	1068	24	1087	43	1096	65	-2.8	1068	24
NA010A-007	341912	184	0.10386	0.00123	4.45781	0.30387	0.31128	0.02090	0.985	1694	22	1723	55	1747	102	-3.6	1694	22
NA010A-008	860846	185	0.07711	0.00088	2.11434	0.14975	0.19886	0.01390	0.987	1124	22	1153	48	1169	74	-4.4	1124	22
NA010A-009	123001	205	0.05789	0.00098	0.63248	0.05404	0.07924	0.00663	0.980	526	37	498	33	492	40	6.8	492	40
NA010A-010	209413	204	0.05823	0.00148	0.58611	0.05057	0.07300	0.00602	0.956	539	54	468	32	454	36	16.2	454	36
NA010A-011	469855	34	0.10092	0.00117	4.14868	0.27624	0.29816	0.01955	0.985	1641	21	1664	53	1682	96	-2.9	1641	21
NA010A-012	784461	49	0.10089	0.00115	4.20521	0.27774	0.30229	0.01967	0.985	1641	21	1675	53	1703	97	-4.3	1641	21
NA010A-013	298487	43	0.05569	0.00090	0.59272	0.04962	0.07719	0.00634	0.981	440	35	473	31	479	38	-9.3	479	38
NA010A-014	369203	35	0.10438	0.00121	4.62223	0.31226	0.32117	0.02138	0.985	1703	21	1753	55	1795	103	-6.2	1703	21
NA010A-015	509581	34	0.05619	0.00090	0.59334	0.04919	0.07659	0.00623	0.981	460	35	473	31	476	37	-3.6	476	37
NA010A-016	123213	39	0.09001	0.00106	3.30887	0.22320	0.26661	0.01771	0.985	1426	22	1483	51	1524	89	-7.7	1426	22
NA010A-017	532208	101	0.08519	0.00102	2.75165	0.18992	0.23426	0.01592	0.985	1320	23	1343	50	1357	83	-3.1	1320	23
NA010A-018	1076743	67	0.07032	0.00081	1.56292	0.10185	0.16119	0.01034	0.984	938	23	956	40	963	57	-2.9	938	23
NA010A-019	391752	207	0.06361	0.00107	0.75680	0.06414	0.08629	0.00717	0.980	729	35	572	36	534	42	27.9	534	42
NA010A-020	767424	41	0.09336	0.00113	3.27865	0.25894	0.25470	0.01988	0.988	1495	23	1476	60	1463	101	2.4	1495	23
NA010A-021	102972	19	0.09726	0.00121	3.73370	0.25459	0.27843	0.01867	0.983	1572	23	1579	53	1583	93	-0.8	1572	23
NA010A-022	292835	16	0.06983	0.00082	1.60933	0.10561	0.16714	0.01079	0.984	923	24	974	40	996	59	-8.5	923	24
NA010A-023	97875	60	0.06092	0.00171	0.63114	0.05538	0.07514	0.00625	0.948	636	59	497	34	467	37	27.6	467	37
NA010A-024	128819	52	0.06011	0.00121	0.67637	0.05971	0.08161	0.00701	0.974	607	43	525	36	506	42	17.4	506	42
NA010A-025	298383	35	0.13033	0.00151	7.07077	0.48335	0.39349	0.02651	0.986	2102	20	2120	59	2139	121	-2.0	2102	20
NA010A-026	24673	17	0.05805	0.00184	0.60957	0.05584	0.07616	0.00655	0.938	532	68	483	35	473	39	11.4	473	39
NA010A-027	96724	64	0.07373	0.00145	1.84522	0.12619	0.18151	0.01189	0.958	1034	39	1062	44	1075	65	-4.3	1034	39
NA010A-028	220568	20	0.08407	0.00099	2.68798	0.17791	0.23190	0.01510	0.984	1294	23	1325	48	1344	79	-4.3	1294	23
NA010A-029	673018	39	0.11306	0.00132	5.37922	0.39185	0.34508	0.02481	0.987	1849	21	1882	61	1911	118	-3.9	1849	21
NA010A-030	691175	41	0.08645	0.00108	2.89062	0.19473	0.24250	0.01605	0.983	1348	24	1379	50	1400	83	-4.2	1348	24
NA010A-031A	271952	40	0.07726	0.00092	2.05218	0.13975	0.19264	0.01292	0.985	1128	24	1133	45	1136	69	-0.8	1128	24
NA010A-031B	24741	40	0.05292	0.00102	0.58263	0.04965	0.07985	0.00663	0.974	325	43	466	31	495	39	-54.3	495	39
NA010A-032	251095	89	0.05650	0.00104	0.56691	0.04790	0.07277	0.00600	0.976	472	40	456	31	453	36	4.2	453	36
NA010A-033	573501	76	0.08544	0.00098	2.87017	0.22354	0.24363	0.01877	0.989	1326	22	1374	57	1406	97	-6.7	1326	22
NA010A-034	198464	46	0.08525	0.00101	2.81584	0.19881	0.23956	0.01667	0.986	1321	23	1360	52	1384	86	-5.3	1321	23
NA010A-035	385078	210	0.06010	0.00112	0.62234	0.05192	0.07510	0.00611	0.975	607	40	491	32	467	37	24.0	467	37
NA010A-036	521755	90	0.08778	0.00104	2.97575	0.19890	0.24588	0.01618	0.984	1378	23	1401	50	1417	83	-3.2	1378	23
NA010A-037	67478	80	0.05465	0.00105	0.54468	0.04704	0.07228	0.00609	0.975	398	43	442	30	450	36	-13.5	450	36
NA010A-038	181364	64	0.08422	0.00102	2.62626	0.17577	0.22616	0.01489	0.984	1298	23	1308	48	1314	78	-1.4	1298	23
NA010A-039	188375	78	0.05520	0.00092	0.54104	0.04600	0.07109	0.00593	0.981	420	37	439	30	443	36	-5.6	443	36
NA010A-040	279802	102	0.05533	0.00094	0.53147	0.04478	0.06967	0.00575	0.979	425	38	433	29	434	35	-2.1	434	35
NA010A-041	205646	38	0.05748	0.00094	0.59698	0.05182	0.07533	0.00642	0.982	510	36	475	32	468	38	8.5	468	38
NA010A-042	71252	27	0.09717	0.00124	3.87954	0.25931	0.28956	0.01900	0.982	1571	24	1609	53	1639	94	-5.0	1571	24
NA010A-043	22140	30	0.09494	0.00251	3.92280	0.30943	0.29969	0.02227	0.942	1527	49	1618	62	1690	110	-12.1	1527	49
NA010A-044	445648	53	0.05735	0.00110	0.60189	0.05279	0.07612	0.00651	0.976	505	42	478	33	473	39	6.6	473	39
NA010A-045	187399	19	0.05641	0.00091	0.58141	0.04856	0.07476	0.00612	0.981	468	35	465	31	465	37	0.8	465	37
NA010A-046	149015	32	0.05589	0.00111	0.57370	0.04868	0.07444	0.00614	0.972	448	44	460	31	463	37	-3.4	463	37
NA010A-047	287449	30	0.11277	0.00130	5.23678	0.36034	0.33681	0.02285	0.986	1844	21	1859	57	1871	109	-1.7	1844	21

Flume Ridge Fm. (NA010A)

										age (Ma)	error (Ma)	age (Ma)	error (Ma)	age (Ma)	error (Ma)	discordance[1]	reported age[2]	
sample name	^{206}Pb (cps)	^{204}Pb (cps)	^{207}Pb/^{206}Pb	2 σ	^{207}Pb/^{235}U	2 σ	^{206}Pb/^{238}U	2 σ	ρ	^{207}Pb/^{206}Pb	2 σ	^{207}Pb/^{235}U	2 σ	^{206}Pb/^{238}U	2 σ	%	(Ma)	2 σ
NA010A-048	*336835*	*1121*	*0.05665*	*0.00451*	*0.55797*	*0.06147*	*0.07144*	*0.00544*	*0.692*	*478*	*167*	*450*	*39*	*445*	*33*	*7.1*	*478*	*167*
NA010A-049	1228633	63	0.10137	0.00114	4.18650	0.28025	0.29952	0.01976	0.986	1649	21	1671	53	1689	97	-2.7	1649	21
NA010A-050	409657	38	0.07450	0.00086	1.89883	0.12598	0.18485	0.01207	0.985	1055	23	1081	43	1093	65	-3.9	1055	23
NA010A-051A	219644	71	0.08977	0.00103	3.12038	0.22160	0.25209	0.01767	0.987	1421	22	1438	53	1449	90	-2.2	1421	22
NA010A-051B	223249	95	0.07913	0.00175	2.20649	0.19220	0.20222	0.01704	0.967	1176	43	1183	59	1187	91	-1.1	1176	43
NA010A-052	114108	107	0.05547	0.00103	0.57266	0.04883	0.07487	0.00623	0.976	431	41	460	31	465	37	-8.2	465	37
NA010A-054	*669649*	*319*	*0.10226*	*0.00172*	*4.04861*	*0.37314*	*0.28715*	*0.02602*	*0.983*	*1666*	*31*	*1644*	*72*	*1627*	*129*	*2.6*	*1666*	*31*
NA010A-055A	96842	104	0.05580	0.00103	0.59674	0.05257	0.07757	0.00668	0.978	444	40	475	33	482	40	-8.7	482	40
NA010A-055B	43694	106	0.05472	0.00109	0.57588	0.05031	0.07634	0.00649	0.974	401	44	462	32	474	39	-19.1	474	39
NA010A-055C	171513	113	0.05621	0.00096	0.59860	0.05129	0.07724	0.00649	0.980	461	37	476	32	480	39	-4.3	480	39
NA010A-056	197317	118	0.05559	0.00093	0.56126	0.05030	0.07323	0.00645	0.982	436	37	452	32	456	39	-4.7	456	39
NA010A-057	*136412*	*399*	*0.08887*	*0.00569*	*3.63907*	*0.35163*	*0.29698*	*0.02149*	*0.749*	*1401*	*118*	*1558*	*74*	*1676*	*106*	*-22.3*	*1401*	*118*
NA010A-058	31682	134	0.06313	0.00279	0.68562	0.06359	0.07877	0.00642	0.879	713	91	530	38	489	38	32.6	489	38
NA010A-059	107872	123	0.05459	0.00095	0.51006	0.04464	0.06777	0.00581	0.980	395	39	418	30	423	35	-7.2	423	35
NA010A-060	176294	141	0.07902	0.00094	2.32780	0.15683	0.21364	0.01417	0.984	1173	23	1221	47	1248	75	-7.1	1173	23
NA010A-061	260911	27	0.10093	0.00116	3.85117	0.25888	0.27674	0.01833	0.985	1641	21	1604	53	1575	92	4.6	1641	21
NA010A-062	154972	43	0.06029	0.00147	0.59260	0.05283	0.07129	0.00611	0.962	614	52	473	33	444	37	28.6	444	37
NA010A-063	181015	20	0.08674	0.00105	2.78688	0.19585	0.23303	0.01613	0.985	1355	23	1352	51	1350	84	0.3	1355	23
NA010A-064	266796	12	0.10163	0.00121	4.16874	0.29483	0.29749	0.02074	0.986	1654	22	1668	56	1679	102	-1.7	1654	22
NA010A-065	230707	12	0.09302	0.00108	3.42692	0.22678	0.26718	0.01741	0.984	1488	22	1511	51	1526	88	-2.9	1488	22
NA010A-066	107770	12	0.05677	0.00093	0.56892	0.04895	0.07268	0.00614	0.982	483	36	457	31	452	37	6.5	452	37
NA010A-067	658274	36	0.10218	0.00117	4.18497	0.30742	0.29705	0.02156	0.988	1664	21	1671	58	1677	106	-0.9	1664	21
NA010A-068	508331	7	0.10561	0.00120	4.49465	0.32515	0.30867	0.02205	0.988	1725	21	1730	58	1734	108	-0.6	1725	21
NA010A-069	220996	14	0.09285	0.00112	3.22104	0.22523	0.25160	0.01733	0.985	1485	23	1462	53	1447	89	2.9	1485	23
NA010A-070	421382	23	0.07792	0.00090	2.15030	0.15693	0.20014	0.01442	0.987	1145	23	1165	49	1176	77	-3.0	1145	23
NA010A-071	*1136140*	*578*	*0.07670*	*0.00129*	*1.86435*	*0.13724*	*0.17628*	*0.01263*	*0.973*	*1114*	*33*	*1069*	*48*	*1047*	*69*	*6.5*	*1114*	*33*
NA010A-072	76768	7	0.07212	0.00107	1.63719	0.12435	0.16464	0.01226	0.981	989	30	985	47	982	68	0.8	989	30
NA010A-073	81856	7	0.07506	0.00095	1.84220	0.12068	0.17800	0.01144	0.981	1070	25	1061	42	1056	62	1.4	1070	25
NA010A-074	145132	7	0.16164	0.00194	10.47351	0.69930	0.46994	0.03087	0.984	2473	20	2478	60	2483	134	-0.5	2473	20
NA010A-075	91065	5	0.05684	0.00096	0.57501	0.04871	0.07337	0.00609	0.980	485	37	461	31	456	36	6.2	456	36
NA010A-076	45713	16	0.07761	0.00111	2.00267	0.13854	0.18715	0.01267	0.978	1137	28	1116	46	1106	68	3.0	1137	28
NA010A-077	759908	18	0.07508	0.00085	1.96054	0.13326	0.18939	0.01269	0.986	1071	23	1102	45	1118	68	-4.8	1071	23
NA010A-078	271056	12	0.09852	0.00114	3.92168	0.27489	0.28871	0.01996	0.986	1596	21	1618	55	1635	99	-2.8	1596	21
NA010A-079	727726	5	0.08459	0.00097	2.65919	0.18660	0.22800	0.01579	0.987	1306	22	1317	51	1324	82	-1.5	1306	22
NA010A-080	458380	8	0.07364	0.00085	1.76822	0.11897	0.17415	0.01155	0.985	1032	23	1034	43	1035	63	-0.3	1032	23
NA010A-081	405797	58	0.18810	0.00215	14.35581	0.98261	0.55351	0.03736	0.986	2726	19	2774	63	2840	153	-5.2	2726	19
NA010A-082	160549	54	0.07648	0.00098	1.91502	0.14463	0.18161	0.01352	0.986	1108	25	1086	49	1076	73	3.1	1108	25
NA010A-083	400800	200	0.06212	0.00155	0.58377	0.05180	0.06815	0.00580	0.959	678	53	467	33	425	35	38.6	425	35
NA010A-084	84366	22	0.05764	0.00153	0.58417	0.05014	0.07351	0.00600	0.951	516	57	467	32	457	36	11.8	457	36
NA010A-085	311680	86	0.10383	0.00122	4.13563	0.31080	0.28889	0.02144	0.988	1694	22	1661	60	1636	106	3.9	1694	22
NA010A-086	567456	39	0.08731	0.00099	2.86461	0.19375	0.23795	0.01587	0.986	1367	22	1373	50	1376	82	-0.7	1367	22
NA010A-087	45495	32	0.06223	0.00114	0.61544	0.05159	0.07173	0.00587	0.976	682	39	487	32	447	35	35.7	447	35
NA010A-088	368436	53	0.10692	0.00130	4.55783	0.31512	0.30917	0.02104	0.984	1748	22	1742	56	1737	103	0.7	1748	22
NA010A-089	571299	45	0.07309	0.00084	1.77808	0.12145	0.17644	0.01188	0.986	1016	23	1037	43	1048	65	-3.3	1016	23
NA010A-090	140134	41	0.05579	0.00092	0.54647	0.04587	0.07104	0.00585	0.981	444	36	443	30	442	35	0.4	442	35
NA010A-091	64110	75	0.06726	0.00101	1.07045	0.07112	0.11544	0.00747	0.974	846	31	739	34	704	43	17.7	846	31
NA010A-092	335259	80	0.05698	0.00091	0.59914	0.05135	0.07626	0.00642	0.982	491	35	477	32	474	38	3.6	474	38
NA010A-093	86927	107	0.07549	0.00109	1.73957	0.11949	0.16714	0.01122	0.978	1081	29	1023	43	996	62	8.5	1081	29

Flume Ridge Fm. (NA010A)

										age (Ma)	error (Ma)	age (Ma)	error (Ma)	age (Ma)	error (Ma)	discordance[1]	reported age[2]	
sample name	^{206}Pb (cps)	^{204}Pb (cps)	^{207}Pb/^{206}Pb	2 σ	^{207}Pb/^{235}U	2 σ	^{206}Pb/^{238}U	2 σ	ρ	^{207}Pb/^{206}Pb	2 σ	^{207}Pb/^{235}U	2 σ	^{206}Pb/^{238}U	2 σ	%	(Ma)	2 σ
NA010A-094	64855	102	0.05713	0.00101	0.58182	0.04892	0.07386	0.00607	0.978	496	39	466	31	459	36	7.7	459	36
NA010A-095	321574	110	0.09020	0.00107	3.04674	0.20912	0.24498	0.01656	0.985	1430	23	1419	51	1413	85	1.3	1430	23
NA010A-096	403790	75	0.07407	0.00086	1.82049	0.12239	0.17826	0.01180	0.985	1043	23	1053	43	1057	64	-1.5	1043	23
NA010A-097	596225	2941	0.07710	0.00194	0.50132	0.04125	0.04716	0.00369	0.952	1124	49	413	28	297	23	75.2	1124	49
NA010A-098	52456	114	0.05887	0.00122	0.64906	0.05687	0.07996	0.00681	0.972	562	44	508	34	496	41	12.3	496	41
NA010A-099	71874	107	0.07348	0.00094	1.81303	0.12527	0.17895	0.01215	0.983	1027	26	1050	44	1061	66	-3.6	1027	26
NA010A-100	1052389	152	0.09249	0.00106	3.31455	0.22263	0.25992	0.01720	0.985	1477	22	1484	51	1489	87	-0.9	1477	22
NA010A-101	1128613	132	0.07364	0.00084	1.76794	0.11791	0.17413	0.01144	0.985	1032	23	1034	42	1035	63	-0.3	1032	23
NA010A-102	325004	101	0.09181	0.00106	3.18324	0.21944	0.25145	0.01709	0.986	1464	22	1453	52	1446	87	1.3	1464	22
NA010A-103	366760	99	0.05598	0.00090	0.56757	0.04766	0.07353	0.00606	0.982	452	35	456	30	457	36	-1.3	457	36
NA010A-104	182102	275	0.08838	0.00144	2.35943	0.16596	0.19362	0.01325	0.973	1391	31	1230	49	1141	71	19.6	1391	31
NA010A-105	528325	128	0.09134	0.00104	3.18240	0.23059	0.25270	0.01808	0.988	1454	22	1453	54	1452	92	0.1	1454	22
NA010A-106	200570	115	0.05664	0.00094	0.59597	0.05234	0.07632	0.00658	0.982	477	36	475	33	474	39	0.7	474	39
NA010A-107	357248	269	0.10291	0.00192	4.19795	0.30430	0.29584	0.02072	0.966	1677	34	1674	58	1671	102	0.5	1677	34
NA010A-108	39363	119	0.08225	0.00136	2.23322	0.16100	0.19693	0.01382	0.973	1251	32	1192	49	1159	74	8.1	1251	32
NA010A-109	124136	94	0.07282	0.00085	1.73467	0.11647	0.17277	0.01142	0.985	1009	23	1021	42	1027	62	-2.0	1009	23
NA010A-110	255222	118	0.09619	0.00113	3.49387	0.24613	0.26343	0.01830	0.986	1552	22	1526	54	1507	93	3.2	1552	22
NA010A-111	320881	88	0.08699	0.00102	2.49296	0.17064	0.20784	0.01402	0.985	1360	22	1270	48	1217	74	11.5	1360	22
NA010A-112	*717999*	*451*	*0.07321*	*0.00153*	*1.81507*	*0.13549*	*0.17980*	*0.01288*	*0.960*	*1020*	*42*	*1051*	*48*	*1066*	*70*	*-4.9*	*1020*	*42*
NA010A-113	690013	83	0.10000	0.00114	4.21923	0.32362	0.30600	0.02321	0.989	1624	21	1678	61	1721	114	-6.8	1624	21
NA010A-114	37879	40	0.05655	0.00137	0.62350	0.05459	0.07996	0.00673	0.961	474	53	492	34	496	40	-4.8	496	40
NA010A-115	109696	57	0.08436	0.00101	2.64982	0.18795	0.22780	0.01593	0.986	1301	23	1315	51	1323	83	-1.9	1301	23
NA010A-116	212134	31	0.10567	0.00124	4.78941	0.32796	0.32873	0.02218	0.985	1726	21	1783	56	1832	107	-7.1	1726	21
NA010A-117	1228135	39	0.07629	0.00088	2.01042	0.13809	0.19113	0.01294	0.986	1103	23	1119	46	1127	70	-2.5	1103	23
NA010A-118	158959	39	0.09165	0.00113	3.30210	0.23535	0.26130	0.01834	0.985	1460	23	1482	54	1496	93	-2.8	1460	23
NA010A-119	357175	55	0.05738	0.00096	0.59298	0.05083	0.07496	0.00630	0.981	506	36	473	32	466	38	8.2	466	38
NA010A-120	48906	18	0.05812	0.00114	0.60345	0.05101	0.07531	0.00619	0.972	534	43	479	32	468	37	12.8	468	37
NA010A-121	*441550*	*167*	*0.05777*	*0.00154*	*0.63080*	*0.05704*	*0.07919*	*0.00684*	*0.956*	*521*	*57*	*497*	*35*	*491*	*41*	*5.9*	*491*	*41*
NA010A-122	130937	16	0.07256	0.00085	1.71648	0.11660	0.17156	0.01148	0.985	1002	24	1015	43	1021	63	-2.0	1002	24
NA010A-123	382736	15	0.05658	0.00090	0.60159	0.05028	0.07711	0.00633	0.982	475	35	478	31	479	38	-0.8	479	38
NA010A-124	272613	20	0.11593	0.00151	5.60035	0.38939	0.35037	0.02393	0.982	1894	23	1916	58	1936	113	-2.6	1894	23
NA010A-125	119116	15	0.05577	0.00093	0.54828	0.04589	0.07130	0.00585	0.980	443	37	444	30	444	35	-0.1	444	35
NA010A-126	364513	42	0.10207	0.00135	3.97524	0.26925	0.28246	0.01876	0.981	1662	24	1629	54	1604	94	4.0	1662	24
NA010A-127	415090	16	0.07631	0.00087	1.98367	0.14108	0.18854	0.01323	0.987	1103	23	1110	47	1113	71	-1.0	1103	23
NA010A-128	603303	3	0.07305	0.00083	1.77311	0.12137	0.17605	0.01188	0.986	1015	23	1036	43	1045	65	-3.2	1015	23
NA010A-129	366328	4	0.07178	0.00082	1.65077	0.10958	0.16680	0.01091	0.985	980	23	990	41	994	60	-1.6	980	23
NA010A-130	37642	19	0.05988	0.00116	0.78029	0.07031	0.09451	0.00832	0.977	599	41	586	39	582	49	3.0	582	49
NA010A-131	182869	120	0.10479	0.00302	3.71335	0.28423	0.25701	0.01823	0.926	1711	52	1574	59	1475	93	15.4	1711	52
NA010A-132	181505	2	0.09205	0.00107	3.07869	0.20485	0.24257	0.01589	0.985	1468	22	1427	50	1400	82	5.2	1468	22
NA010A-133	*2045756*	*1545*	*0.07496*	*0.00131*	*1.63224*	*0.13550*	*0.15793*	*0.01282*	*0.978*	*1067*	*35*	*983*	*51*	*945*	*71*	*12.3*	*1067*	*35*
NA010A-134	231033	9	0.05631	0.00091	0.53615	0.04441	0.06905	0.00561	0.981	465	36	436	29	430	34	7.6	430	34
NA010A-135	339390	2	0.09619	0.00116	3.40814	0.24465	0.25698	0.01819	0.986	1551	22	1506	55	1474	93	5.6	1551	22
NA010A-136	258132	0	0.07467	0.00087	1.65208	0.10903	0.16048	0.01042	0.984	1060	23	990	41	959	58	10.2	1060	23
NA010A-137	163348	5	0.09303	0.00115	2.68758	0.24350	0.20952	0.01880	0.991	1489	23	1325	65	1226	99	19.3	1489	23
NA010A-138	28403	0	0.07972	0.00125	1.94392	0.13661	0.17686	0.01211	0.975	1190	31	1096	46	1050	66	12.8	1190	31
NA010A-139	611665	0	0.07812	0.00089	1.92634	0.15427	0.17885	0.01418	0.990	1150	23	1090	52	1061	77	8.4	1150	23
NA010A-140	83965	0	0.07215	0.00096	1.50349	0.10289	0.15113	0.01014	0.981	990	27	932	41	907	57	9.0	990	27

Concordia diagrams for NA010A, Flume Ridge Fm.

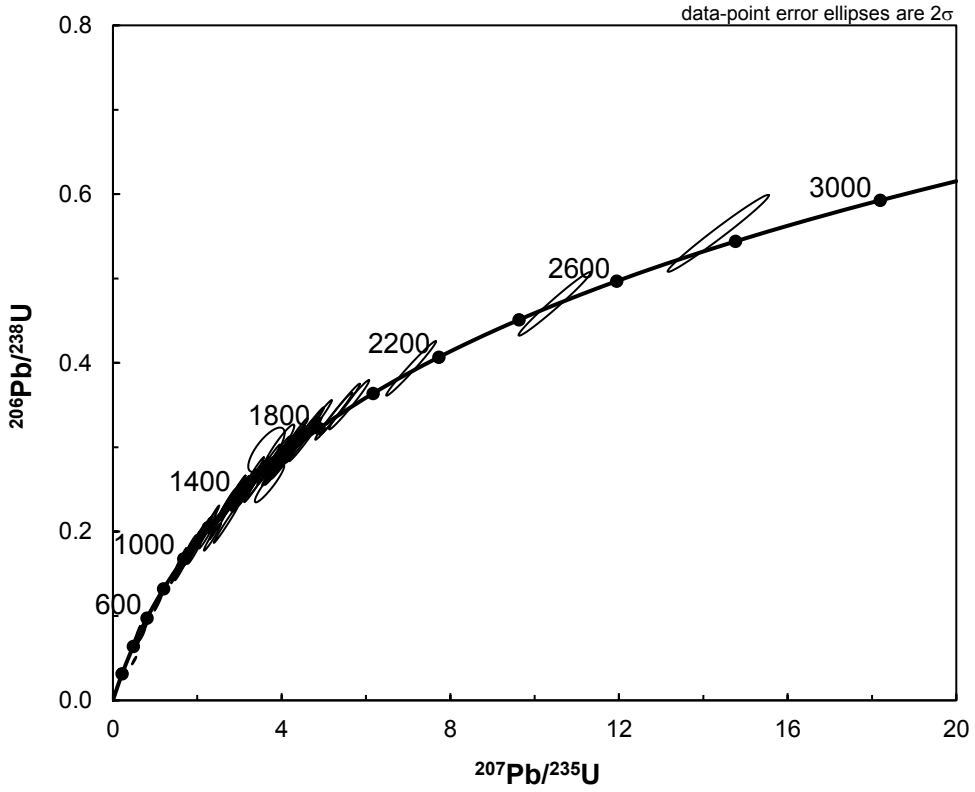

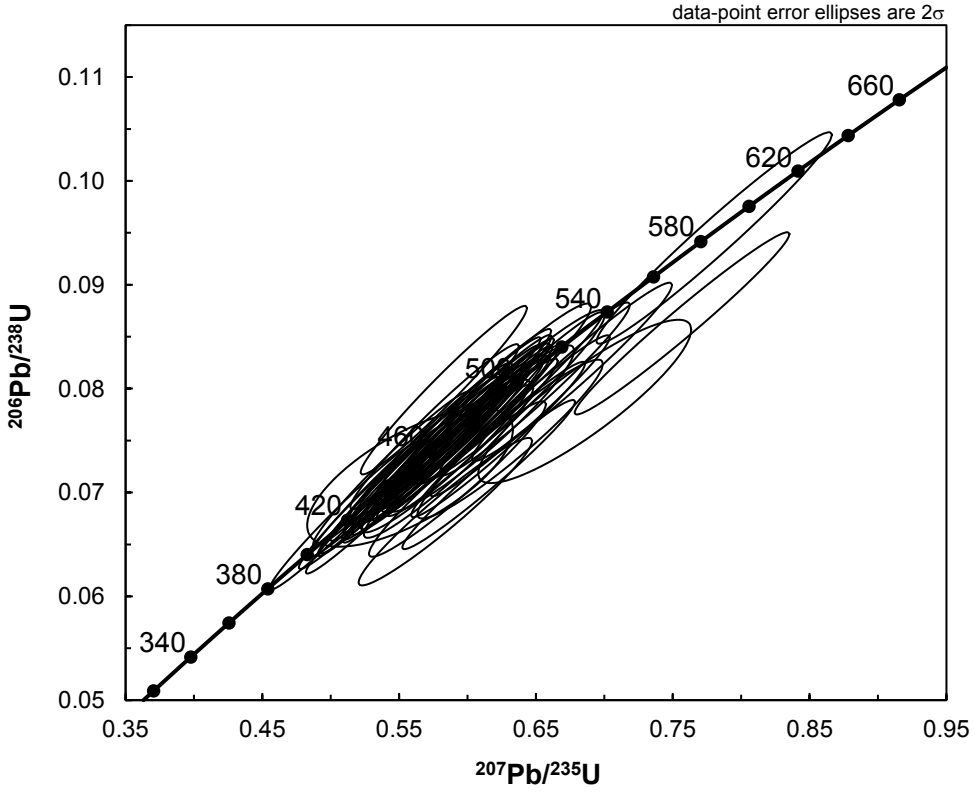

Histogram and kernel density plot for NA010A, Flume Ridge Fm. Bandwidth and bin width is equal to median 2σ, 23.3 Ma.

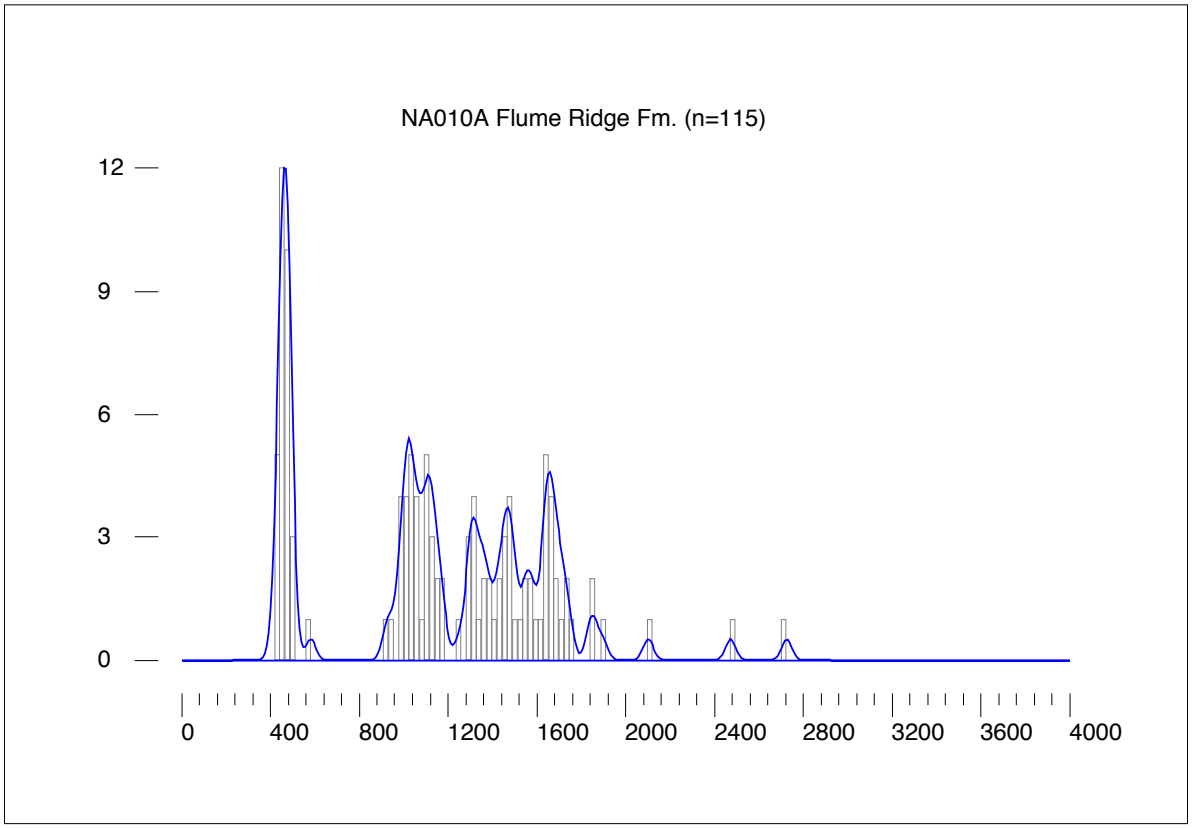

Appendix B: Mascarene Basin detrital zircon data and diagrams

Notes to appendix:

[1]Percent discordance between $^{206}Pb/^{238}U$ and $^{207}Pb/^{206}Pb$, as per the following formula:

$[(e^{0.000155125 \times 207Pb/206Pb\ age} - 1) - {}^{207}Pb/^{206}Pb\ ratio] \times 100 / [(e^{0.000155125 \times 207Pb/206Pb\ age} - 1)]$

[2] $^{207}Pb/^{206}Pb$ ages are reported for $^{207}Pb/^{206}Pb$ ratios greater than 0.0658 (800 Ma); $^{206}Pb/^{238}U$ ages reported otherwise.

Samples in *italics* are corrected for common lead. A discordance cutoff of 10% is applied: analyses which fall outside of the -10% to +10% range are greyed out.

Concordia diagrams do not exclude discordant analyses.

Correlation coefficients (ρ) calculated by the following formula:

$[(2\sigma^{207}Pb/^{235}U / {}^{207}Pb/^{235}U)^2 + (2\sigma^{206}Pb/^{238}U / {}^{206}Pb/^{238}U)^2 - (2\sigma^{207}Pb/^{206}Pb / {}^{207}Pb/^{206}Pb)^2] / [(2)(2\sigma^{206}Pb/^{238}U / {}^{206}Pb/^{238}U)(2\sigma^{207}Pb/^{235}U / {}^{207}Pb/^{235}U)]$

$^{207}Pb/^{235}U$ ratios are calculated as 137.88 x $^{206}Pb/^{238}U$ x $^{207}Pb/^{206}Pb$.

Histograms and KDEs were generated using DensityPlotter 7.3 (Vermeesch, 2012), and concordia diagrams with Isoplot 3.75 (Ludwig, 2012).

Waweig Fm. (PG035A)

sample name	^{206}Pb (cps)	^{204}Pb (cps)	$^{207}Pb/^{206}Pb$	2 σ	$^{207}Pb/^{235}U$	2 σ	$^{206}Pb/^{238}U$	2 σ	ρ	age (Ma) $^{207}Pb/^{206}Pb$	error (Ma) 2 σ	age (Ma) $^{207}Pb/^{235}U$	error (Ma) 2 σ	age (Ma) $^{206}Pb/^{238}U$	error (Ma) 2 σ	discordance[1] %	reported age[2] (Ma)	2 σ
PG035A-001	8707	95	0.05636	0.00142	0.54136	0.02743	0.06966	0.00306	0.867	467	55	439	18	434	18	7.2	434	18
PG035A-002	65361	110	0.05675	0.00071	0.57092	0.02415	0.07296	0.00295	0.956	482	27	459	15	454	18	6.0	454	18
PG035A-003	7415	105	0.05433	0.00184	0.51635	0.02846	0.06893	0.00300	0.789	385	74	423	19	430	18	-12.1	430	18
PG035A-004	1945	110	0.04731	0.00519	0.54870	0.07673	0.08411	0.00731	0.621	65	242	444	49	521	43	-730.2	521	43
PG035A-005	631985	129	0.05645	0.00065	0.55066	0.02501	0.07075	0.00311	0.967	470	25	445	16	441	19	6.5	441	19
PG035A-006	9200	112	0.06855	0.00303	0.66196	0.07483	0.07004	0.00729	0.920	885	89	516	45	436	44	52.4	885	89
PG035A-007	9356	101	0.05330	0.00114	0.51272	0.02363	0.06976	0.00285	0.887	342	48	420	16	435	17	-28.1	435	17
PG035A-008	20723	92	0.05435	0.00112	0.51322	0.02285	0.06848	0.00270	0.886	386	46	421	15	427	16	-11.1	427	16
PG035A-009	4720	119	0.05163	0.00198	0.55468	0.03422	0.07792	0.00377	0.784	269	86	448	22	484	23	-82.8	484	23
PG035A-010	6407842	110	0.06060	0.00144	0.59798	0.02440	0.07156	0.00238	0.814	625	50	476	15	446	14	29.7	446	14
PG035A-011	83678	81	0.05688	0.00066	0.56091	0.02934	0.07152	0.00365	0.975	487	25	452	19	445	22	8.8	445	22
PG035A-012	27235	33	0.05581	0.00085	0.54097	0.02275	0.07030	0.00276	0.932	445	34	439	15	438	17	1.6	438	17
PG035A-013	30050	32	0.05619	0.00089	0.51751	0.02861	0.06680	0.00354	0.958	460	35	423	19	417	21	9.7	417	21
PG035A-014	15655	24	0.05562	0.00115	0.52083	0.02749	0.06792	0.00330	0.920	437	45	426	18	424	20	3.2	424	20
PG035A-015	11974	40	0.05626	0.00118	0.51618	0.02556	0.06654	0.00298	0.906	463	46	423	17	415	18	10.6	415	18
PG035A-016	189905	71	0.10701	0.00115	4.19954	0.32437	0.28462	0.02177	0.990	1749	20	1674	61	1615	108	8.7	1749	20
PG035A-017	34317	51	0.05831	0.00079	0.55257	0.02190	0.06873	0.00256	0.940	541	29	447	14	429	15	21.5	429	15
PG035A-018	30038	55	0.05833	0.00104	0.55103	0.02283	0.06851	0.00257	0.904	542	38	446	15	427	15	21.9	427	15
PG035A-019	13121	48	0.06584	0.00146	0.86137	0.06462	0.09488	0.00680	0.956	801	46	631	35	584	40	28.3	801	46
PG035A-020	331522	86	0.05773	0.00078	0.57222	0.02957	0.07189	0.00359	0.966	520	29	459	19	448	22	14.4	448	22
PG035A-021	15916	42	0.06116	0.00201	0.70658	0.04634	0.08379	0.00475	0.865	645	69	543	27	519	28	20.4	519	28
PG035A-022	17109	37	0.05687	0.00143	0.54627	0.03727	0.06966	0.00442	0.929	487	55	443	24	434	27	11.2	434	27
PG035A-023	46779	34	0.05668	0.00077	0.54834	0.02269	0.07016	0.00274	0.945	479	30	444	15	437	17	9.1	437	17
PG035A-024	9295	25	0.05559	0.00152	0.52645	0.02791	0.06869	0.00312	0.858	436	60	429	18	428	19	1.8	428	19
PG035A-025	58511	34	0.05532	0.00071	0.56313	0.02959	0.07383	0.00376	0.970	425	28	454	19	459	23	-8.3	459	23
PG035A-026	22878	29	0.05809	0.00118	0.54452	0.02483	0.06798	0.00277	0.894	533	44	441	16	424	17	21.1	424	17
PG035A-027	225400	19	0.05619	0.00063	0.50367	0.02153	0.06501	0.00268	0.965	460	25	414	14	406	16	12.1	406	16
PG035A-028	30266	17	0.05607	0.00089	0.55274	0.02132	0.07150	0.00252	0.912	455	35	447	14	445	15	2.3	445	15
PG035A-029	44090	4	0.05791	0.00145	0.51558	0.02876	0.06458	0.00322	0.894	526	54	422	19	403	19	24.1	403	19
PG035A-030	15307	10	0.05534	0.00109	0.51341	0.02921	0.06728	0.00359	0.938	426	43	421	19	420	22	1.6	420	22
PG035A-031	23929	8	0.05603	0.00090	0.52711	0.02901	0.06824	0.00359	0.956	453	35	430	19	426	22	6.3	426	22
PG035A-032	39933	4	0.05603	0.00074	0.52688	0.02724	0.06820	0.00341	0.966	454	29	430	18	425	21	6.5	425	21
PG035A-033	90951	3	0.05667	0.00072	0.52100	0.03470	0.06667	0.00436	0.982	479	28	426	23	416	26	13.5	416	26
PG035A-034	62221	1	0.05597	0.00069	0.51178	0.02930	0.06632	0.00371	0.976	451	27	420	19	414	22	8.5	414	22
PG035A-035	57302	4	0.05582	0.00069	0.54555	0.02382	0.07089	0.00297	0.959	445	27	442	16	442	18	0.8	442	18
PG035A-036	34474	4	0.05705	0.00087	0.55510	0.02215	0.07057	0.00260	0.925	493	33	448	14	440	16	11.3	440	16
PG035A-037	11545	11	0.05560	0.00153	0.52868	0.02623	0.06896	0.00284	0.831	437	60	431	17	430	17	1.6	430	17
PG035A-038	58920	13	0.05604	0.00072	0.52596	0.03261	0.06807	0.00413	0.978	454	28	429	21	425	25	6.7	425	25
PG035A-039	41884	5	0.05596	0.00084	0.53289	0.02512	0.06907	0.00309	0.948	451	33	434	17	431	19	4.6	431	19
PG035A-040	171724	12	0.11702	0.00149	1.65722	0.18884	0.10271	0.01163	0.994	1911	23	992	70	630	68	70.2	1911	23
PG035A-041	23156	49	0.05862	0.00107	0.57612	0.02784	0.07128	0.00319	0.926	553	39	462	18	444	19	20.4	444	19
PG035A-042	52416	2	0.05604	0.00068	0.52635	0.02161	0.06812	0.00267	0.955	454	27	429	14	425	16	6.6	425	16
PG035A-043	75770	2	0.05591	0.00071	0.54610	0.02811	0.07084	0.00353	0.969	449	28	442	18	441	21	1.7	441	21
PG035A-044	14411	3	0.05591	0.00156	0.52428	0.02611	0.06801	0.00281	0.828	449	61	428	17	424	17	5.7	424	17
PG035A-045	74780	5	0.05582	0.00070	0.51392	0.03449	0.06677	0.00440	0.982	445	28	421	23	417	27	6.7	417	27
PG035A-046	37775	9	0.05673	0.00071	0.51747	0.02281	0.06615	0.00280	0.959	481	27	423	15	413	17	14.7	413	17
PG035A-047	14560	4	0.05508	0.00118	0.51685	0.02309	0.06806	0.00267	0.877	415	47	423	15	424	16	-2.3	424	16
PG035A-048	649954	45	0.05548	0.00057	0.57060	0.02692	0.07459	0.00343	0.976	432	23	458	17	464	21	-7.7	464	21

Waweig Fm. (PG035A)

sample name	^{206}Pb (cps)	^{204}Pb (cps)	^{207}Pb/^{206}Pb	2 σ	^{207}Pb/^{235}U	2 σ	^{206}Pb/^{238}U	2 σ	ρ	age (Ma) ^{207}Pb/^{206}Pb	error (Ma) 2 σ	age (Ma) ^{207}Pb/^{235}U	error (Ma) 2 σ	age (Ma) ^{206}Pb/^{238}U	error (Ma) 2 σ	discordance[1] %	reported age[2] (Ma)	2 σ
PG035A-049	36307	46	0.05644	0.00086	0.53172	0.02086	0.06833	0.00247	0.922	470	33	433	14	426	15	9.6	426	15
PG035A-050	16686	4	0.05734	0.00095	0.53689	0.02198	0.06791	0.00254	0.914	505	36	436	14	424	15	16.6	424	15
PG035A-051	23375	4	0.05661	0.00098	0.54634	0.02135	0.06999	0.00245	0.896	477	38	443	14	436	15	8.8	436	15
PG035A-052	34905	9	0.05615	0.00082	0.53238	0.03067	0.06877	0.00383	0.967	458	32	433	20	429	23	6.7	429	23
PG035A-053	81465	2	0.05536	0.00067	0.52433	0.02854	0.06869	0.00365	0.975	427	27	428	19	428	22	-0.3	428	22
PG035A-054	30294	14	0.05515	0.00086	0.52778	0.02825	0.06941	0.00355	0.956	418	35	430	19	433	21	-3.6	433	21
PG035A-055	14247	0	0.05520	0.00127	0.50400	0.02360	0.06622	0.00270	0.870	420	51	414	16	413	16	1.8	413	16
PG035A-056	18699	5	0.05538	0.00099	0.51884	0.02227	0.06795	0.00265	0.910	427	39	424	15	424	16	0.9	424	16
PG035A-057	18596	7	0.05623	0.00102	0.52687	0.02682	0.06795	0.00323	0.934	462	40	430	18	424	19	8.5	424	19
PG035A-058	8513	4	0.05599	0.00156	0.53908	0.02844	0.06982	0.00313	0.848	452	61	438	19	435	19	3.9	435	19
PG035A-059	17354	6	0.05566	0.00090	0.51924	0.02759	0.06766	0.00342	0.952	439	36	425	18	422	21	4.0	422	21
PG035A-060	150231	6	0.05577	0.00065	0.56541	0.02912	0.07353	0.00369	0.974	443	26	455	19	457	22	-3.3	457	22
PG035A-061	89665	12	0.05734	0.00072	0.55413	0.02034	0.07009	0.00242	0.940	505	27	448	13	437	15	13.9	437	15
PG035A-062	49345	5	0.05607	0.00075	0.52872	0.02208	0.06839	0.00271	0.947	455	29	431	15	426	16	6.5	426	16
PG035A-063	217643	6	0.05581	0.00060	0.58084	0.02748	0.07548	0.00348	0.974	445	24	465	18	469	21	-5.6	469	21
PG035A-064	9945	7	0.07574	0.00189	0.74102	0.05403	0.07096	0.00486	0.940	1088	49	563	31	442	29	61.4	1088	49
PG035A-065	53474	18	0.06251	0.00097	0.61992	0.02756	0.07192	0.00299	0.937	692	33	490	17	448	18	36.5	448	18
PG035A-066	52718	10	0.05680	0.00084	0.53501	0.02907	0.06831	0.00357	0.962	484	32	435	19	426	22	12.4	426	22
PG035A-067	32451	7	0.05633	0.00088	0.53090	0.02134	0.06836	0.00253	0.922	465	34	432	14	426	15	8.7	426	15
PG035A-068	16956	1	0.05698	0.00111	0.52285	0.02315	0.06655	0.00264	0.898	491	42	427	15	415	16	15.9	415	16
PG035A-069	20035	3	0.05552	0.00102	0.51535	0.02055	0.06732	0.00239	0.888	433	40	422	14	420	14	3.2	420	14
PG035A-070	118653	9	0.05919	0.00099	0.53889	0.02228	0.06603	0.00250	0.914	574	36	438	15	412	15	29.1	412	15
PG035A-071	47819	19	0.05551	0.00085	0.51905	0.03179	0.06782	0.00402	0.968	433	34	425	21	423	24	2.3	423	24
PG035A-072	120136	32	0.08745	0.00457	0.41798	0.05743	0.03467	0.00441	0.925	1370	97	355	40	220	27	85.4	1370	97
PG035A-073	44824	17	0.05577	0.00080	0.53175	0.02695	0.06915	0.00336	0.959	443	32	433	18	431	20	2.8	431	20
PG035A-074	27230	14	0.05583	0.00098	0.51481	0.03444	0.06688	0.00432	0.965	446	39	422	23	417	26	6.5	417	26
PG035A-075	869896	33	0.05689	0.00065	0.57144	0.03329	0.07285	0.00416	0.981	487	25	459	21	453	25	7.2	453	25
PG035A-076	82358	22	0.05581	0.00066	0.56541	0.02498	0.07347	0.00313	0.964	445	26	455	16	457	19	-2.8	457	19
PG035A-077	387202	113	0.05917	0.00113	0.62281	0.04076	0.07634	0.00478	0.957	573	41	492	25	474	29	17.9	474	29
PG035A-078	33770	48	0.07855	0.00238	0.69519	0.03609	0.06419	0.00271	0.812	1161	59	536	21	401	16	67.5	1161	59
PG035A-079	160293	17	0.06182	0.00073	0.94184	0.04927	0.11050	0.00563	0.975	668	25	674	25	676	33	-1.2	676	33
PG035A-080	40319	11	0.05529	0.00079	0.53985	0.02632	0.07082	0.00330	0.956	424	32	438	17	441	20	-4.2	441	20
PG035A-081	33036	2	0.05616	0.00088	0.50072	0.02474	0.06466	0.00303	0.949	459	34	412	17	404	18	12.3	404	18
PG035A-082	15063	6	0.05739	0.00111	0.54313	0.02785	0.06864	0.00326	0.927	507	42	440	18	428	20	16.0	428	20
PG035A-083	10576	5	0.05575	0.00132	0.53203	0.02698	0.06921	0.00310	0.884	443	52	433	18	431	19	2.6	431	19
PG035A-084	87216	7	0.05748	0.00086	0.52874	0.02366	0.06671	0.00281	0.942	510	33	431	16	416	17	19.0	416	17
PG035A-085	12146	3	0.05440	0.00138	0.54179	0.03303	0.07223	0.00400	0.909	388	56	440	22	450	24	-16.5	450	24
PG035A-086	13371	3	0.05492	0.00090	0.50567	0.02523	0.06678	0.00315	0.944	409	36	416	17	417	19	-1.9	417	19
PG035A-087	16449	0	0.05496	0.00105	0.51438	0.02702	0.06788	0.00332	0.931	411	42	421	18	423	20	-3.2	423	20
PG035A-088	11109	1	0.05655	0.00110	0.53037	0.02821	0.06802	0.00337	0.931	474	42	432	19	424	20	10.9	424	20
PG035A-089	25823	2	0.05525	0.00100	0.50365	0.02492	0.06611	0.00304	0.930	423	40	414	17	413	18	2.4	413	18
PG035A-090	36032	2	0.05671	0.00102	0.53943	0.02623	0.06899	0.00311	0.929	480	39	438	17	430	19	10.8	430	19
PG035A-091	9713	0	0.05618	0.00136	0.53775	0.02702	0.06942	0.00305	0.875	459	53	437	18	433	18	6.0	433	18
PG035A-092	13389	0	0.05480	0.00129	0.51099	0.03120	0.06763	0.00381	0.922	404	52	419	21	422	23	-4.6	422	23
PG035A-093	34148	0	0.05847	0.00122	0.54210	0.02834	0.06724	0.00322	0.916	547	45	440	18	420	19	24.1	420	19
PG035A-094	10873	3	0.05705	0.00155	0.55388	0.04129	0.07042	0.00489	0.931	493	59	448	27	439	29	11.5	439	29
PG035A-095A	3431	0	0.04723	0.00269	0.46159	0.03590	0.07089	0.00375	0.681	61	130	385	25	441	23	-648.6	441	23
PG035A-095B	9880	1	0.05489	0.00151	0.49349	0.02775	0.06520	0.00320	0.872	408	60	407	19	407	19	0.2	407	19

Waweig Fm. (PG035A)

sample name	^{206}Pb (cps)	^{204}Pb (cps)	^{207}Pb/^{206}Pb	2 σ	^{207}Pb/^{235}U	2 σ	^{206}Pb/^{238}U	2 σ	ρ	age (Ma) ^{207}Pb/^{206}Pb	error (Ma) 2 σ	age (Ma) ^{207}Pb/^{235}U	error (Ma) 2 σ	age (Ma) ^{206}Pb/^{238}U	error (Ma) 2 σ	discordance[1] %	reported age[2] (Ma)	2 σ
PG035A-096	32566	0	0.05552	0.00087	0.52403	0.02888	0.06846	0.00362	0.959	433	35	428	19	427	22	1.5	427	22
PG035A-097	65606	0	0.05622	0.00087	0.58402	0.03274	0.07534	0.00406	0.961	461	34	467	21	468	24	-1.6	468	24
PG035A-098	20987	1	0.05567	0.00099	0.51652	0.03192	0.06729	0.00398	0.958	439	39	423	21	420	24	4.6	420	24
PG035A-099	19304	0	0.05663	0.00101	0.54482	0.03107	0.06977	0.00378	0.950	477	39	442	20	435	23	9.2	435	23
PG035A-100	30173	0	0.05603	0.00083	0.51087	0.02969	0.06613	0.00372	0.967	454	32	419	20	413	22	9.3	413	22
PG035A-101	24133	1	0.05482	0.00096	0.54641	0.03324	0.07229	0.00421	0.958	405	39	443	22	450	25	-11.5	450	25
PG035A-102	25924	3	0.05595	0.00089	0.49743	0.02420	0.06448	0.00296	0.945	451	35	410	16	403	18	10.9	403	18
PG035A-103	13069	5	0.05424	0.00132	0.50407	0.02906	0.06741	0.00353	0.907	381	54	414	19	421	21	-10.8	421	21
PG035A-104	6825	2	0.05421	0.00214	0.50430	0.03152	0.06747	0.00327	0.776	380	86	415	21	421	20	-11.2	421	20
PG035A-105	4700	1	0.05294	0.00175	0.47795	0.02902	0.06547	0.00333	0.838	326	73	397	20	409	20	-26.1	409	20
PG035A-106	6157	0	0.05340	0.00178	0.47207	0.03484	0.06411	0.00422	0.892	346	74	393	24	401	26	-16.3	401	26
PG035A-107	9446	0	0.05497	0.00150	0.49538	0.02695	0.06536	0.00308	0.866	411	60	409	18	408	19	0.7	408	19
PG035A-108	35089	0	0.05480	0.00081	0.50345	0.02572	0.06663	0.00326	0.958	404	33	414	17	416	20	-3.0	416	20
PG035A-109	10704	2	0.05466	0.00113	0.50008	0.02470	0.06635	0.00297	0.908	399	46	412	17	414	18	-4.0	414	18
PG035A-110	16008	0	0.05543	0.00104	0.51829	0.02557	0.06782	0.00309	0.924	430	41	424	17	423	19	1.6	423	19
PG035A-111	6417	0	0.05898	0.00253	0.57256	0.03714	0.07041	0.00342	0.750	566	91	460	24	439	21	23.3	439	21
PG035A-112	12558	0	0.05442	0.00146	0.51240	0.03146	0.06828	0.00377	0.900	389	59	420	21	426	23	-9.9	426	23
PG035A-113	5433	0	0.06270	0.00180	0.55399	0.03221	0.06408	0.00324	0.870	698	60	448	21	400	20	44.0	400	20
PG035A-114	6029	1	0.05559	0.00181	0.50854	0.03031	0.06635	0.00331	0.837	436	71	417	20	414	20	5.2	414	20
PG035A-115	32069	1	0.05610	0.00076	0.56638	0.03075	0.07322	0.00385	0.968	456	30	456	20	456	23	0.2	456	23
PG035A-116	16699	0	0.05846	0.00136	0.56448	0.03380	0.07003	0.00386	0.921	547	50	454	22	436	23	20.9	436	23
PG035A-117	28275	0	0.05588	0.00085	0.53009	0.02541	0.06881	0.00313	0.948	447	34	432	17	429	19	4.3	429	19
PG035A-118	6284	0	0.05413	0.00152	0.53755	0.03188	0.07202	0.00376	0.880	377	62	437	21	448	23	-19.7	448	23
PG035A-119	9595	0	0.05459	0.00134	0.52695	0.03486	0.07001	0.00430	0.929	396	54	430	23	436	26	-10.6	436	26
PG035A-120	13777	0	0.05513	0.00103	0.51542	0.03315	0.06781	0.00418	0.957	417	41	422	22	423	25	-1.4	423	25
PG035A-121	11526	0	0.05436	0.00124	0.54667	0.02997	0.07293	0.00364	0.910	386	50	443	19	454	22	-18.1	454	22
PG035A-122	7986	0	0.05288	0.00149	0.49888	0.02680	0.06843	0.00313	0.852	324	63	411	18	427	19	-32.9	427	19
PG035A-123	50995	0	0.05556	0.00084	0.56141	0.02750	0.07328	0.00341	0.951	435	33	452	18	456	20	-5.0	456	20
PG035A-124	1828	0	0.04656	0.00465	0.43988	0.04986	0.06851	0.00366	0.471	27	224	370	35	427	22	-1537.4	427	22
PG035A-125	2676	0	0.05431	0.00450	0.48276	0.05085	0.06447	0.00419	0.617	384	176	400	34	403	25	-5.1	403	25
PG035A-126	5606	0	0.05309	0.00204	0.48722	0.03340	0.06656	0.00378	0.829	333	85	403	23	415	23	-25.7	415	23
PG035A-127	5118	0	0.05830	0.00305	0.56420	0.04014	0.07019	0.00339	0.678	541	110	454	26	437	20	19.8	437	20
PG035A-128	9345	0	0.05431	0.00150	0.53753	0.03219	0.07178	0.00382	0.888	384	61	437	21	447	23	-16.9	447	23
PG035A-129	8478	0	0.05326	0.00192	0.51817	0.03033	0.07057	0.00325	0.787	340	80	424	20	440	20	-30.4	440	20
PG035A-130	14902	0	0.06333	0.00176	0.63638	0.03549	0.07289	0.00352	0.867	719	58	500	22	454	21	38.2	454	21
PG035A-131	3647	0	0.05255	0.00431	0.47504	0.05108	0.06556	0.00456	0.646	309	177	395	35	409	28	-33.4	409	28
PG035A-132	4032	0	0.05283	0.00310	0.49113	0.03910	0.06742	0.00363	0.677	322	128	406	26	421	22	-31.8	421	22
PG035A-133	5308	0	0.05844	0.00232	0.53207	0.03963	0.06603	0.00416	0.846	546	85	433	26	412	25	25.3	412	25
PG035A-134	16101	0	0.05376	0.00117	0.50714	0.03172	0.06842	0.00401	0.938	361	48	417	21	427	24	-18.8	427	24
PG035A-135	46382	0	0.05780	0.00088	0.55357	0.02894	0.06946	0.00347	0.957	522	33	447	19	433	21	17.7	433	21
PG035A-136	23093	0	0.05565	0.00102	0.51222	0.02544	0.06675	0.00308	0.929	438	40	420	17	417	19	5.2	417	19
PG035A-137	36591	0	0.05653	0.00104	0.50672	0.02690	0.06501	0.00324	0.938	473	40	416	18	406	20	14.7	406	20
PG035A-138	11086	0	0.05339	0.00148	0.48370	0.02709	0.06571	0.00319	0.868	345	62	401	18	410	19	-19.3	410	19
PG035A-139	151263	0	0.05626	0.00075	0.51913	0.03338	0.06692	0.00421	0.978	463	29	425	22	418	25	10.1	418	25
PG035A-140	21492	0	0.05683	0.00130	0.53740	0.02902	0.06858	0.00336	0.906	485	50	437	19	428	20	12.2	428	20

Concordia diagrams for PG035A, Waweig Fm.

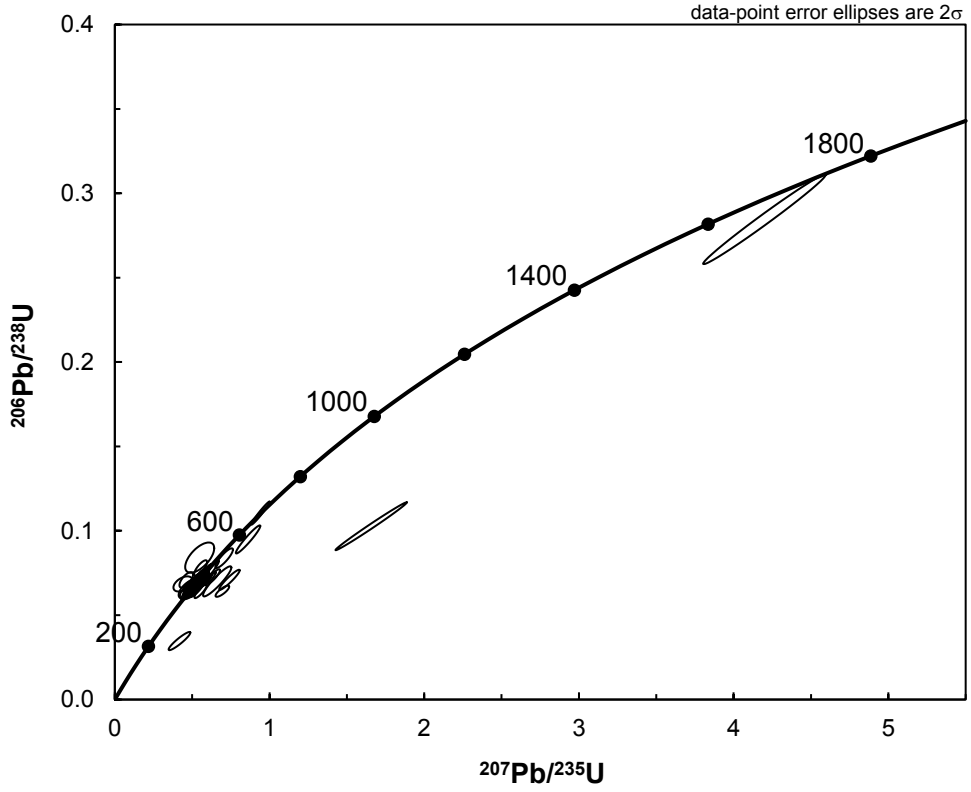

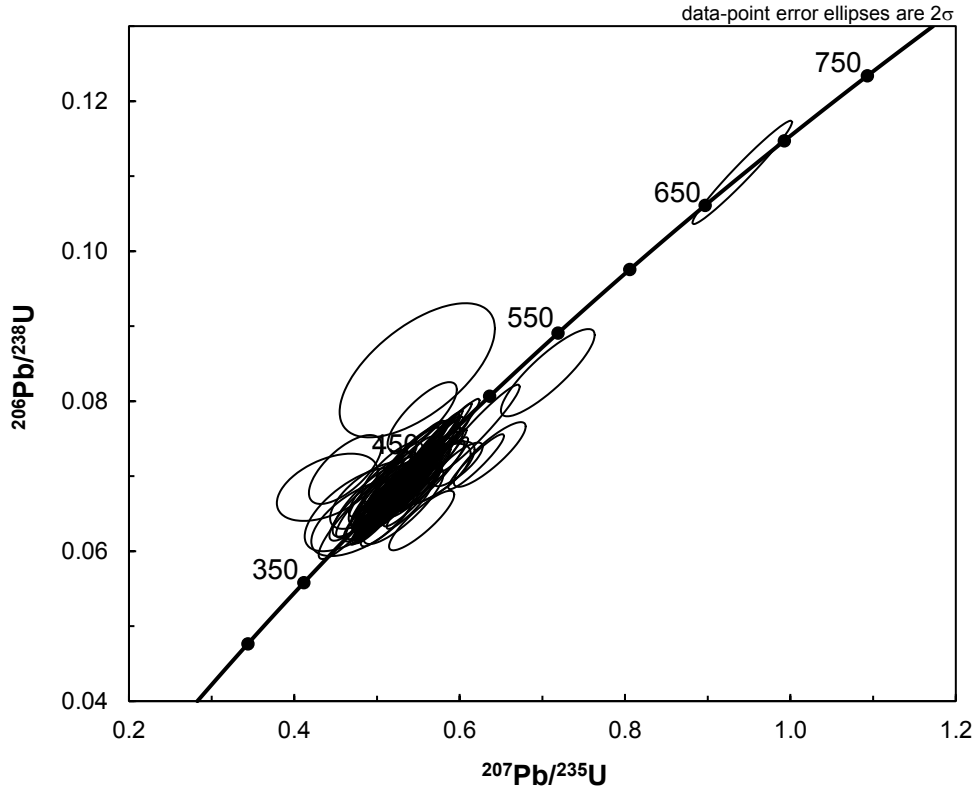

Histogram and kernel density plot for PG035A, Waweig Fm. Bandwidth and bin width is equal to median 2 σ , 19.9 Ma.

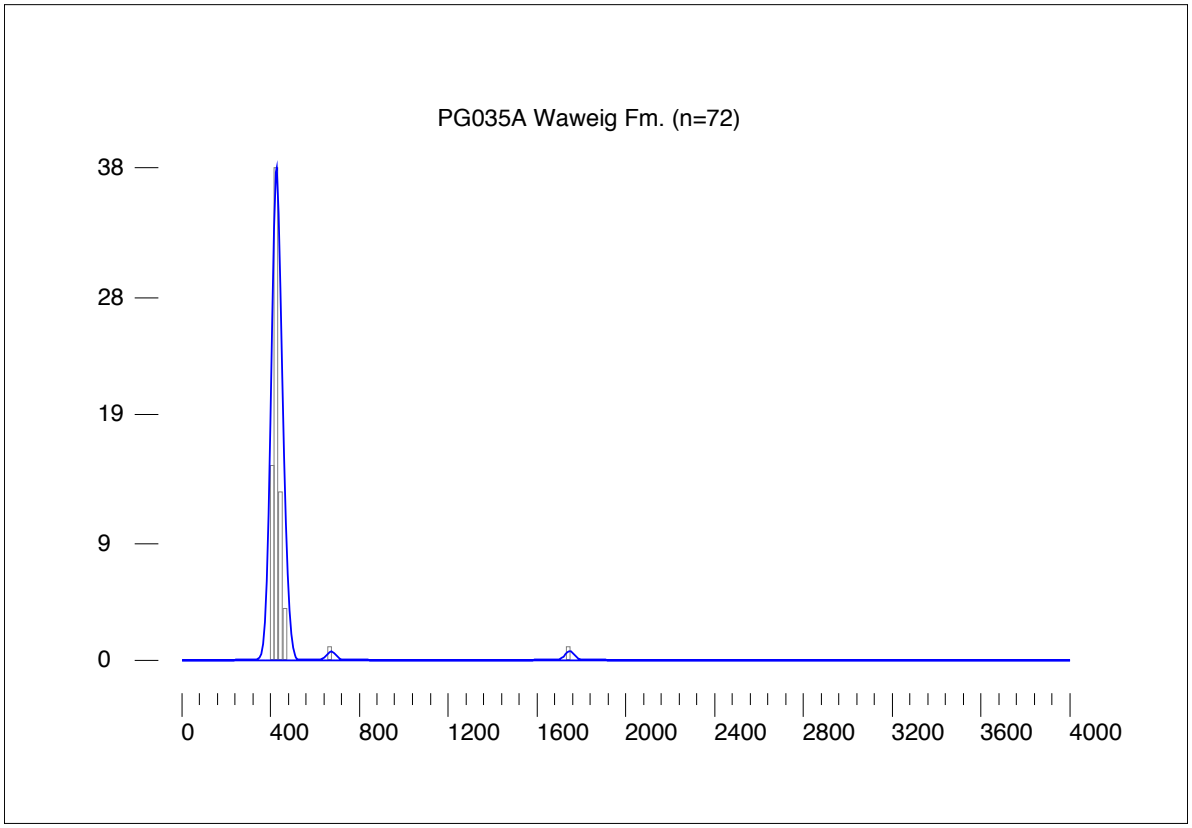

Eastport Fm. (PG036A)

sample name	^{206}Pb (cps)	^{204}Pb (cps)	^{207}Pb/^{206}Pb	2 σ	^{207}Pb/^{235}U	2 σ	^{206}Pb/^{238}U	2 σ	ρ	age (Ma) ^{207}Pb/^{206}Pb	error (Ma) 2 σ	age (Ma) ^{207}Pb/^{235}U	error (Ma) 2 σ	age (Ma) ^{206}Pb/^{238}U	error (Ma) 2 σ	discordance[1] %	reported age[2] (Ma)	2 σ
PG036A-001	314985	27	0.08652	0.00094	2.65195	0.15673	0.22231	0.01291	0.983	1350	21	1315	43	1294	68	4.6	1350	21
PG036A-002	290255	22	0.08040	0.00083	2.20180	0.12857	0.19862	0.01141	0.984	1207	20	1182	40	1168	61	3.5	1207	20
PG036A-003	122211	23	0.05603	0.00065	0.53080	0.02070	0.06871	0.00256	0.954	454	26	432	14	428	15	5.7	428	15
PG036A-004	99879	20	0.05653	0.00070	0.53402	0.02021	0.06851	0.00245	0.944	473	27	434	13	427	15	10.1	427	15
PG036A-005	216511	9	0.05944	0.00067	0.67747	0.03665	0.08266	0.00437	0.978	583	24	525	22	512	26	12.7	512	26
PG036A-006	140706	8	0.05991	0.00070	0.63954	0.02443	0.07742	0.00281	0.952	600	25	502	15	481	17	20.7	481	17
PG036A-007	88763	8	0.05781	0.00074	0.64687	0.02720	0.08115	0.00325	0.953	523	28	507	17	503	19	3.9	503	19
PG036A-008	153680	1	0.06172	0.00069	0.82514	0.03030	0.09696	0.00339	0.953	664	24	611	17	597	20	10.7	597	20
PG036A-009	138380	2	0.08132	0.00097	2.22258	0.13463	0.19822	0.01177	0.980	1229	23	1188	42	1166	63	5.6	1229	23
PG036A-010	205773	0	0.05607	0.00061	0.52910	0.01924	0.06844	0.00238	0.955	455	24	431	13	427	14	6.4	427	14
PG036A-011	178254	0	0.06402	0.00076	0.92148	0.04963	0.10440	0.00549	0.976	742	25	663	26	640	32	14.4	640	32
PG036A-012	28136	0	0.05857	0.00113	0.65211	0.03311	0.08075	0.00379	0.925	551	42	510	20	501	23	9.5	501	23
PG036A-013	56374	0	0.05642	0.00082	0.51979	0.02002	0.06681	0.00239	0.927	469	32	425	13	417	14	11.5	417	14
PG036A-014	146214	0	0.05897	0.00072	0.61873	0.02978	0.07609	0.00354	0.967	566	26	489	19	473	21	17.1	473	21
PG036A-015	124217	0	0.05757	0.00067	0.59333	0.02549	0.07474	0.00309	0.962	514	25	473	16	465	19	9.9	465	19
PG036A-016	314805	0	0.05535	0.00062	0.52138	0.02017	0.06832	0.00253	0.957	426	25	426	13	426	15	0.1	426	15
PG036A-017	482710	0	0.09406	0.00113	3.02436	0.18157	0.23320	0.01372	0.980	1509	23	1414	45	1351	71	11.6	1509	23
PG036A-018	383566	0	0.06065	0.00063	0.82465	0.03389	0.09861	0.00392	0.968	627	22	611	19	606	23	3.5	606	23
PG036A-019	97343	0	0.05559	0.00073	0.50724	0.01814	0.06618	0.00220	0.931	436	29	417	12	413	13	5.4	413	13
PG036A-020	235298	0	0.07283	0.00085	1.76730	0.09763	0.17601	0.00951	0.978	1009	23	1034	35	1045	52	-3.9	1009	23
PG036A-021	240725	0	0.05929	0.00069	0.61671	0.02308	0.07544	0.00268	0.950	578	25	488	14	469	16	19.5	469	16
PG036A-022	98248	0	0.06129	0.00084	0.81887	0.03352	0.09690	0.00374	0.942	649	29	607	19	596	22	8.6	596	22
PG036A-023	45120	0	0.05782	0.00080	0.59118	0.02979	0.07415	0.00359	0.962	523	30	472	19	461	22	12.3	461	22
PG036A-024A	207570	0	0.05557	0.00062	0.52297	0.01961	0.06825	0.00244	0.954	435	25	427	13	426	15	2.3	426	15
PG036A-024B-20micron	101385	0	0.05683	0.00105	0.50983	0.02186	0.06507	0.00252	0.902	485	40	418	15	406	15	16.7	406	15
PG036A-025	89572	0	0.05596	0.00067	0.49944	0.02201	0.06473	0.00274	0.962	451	27	411	15	404	17	10.6	404	17
PG036A-026	458922	0	0.05642	0.00059	0.48846	0.01786	0.06279	0.00220	0.958	469	23	404	12	393	13	16.8	393	13
PG036A-027	143425	0	0.06047	0.00066	0.79508	0.03255	0.09536	0.00376	0.963	620	23	594	18	587	22	5.6	587	22
PG036A-028	34661	0	0.05739	0.00090	0.59156	0.02590	0.07476	0.00306	0.934	506	34	472	16	465	18	8.5	465	18
PG036A-029	79062	0	0.05536	0.00072	0.50593	0.02110	0.06628	0.00263	0.950	427	29	416	14	414	16	3.1	414	16
PG036A-030	58470	0	0.06348	0.00095	0.90730	0.03841	0.10366	0.00410	0.935	724	32	656	20	636	24	12.8	636	24
PG036A-031	1569215	153	0.05558	0.00065	0.50731	0.02211	0.06620	0.00278	0.963	436	26	417	15	413	17	5.3	413	17
PG036A-032	194014	40	0.09416	0.00099	3.23269	0.18946	0.24900	0.01436	0.984	1511	20	1465	44	1433	74	5.8	1511	20
PG036A-033	92757	26	0.05661	0.00065	0.51037	0.02070	0.06538	0.00254	0.959	477	25	419	14	408	15	14.8	408	15
PG036A-034	177347	60	0.06116	0.00070	0.86033	0.03066	0.10202	0.00344	0.946	645	25	630	17	626	20	3.1	626	20
PG036A-035	116628	53	0.05757	0.00084	0.51062	0.02089	0.06432	0.00246	0.935	514	32	419	14	402	15	22.4	402	15
PG036A-036	*2063997*	*451*	*0.05466*	*0.00120*	*0.52737*	*0.04919*	*0.06998*	*0.00634*	*0.972*	*398*	*49*	*430*	*32*	*436*	*38*	*-9.8*	*423*	*13*
PG036A-037	107494	111	0.05591	0.00072	0.51200	0.02023	0.06641	0.00248	0.945	449	29	420	13	415	15	7.9	415	15
PG036A-038A	1327186	219	0.05586	0.00061	0.52072	0.01919	0.06761	0.00238	0.956	447	24	426	13	422	14	5.8	422	14
PG036A-038B	1430543	117	0.05524	0.00058	0.54431	0.02229	0.07146	0.00283	0.967	422	23	441	15	445	17	-5.6	445	17
PG036A-039	122414	106	0.05612	0.00067	0.51905	0.02014	0.06708	0.00247	0.951	457	26	425	13	419	15	8.7	419	15
PG036A-040	211123	102	0.07995	0.00085	2.26930	0.12670	0.20586	0.01128	0.982	1196	21	1203	39	1207	60	-1.0	1196	21
PG036A-041	400474	91	0.05601	0.00061	0.49181	0.01825	0.06369	0.00226	0.956	453	24	406	12	398	14	12.4	398	14
PG036A-042	133690	175	0.05931	0.00112	0.55943	0.02599	0.06841	0.00291	0.914	578	40	451	17	427	18	27.1	427	18
PG036A-043	261295	223	0.05850	0.00094	0.52427	0.01972	0.06500	0.00221	0.904	548	35	428	13	406	13	26.8	406	13
PG036A-044	310948	168	0.05716	0.00068	0.55077	0.02422	0.06988	0.00296	0.962	498	26	446	16	435	18	13.0	435	18
PG036A-045	825279	207	0.08783	0.00090	2.77502	0.15736	0.22915	0.01278	0.984	1379	20	1349	41	1330	67	3.9	1379	20
PG036A-046	*1043714*	*316*	*0.07267*	*0.00133*	*1.59559*	*0.11778*	*0.15924*	*0.01139*	*0.969*	*1005*	*37*	*968*	*45*	*953*	*63*	*5.6*	*1017*	*30*

Eastport Fm. (PG036A)

										age (Ma)	error (Ma)	age (Ma)	error (Ma)	age (Ma)	error (Ma)	discordance[1]	reported age[2]	
sample name	^{206}Pb (cps)	^{204}Pb (cps)	^{207}Pb/^{206}Pb	2 σ	^{207}Pb/^{235}U	2 σ	^{206}Pb/^{238}U	2 σ	ρ	^{207}Pb/^{206}Pb	2 σ	^{207}Pb/^{235}U	2 σ	^{206}Pb/^{238}U	2 σ	%	(Ma)	2 σ
PG036A-047	244868	110	0.06090	0.00068	0.81368	0.02877	0.09690	0.00325	0.949	636	24	605	16	596	19	6.5	596	19
PG036A-048	1416461	106	0.10029	0.00102	3.88072	0.22459	0.28064	0.01599	0.984	1630	19	1610	46	1595	80	2.4	1630	19
PG036A-049	456232	112	0.05813	0.00072	0.59271	0.02607	0.07394	0.00312	0.960	535	27	473	16	460	19	14.5	460	19
PG036A-050	819530	7725	0.19673	0.01964	1.84661	0.21636	0.06808	0.00417	0.523	2799	155	1062	74	425	25	87.5	2799	155
PG036A-051	190862	49	0.06255	0.00074	0.82069	0.03089	0.09516	0.00340	0.950	693	25	608	17	586	20	16.2	586	20
PG036A-052	293843	34	0.06017	0.00065	0.74165	0.03115	0.08939	0.00363	0.966	610	23	563	18	552	21	9.9	552	21
PG036A-053	112658	8	0.05601	0.00063	0.51018	0.01907	0.06607	0.00235	0.953	453	25	419	13	412	14	9.2	412	14
PG036A-054	137249	18	0.05610	0.00062	0.53045	0.01936	0.06857	0.00239	0.953	456	24	432	13	428	14	6.5	428	14
PG036A-055	41166	30	0.05819	0.00096	0.55440	0.02017	0.06910	0.00224	0.890	537	36	448	13	431	13	20.4	431	13
PG036A-056	322376	51	0.06120	0.00065	0.81349	0.03478	0.09641	0.00399	0.969	646	23	604	19	593	23	8.6	593	23
PG036A-057	93254	47	0.05699	0.00071	0.53931	0.02168	0.06863	0.00262	0.950	491	27	438	14	428	16	13.3	428	16
PG036A-058	469973	30	0.05679	0.00061	0.55484	0.02796	0.07085	0.00349	0.977	484	24	448	18	441	21	9.0	441	21
PG036A-059	129411	36	0.07468	0.00084	1.62153	0.09562	0.15747	0.00912	0.982	1060	22	979	36	943	51	11.9	1060	22
PG036A-060	159915	33	0.07458	0.00083	1.70775	0.09593	0.16607	0.00915	0.980	1057	22	1011	35	990	50	6.8	1057	22
PG036A-061	155100	94	0.05845	0.00063	0.51606	0.01934	0.06404	0.00230	0.957	547	24	423	13	400	14	27.6	400	14
PG036A-062	244857	46	0.05957	0.00064	0.70046	0.02748	0.08529	0.00322	0.961	588	23	539	16	528	19	10.7	528	19
PG036A-063	73984	96	0.06326	0.00078	0.90896	0.04131	0.10421	0.00456	0.963	717	26	657	22	639	27	11.4	639	27
PG036A-064	68199	85	0.06023	0.00080	0.58891	0.02199	0.07091	0.00248	0.935	612	28	470	14	442	15	28.8	442	15
PG036A-065	380633	111	0.09364	0.00130	3.06770	0.17618	0.23759	0.01324	0.971	1501	26	1425	43	1374	69	9.4	1501	26
PG036A-066	51365	135	0.05886	0.00083	0.59003	0.02390	0.07270	0.00276	0.937	562	31	471	15	452	17	20.2	452	17
PG036A-067	112270	107	0.05837	0.00067	0.57120	0.02198	0.07098	0.00261	0.954	544	25	459	14	442	16	19.3	442	16
PG036A-068	69178	114	0.05877	0.00084	0.58122	0.02569	0.07173	0.00300	0.946	558	31	465	16	447	18	20.7	447	18
PG036A-069	111369	208	0.06671	0.00421	0.67284	0.05587	0.07315	0.00395	0.650	829	126	522	33	455	24	46.7	829	126
PG036A-070	598854	119	0.05586	0.00058	0.52313	0.02237	0.06792	0.00282	0.971	447	23	427	15	424	17	5.4	424	17
PG036A-071	100951	22	0.05695	0.00068	0.52114	0.02175	0.06637	0.00265	0.958	489	26	426	14	414	16	15.9	414	16
PG036A-072	82732	47	0.06139	0.00082	0.76602	0.02927	0.09050	0.00324	0.937	653	28	577	17	558	19	15.1	558	19
PG036A-074	72746	46	0.05993	0.00074	0.70348	0.02625	0.08514	0.00300	0.943	601	27	541	16	527	18	12.9	527	18
PG036A-075	608439	21	0.09574	0.00104	3.33635	0.17905	0.25275	0.01328	0.979	1543	20	1490	41	1453	68	6.5	1543	20
PG036A-076	384263	130	0.05805	0.00065	0.55133	0.02246	0.06888	0.00270	0.962	532	24	446	15	429	16	19.9	429	16
PG036A-077	339110	38	0.05726	0.00070	0.65447	0.02712	0.08289	0.00328	0.955	502	27	511	17	513	20	-2.4	513	20
PG036A-078	89543	20	0.05780	0.00067	0.59257	0.02207	0.07436	0.00263	0.950	522	25	473	14	462	16	11.9	462	16
PG036A-079	147064	29	0.05628	0.00064	0.50953	0.01800	0.06566	0.00220	0.947	463	25	418	12	410	13	11.9	410	13
PG036A-080	569339	303	0.06229	0.00111	0.53967	0.02247	0.06283	0.00236	0.904	684	38	438	15	393	14	43.9	393	14
PG036A-081	118449	7	0.06235	0.00072	0.80640	0.03369	0.09381	0.00377	0.961	686	24	600	19	578	22	16.5	578	22
PG036A-082	185334	44	0.05982	0.00099	0.57467	0.02874	0.06967	0.00329	0.943	597	36	461	18	434	20	28.2	434	20
PG036A-083	1291821	16	0.09366	0.00097	3.10429	0.17405	0.24039	0.01325	0.983	1501	19	1434	42	1389	68	8.3	1501	19
PG036A-084	261292	4	0.05652	0.00059	0.57273	0.02380	0.07349	0.00296	0.968	473	23	460	15	457	18	3.4	457	18
PG036A-085	410261	14	0.05573	0.00063	0.52655	0.01862	0.06852	0.00229	0.947	442	25	430	12	427	14	3.4	427	14
PG036A-086	1003375	117	0.10514	0.00108	4.20333	0.22428	0.28996	0.01518	0.981	1717	19	1675	43	1641	75	5.0	1717	19
PG036A-087	271127	36	0.05592	0.00064	0.51448	0.02383	0.06672	0.00299	0.969	449	25	421	16	416	18	7.6	416	18
PG036A-088	37867	33	0.06974	0.00112	0.94192	0.05691	0.09796	0.00570	0.964	921	33	674	29	602	33	36.2	921	33
PG036A-089	151921	8	0.07850	0.00093	2.04959	0.10686	0.18936	0.00961	0.974	1160	23	1132	35	1118	52	3.9	1160	23
PG036A-090	100041	4955	0.78323	0.00879	61.32434	5.06782	0.56786	0.04649	0.991	4892	16	4196	79	2899	188	50.0	4892	16
PG036A-091	252172	63	0.05744	0.00061	0.57937	0.02468	0.07315	0.00302	0.969	508	23	464	16	455	18	10.9	455	18
PG036A-092	142446	81	0.05921	0.00072	0.63996	0.02327	0.07839	0.00269	0.942	575	26	502	14	487	16	15.9	487	16
PG036A-093	470857	64	0.09672	0.00106	3.55089	0.18937	0.26626	0.01390	0.979	1562	20	1539	41	1522	70	2.9	1562	20
PG036A-094	293017	41	0.05608	0.00072	0.47172	0.01594	0.06101	0.00191	0.924	456	28	392	11	382	12	16.7	382	12
PG036A-095	198074	73	0.05839	0.00070	0.50003	0.01880	0.06211	0.00221	0.948	545	26	412	13	388	13	29.5	388	13

Eastport Fm. (PG036A)

sample name	^{206}Pb (cps)	^{204}Pb (cps)	$^{207}Pb/^{206}Pb$	2 σ	$^{207}Pb/^{235}U$	2 σ	$^{206}Pb/^{238}U$	2 σ	ρ	age (Ma) $^{207}Pb/^{206}Pb$	error (Ma) 2 σ	age (Ma) $^{207}Pb/^{235}U$	error (Ma) 2 σ	age (Ma) $^{206}Pb/^{238}U$	error (Ma) 2 σ	discordance[1] %	reported age[2] (Ma)	2 σ
PG036A-096	409474	83	0.06250	0.00069	0.93103	0.03908	0.10804	0.00438	0.965	691	23	668	20	661	25	4.5	661	25
PG036A-097	71345	92	0.05930	0.00095	0.61689	0.02563	0.07544	0.00289	0.923	578	34	488	16	469	17	19.6	469	17
PG036A-098	265729	130	0.09356	0.00112	2.86552	0.17045	0.22213	0.01295	0.980	1499	22	1373	44	1293	68	15.2	1499	22
PG036A-099	293147	339	0.07070	0.00202	0.67427	0.04189	0.06916	0.00382	0.888	949	57	523	25	431	23	56.4	949	57
PG036A-100	69937	64	0.06225	0.00120	0.78614	0.04642	0.09159	0.00511	0.946	683	41	589	26	565	30	18.0	565	30
PG036A-101	52098	9	0.05884	0.00078	0.64753	0.02464	0.07982	0.00285	0.938	561	28	507	15	495	17	12.2	495	17
PG036A-102	420293	9	0.09826	0.00103	3.55895	0.20326	0.26269	0.01475	0.983	1591	19	1540	44	1504	75	6.2	1591	19
PG036A-103	361387	4	0.08601	0.00089	2.60237	0.15262	0.21945	0.01267	0.984	1338	20	1301	42	1279	67	4.9	1338	20
PG036A-104	69002	0	0.05763	0.00068	0.57072	0.02480	0.07183	0.00301	0.963	516	26	458	16	447	18	13.8	447	18
PG036A-105	129137	17	0.06155	0.00084	0.83841	0.04122	0.09880	0.00467	0.961	658	29	618	23	607	27	8.1	607	27
PG036A-106	375991	1	0.10043	0.00108	3.72274	0.21155	0.26885	0.01500	0.982	1632	20	1576	44	1535	76	6.7	1632	20
PG036A-107	89941	132	0.06119	0.00129	0.66627	0.02771	0.07897	0.00283	0.862	646	45	518	17	490	17	25.1	490	17
PG036A-108	310973	187	0.05849	0.00076	0.60313	0.02413	0.07479	0.00283	0.947	548	28	479	15	465	17	15.7	465	17
PG036A-109	297801	132	0.05720	0.00061	0.72981	0.03795	0.09254	0.00471	0.979	499	23	556	22	571	28	-14.9	571	28
PG036A-110	219759	176	0.06061	0.00075	0.77267	0.03218	0.09246	0.00368	0.955	625	26	581	18	570	22	9.2	570	22
PG036A-111	296773	252	0.05834	0.00063	0.61130	0.02878	0.07599	0.00348	0.974	543	23	484	18	472	21	13.5	472	21
PG036A-112	263856	262	0.10451	0.00116	4.25272	0.32682	0.29513	0.02244	0.989	1706	20	1684	61	1667	111	2.6	1706	20
PG036A-113	155913	251	0.05940	0.00087	0.64251	0.03229	0.07845	0.00377	0.957	582	31	504	20	487	23	16.9	487	23
PG036A-114	772386	260	0.06691	0.00069	1.29373	0.10135	0.14024	0.01089	0.991	835	21	843	44	846	61	-1.4	835	21
PG036A-115	260800	291	0.07467	0.00083	1.86027	0.14580	0.18069	0.01402	0.990	1060	22	1067	50	1071	76	-1.1	1060	22
PG036A-116	90673	250	0.05612	0.00065	0.57213	0.03195	0.07394	0.00404	0.978	457	26	459	20	460	24	-0.6	460	24
PG036A-117	308033	273	0.09308	0.00098	3.29502	0.25834	0.25674	0.01995	0.991	1490	20	1480	59	1473	102	1.2	1490	20
PG036A-118	125310	48	0.05807	0.00079	0.55120	0.02193	0.06884	0.00258	0.940	532	29	446	14	429	16	20.0	429	16
PG036A-119	71792	69	0.06593	0.00111	0.89976	0.07008	0.09898	0.00753	0.977	804	35	652	37	608	44	25.5	804	35
PG036A-120	201672	44	0.06047	0.00066	0.82324	0.02988	0.09874	0.00342	0.954	620	23	610	17	607	20	2.3	607	20
PG036A-121	787879	25	0.05582	0.00058	0.61325	0.02599	0.07968	0.00327	0.970	445	23	486	16	494	20	-11.5	494	20
PG036A-122	577374	64	0.18163	0.00183	12.81054	1.03391	0.51155	0.04096	0.992	2668	17	2666	73	2663	172	0.2	2668	17
PG036A-123	458808	53	0.08093	0.00084	2.35704	0.18758	0.21124	0.01667	0.992	1220	20	1230	55	1235	88	-1.4	1220	20
PG036A-124	291147	14	0.07405	0.00079	1.80119	0.13905	0.17641	0.01349	0.990	1043	21	1046	49	1047	73	-0.5	1043	21
PG036A-125	104508	27	0.05786	0.00067	0.61389	0.02436	0.07695	0.00292	0.956	525	25	486	15	478	17	9.2	478	17
PG036A-126	270217	14	0.08730	0.00092	2.85754	0.24068	0.23739	0.01984	0.992	1367	20	1371	61	1373	103	-0.5	1367	20
PG036A-127	443414	35	0.13889	0.00142	7.88744	0.62300	0.41186	0.03226	0.992	2213	18	2218	69	2223	146	-0.5	2213	18
PG036A-128	96024	35	0.05558	0.00062	0.54211	0.02155	0.07074	0.00270	0.960	436	25	440	14	441	16	-1.2	441	16
PG036A-129	245116	74	0.05684	0.00064	0.55905	0.02179	0.07134	0.00266	0.958	485	25	451	14	444	16	8.8	444	16
PG036A-130	187590	59	0.05619	0.00060	0.56950	0.02400	0.07350	0.00300	0.967	460	24	458	15	457	18	0.6	457	18
PG036A-131	285430	83	0.05730	0.00067	0.64150	0.02904	0.08120	0.00355	0.966	503	26	503	18	503	21	0.0	503	21
PG036A-132	62518	104	0.05658	0.00068	0.54230	0.02425	0.06951	0.00299	0.963	475	26	440	16	433	18	9.2	433	18
PG036A-133	71751	3603	0.75895	0.00859	45.19337	3.50716	0.43188	0.03316	0.989	4847	16	3892	74	2314	148	61.5	4847	16
PG036A-134	24965	154	0.08356	0.00284	0.98870	0.08230	0.08581	0.00652	0.913	1282	65	698	41	531	39	61.0	1282	65
PG036A-135	83134	153	0.05764	0.00081	0.55888	0.02197	0.07032	0.00258	0.933	516	31	451	14	438	16	15.7	438	16
PG036A-136	36068	154	0.06882	0.00199	1.00072	0.08233	0.10545	0.00812	0.936	893	59	704	41	646	47	29.1	893	59
PG036A-137	194678	149	0.05612	0.00062	0.54130	0.02012	0.06995	0.00248	0.955	457	24	439	13	436	15	4.8	436	15
PG036A-138	148863	146	0.05595	0.00061	0.53875	0.02130	0.06984	0.00266	0.962	450	24	438	14	435	16	3.4	435	16
PG036A-139	350882	220	0.05941	0.00066	0.63426	0.02774	0.07743	0.00328	0.967	582	24	499	17	481	20	18.1	481	20
PG036A-140	162736	234	0.06346	0.00104	0.60663	0.04843	0.06933	0.00542	0.979	724	34	481	30	432	33	41.6	432	33
PG036A-141	694665	110	0.07245	0.00117	0.96710	0.07427	0.09681	0.00727	0.978	999	32	687	38	596	43	42.2	999	32
PG036A-142	108257	10	0.06045	0.00068	0.79091	0.03065	0.09489	0.00352	0.957	620	24	592	17	584	21	6.0	584	21
PG036A-143	263603	31	0.06372	0.00072	0.92658	0.07757	0.10546	0.00875	0.991	732	24	666	40	646	51	12.3	646	51

Eastport Fm. (PG036A)

sample name	^{206}Pb (cps)	^{204}Pb (cps)	$^{207}Pb/^{206}Pb$	2 σ	$^{207}Pb/^{235}U$	2 σ	$^{206}Pb/^{238}U$	2 σ	ρ	age (Ma) $^{207}Pb/^{206}Pb$	error (Ma) 2 σ	age (Ma) $^{207}Pb/^{235}U$	error (Ma) 2 σ	age (Ma) $^{206}Pb/^{238}U$	error (Ma) 2 σ	discordance[1] %	reported age[2] (Ma)	2 σ
PG036A-144	98145	21	0.05725	0.00068	0.53864	0.02129	0.06824	0.00257	0.954	501	26	438	14	426	16	15.6	426	16
PG036A-145	1240993	166	0.05901	0.00061	0.62629	0.03058	0.07697	0.00367	0.977	567	22	494	19	478	22	16.4	478	22
PG036A-146	92564	3	0.05690	0.00072	0.54896	0.02096	0.06997	0.00252	0.943	488	28	444	14	436	15	11.0	436	15
PG036A-147	120381	4	0.05686	0.00064	0.54059	0.01965	0.06896	0.00238	0.950	486	25	439	13	430	14	11.9	430	14
PG036A-148	87661	3	0.06140	0.00077	0.78913	0.03291	0.09321	0.00371	0.954	653	27	591	19	575	22	12.6	575	22
PG036A-149	106251	0	0.07776	0.00085	1.82040	0.14109	0.16979	0.01303	0.990	1141	22	1053	50	1011	71	12.3	1141	22
PG036A-150	63893	1	0.10299	0.00126	3.90007	0.29915	0.27465	0.02080	0.987	1679	22	1614	60	1564	104	7.7	1679	22
PG036A-151	144405	7	0.06120	0.00079	0.54767	0.02269	0.06491	0.00255	0.950	646	28	443	15	405	15	38.4	405	15
PG036A-152	43175	42	0.05851	0.00087	0.56549	0.02480	0.07010	0.00289	0.940	549	32	455	16	437	17	21.1	437	17
PG036A-153	252538	18	0.05779	0.00063	0.64281	0.02646	0.08067	0.00320	0.964	522	24	504	16	500	19	4.3	500	19
PG036A-154	39729	33	0.07639	0.00120	1.57093	0.12464	0.14915	0.01160	0.980	1105	31	959	48	896	65	20.3	1105	31
PG036A-155	90263	25	0.06125	0.00104	0.65990	0.02684	0.07814	0.00289	0.910	648	36	515	16	485	17	26.1	485	17
PG036A-156	43486	29	0.06260	0.00079	0.76307	0.02970	0.08840	0.00326	0.947	695	27	576	17	546	19	22.3	546	19
PG036A-157	76637	11	0.05800	0.00085	0.54115	0.02039	0.06767	0.00235	0.922	530	32	439	13	422	14	21.0	422	14
PG036A-158	93569	25	0.06199	0.00070	0.88975	0.03334	0.10410	0.00372	0.954	674	24	646	18	638	22	5.5	638	22
PG036A-159	44092	27	0.05934	0.00144	0.51181	0.02597	0.06256	0.00279	0.878	580	52	420	17	391	17	33.5	391	17
PG036A-160	714539	1650	0.09058	0.00461	0.86675	0.07849	0.06940	0.00520	0.827	1438	94	634	42	433	31	72.2	1438	94
PG036A-161	68614	6	0.06677	0.00086	1.03395	0.05984	0.11231	0.00634	0.975	831	27	721	29	686	37	18.3	831	27
PG036A-162	436785	6	0.05610	0.00060	0.61928	0.02525	0.08005	0.00315	0.965	457	23	489	16	496	19	-9.1	496	19
PG036A-163	54483	9	0.06026	0.00069	0.66105	0.02533	0.07956	0.00291	0.954	613	25	515	15	493	17	20.2	493	17
PG036A-164	93582	33	0.05976	0.00069	0.64257	0.02600	0.07799	0.00302	0.958	595	25	504	16	484	18	19.3	484	18
PG036A-165	99422	12	0.05949	0.00075	0.63936	0.03158	0.07794	0.00372	0.967	585	27	502	19	484	22	18.0	484	22
PG036A-166	188012	11	0.05795	0.00067	0.53776	0.01978	0.06730	0.00235	0.950	528	25	437	13	420	14	21.1	420	14
PG036A-167	530070	12	0.05513	0.00056	0.52907	0.02136	0.06960	0.00272	0.968	418	23	431	14	434	16	-4.0	434	16
PG036A-168	243448	5	0.06183	0.00067	0.91423	0.05087	0.10724	0.00585	0.981	668	23	659	27	657	34	1.8	657	34
PG036A-169	42704	1	0.08014	0.00105	1.81900	0.10767	0.16461	0.00950	0.975	1201	26	1052	38	982	52	19.6	1201	26
PG036A-170	351703	0	0.08663	0.00089	2.60283	0.15141	0.21792	0.01248	0.984	1352	20	1301	42	1271	66	6.6	1352	20
PG036A-171	195606	0	0.06157	0.00066	0.82182	0.03577	0.09680	0.00408	0.969	659	23	609	20	596	24	10.1	596	24
PG036A-172	108808	2	0.05739	0.00066	0.53177	0.02135	0.06720	0.00258	0.958	507	25	433	14	419	16	17.8	419	16
PG036A-173	224811	0	0.13412	0.00142	6.83867	0.42541	0.36981	0.02267	0.985	2153	18	2091	54	2029	106	6.7	2153	18
PG036A-174	178710	8	0.13437	0.00139	8.08481	0.46199	0.43638	0.02453	0.984	2156	18	2241	50	2334	109	-9.9	2156	18
PG036A-175	110242	4	0.05880	0.00066	0.62392	0.02400	0.07696	0.00283	0.957	560	24	492	15	478	17	15.1	478	17
PG036A-176	95480	6	0.06138	0.00075	0.58231	0.02349	0.06881	0.00264	0.953	652	26	466	15	429	16	35.4	429	16
PG036A-200	203700	261	0.08920	0.00210	1.88788	0.29850	0.15350	0.02400	0.989	1408	44	1077	100	921	133	37.1	1408	44
PG036A-201	20220	269	0.07710	0.00270	0.88978	0.14167	0.08370	0.01300	0.976	1124	68	646	73	518	77	56.0	1124	68
PG036A-202	22000	305	0.06220	0.00250	0.82674	0.03780	0.09640	0.00210	0.477	681	84	612	21	593	12	13.5	593	12
PG036A-203	80200	380	0.06110	0.00140	1.03537	0.03117	0.12290	0.00240	0.649	643	49	722	15	747	14	-17.2	747	14
PG036A-204	20300	296	0.06200	0.00350	0.56651	0.03386	0.06627	0.00130	0.328	674	116	456	22	414	8	39.9	414	8
PG036A-205	31530	398	0.06600	0.00330	0.66977	0.11422	0.07360	0.01200	0.956	806	101	521	67	458	72	44.8	806	101
PG036A-206	17890	809	0.13770	0.00470	4.40477	0.69984	0.23200	0.03600	0.977	2198	58	1713	124	1345	186	42.9	2198	58
PG036A-207	14500	362	0.07480	0.00350	0.70131	0.11810	0.06800	0.01100	0.961	1063	91	540	68	424	66	62.1	1063	91
PG036A-208	23100	360	0.06290	0.00240	0.60795	0.02660	0.07010	0.00150	0.489	705	79	482	17	437	9	39.3	437	9
PG036A-209	25420	316	0.05840	0.00300	0.61342	0.03375	0.07618	0.00150	0.358	545	108	486	21	473	9	13.6	473	9
PG036A-210	5930	329	0.06130	0.00500	0.65419	0.05572	0.07740	0.00190	0.288	650	166	511	34	481	11	27.0	481	11
PG036A-211	2800	306	0.06790	0.00720	0.74147	0.13712	0.07920	0.01200	0.819	866	206	563	77	491	71	44.9	866	206
PG036A-212	21260	299	0.05590	0.00210	0.51771	0.02154	0.06717	0.00120	0.429	448	81	424	14	419	7	6.8	419	7
PG036A-213	8290	341	0.06750	0.00440	0.73431	0.12151	0.07890	0.01200	0.919	853	130	559	69	490	71	44.2	853	130
PG036A-214	38100	443	0.08090	0.00260	0.77301	0.12519	0.06930	0.01100	0.980	1219	62	581	69	432	66	66.7	1219	62

Eastport Fm. (PG036A)

sample name	^{206}Pb (cps)	^{204}Pb (cps)	$^{207}Pb/^{206}Pb$	2 σ	$^{207}Pb/^{235}U$	2 σ	$^{206}Pb/^{238}U$	2 σ	ρ	age (Ma) $^{207}Pb/^{206}Pb$	error (Ma) 2 σ	age (Ma) $^{207}Pb/^{235}U$	error (Ma) 2 σ	age (Ma) $^{206}Pb/^{238}U$	error (Ma) 2 σ	discordance[1] %	reported age[2] (Ma)	2 σ
PG036A-215	43040	310	0.06380	0.00180	0.87967	0.03316	0.10000	0.00250	0.663	735	59	641	18	614	15	17.2	614	15
PG036A-216	16270	348	0.05580	0.00300	0.51509	0.02971	0.06695	0.00140	0.362	444	115	422	20	418	8	6.2	418	8
PG036A-217	26680	419	0.05920	0.00180	0.55064	0.01982	0.06746	0.00130	0.535	574	65	445	13	421	8	27.6	421	8
PG036A-218	149300	911	0.10530	0.00570	1.10052	0.18413	0.07580	0.01200	0.946	1720	96	754	85	471	72	75.2	1720	96
PG036A-219	17710	450	0.06330	0.00270	0.85271	0.04034	0.09770	0.00200	0.433	718	88	626	22	601	12	17.1	601	12
PG036A-220	116800	466	0.06210	0.00140	0.57693	0.01712	0.06738	0.00130	0.650	678	47	462	11	420	8	39.2	420	8
PG036A-221	33960	361	0.05560	0.00170	0.53126	0.01990	0.06930	0.00150	0.578	436	67	433	13	432	9	1.1	432	9
PG036A-222	187000	528	0.05750	0.00150	0.53673	0.01889	0.06770	0.00160	0.671	511	56	436	12	422	10	17.9	422	10
PG036A-223	13320	351	0.06230	0.00370	0.76107	0.04867	0.08860	0.00210	0.371	684	122	575	28	547	12	20.9	547	12
PG036A-224	23200	336	0.07000	0.00280	1.00570	0.15958	0.10420	0.01600	0.968	928	80	707	78	639	93	32.7	928	80
PG036A-225	31940	373	0.06290	0.00190	0.60448	0.02242	0.06970	0.00150	0.580	705	63	480	14	434	9	39.7	434	9
PG036A-226	8140	409	0.07650	0.00440	0.84488	0.14548	0.08010	0.01300	0.943	1108	111	622	77	497	77	57.3	1108	111
PG036A-227	14560	318	0.05990	0.00290	0.57896	0.03135	0.07010	0.00170	0.448	600	102	464	20	437	10	28.1	437	10
PG036A-228	46200	314	0.06030	0.00210	0.53876	0.02739	0.06480	0.00240	0.729	614	73	438	18	405	15	35.2	405	15
PG036A-229	40420	336	0.06140	0.00170	0.56552	0.02070	0.06680	0.00160	0.654	653	58	455	13	417	10	37.4	417	10
PG036A-230	24700	269	0.05570	0.00190	0.53137	0.02107	0.06919	0.00140	0.510	440	74	433	14	431	8	2.1	431	8
PG036A-231	24770	251	0.06190	0.00210	0.93370	0.03640	0.10940	0.00210	0.492	671	71	670	19	669	12	0.2	669	12
PG036A-232	28540	281	0.06210	0.00210	0.85367	0.03272	0.09970	0.00180	0.471	678	71	627	18	613	11	10.0	613	11
PG036A-233	39940	351	0.07880	0.00220	1.76881	0.27608	0.16280	0.02500	0.984	1167	54	1034	97	972	137	18.0	1167	54
PG036A-234	282800	293	0.10244	0.00071	3.82348	0.59382	0.27070	0.04200	0.999	1669	13	1598	118	1544	210	8.4	1669	13
PG036A-235	53400	327	0.06150	0.00150	0.82591	0.02579	0.09740	0.00190	0.625	657	51	611	14	599	11	9.2	599	11
PG036A-236	15610	236	0.07510	0.00280	1.70129	0.27660	0.16430	0.02600	0.973	1071	73	1009	99	981	142	9.1	1071	73
PG036A-237	7440	262	0.06240	0.00290	0.65388	0.03336	0.07600	0.00160	0.413	688	96	511	20	472	10	32.5	472	10
PG036A-238	172900	761	0.09600	0.00230	1.01034	0.16067	0.07633	0.01200	0.989	1548	44	709	78	474	71	71.9	1548	44
PG036A-239	22250	275	0.05870	0.00250	0.74218	0.03551	0.09170	0.00200	0.456	556	90	564	20	566	12	-1.8	566	12
PG036A-240	43300	229	0.08070	0.00140	2.30995	0.35831	0.20760	0.03200	0.994	1214	34	1215	104	1216	169	-0.2	1214	34
PG036A-241	20430	295	0.06050	0.00250	0.64248	0.02935	0.07702	0.00150	0.426	622	87	504	18	478	9	23.9	478	9
PG036A-242	67800	255	0.09740	0.00160	3.69849	0.58066	0.27540	0.04300	0.995	1575	30	1571	118	1568	214	0.5	1575	30
PG036A-243	45590	240	0.08720	0.00180	2.67034	0.42440	0.22210	0.03500	0.992	1365	39	1320	111	1293	182	5.8	1365	39
PG036A-244	39600	346	0.07960	0.00400	0.75905	0.12661	0.06916	0.01100	0.954	1187	96	573	71	431	66	65.8	1187	96
PG036A-245	20140	242	0.06340	0.00220	0.89400	0.03478	0.10227	0.00180	0.452	722	72	649	18	628	11	13.7	628	11
PG036A-246	24210	238	0.05960	0.00200	0.56094	0.02088	0.06826	0.00110	0.433	589	71	452	13	426	7	28.7	426	7
PG036A-247	59000	286	0.06750	0.00180	0.93441	0.15098	0.10040	0.01600	0.986	853	54	670	76	617	93	29.1	853	54
PG036A-248	10850	199	0.06550	0.00320	0.80287	0.13238	0.08890	0.01400	0.955	790	99	598	72	549	82	31.9	549	82
PG036A-249	52100	459	0.12610	0.00490	1.34747	0.21511	0.07750	0.01200	0.970	2044	67	866	89	481	71	79.2	2044	67
PG036A-250	38000	330	0.08170	0.00590	0.79935	0.13670	0.07096	0.01100	0.906	1238	135	596	74	442	66	66.5	1238	135
PG036A-251	10870	294	0.11960	0.00770	1.77602	0.30276	0.10770	0.01700	0.926	1950	111	1037	105	659	98	69.5	1950	111
PG036A-252	33300	198	0.05830	0.00210	0.62740	0.02525	0.07805	0.00140	0.446	541	77	494	16	484	8	10.9	484	8
PG036A-253	48000	193	0.09900	0.00180	3.65960	0.57715	0.26810	0.04200	0.993	1605	34	1563	119	1531	210	5.2	1605	34
PG036A-254	13030	183	0.06030	0.00330	0.65898	0.03816	0.07926	0.00150	0.327	614	114	514	23	492	9	20.7	492	9
PG036A-255	15520	274	0.07470	0.00340	0.93521	0.15035	0.09080	0.01400	0.959	1060	89	670	76	560	82	49.2	1060	89
PG036A-256	10120	242	0.06620	0.00440	0.77950	0.12948	0.08540	0.01300	0.916	813	133	585	71	528	77	36.4	813	133
PG036A-257	16570	214	0.06380	0.00320	0.60363	0.03269	0.06862	0.00140	0.377	735	103	480	20	428	8	43.2	428	8
PG036A-258	44280	208	0.06170	0.00190	0.86348	0.03203	0.10150	0.00210	0.558	664	65	632	17	623	12	6.4	623	12
PG036A-259	125900	229	0.09500	0.00110	3.48030	0.53855	0.26570	0.04100	0.997	1528	22	1523	115	1519	206	0.7	1528	22
PG036A-260	43710	205	0.05690	0.00170	0.53662	0.01989	0.06840	0.00150	0.592	488	65	436	13	427	9	13.0	427	9
PG036A-261	36390	280	0.07290	0.00190	1.65849	0.26489	0.16500	0.02600	0.987	1011	52	993	96	985	142	2.8	1011	52
PG036A-262	13180	331	0.08130	0.00400	1.01559	0.16470	0.09060	0.01400	0.953	1229	94	712	80	559	82	56.9	1229	94

Eastport Fm. (PG036A)

										age (Ma)	error (Ma)	age (Ma)	error (Ma)	age (Ma)	error (Ma)	discordance[1]	reported age[2]	
sample name	^{206}Pb (cps)	^{204}Pb (cps)	^{207}Pb/^{206}Pb	2 σ	^{207}Pb/^{235}U	2 σ	^{206}Pb/^{238}U	2 σ	ρ	^{207}Pb/^{206}Pb	2 σ	^{207}Pb/^{235}U	2 σ	^{206}Pb/^{238}U	2 σ	%	(Ma)	2 σ
PG036A-263	21400	327	0.09000	0.00250	0.84358	0.13850	0.06798	0.01100	0.986	1426	52	621	74	424	66	72.5	1426	52
PG036A-264	76600	333	0.07310	0.00200	0.67933	0.11242	0.06740	0.01100	0.986	1017	54	526	66	420	66	60.5	1017	54
PG036A-265	63900	259	0.10230	0.00260	3.27944	0.52850	0.23250	0.03700	0.987	1666	46	1476	118	1348	191	21.2	1666	46
PG036A-266	133600	372	0.07160	0.00130	0.83351	0.12923	0.08443	0.01300	0.993	975	37	616	69	523	77	48.3	975	37
PG036A-267	3480	238	0.09000	0.01100	1.21982	0.24829	0.09830	0.01600	0.800	1426	217	810	108	604	93	60.3	1426	217
PG036A-268	12310	154	0.06050	0.00300	0.57975	0.03206	0.06950	0.00170	0.442	622	104	464	20	433	10	31.3	433	10
PG036A-269	24700	204	0.06230	0.00220	0.64768	0.02625	0.07540	0.00150	0.491	684	74	507	16	469	9	32.7	469	9
PG036A-270	31020	174	0.06160	0.00190	0.85104	0.03272	0.10020	0.00230	0.597	660	65	625	18	616	13	7.1	616	13
PG036A-271	11960	169	0.05830	0.00290	0.61815	0.03365	0.07690	0.00170	0.406	541	105	489	21	478	10	12.2	478	10
PG036A-272	14620	153	0.07470	0.00260	1.69429	0.27421	0.16450	0.02600	0.977	1060	68	1006	98	982	142	8.0	1060	68
PG036A-273	12870	165	0.06640	0.00280	0.71136	0.11388	0.07770	0.01200	0.965	819	86	546	65	482	71	42.6	819	86
PG036A-274	21050	157	0.06050	0.00190	0.56090	0.02069	0.06724	0.00130	0.524	622	66	452	13	420	8	33.6	420	8
PG036A-275	21490	137	0.05740	0.00220	0.53572	0.02333	0.06769	0.00140	0.475	507	82	436	15	422	8	17.3	422	8
PG036A-276	11000	186	0.06920	0.00520	0.63354	0.10663	0.06640	0.01000	0.895	905	148	498	64	414	60	55.9	905	148
PG036A-277	23650	176	0.05920	0.00160	0.55897	0.01894	0.06848	0.00140	0.603	574	58	451	12	427	8	26.5	427	8
PG036A-278	12080	183	0.07870	0.00350	1.10031	0.18038	0.10140	0.01600	0.963	1165	86	753	84	623	93	48.8	1165	86
PG036A-279	15490	163	0.09080	0.00350	2.97964	0.47725	0.23800	0.03700	0.971	1442	72	1402	115	1376	190	5.1	1442	72
PG036A-280	3430	188	0.07350	0.00740	0.79351	0.14550	0.07830	0.01200	0.836	1028	191	593	79	486	71	54.7	1028	191
PG036A-281	12790	180	0.07430	0.00590	0.76936	0.13728	0.07510	0.01200	0.896	1050	152	579	76	467	72	57.5	1050	152
PG036A-282	20620	182	0.05830	0.00260	0.54420	0.02710	0.06770	0.00150	0.445	541	95	441	18	422	9	22.7	422	9
PG036A-283	24480	172	0.06000	0.00200	0.55841	0.02333	0.06750	0.00170	0.603	604	71	450	15	421	10	31.2	421	10
PG036A-284	16400	155	0.06680	0.00260	0.68802	0.11372	0.07470	0.01200	0.972	832	79	532	66	464	72	45.7	832	79
PG036A-285	72500	193	0.08640	0.00170	2.65061	0.42020	0.22250	0.03500	0.992	1347	38	1315	111	1295	182	4.3	1347	38
PG036A-286	9200	170	0.06310	0.00480	0.68210	0.05530	0.07840	0.00220	0.346	712	154	528	33	487	13	32.8	487	13
PG036A-287	33800	218	0.06740	0.00200	1.03154	0.16092	0.11100	0.01700	0.982	850	60	720	77	679	98	21.3	850	60
PG036A-288	67900	318	0.06750	0.00150	0.66991	0.10345	0.07198	0.01100	0.990	853	46	521	61	448	66	49.1	853	46
PG036A-289	16990	172	0.06340	0.00280	0.77625	0.03931	0.08880	0.00220	0.489	722	91	583	22	548	13	25.0	548	13
PG036A-290	213500	223	0.06020	0.00180	0.59638	0.02043	0.07185	0.00120	0.488	611	63	475	13	447	7	27.7	447	7
PG036A-291	26000	168	0.06730	0.00230	1.02165	0.16157	0.11010	0.01700	0.976	847	70	715	78	673	98	21.6	847	70
PG036A-292	63100	168	0.05980	0.00140	0.56488	0.01755	0.06851	0.00140	0.658	596	50	455	11	427	8	29.3	427	8
PG036A-293	23700	215	0.06960	0.00260	0.68039	0.10858	0.07090	0.01100	0.972	917	75	527	64	442	66	53.6	917	75
PG036A-294	6020	190	0.08870	0.00870	0.94415	0.17353	0.07720	0.01200	0.846	1398	177	675	87	479	71	68.1	1398	177
PG036A-295	106200	148	0.05740	0.00130	0.56350	0.01913	0.07120	0.00180	0.745	507	49	454	12	443	11	13.0	443	11
PG036A-296	48470	164	0.06040	0.00210	0.62959	0.02563	0.07560	0.00160	0.520	618	73	496	16	470	10	24.9	470	10
PG036A-297	98100	152	0.07257	0.00095	1.64098	0.26104	0.16400	0.02600	0.997	1002	26	986	96	979	142	2.5	1002	26
PG036A-298	14500	185	0.07990	0.00300	0.74285	0.12435	0.06743	0.01100	0.975	1195	72	564	70	421	66	66.9	1195	72
PG036A-299	12130	171	0.07290	0.00400	0.66601	0.10695	0.06626	0.01000	0.940	1011	107	518	63	414	60	61.0	1011	107
PG036A-299B	9900	146	0.06530	0.00390	0.60684	0.10546	0.06740	0.01100	0.939	784	121	482	65	420	66	47.9	420	66
PG036A-300	37270	178	0.10140	0.00230	3.74272	0.59331	0.26770	0.04200	0.990	1650	41	1581	120	1529	210	8.2	1650	41
PG036A-301	23200	189	0.06540	0.00240	0.66097	0.10211	0.07330	0.01100	0.971	787	75	515	61	456	66	43.6	456	66
PG036A-302	10130	181	0.08330	0.00720	0.83499	0.14550	0.07270	0.01100	0.868	1276	160	616	77	452	66	66.8	1276	160
PG036A-303	17760	242	0.06350	0.00270	0.59353	0.02806	0.06779	0.00140	0.437	725	88	473	18	423	8	43.1	423	8
PG036A-304	71700	200	0.08020	0.00160	2.31222	0.36782	0.20910	0.03300	0.992	1202	39	1216	107	1224	174	-2.0	1202	39
PG036A-305	37570	317	0.07390	0.00330	0.77133	0.12703	0.07570	0.01200	0.963	1039	88	581	70	470	72	56.7	1039	88
PG036A-306	20430	219	0.06380	0.00430	0.83657	0.05906	0.09510	0.00200	0.298	735	137	617	32	586	12	21.3	586	12
PG036A-307	21740	269	0.07440	0.00390	1.03403	0.17285	0.10080	0.01600	0.950	1052	102	721	83	619	93	43.2	1052	102
PG036A-308	30000	220	0.06800	0.00280	1.05009	0.16515	0.11200	0.01700	0.965	869	83	729	79	684	98	22.3	869	83
PG036A-309	18070	211	0.06140	0.00290	0.56975	0.03013	0.06730	0.00160	0.450	653	98	458	19	420	10	36.9	420	10

Eastport Fm. (PG036A)

										age (Ma)	error (Ma)	age (Ma)	error (Ma)	age (Ma)	error (Ma)	discordance[1]	reported age[2]	
sample name	^{206}Pb (cps)	^{204}Pb (cps)	^{207}Pb/^{206}Pb	2 σ	^{207}Pb/^{235}U	2 σ	^{206}Pb/^{238}U	2 σ	ρ	^{207}Pb/^{206}Pb	2 σ	^{207}Pb/^{235}U	2 σ	^{206}Pb/^{238}U	2 σ	%	(Ma)	2 σ
PG036A-310	20420	200	0.05940	0.00280	0.57167	0.02929	0.06980	0.00140	0.392	582	99	459	19	435	8	26.1	435	8
PG036A-311	24130	209	0.06060	0.00300	0.57319	0.03173	0.06860	0.00170	0.448	625	103	460	20	428	10	32.6	428	10
PG036A-312	60600	204	0.05800	0.00160	0.61737	0.02179	0.07720	0.00170	0.624	530	59	488	14	479	10	9.9	479	10
PG036A-313	59300	203	0.05820	0.00160	0.55611	0.01996	0.06930	0.00160	0.643	537	59	449	13	432	10	20.3	432	10
PG036A-314	103300	266	0.10590	0.00150	4.88420	0.76242	0.33450	0.05200	0.996	1730	26	1800	124	1860	246	-8.7	1730	26
PG036A-315	16060	177	0.08070	0.00340	2.55251	0.41475	0.22940	0.03600	0.966	1214	81	1287	112	1331	186	-10.7	1214	81
PG036A-316	26750	152	0.05660	0.00190	0.53848	0.02197	0.06900	0.00160	0.568	476	73	437	14	430	10	10.0	430	10
PG036A-317	30900	183	0.06100	0.00180	0.65099	0.02345	0.07740	0.00160	0.574	639	62	509	14	481	10	25.8	481	10
PG036A-318	20800	207	0.07480	0.00500	0.82714	0.14503	0.08020	0.01300	0.924	1063	129	612	78	497	77	55.3	1063	129
PG036A-319	43400	171	0.11210	0.00190	5.62457	0.88615	0.36390	0.05700	0.994	1834	30	1920	127	2001	264	-10.6	1834	30
PG036A-320	72300	159	0.07570	0.00150	2.23676	0.34728	0.21430	0.03300	0.992	1087	39	1193	103	1252	173	-16.7	1087	39
PG036A-321	21140	145	0.06220	0.00240	0.85761	0.03651	0.10000	0.00180	0.423	681	80	629	20	614	11	10.2	614	11
PG036A-322	47300	165	0.05780	0.00180	0.55125	0.02047	0.06917	0.00140	0.545	522	67	446	13	431	8	18.0	431	8
PG036A-323	17600	164	0.06630	0.00350	1.10886	0.18329	0.12130	0.01900	0.948	816	107	758	85	738	108	10.1	816	107
PG036A-324	7440	148	0.06440	0.00390	0.89150	0.05804	0.10040	0.00240	0.367	755	123	647	31	617	14	19.2	617	14
PG036A-325	69500	201	0.06380	0.00200	0.89903	0.03370	0.10220	0.00210	0.548	735	65	651	18	627	12	15.4	627	12
PG036A-326	19880	159	0.06720	0.00310	1.19896	0.20228	0.12940	0.02100	0.962	844	93	800	89	784	119	7.5	844	93
PG036A-327	17220	181	0.07570	0.00340	1.16378	0.18498	0.11150	0.01700	0.959	1087	87	784	83	681	98	39.3	1087	87
PG036A-328	89800	174	0.06880	0.00110	1.27399	0.20025	0.13430	0.02100	0.995	893	33	834	86	812	118	9.6	893	33
PG036A-329	14270	135	0.05870	0.00250	0.73409	0.03484	0.09070	0.00190	0.441	556	90	559	20	560	11	-0.7	560	11
PG036A-330	18500	148	0.05890	0.00350	0.55711	0.03556	0.06860	0.00160	0.365	563	124	450	23	428	10	24.9	428	10
PG036A-331	16350	170	0.07160	0.00390	0.82532	0.13598	0.08360	0.01300	0.944	975	107	611	73	518	77	48.8	975	107
PG036A-332	88600	147	0.09620	0.00140	4.38510	0.67947	0.33060	0.05100	0.996	1552	27	1710	121	1841	242	-21.5	1552	27
PG036A-333	60500	194	0.09610	0.00200	4.14866	0.65498	0.31310	0.04900	0.991	1550	39	1664	122	1756	236	-15.2	1550	39
PG036A-334	28870	147	0.05910	0.00170	0.56634	0.02087	0.06950	0.00160	0.625	571	61	456	13	433	10	24.9	433	10
PG036A-335	12110	160	0.08040	0.00360	2.29138	0.36928	0.20670	0.03200	0.961	1207	86	1210	108	1211	169	-0.4	1207	86
PG036A-336	86900	142	0.06101	0.00120	0.89841	0.02878	0.10680	0.00270	0.789	640	42	651	15	654	16	-2.4	654	16
PG036A-337	56200	166	0.05650	0.00150	0.61153	0.02250	0.07850	0.00200	0.692	472	58	485	14	487	12	-3.3	487	12
PG036A-338	78000	257	0.07410	0.00250	0.95222	0.15658	0.09320	0.01500	0.979	1044	67	679	78	574	88	47.0	1044	67
PG036A-339	8050	127	0.06020	0.00390	0.57854	0.04005	0.06970	0.00170	0.352	611	134	464	25	434	10	29.9	434	10
PG036A-340	12020	152	0.06320	0.00340	0.83393	0.04914	0.09570	0.00230	0.408	715	110	616	27	589	14	18.4	589	14
PG036A-341	66300	171	0.09470	0.00250	2.40906	0.38396	0.18450	0.02900	0.986	1522	49	1245	108	1092	156	30.7	1522	49
PG036A-342	32150	164	0.06130	0.00190	0.75840	0.02712	0.08973	0.00160	0.499	650	65	573	16	554	9	15.4	554	9
PG036A-343	78600	144	0.18530	0.00210	15.58499	2.43359	0.61000	0.09500	0.997	2701	19	2852	139	3070	370	-17.2	2701	19
PG036A-344	98100	137	0.10180	0.00150	5.08110	0.78958	0.36200	0.05600	0.995	1657	27	1833	124	1992	260	-23.5	1657	27
PG036A-345	22300	183	0.06130	0.00210	0.59418	0.02354	0.07030	0.00140	0.503	650	72	474	15	438	8	33.7	438	8
PG036A-346	22920	142	0.06630	0.00250	1.11069	0.17867	0.12150	0.01900	0.972	816	77	759	83	739	108	9.9	816	77
PG036A-347	11180	113	0.07740	0.00390	2.18347	0.35879	0.20460	0.03200	0.952	1132	97	1176	108	1200	169	-6.6	1132	97
PG036A-348	57500	127	0.08250	0.00130	2.82671	0.44586	0.24850	0.03900	0.995	1257	31	1363	112	1431	198	-15.4	1257	31
PG036A-349	4700	365	0.60000	0.14000	19.77199	6.03343	0.23900	0.04700	0.644	4508	302	3080	259	1381	240	76.4	4508	302
PG036A-350	12610	129	0.06480	0.00300	0.92563	0.04715	0.10360	0.00220	0.417	768	95	665	25	635	13	18.1	635	13

Concordia diagrams for PG036A, Eastport Fm.

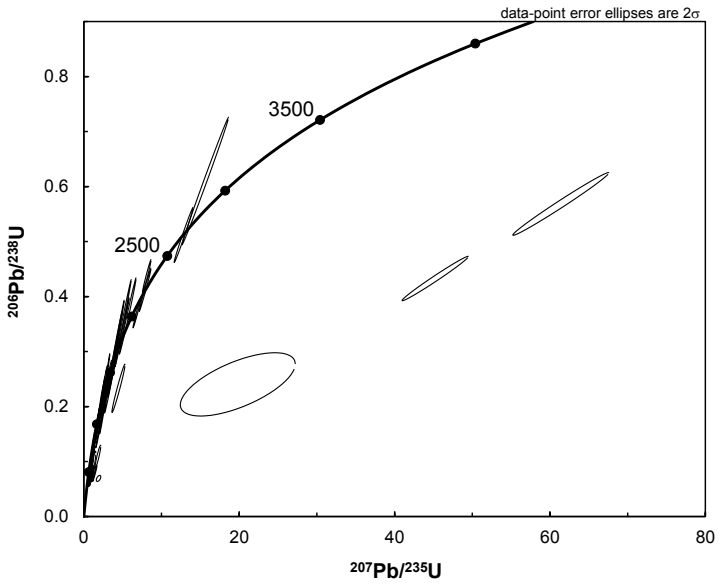

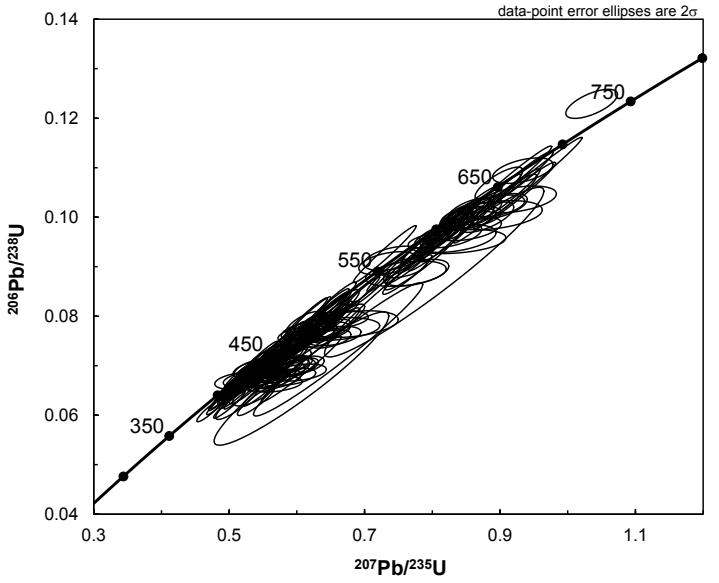

Histogram and kernel density plot for PG036A, Eastport Fm. Bandwidth and bin width is equal to median 2 σ , 19.7 Ma.

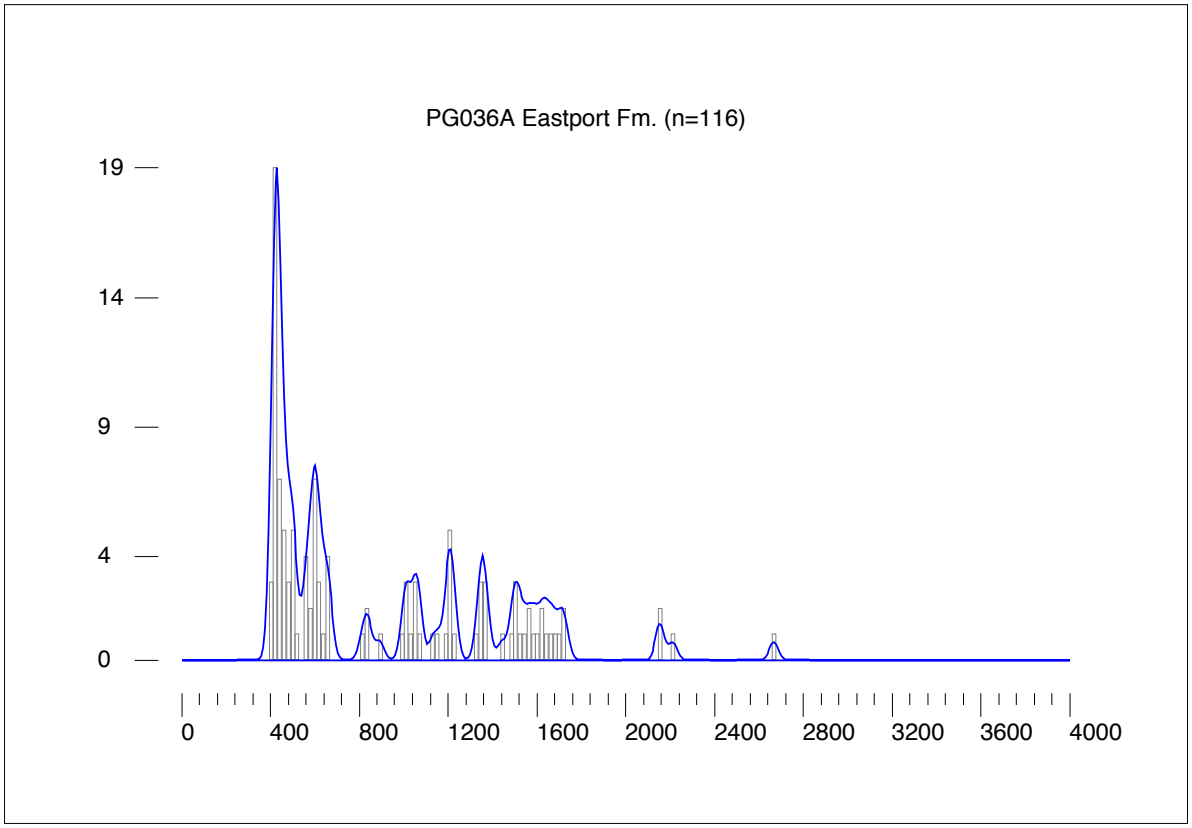

Back Bay Fm. (PG044A)

										age (Ma)	error (Ma)	age (Ma)	error (Ma)	age (Ma)	error (Ma)	discordance[1]	reported age[2]	
sample name	^{206}Pb (cps)	^{204}Pb (cps)	^{207}Pb/^{206}Pb	2 σ	^{207}Pb/^{235}U	2 σ	^{206}Pb/^{238}U	2 σ	ρ	^{207}Pb/^{206}Pb	2 σ	^{207}Pb/^{235}U	2 σ	^{206}Pb/^{238}U	2 σ	%	(Ma)	2 σ
PG044A-001	110456	93	0.06218	0.00109	0.89124	0.04374	0.10396	0.00476	0.934	680	37	647	23	638	28	6.6	629	25
PG044A-002	120827	26	0.06091	0.00088	0.85658	0.03677	0.10199	0.00412	0.941	636	31	628	20	626	24	1.7	618	21
PG044A-003	93559	18	0.06146	0.00096	0.83604	0.03569	0.09866	0.00392	0.930	655	33	617	20	607	23	7.8	599	20
PG044A-004	87711	3	0.06070	0.00091	0.79374	0.04215	0.09484	0.00483	0.960	629	32	593	24	584	28	7.4	576	26
PG044A-005	54747	1	0.05602	0.00087	0.51287	0.02247	0.06640	0.00272	0.935	453	34	420	15	414	16	8.8	409	15
PG044A-006	78335	1	0.06120	0.00088	0.81297	0.04034	0.09635	0.00458	0.957	646	30	604	22	593	27	8.6	585	25
PG044A-007	109763	3	0.06065	0.00087	0.86158	0.04134	0.10302	0.00472	0.955	627	30	631	22	632	28	-0.9	624	25
PG044A-008	30870	1	0.05700	0.00101	0.53486	0.02885	0.06805	0.00347	0.944	492	39	435	19	424	21	14.1	419	19
PG044A-009	98876	6	0.06118	0.00091	0.82509	0.03880	0.09781	0.00436	0.949	646	32	611	21	602	26	7.2	594	23
PG044A-010	108542	33	0.06111	0.00135	0.82372	0.03727	0.09776	0.00386	0.872	643	47	610	21	601	23	6.8	593	20
PG044A-011	13885	88	0.19792	0.02283	2.07521	0.27375	0.07605	0.00486	0.485	2809	177	1141	87	472	29	86.1	2812	179
PG044A-012	101060	21	0.06212	0.00096	0.86986	0.04527	0.10156	0.00505	0.955	678	33	635	24	624	29	8.5	614	27
PG044A-013	100545	66	0.06042	0.00089	0.84594	0.04100	0.10155	0.00469	0.953	618	31	622	22	624	27	-0.9	614	25
PG044A-014	56259	39	0.06077	0.00098	0.84353	0.04514	0.10067	0.00514	0.954	631	34	621	25	618	30	2.1	609	28
PG044A-015	39897	47	0.05679	0.00106	0.57077	0.03042	0.07289	0.00364	0.936	483	41	459	19	454	22	6.4	447	20
PG044A-016	19524	20	0.05811	0.00103	0.53883	0.02904	0.06725	0.00342	0.944	534	38	438	19	420	21	22.1	413	19
PG044A-017	53331	4	0.06002	0.00094	0.76242	0.03743	0.09213	0.00429	0.948	604	33	575	21	568	25	6.2	560	23
PG044A-018	89082	3	0.06064	0.00093	0.85857	0.04401	0.10269	0.00502	0.954	626	33	629	24	630	29	-0.6	621	27
PG044A-019	594577	15	0.11423	0.00122	4.98413	0.20721	0.31644	0.01272	0.967	1868	19	1817	35	1772	62	5.8	1871	34
PG044A-020	60818	17	0.06068	0.00102	0.85018	0.03809	0.10161	0.00422	0.927	628	36	625	21	624	25	0.7	615	22
PG044A-021	31134	0	0.06112	0.00118	0.80096	0.03842	0.09504	0.00417	0.915	644	41	597	21	585	25	9.5	580	28
PG044A-022	33738	4	0.06018	0.00163	0.56214	0.02625	0.06775	0.00258	0.814	610	58	453	17	423	16	31.7	419	18
PG044A-023	83484	38	0.06079	0.00100	0.85208	0.04119	0.10166	0.00462	0.940	632	35	626	22	624	27	1.3	619	30
PG044A-024	38624	4	0.06168	0.00106	0.84334	0.03795	0.09917	0.00413	0.925	663	36	621	21	610	24	8.5	604	27
PG044A-025	80329	14	0.06132	0.00109	0.82653	0.03471	0.09776	0.00372	0.905	650	38	612	19	601	22	7.9	596	25
PG044A-026	86884	16	0.06046	0.00089	0.76324	0.04314	0.09156	0.00500	0.965	620	31	576	25	565	29	9.3	560	32
PG044A-027	173690	2	0.06022	0.00098	0.68516	0.04497	0.08252	0.00525	0.969	611	35	530	27	511	31	17.0	507	33
PG044A-028	125036	0	0.06014	0.00085	0.81710	0.04367	0.09854	0.00508	0.964	609	30	606	24	606	30	0.5	601	32
PG044A-029	91731	1	0.06055	0.00094	0.83482	0.04420	0.09999	0.00506	0.956	623	33	616	24	614	30	1.5	609	32
PG044A-030	15783	4	0.05580	0.00121	0.50674	0.02363	0.06586	0.00272	0.885	444	48	416	16	411	16	7.7	408	19
PG044A-031	49680	7	0.06276	0.00123	0.74132	0.04059	0.08566	0.00438	0.933	700	41	563	23	530	26	25.3	531	25
PG044A-032	11218	0	0.05150	0.00164	0.21541	0.01166	0.03034	0.00133	0.808	263	72	198	10	193	8	27.3	193	8
PG044A-033	19689	2	0.06861	0.00118	0.63736	0.02942	0.06737	0.00289	0.928	887	35	501	18	420	17	54.3	901	35
PG044A-034	69774	5	0.06057	0.00085	0.86069	0.03864	0.10306	0.00440	0.950	624	30	630	21	632	26	-1.4	634	24
PG044A-035	110473	55	0.06070	0.00094	0.79047	0.04066	0.09445	0.00463	0.954	629	33	591	23	582	27	7.8	583	26
PG044A-036	98605	13	0.06039	0.00094	0.82470	0.03707	0.09905	0.00418	0.939	618	33	611	20	609	24	1.5	610	22
PG044A-037	84071	14	0.06058	0.00100	0.82264	0.03920	0.09849	0.00440	0.938	624	35	610	22	606	26	3.1	607	24
PG044A-038	113267	14	0.05883	0.00085	0.75140	0.03854	0.09263	0.00456	0.959	561	31	569	22	571	27	-1.9	572	25
PG044A-039	102995	11	0.06151	0.00092	0.88814	0.04023	0.10472	0.00448	0.944	657	32	645	21	642	26	2.4	643	24
PG044A-040	160508	5	0.06445	0.00098	1.00608	0.04842	0.11322	0.00517	0.949	756	32	707	24	691	30	9.1	693	28
PG044A-041	86289	1	0.06132	0.00100	0.83903	0.05074	0.09924	0.00578	0.963	650	34	619	28	610	34	6.5	611	32
PG044A-042	31687	0	0.06105	0.00116	0.85572	0.03978	0.10165	0.00431	0.913	641	40	628	22	624	25	2.8	626	23
PG044A-043	59448	4	0.06203	0.00108	0.88537	0.04256	0.10352	0.00464	0.932	675	37	644	23	635	27	6.2	636	25
PG044A-044	53202	40	0.06180	0.00111	0.88106	0.03999	0.10339	0.00431	0.918	667	38	642	21	634	25	5.2	636	23
PG044A-045	275935	0	0.05898	0.00081	0.81640	0.03539	0.10039	0.00413	0.949	566	30	606	20	617	24	-9.3	618	22
PG044A-046	66236	3	0.06095	0.00087	0.84207	0.04665	0.10020	0.00537	0.967	637	30	620	25	616	31	3.6	619	30
PG044A-047	69821	49	0.06101	0.00096	0.89035	0.04479	0.10584	0.00506	0.949	640	34	647	24	649	29	-1.5	652	27
PG044A-048	115553	0	0.06013	0.00090	0.80104	0.03641	0.09661	0.00415	0.944	608	32	597	20	595	24	2.4	598	22

Back Bay Fm. (PG044A)

sample name	^{206}Pb (cps)	^{204}Pb (cps)	^{207}Pb/^{206}Pb	2 σ	^{207}Pb/^{235}U	2 σ	^{206}Pb/^{238}U	2 σ	ρ	age (Ma) ^{207}Pb/^{206}Pb	error (Ma) 2 σ	age (Ma) ^{207}Pb/^{235}U	error (Ma) 2 σ	age (Ma) ^{206}Pb/^{238}U	error (Ma) 2 σ	discordance[1] %	reported age[2] (Ma)	2 σ
PG044A-050	37034	10	0.07164	0.00112	0.91899	0.03657	0.09303	0.00341	0.920	976	31	662	19	573	20	43.1	994	31
PG044A-051	56478	5	0.06383	0.00108	0.92604	0.04916	0.10521	0.00529	0.947	736	36	666	26	645	31	13.0	649	29
PG044A-052	29298	7	0.06401	0.00119	0.92124	0.04109	0.10438	0.00423	0.910	742	39	663	21	640	25	14.4	644	22
PG044A-053	15054	3	0.06240	0.00168	0.59422	0.02825	0.06907	0.00271	0.825	688	56	474	18	431	16	38.7	433	15
PG044A-054	17814	6	0.05506	0.00137	0.52329	0.02852	0.06893	0.00334	0.889	415	55	427	19	430	20	-3.7	432	19
PG044A-055	18597	42	0.05960	0.00141	0.66164	0.03755	0.08051	0.00415	0.909	589	50	516	23	499	25	15.9	499	25
PG044A-056	57241	41	0.06096	0.00105	0.83662	0.03960	0.09954	0.00439	0.931	638	37	617	22	612	26	4.3	611	26
PG044A-057	75056	36	0.06367	0.00169	0.90682	0.04488	0.10329	0.00432	0.845	731	55	655	24	634	25	14.0	633	26
PG044A-058	122263	43	0.06109	0.00089	0.82613	0.03674	0.09809	0.00412	0.944	642	31	611	20	603	24	6.4	602	25
PG044A-059	26969	38	0.05816	0.00120	0.54015	0.02657	0.06736	0.00301	0.908	536	45	439	17	420	18	22.2	420	19
PG044A-060	43546	39	0.06354	0.00107	0.90686	0.03801	0.10351	0.00398	0.916	726	35	655	20	635	23	13.2	634	24
PG044A-061	13489	44	0.06168	0.00194	0.58197	0.03231	0.06843	0.00313	0.823	663	66	466	21	427	19	36.8	426	19
PG044A-062	13068	59	0.06985	0.00205	0.87234	0.04360	0.09058	0.00367	0.810	924	59	637	23	559	22	41.2	921	59
PG044A-063	111383	69	0.07687	0.00106	1.86531	0.07346	0.17599	0.00649	0.937	1118	27	1069	26	1045	36	7.1	1115	27
PG044A-064	36566	66	0.06294	0.00140	0.89852	0.04391	0.10354	0.00451	0.891	706	46	651	23	635	26	10.6	634	27
PG044A-065	60643	75	0.05904	0.00089	0.77057	0.03900	0.09466	0.00458	0.955	569	32	580	22	583	27	-2.7	582	28
PG044A-066	25617	81	0.05631	0.00103	0.52415	0.02809	0.06752	0.00340	0.940	464	40	428	19	421	21	9.6	426	20
PG044A-067	16562	75	0.05845	0.00118	0.55054	0.02971	0.06831	0.00342	0.927	547	44	445	19	426	21	22.8	425	21
PG044A-068	105495	59	0.06067	0.00086	0.86164	0.04183	0.10301	0.00478	0.956	627	30	631	23	632	28	-0.8	631	29
PG044A-069	88679	43	0.06074	0.00089	0.81904	0.04330	0.09779	0.00497	0.961	630	31	608	24	601	29	4.8	601	30
PG044A-070	64813	31	0.05662	0.00091	0.54845	0.02602	0.07025	0.00314	0.941	477	35	444	17	438	19	8.5	437	19
PG044A-071	74510	122	0.05595	0.00094	0.52049	0.02913	0.06747	0.00360	0.954	450	37	425	19	421	22	6.8	427	17
PG044A-072	61769	40	0.06237	0.00109	0.89607	0.05178	0.10419	0.00574	0.953	687	37	650	27	639	33	7.3	644	32
PG044A-073	66948	40	0.06336	0.00098	0.87565	0.04676	0.10023	0.00512	0.957	720	32	639	25	616	30	15.2	621	28
PG044A-074	117227	57	0.06246	0.00099	0.86210	0.04497	0.10010	0.00497	0.953	690	33	631	24	615	29	11.4	620	27
PG044A-075	88238	42	0.05989	0.00086	0.77097	0.04031	0.09336	0.00469	0.961	600	31	580	23	575	28	4.2	580	26
PG044A-076	136738	162	0.06187	0.00109	0.85167	0.04374	0.09983	0.00482	0.940	670	37	626	24	613	28	8.8	619	26
PG044A-077	72922	58	0.06098	0.00099	0.86191	0.03707	0.10252	0.00408	0.926	638	35	631	20	629	24	1.5	634	21
PG044A-078	37985	68	0.06118	0.00112	0.76382	0.03256	0.09055	0.00349	0.904	645	39	576	19	559	21	14.0	564	18
PG044A-079	40745	88	0.06661	0.00178	0.84550	0.03986	0.09205	0.00358	0.824	826	55	622	22	568	21	32.6	820	55
PG044A-080	70018	273	0.11198	0.00449	1.71062	0.09928	0.11079	0.00465	0.723	1832	71	1013	37	677	27	66.3	1827	71
PG044A-081	55468	81	0.06407	0.00105	0.97504	0.04406	0.11037	0.00464	0.931	744	34	691	22	675	27	9.8	681	25
PG044A-082	69216	61	0.05887	0.00097	0.56773	0.02838	0.06994	0.00330	0.945	562	35	457	18	436	20	23.3	440	19
PG044A-083	67433	51	0.06070	0.00089	0.82700	0.04674	0.09881	0.00539	0.966	629	31	612	26	607	32	3.5	613	30
PG044A-084	111395	62	0.06092	0.00085	0.88161	0.04421	0.10495	0.00505	0.960	636	30	642	24	643	29	-1.1	649	27
PG044A-085	121198	113	0.11495	0.00124	4.90301	0.26828	0.30935	0.01659	0.980	1879	19	1803	45	1738	81	8.6	1874	19
PG044A-086	23287	75	0.06154	0.00120	0.57344	0.02950	0.06758	0.00322	0.925	658	41	460	19	422	19	37.1	423	18
PG044A-087	89036	63	0.06076	0.00090	0.82039	0.03921	0.09793	0.00445	0.950	631	32	608	22	602	26	4.7	604	24
PG044A-088	91619	76	0.06176	0.00101	0.84860	0.03901	0.09965	0.00428	0.934	666	35	624	21	612	25	8.4	614	23
PG044A-089	29708	60	0.05764	0.00108	0.53832	0.02726	0.06773	0.00319	0.929	516	41	437	18	422	19	18.8	424	18
PG044A-090	20506	44	0.05910	0.00126	0.55443	0.02600	0.06804	0.00284	0.891	571	46	448	17	424	17	26.5	426	16
PG044A-091	57148	42	0.06073	0.00094	0.83427	0.03792	0.09963	0.00426	0.941	630	33	616	21	612	25	2.9	614	23
PG044A-092	100940	69	0.06066	0.00088	0.85763	0.04655	0.10255	0.00536	0.963	627	31	629	25	629	31	-0.4	631	29
PG044A-093	67272	66	0.06184	0.00088	0.76761	0.03643	0.09003	0.00408	0.954	669	30	578	21	556	24	17.6	558	22
PG044A-094	88619	98	0.05939	0.00087	0.73476	0.03748	0.08972	0.00439	0.958	582	31	559	22	554	26	5.0	556	24
PG044A-095	42035	98	0.07240	0.00165	0.98521	0.04273	0.09869	0.00364	0.851	997	46	696	22	607	21	41.0	991	46
PG044A-096	48110	230	0.10098	0.00464	1.41306	0.08655	0.10149	0.00411	0.660	1642	83	894	36	623	24	65.0	1637	83
PG044A-097	41631	86	0.06262	0.00101	0.85392	0.04477	0.09891	0.00493	0.951	695	34	627	24	608	29	13.2	610	27

Back Bay Fm. (PG044A)

sample name	^{206}Pb (cps)	^{204}Pb (cps)	$^{207}Pb/^{206}Pb$	2 σ	$^{207}Pb/^{235}U$	2 σ	$^{206}Pb/^{238}U$	2 σ	ρ	age (Ma) $^{207}Pb/^{206}Pb$	error (Ma) 2 σ	age (Ma) $^{207}Pb/^{235}U$	error (Ma) 2 σ	age (Ma) $^{206}Pb/^{238}U$	error (Ma) 2 σ	discordance[1] %	reported age[2] (Ma)	2 σ
PG044A-098	56515	128	0.06105	0.00099	0.81830	0.03710	0.09722	0.00412	0.934	641	34	607	21	598	24	7.0	600	22
PG044A-099	56998	99	0.06108	0.00094	0.86150	0.03650	0.10230	0.00404	0.932	642	33	631	20	628	24	2.3	630	21
PG044A-100	75291	121	0.10434	0.00127	3.74393	0.15329	0.26024	0.01018	0.955	1703	22	1581	32	1491	52	13.9	1697	22
PG044A-101	15862	111	0.06245	0.00145	0.82485	0.04585	0.09579	0.00483	0.908	690	49	611	25	590	28	15.2	597	32
PG044A-102	128124	104	0.10594	0.00122	4.10097	0.15991	0.28075	0.01046	0.956	1731	21	1654	31	1595	52	8.8	1722	21
PG044A-103	131820	144	0.06170	0.00091	0.80816	0.04659	0.09500	0.00530	0.967	664	31	601	26	585	31	12.4	592	34
PG044A-104	46172	111	0.06124	0.00101	0.85460	0.03883	0.10121	0.00429	0.932	648	35	627	21	622	25	4.2	629	29
PG044A-105	31520	107	0.06037	0.00102	0.73299	0.03375	0.08805	0.00377	0.930	617	36	558	20	544	22	12.3	551	26
PG044A-106	101989	158	0.06103	0.00094	0.83539	0.04015	0.09927	0.00452	0.948	640	33	617	22	610	26	4.9	617	30
PG044A-107	157950	108	0.07538	0.00084	1.70568	0.09412	0.16411	0.00887	0.979	1079	22	1011	35	980	49	9.9	1070	22
PG044A-108	68471	113	0.06135	0.00093	0.86537	0.04497	0.10230	0.00508	0.956	652	32	633	24	628	30	3.8	635	33
PG044A-109	88509	118	0.06084	0.00090	0.83239	0.04319	0.09922	0.00493	0.958	634	32	615	24	610	29	4.0	617	32
PG044A-110	59356	120	0.05916	0.00100	0.75682	0.03446	0.09278	0.00392	0.928	573	36	572	20	572	23	0.2	579	27
PG044A-111	65570	150	0.06021	0.00102	0.75274	0.03792	0.09068	0.00430	0.942	611	36	570	22	560	25	8.8	566	29
PG044A-112	33207	96	0.05663	0.00095	0.52170	0.02687	0.06682	0.00325	0.945	477	37	426	18	417	20	13.0	422	22
PG044A-113	47543	131	0.06036	0.00094	0.75592	0.03855	0.09083	0.00441	0.952	616	33	572	22	560	26	9.5	567	29
PG044A-114	104344	125	0.06322	0.00093	0.89744	0.04169	0.10296	0.00454	0.949	716	31	650	22	632	26	12.3	639	30
PG044A-115	136379	113	0.06165	0.00089	0.83166	0.03927	0.09783	0.00440	0.952	662	31	615	22	602	26	9.6	609	30
PG044A-116	111807	152	0.06429	0.00100	0.89712	0.04739	0.10120	0.00511	0.955	751	33	650	25	621	30	18.1	629	33
PG044A-117	102094	191	0.07211	0.00138	0.94899	0.04907	0.09544	0.00458	0.929	989	38	678	25	588	27	42.5	980	39
PG044A-118	33939	93	0.06287	0.00123	0.76171	0.04185	0.08787	0.00451	0.934	704	41	575	24	543	27	23.8	550	30
PG044A-120	16623	89	0.06063	0.00114	0.55151	0.03903	0.06597	0.00450	0.964	626	40	446	25	412	27	35.3	417	29
PG044A-121	67562	98	0.06122	0.00096	0.83020	0.04099	0.09836	0.00460	0.948	647	33	614	22	605	27	6.8	614	31
PG044A-122	129083	127	0.06183	0.00094	0.85338	0.03822	0.10010	0.00422	0.940	668	32	627	21	615	25	8.4	625	29
PG044A-123	74836	118	0.06106	0.00094	0.79333	0.03724	0.09424	0.00418	0.945	641	33	593	21	581	25	9.9	590	28
PG044A-124	98367	119	0.06133	0.00089	0.82292	0.03862	0.09732	0.00434	0.951	651	31	610	21	599	25	8.4	608	29
PG044A-125	266586	134	0.06569	0.00073	0.95784	0.06235	0.10575	0.00678	0.985	797	23	682	32	648	39	19.6	652	39
PG044A-126	186700	72	0.06065	0.00086	0.79940	0.04150	0.09559	0.00477	0.962	627	30	596	23	589	28	6.4	598	31
PG044A-127	46766	78	0.06226	0.00105	0.83999	0.03920	0.09784	0.00426	0.933	683	36	619	21	602	25	12.5	611	29
PG044A-128	75672	99	0.06117	0.00088	0.83765	0.04288	0.09932	0.00488	0.959	645	31	618	23	610	29	5.7	620	32
PG044A-129	140734	97	0.06103	0.00086	0.82856	0.03831	0.09847	0.00434	0.953	640	30	613	21	605	25	5.7	615	29
PG044A-130	33810	94	0.06134	0.00105	0.79162	0.03930	0.09359	0.00436	0.939	651	36	592	22	577	26	12.0	586	29

Concordia diagrams for PG044A, Back Bay Fm.

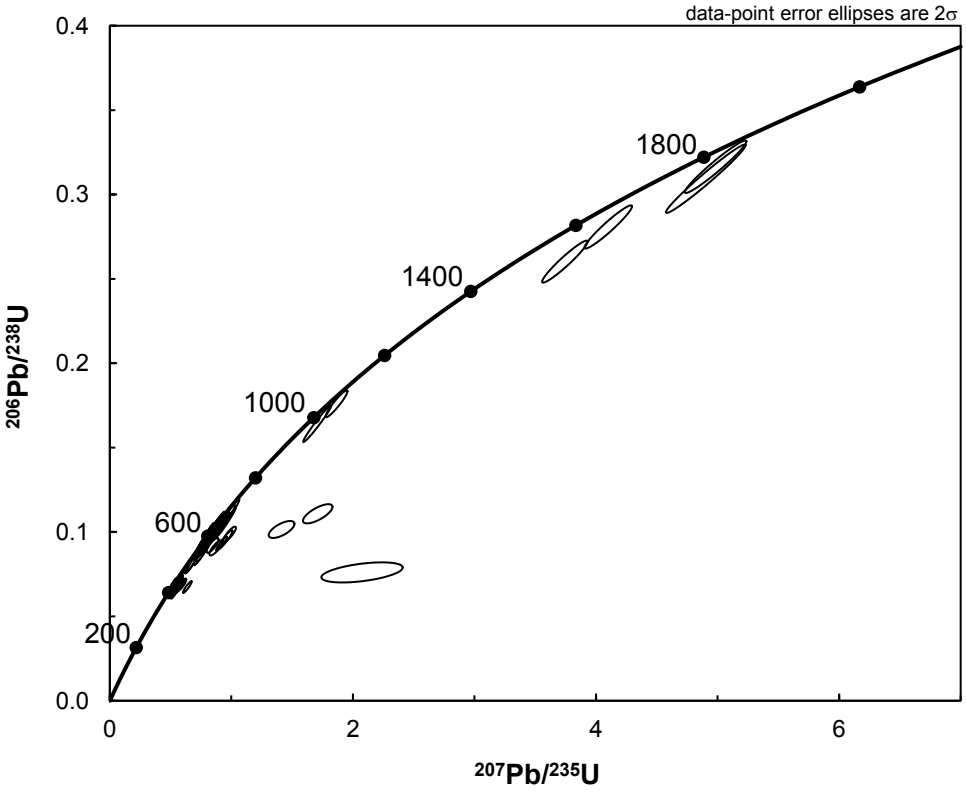

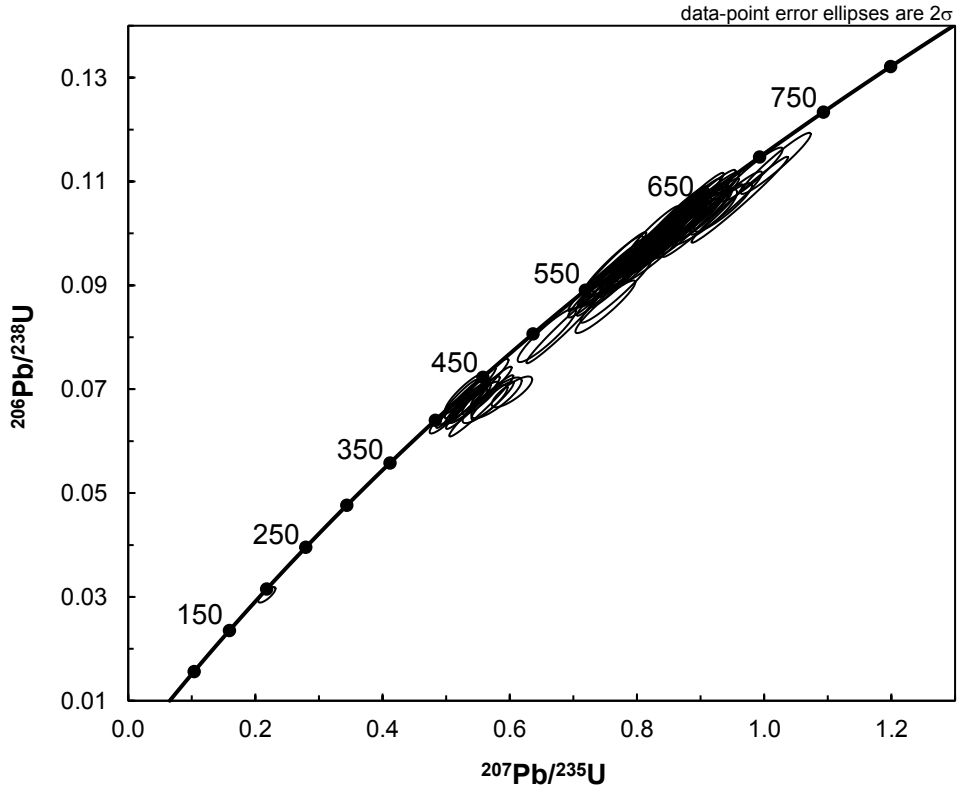

Histogram and kernel density plot for PG044A, Back Bay Fm. Bandwidth and bin width is equal to median 2 σ , 26.4 Ma.